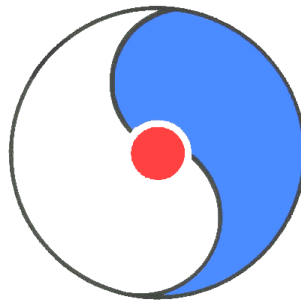


# Baryon Dynamics at RHIC

March 28-30, 2002



Organizers:

M. Gyulassy, D. Kharzeev, and N. Xu

**RIKEN BNL Research Center**

Building 510A, Brookhaven National Laboratory, Upton, NY 11973-5000, USA

## DISCLAIMER

*This report was prepared as an account of work sponsored by an agency of the United States Government. Neither the United States Government nor any agency thereof, nor any employees, nor any of their contractors, subcontractors or their employees, makes any warranty, express or implied, or assumes any legal liability or responsibility for the accuracy, completeness, or any third party's use or the results of such use of any information, apparatus, product, or process disclosed, or represents that its use would not infringe privately owned rights. Reference herein to any specific commercial product, process, or service by trade name, trademark, manufacturer, or otherwise, does not necessarily constitute or imply its endorsement, recommendation, or favoring by the United States Government or any agency thereof or its contractors or subcontractors. The views and opinions of authors expressed herein do not necessarily state or reflect those of the United States Government or any agency thereof.*

Available electronically at-

<http://www.doe.gov/bridge>

Available to U.S. Department of Energy and its contractors in paper from-

U.S. Department of Energy  
Office of Scientific and Technical Information  
P.O. Box 62  
Oak Ridge, TN 37831  
(423) 576-8401

Available to the public from-

U.S. Department of Commerce  
National Technical Information Service  
5285 Port Royal Road  
Springfield, VA 22131  
(703) 487-4650



Printed on recycled paper

## Preface to the Series

The RIKEN BNL Research Center (RBRC) was established in April 1997 at Brookhaven National Laboratory. It is funded by the "Rikagaku Kenkyusho" (RIKEN, The Institute of Physical and Chemical Research) of Japan. The Center is dedicated to the study of strong interactions, including spin physics, lattice QCD, and RHIC physics through the nurturing of a new generation of young physicists.

During the first year, the Center had only a Theory Group. In the second year, an Experimental Group was also established at the Center. At present, there are seven Fellows and eight Research Associates in these two groups. During the third year, we started a new Tenure Track Strong Interaction Theory RHIC Physics Fellow Program, with six positions in the first academic year, 1999-2000. This program has increased to include ten theorists and one experimentalist in the current academic year, 2001-2002. Beginning this year there is a new RIKEN Spin Program at RBRC with four Researchers and three Research Associates.

In addition, the Center has an active workshop program on strong interaction physics with each workshop focused on a specific physics problem. Each workshop speaker is encouraged to select a few of the most important transparencies from his or her presentation, accompanied by a page of explanation. This material is collected at the end of the workshop by the organizer to form proceedings, which can therefore be available within a short time. To date there are forty-one proceeding volumes available.

The construction of a 0.6 teraflops parallel processor, dedicated to lattice QCD, begun at the Center on February 19, 1998, was completed on August 28, 1998.

T. D. Lee  
August 2, 2001

\*Work performed under the auspices of U.S.D.O.E. Contract No. DE-AC02-98CH10886.



# CONTENTS

Preface to the Series.....	i
Introduction	
<i>M. Gyulassy, D. Kharzeev, N. Xu</i> .....	1
Lattice QCD at finite T and $\mu$ , and the Critical Point	
<i>S. Katz</i> .....	3
The Detailed Analysis of the Three-Quark Potential $V_{3Q}$ in SU(3) Lattice QCD	
<i>T. T. Takahashi</i> .....	13
The Groundstate of 3 Static Quarks	
<i>P. de Forcrand</i> .....	19
High-Baryon Density QCD Matter	
<i>D. Rischke</i> .....	25
Effects of Strong Color Fields on Baryon Dynamics	
<i>S. Soff</i> .....	31
AntiBaryon/Baryon vs. Rapidity: Results from BRAHMS	
<i>I. Bearden</i> .....	35
Overview of PHENIX Results on Baryons and Identified Hadrons	
<i>T. Chujo</i> .....	43
Baryons in PHOBOS	
<i>K. Gulbrandsen</i> .....	49
Proton and Anti-Proton Distributions from STAR	
<i>K. Schweda</i> .....	57
Baryon Production and Gluonic Dynamics	
<i>H. Huang</i> .....	65

Hadronization, Baryon- and Meson- Dynamics at RHIC <i>S. Bass</i> .....	71
Baryon Transport at RHIC <i>V. Topor Pop</i> .....	83
The Relativistic Advection-Diffusion Equation <i>D. Teaney</i> .....	93
The Pbar/pi- Anomaly at High P <sub>T</sub> <i>Ivan Vitev</i> .....	99
Color Glass Condensate of Baryon Junctions <i>B. Kopeliovich</i> .....	107
Baryon Fluctuation <i>S. Jeon</i> .....	113
Baryons in AMPT Model <i>Z. Lin</i> .....	117
Reviving the Strong Coupling Expansion: Baryon Junctions and Other “Resonances” <i>M. Velkovsky</i> .....	125
Baryon Stopping From SIS to High Energies – Expectations and Reality <i>F. Videbaek</i> .....	133
Strange Baryon Production in p+A Collisions <i>B. Cole</i> .....	139
Baryon and Baryon Pair Production in Elementary and Nuclear Hadronic Interactions <i>H. G. Fischer</i> .....	147
Baryon Results from E917 and the AGS <i>D. Hofman</i> .....	153
K/π vs. Collision Energy and Centrality: What we learn from the systematics? <i>F. Wang</i> .....	161

Evidence for Topological Defect Production in Heavy Ion Collisions <i>J. Kapusta</i> .....	165
Buckyballs and Gluon Junction Networks on the Femtometer Scale <i>T. Csörgő</i> .....	171
Theory and Phenomenology of Baryon Junctions <i>D. Kharzeev</i> .....	179
Recent Results on Strange Baryons From STAR <i>H. Long</i> .....	187
Anti-Baryon/Baryon Ratios in PHENIX <i>I. Ravinovich</i> .....	197
Systematics of Nuclear Cluster Formation Rates <i>Z. Xu</i> .....	201
Theory Summary <i>X. Wang</i> .....	209
Experiment Summary <i>C. Ogilvie</i> .....	215
List of Registered Participants.....	218
Agenda.....	224
Pictures	227
Additional RIKEN BNL Research Center Proceeding Volumes	228
Contact Information	





One of the striking observations at RHIC is the large valence baryon rapidity density observed at mid rapidity in central Au+Au at 130 A GeV. There are about twice as many valence protons at mid-rapidity than predicted based on extrapolation from p+p collisions. Even more striking PHENIX observed that the high pt spectrum is dominated by baryons and anti-baryons. The STAR measured event anisotropy parameter  $v_2$  for lambdas are as high as charged particles at  $pt \sim 2.5$  GeV/c. These are completely unexpected based on conventional pQCD parton fragmentation phenomenology.

One exciting possibility is that these observables reveal the topological gluon field origin of baryon number transport referred to as baryon junctions. Another is that hydrodynamics may apply up to high pt in A+A. There is no consensus on what are the correct mechanisms for producing baryons and hyperons at high pt and large rapidity shifts and the new RHIC data provide a strong motivation to hold a meeting focusing on this class of observables. The possible role of junctions in forming CP violating domain walls and novel nuclear bucky-ball configurations would also be discussed.

In this workshop, we focused on all measured baryon distributions at RHIC energies and related theoretical considerations. To facilitate the discussions, results of heavy ion collisions at lower beam energies, results from p+A /p+p/e+e collisions were included. Some suggestions for future measurements have been made at the workshop.

M. Gyulassy, D. Kharzeev, and N. Xu



# Lattice QCD at finite $T$ and $\mu$ , and the Critical Point

Sándor Katz, DESY Hamburg  
March 28, 2002

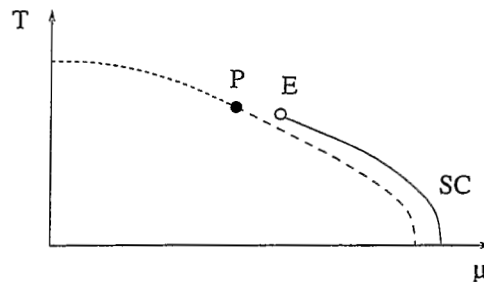
for  
Baryon Dynamics at RHIC Workshop  
RIKEN BNL Research Center

Z. Fodor, S. D. Katz, hep-lat/0104001

Z. Fodor, S. D. Katz, JHEP03 (2002) 014; hep-lat/0106002

1. Introduction
2. Overlap ensuring multi-parameter reweighting
3. Four-flavor dynamical, staggered QCD
4. Critical endpoint in  $n_f = 2 + 1$  dynamical QCD
5. Summary

Introduction, experimental motivation



• Chiral phase transition (PT)

$n_f = 2$  with  $m_q = 0$  at  $\mu = 0 \Rightarrow 2^{nd}$  order PT

$n_f = 2$  with  $m_q = 0$  at  $T = 0 \Rightarrow 1^{st}$  order PT

$n_f = 2$  with  $m_q = 0 \Rightarrow$  tricritical point (P) at  $\mu, T \neq 0$

$n_f = 3$  with  $m_q = 0$  at  $\mu = 0 \Rightarrow 1^{st}$  order PT

increasing  $m_s$  weakens the  $1^{st}$  order PT  $\Rightarrow$  cross-over

$n_f = 2 + 1$  with physical  $m_q$  at  $\mu = 0 \Rightarrow$  cross-over

$n_f = 2 + 1$  with physical  $m_q$  at  $T = 0 \Rightarrow 1^{st}$  order PT

$n_f = 2 + 1$  with physical  $m_q \Rightarrow$  critical endpoint (E) at  $\mu, T \neq 0$

"If and when the critical point E is discovered, it will appear prominently on the map of the phase diagram featured in any future textbook of QCD." (F. Wilczek)

- locate the endpoint: nonperturbative prediction of QCD lattice gauge theory: serious problems at  $\mu \neq 0$   
measure (Dirac determinant) complex  $\Rightarrow$  no importance sampling

I.M. Barbour et al., Nucl. Phys. B (Proc. Supl.) 60A, 220 (1998)

Glasgow method:  $\mu$  reweighting based on an ensemble at  $\mu = 0$  after collecting 20 million configurations only unphysical results  
 $T = \mu = 0$  ensemble does not overlap with the transition states

M.A. Halasz et al., Phys. Rev. D58, 096007 (1998)

random matrix model for the Dirac operator can be solved  
 $\Rightarrow T_E \approx 120$  MeV and  $\mu_E \approx 700$  MeV, can be off by a factor of 2-3

T.M. Schwarz, S.P. Klevansky, G. Papp, Phys. Rev. C60 055205 (1999)

Nambu-Jona-Lasinio model,  $T - \mu$  phase diagram

Overlap ensuring multi-parameter reweighting

- generic system with  $\psi$  fermions and  $\phi$  bosons

fermionic Lagrangian:  $\bar{\psi}M(\phi)\psi \Rightarrow$  after Grassmann integration

$$Z(\alpha) = \int \mathcal{D}\phi \exp[-S_{bos}(\alpha, \phi)] \det M(\phi, \alpha)$$

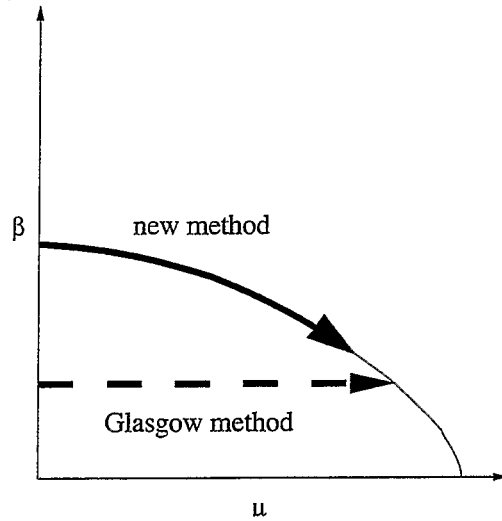
$\alpha$ : parameter set (gauge coupling, mass, chemical potential)

include  $\mu$ : forward/backward links multiplied with  $\exp(\pm\mu)$   
for some parameters  $\alpha_0$  importance sampling can be done

$$Z(\alpha) = \int \mathcal{D}\phi \exp[-S_{bos}(\alpha_0, \phi)] \det M(\phi, \alpha_0) \{ \exp[-S_{bos}(\alpha, \phi) + S_{bos}(\alpha_0, \phi)] \det M(\phi, \alpha) / \det M(\phi, \alpha_0) \}$$

first line: measure; curly bracket: observable (will be measured)  
simultaneously changing several parameters: better overlap  
e.g. transition configurations are mapped to transition ones

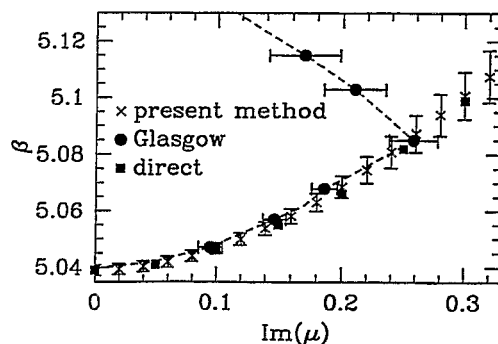
## Comparison with the Glasgow method



Glasgow  
single parameter ( $\mu$ )  
purely hadronic  
configurations

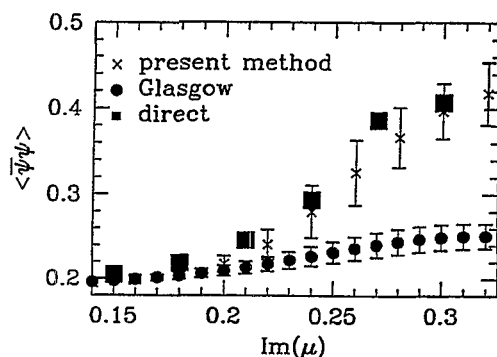
New method  
two parameters ( $\mu$  and  $\beta$ )  
transition configurations

- direct test:  $n_f=4$  dynamical QCD with imaginary  $\mu$   
 $m_q=0.05$  staggered fermions on  $4 \cdot 6^3$  lattices
- compare: direct method and different types of reweighting:  
our method: measuring the determinants and bosonic action  
Glasgow method: only determinants  
phase diagram in the  $\text{Im}(\mu)$ - $\beta$  plane



overlap is much better for our method  
no premature (Glasgow type) onset transition  
no "fake" transitions (with correct  $\mu$ - $\beta$ )

- chiral condensate at  $\mu \approx 0.25$  for the three methods



no “fake” transitions (with correct  $\mu$ - $\beta$ )

Glasgow-method: based on an ensemble of the high-T phase

high- $\mu$  phase does not overlap with the states of interest

statistical errors: two-parameter reweighting more trustworthy

transition points can be defined by susceptibility peaks,

turning points, real part of Lee-Yang zeros (see later)

we expect that our method is also superior at  $\text{Re}(\mu) \neq 0$

QCD with  $n_f=2+1$  dynamical staggered fermions

- partition function with multi-parameter reweighting

$$Z(\alpha) = \int \mathcal{D}\phi \exp[-S_{bos}(\alpha_0, \phi)] [\det M(\phi, \alpha_0)]^{n_f/4} \{ \exp[-S_{bos}(\alpha, \phi) + S_{bos}(\alpha_0, \phi)] [\det M(\phi, \alpha)]^{n_f/4} / [\det M(\phi, \alpha_0)]^{n_f/4} \}$$

we measure fractional powers of the complex determinants

$\Rightarrow$  choose among the possible Riemann-sheets

a. gauge fix to  $A_0 = 0$  on all but the last timeslice

b. multiply the  $j$ -th row/column by  $e^{\pm j\mu}$

c. rearrange the columns of the matrix

d.  $L_t-2$  Gauss elimination step gives a  $6L_s^3 \times 6L_s^3$  matrix

$$\det M(\mu) = e^{-3V\mu} \prod_{i=1}^{6L_s^3} (e^{L_t\mu} - \lambda_i)$$

$\Rightarrow$  gives  $Z$  for “arbitrary”  $\mu$  and  $\beta$

# Lee-Yang zeros of the partition function

C.N. Yang and T.D. Lee, Phys. Rev. 87, 404 (1952)

- distinguish between a crossover and a 1<sup>st</sup> order PT

1<sup>st</sup> order PT: free energy  $\propto \log Z(\beta)$  non-analytic

PT appears not at finite  $V$ , but only at  $V \rightarrow \infty$

$Z$  has zeros even at finite  $V$ , at complex parameters ( $\beta$ )

$\text{Re}(\beta_0)$ , zero with smallest imaginary part: transition point

for 1<sup>st</sup> order PT: zeros approach the real axis

$1/V$  scaling in the  $V \rightarrow \infty$  limit

generates the non-analyticity of the free energy

crossover: zeros do not approach the real axis

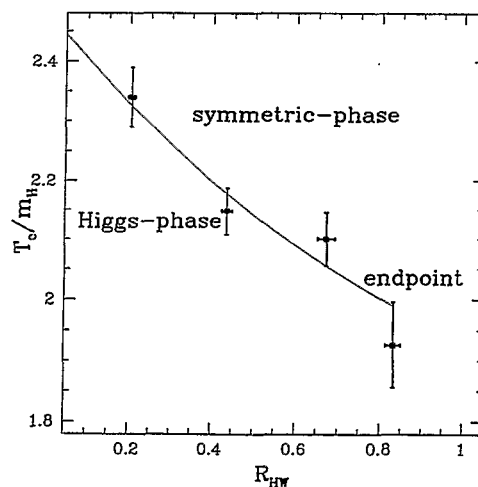
overlap ensuring multi-parameter reweighting

combined with Lee-Yang zeros of the partition function

finite  $T$  endpoint of the 4-D electroweak phase transition

hypothetical Higgs boson mass:  $\approx 72$  GeV (at least upto  $V=60^3$ )

F. Csikor, Z. Fodor and J. Heitger, Phys. Rev. Lett. 82, 21 (1999)





## Endpoint of 2+1 flavor QCD on $L_t = 4$ lattices

- three basic steps of the analysis

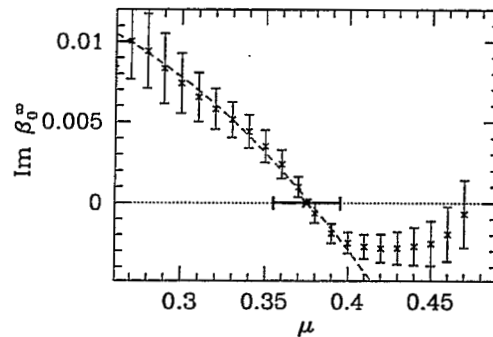
$m_s=0.2$  (approx. physical),  $m_{ud}=0.025$  ( $\approx 3-4\times$  heavier)

a. determine the transition points,  $\text{Re}(\beta_0)$ , on  $L_s=4,6,8$  lattices as a function of  $\mu$  by the Lee-Yang zeros for  $\mu \neq 0$  overlap ensuring multi-parameter reweighting (14000, 3600 and 840 independent configurations, respectively)

b. by inspecting the  $V \rightarrow \infty$  limit of  $\text{Im}(\beta_0)$  separate the crossover and the 1<sup>st</sup> order PT regions in  $\mu$

c. connect  $\mu=T=0$  lattice parameters with observables: physical scale by  $R_0$  (1/403 MeV),  $m_\rho$  (770 MeV),  $\sqrt{\sigma}$  (440 MeV) (2 $\times$ 220 independent configurations on  $10^3 \cdot 16$  lattices)

- separate the crossover and the 1<sup>st</sup> order PT  $V \rightarrow \infty$  limit of  $\text{Im}(\beta_0)$  as a function of  $\mu$



small  $\mu$ :  $\text{Im}(\beta_0^\infty)$  inconsistent with 0  $\Rightarrow$  crossover

increasing  $\mu$ :  $\text{Im}(\beta_0^\infty)$  decreases  $\Rightarrow$

transition becomes consistent with a 1<sup>st</sup> order PT

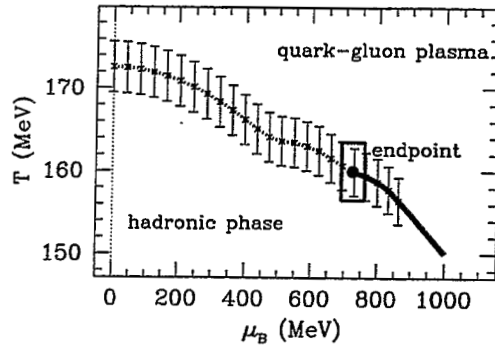
errors decrease close to E, and  $\text{Im}(\beta_0^\infty)$  slightly overshoots:  
known effects of the Lee-Yang technique for relatively small V-s

endpoint chemical potential:  $\mu_{end} = 0.375(20)$

- phase diagram in physical units  
results at  $T=0$  with  $R_0 \cdot m_\pi = 0.73(6)$  (twice too much)

$\beta$	$m_\pi$	$m_\rho$	$R_0$	$\sqrt{\sigma}$
5.208	0.393(2)	1.22(2)	1.87(3)	0.58(7)
5.164	0.393(2)	1.28(3)	1.76(5)	0.75(5)

- $T$  as a function of the baryonic chemical potential  $\mu_B$



- lattice result for QCD with  $n_f=2+1$  fermions and  $L_t = 4$

endpoint:  $T_E = 160 \pm 3.5$  MeV,  $\mu_E = 725 \pm 35$  MeV  
at  $\mu_B=0$  transition temperature:  $T_c = 172 \pm 3$  MeV.

### Summary, outlook

- critical endpoint in the  $\mu$ - $T$  plane: unambiguous, non-perturbative prediction of the QCD Lagrangian  $\Rightarrow$  important experimental consequences for heavy ion collisions
- lattice QCD at finite  $\mu$  is an old, unsolved problem  
new method: overlap ensuring multi-parameter reweighting  
presumably good enough to locate the above endpoint  
(though, can not describe the color superconducting phase)
- overlap ensuring multi-parameter reweighting:  
standard importance sampling with reweighting in  $\beta$  and  $\mu$   
maps transition configurations to transition ones  
(or hadronic/QGP configurations to hadronic/QGP ones)
- can be applied to any number of Wilson or staggered quarks  
analytic expression for the determinants for any  $\mu$

- direct test for  $n_f=4$  dynamical QCD at imaginary  $\mu$   
our method: complete agreement with direct results  
Glasgow method: premature onset, “fake” transitions
- $T=0$  and  $T\neq 0$  simulations in QCD with  $n_f=2+1$  quarks  
infinite volume behavior of the Lee-Yang zeros  
tells the difference between a 1<sup>st</sup> order PT and a crossover

endpoint:  $T_E = 160 \pm 3.5$  MeV,  $\mu_E = 725 \pm 35$  MeV  
at  $\mu_B=0$  transition temperature:  $T_c = 172 \pm 3$  MeV.

- future plans: approaching the chiral and continuum limits

for our  $m_{ud}$  production and reweighting need similar CPU-times  
for physical masses reweighting in  $\mu$  is subdominant  
evaluating determinants/eigenvalues  $\propto L_s^9$   
configuration production is at least  $\propto L_s^9$   
 $\Rightarrow$  reweighting in  $\mu$  remains subdominant



# The Detailed Analysis of the Three-Quark Potential $V_{3Q}$ in SU(3) Lattice QCD

T. T. Takahashi, RCNP Osaka University  
March 28, 2002

for  
Baryon Dynamics at RHIC Workshop  
RIKEN BNL Research Center

# The Detailed Analysis of the Three-Quark Potential $V_{3Q}$ in SU(3) Lattice QCD

T. T. Takahashi (RCNP Osaka Univ.)  
 H. Suganuma (Tokyo Inst. of Technology)  
 Y. Nemoto (RIKEN BNL)  
 H. Matsufuru (YITP Kyoto Univ.)

- Phys.Rev.Lett. **86** 18-21 (2001)
- Proc. of the Int. Symp. on “Dynamics of Gauge Fields”, Tokyo, Dec. 13-15, 1999, (Universal Academy Press, 179-180, 2000)
- Nucl.Phys. **A680** 159-162 (2000)
- Proc. of Int. Symp. on “Hadrons and Nuclei”, Seoul, Korea, Feb. 20-22, 2001. (AIP Conference Proceedings **CP594**, 341-348, 2001)

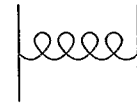
## Theoretical consideration(1)

### *Theoretical Consideration*

- short distance -

Coulomb type due to one-gluon-exchange

$$- \sum_{i < j} \frac{A_{3Q}}{|r_i - r_j|}$$

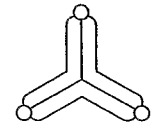


- long distance -

Three-body force proportional to the length of flux

$$\sigma_{3Q} L$$

(L: length of flux)

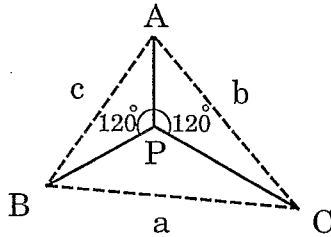


+ Constant term

## Theoretical consideration(2)

$$V_{3Q} = - \sum_{i < j} \frac{A_{3Q}}{|r_i - r_j|} + \sigma_{3Q} L_{\min} + C_{3Q}$$

- Minimal linking length -

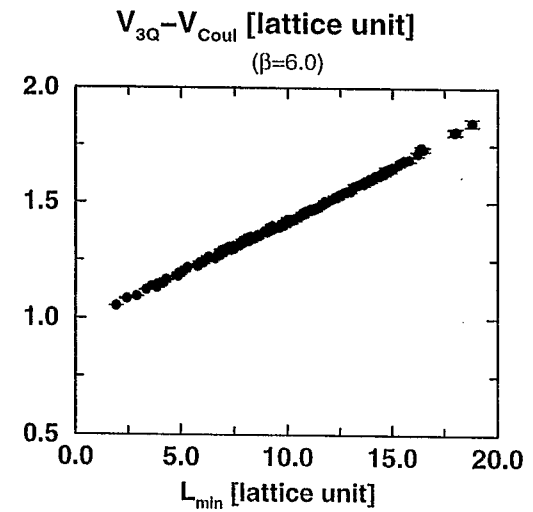
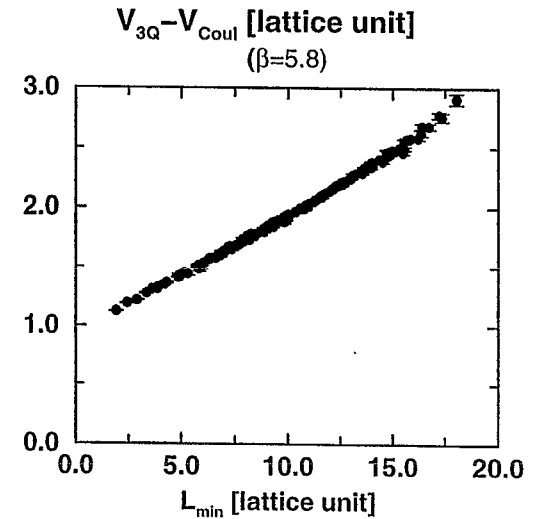


$$\begin{aligned} L_{\min} &= \overline{AP} + \overline{BP} + \overline{CP} \\ &= \left( \frac{1}{2}(a^2 + b^2 + c^2) + \frac{\sqrt{3}}{2} \sqrt{(-a+b+c)(a-b+c)(a+b-c)(a+b+c)} \right)^{1/2} \end{aligned}$$

Direct calculation of 3Q Potential  
in lattice QCD

→ Comparison with the theoretical form

## Y-ansatz plot ( $V_{3Q} - V_{\text{Coul}}$ as a func. of $L_{\min}$ )



$\beta = 5.7$  (lattice unit  $a \simeq 0.19$  fm)

	$\sigma$	$A$	$C$	$\chi^2/N_{DF}$
$3Q_Y$	0.1524(28)	0.1331( 66)	0.9182(213)	3.76
$3Q_Y$ (Latt. Coul.)	0.1556(24)	0.1185( 53)	0.8876(179)	1.81
$Q\bar{Q}$ (on-axis)	0.1629(47)	0.2793(116)	0.6203(161)	0.59
$Q\bar{Q}$ (on-axis, Latt. Coul.)	0.1603(48)	0.2627(109)	0.6271(165)	0.51
$Q\bar{Q}$ (off-axis, Latt. Coul.)	0.1611(18)	0.2780( 44)	0.6430( 63)	3.57

$\beta = 5.8$  (lattice unit  $a \simeq 0.14$  fm)

	$\sigma$	$A$	$C$	$\chi^2/N_{DF}$
$3Q_Y$	0.1027( 6)	0.1230( 20)	0.9085( 55)	5.03
$3Q_Y$ (Latt. Coul.)	0.1031( 6)	0.1141( 18)	0.8999( 54)	4.29
$Q\bar{Q}$ (on-axis)	0.1079(28)	0.2607(174)	0.6115(197)	0.92
$Q\bar{Q}$ (on-axis, Latt. Coul.)	0.1080(28)	0.2377(159)	0.6074(194)	0.76
$Q\bar{Q}$ (off-axis, Latt. Coul.)	0.1018(11)	0.2795( 51)	0.6596( 53)	1.28

$\beta = 6.0$  (lattice unit  $a \simeq 0.1$  fm)

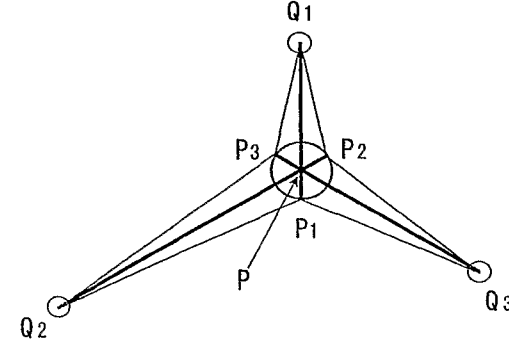
	$\sigma$	$A$	$C$	$\chi^2/N_{DF}$
$3Q_Y$	0.0460( 4)	0.1366( 11)	0.9599( 35)	2.81
$3Q_Y$ (Latt. Coul.)	0.0467( 4)	0.1256( 10)	0.9467( 34)	2.22
$Q\bar{Q}$ (on-axis)	0.0506( 7)	0.2768( 24)	0.6374( 30)	3.56
$Q\bar{Q}$ (on-axis, Latt. Coul.)	0.0500( 7)	0.2557( 22)	0.6373( 30)	1.22
$Q\bar{Q}$ (off-axis, Latt. Coul.)	0.0497( 5)	0.2572( 15)	0.6389( 20)	1.59

- universality of string tension  $\sigma_{Q\bar{Q}} \simeq \sigma_{3Q}$
- consistency with P-QCD  $A_{Q\bar{Q}} \simeq 2A_{3Q}$

(Latt. Coul.) means that the fitting is done with lattice Coulomb potential which contains the lattice discretization effect in the short range.

## Generalized Y-ansatz(2)

The generalized Y-ansatz is defined as follows, which however needs one more parameter corresponding to the flux core radius.



$$L_{\min}^{\text{general}} \equiv \frac{1}{2} (\overline{Q_1 P_3} + \overline{P_3 Q_2} + \overline{Q_2 P_1} + \overline{P_1 Q_3} + \overline{Q_3 P_2} + \overline{P_2 Q_1})$$

(On detailed definition, please read hep-lat.xxx)

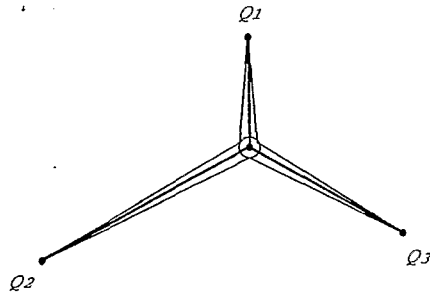


### Generalized Y-ansatz(3)

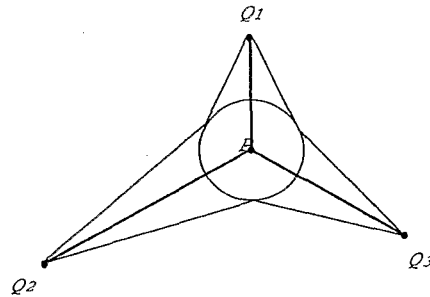
This ansatz has two asymptotic form:

Y-ansatz( $R_{\text{core}} = 0$ ) and

$\Delta$ -ansatz( $R_{\text{core}} = \infty$ )



small  $R_{\text{core}}$   
Y-ansatz like



large  $R_{\text{core}}$   
 $\Delta$ -ansatz like

We fit the 3Q potential by the form

$$V_{3Q} = - \sum_{i < j} \frac{A_{3Q}}{|r_i - r_j|} + \sigma_{3Q} L_{\text{min}}^{\text{general}}(r_1, r_2, r_3; R_{\text{core}}) + C_{3Q}$$

### Generalized Y-ansatz(4)

$\beta$	$\sigma$	$A$	$C$	$R_{\text{core}}$	$\chi^2/N_{DF}$
5.8	$0.98\sigma_{Q\bar{Q}}$	$0.1354(18)$	$0.9569(53)$	0.08 fm	2.63
6.0	$0.95\sigma_{Q\bar{Q}}$	$0.1451(11)$	$0.9837(33)$	0.08 fm	1.23

- We observe the best fitting with  $R_{\text{core}} \simeq 0.1\text{fm}$ , which is independent of  $\beta$  or lattice spacing.

The radius of the flux-core estimated in this analysis is rather small, and therefore we can see that in the hadronic scale ( $r \gg 0.1\text{fm}$ ) Y-ansatz is more preferable than  $\Delta$ -ansatz.

## Summary and Concluding Remarks

We have carried out the detailed analysis of 3Q potential  $V_{3Q}$  with the smearing technique using SU(3) lattice QCD at quenched level. For more than 300 patterns of the 3Q system, we have measured  $V_{3Q}$ .  $V_{3Q}$  is well described with Y-ansatz as

$$V_{3Q} = - \sum_{i < j} \frac{A_{3Q}}{|r_i - r_j|} + \sigma_{3Q} L_{\min} + C_{3Q}$$

18  $L_{\min}$ : minimal linking length for 3 quarks

Here, we have observed two remarkable features.

- universality of string tension  $\sigma_{3Q} \simeq \sigma_{Q\bar{Q}}$
- consistency with P-QCD  $A_{Q\bar{Q}} \sim \frac{1}{2} A_{3Q}$

The static three-quark (3Q) potential is studied in detail using SU(3) lattice QCD with  $12^3 \times 24$  at  $\beta = 5.7$  and  $16^3 \times 32$  at  $\beta = 5.8, 6.0$  at the quenched level. For more than 300 different patterns of the 3Q systems, we perform the accurate measurement of the 3Q Wilson loop with the smearing method, which reduces excited-state contaminations, and present the lattice QCD data of the 3Q ground-state potential  $V_{3Q}$ . We perform the detailed fit analysis on  $V_{3Q}$  in terms of the Y-ansatz both with the continuum Coulomb potential and with the lattice Coulomb potential, and find that the lattice QCD data of the 3Q potential  $V_{3Q}$  are well reproduced within a few % deviation by the sum of a constant, the two-body Coulomb term and the three-body linear confinement term  $\sigma_{3Q} L_{\min}$ , with  $L_{\min}$  the minimal value of the total length of color flux tubes linking the three quarks. From the comparison with the  $Q\bar{Q}$  potential, we find a universality of the string tension as  $\sigma_{3Q} \simeq \sigma_{Q\bar{Q}}$  and the one-gluon-exchange result for the Coulomb coefficients as  $A_{3Q} \simeq \frac{1}{2} A_{Q\bar{Q}}$ . We investigate also the several fit analyses with the various ansätze: the Y-ansatz with the Yukawa potential, the  $\Delta$ -ansatz and a more general ansatz including the Y and the  $\Delta$  ansätze in some limits. All these fit analyses support the Y-ansatz on the confinement part in the 3Q potential  $V_{3Q}$ , although  $V_{3Q}$  seems to be approximated by the  $\Delta$ -ansatz with  $\sigma_{\Delta} \simeq 0.53\sigma$ .

# The groundstate of 3 static quarks

**Philippe de Forcrand**

**ETH Zürich and CERN**

**with**

**Constantia Alexandrou and Antonis Tsapalis**

**Univ. Cyprus**

**Univ. Athens**

**hep-lat/0107006, hep-lat/0110115,  
nucl-th/0111046**

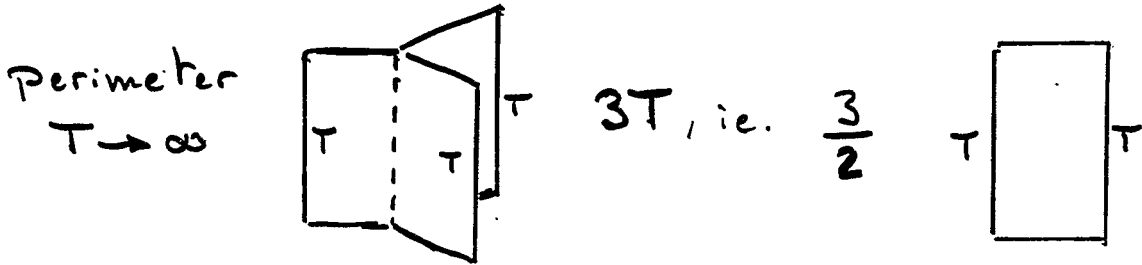
Riken-BNL, March 28, 2002

– Typeset by Foil $\TeX$  –

The baryonic potential.

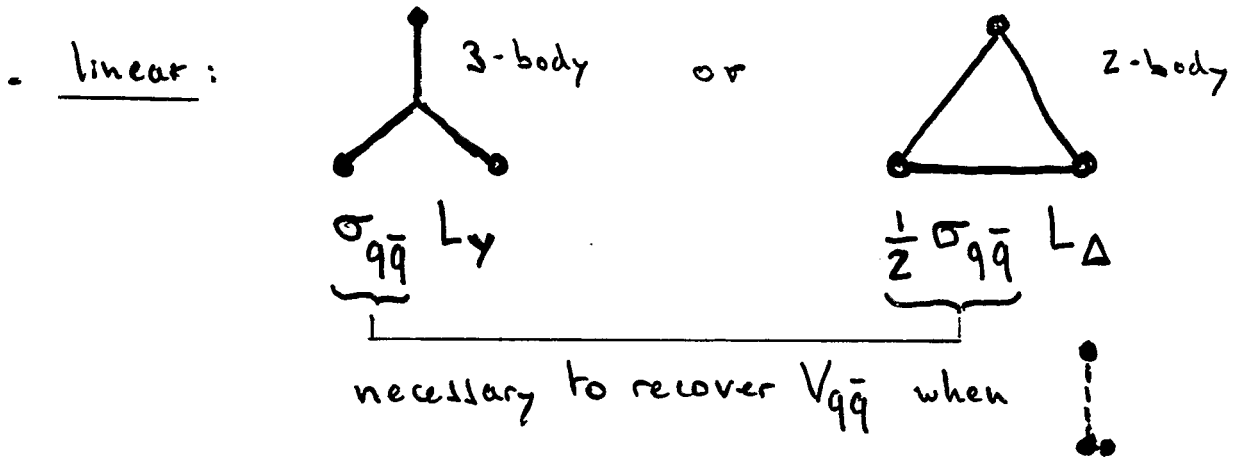
$V_{qqq} = \text{Constant} + \text{Coulomb} + \text{linear}$

- constant  $V_0$ : comes from perimeter term  
 $\langle W \rangle \sim e^{-T(V_0 + \dots)}$



$V_{qqq} = \frac{3}{2} V_{q\bar{q}}$  not to be fitted

- Coulomb: perturbative  $\frac{1}{2} \sum_{i < j} \frac{\alpha}{r_{ij}}$  not to be fitted



No tunable parameters:

$$V_{qqq} = \underbrace{\frac{1}{2} \sum_{i < j} V_{q\bar{q}}(r_i, r_j)}_{\Delta\text{-ansatz}} + \underbrace{\sigma_{q\bar{q}} \left( L_Y - \frac{L_\Delta}{2} \right)}_{Y\text{-ansatz}}$$

# Motivation for Y-law:

## Abelian monopoles

• Abelian projection:  $SU(3) \rightarrow U(1)^2$

ie.  $\begin{pmatrix} e^{i\theta_1} & & \\ & e^{i\theta_2} & \\ & & e^{i\theta_3} \end{pmatrix}, \theta_1 + \theta_2 + \theta_3 = 0 \pmod{2\pi}$

• Dual superconductivity:

3 Higgs fields  $\rightarrow$  Abrikosov flux strings of 3 types



Phase of Higgs field rotates by  $2\pi$  around string

$U(1)^2 \Rightarrow$  constraint:  $\sum_3 \text{Phases of Higgs} = 0 \pmod{2\pi}$

Forces strings to come in pairs:

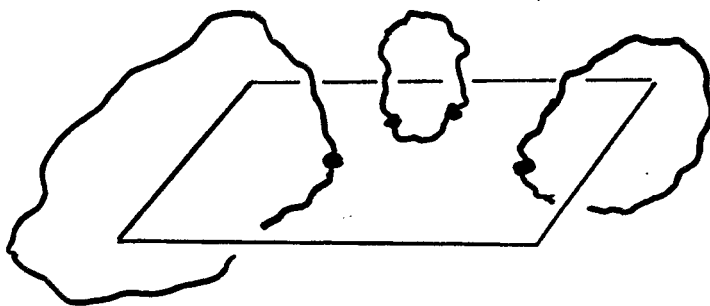


Minimal action (classical)

$\rightarrow$  M is Steiner point  
(minimal length  $L_Y$ )

Center vortices

\* qq: Assume Wilson loop is determined by center vortices piercing it (Mack & Pethoua; 't Hooft)



eg.  $SU(2)$ :  $W \approx (-1)^{\# \text{c.v.}}$

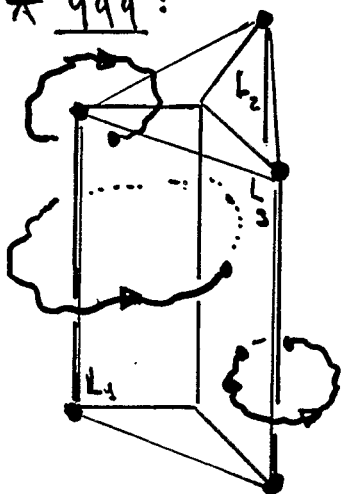
Assume random locations with density  $\rho$

$$\rightarrow \langle W(A) \rangle = \lim_{a \rightarrow 0} (-\rho a^2 + (1 - \rho a^2))^{A/a^2} = e^{-\sigma A}$$

$A$  is minimal area

area law  
 $\sigma = 2\rho$

\* qqq:



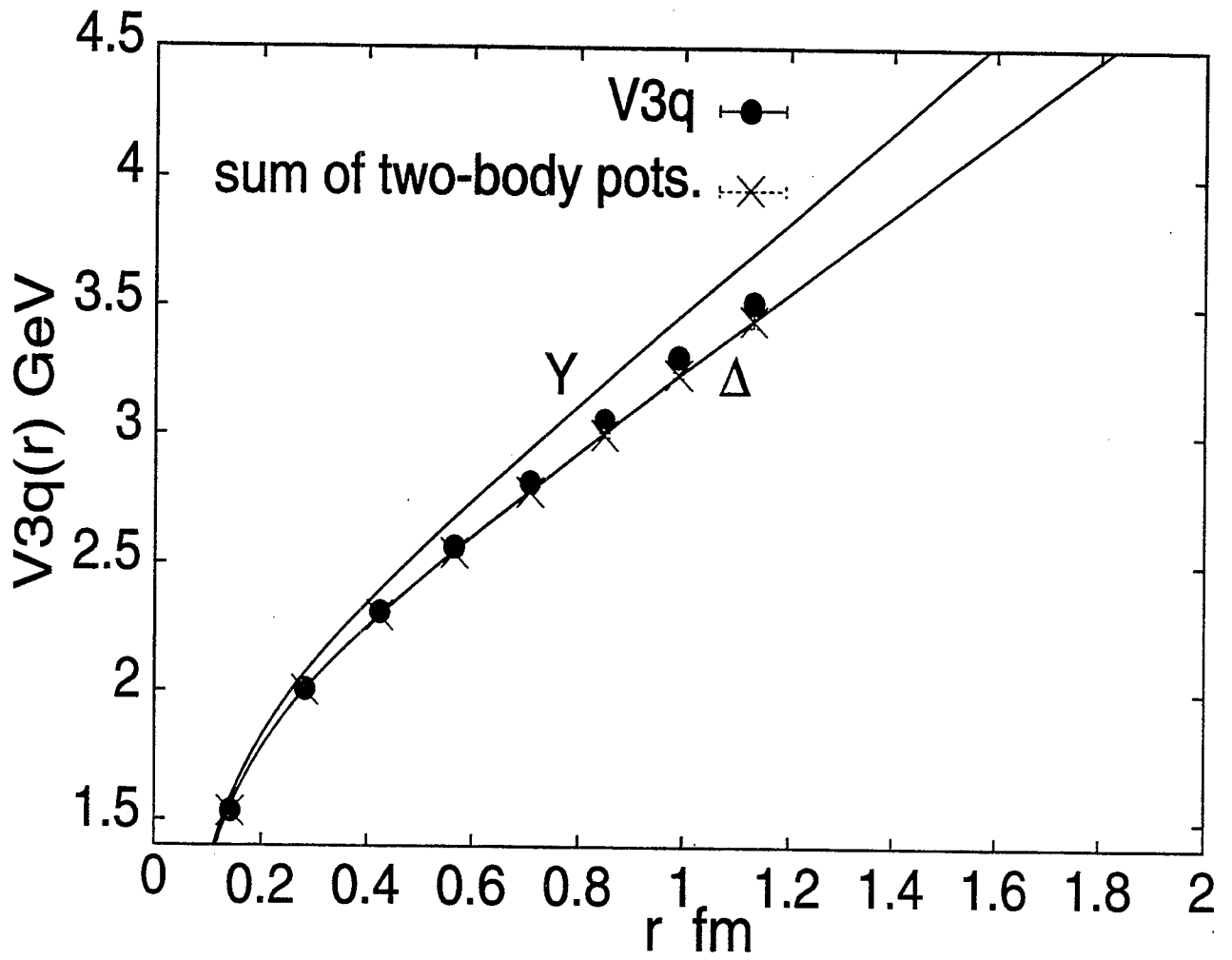
$$W_{qqq} \approx e^{i \frac{2\pi}{3} (L_1 + L_2 + L_3)}$$

does not depend on location of junction

$L_i = \pm 1 \Rightarrow$  must pierce two sides of prism

$$\rightarrow \langle W_{qqq} \rangle = e^{-\frac{1}{2} A \sigma}$$

$\downarrow$   
 $\Delta$   
 $\downarrow$   
 area of prism



$$\beta = 6.0$$

## - Conclusions -

- $\Upsilon$  vs  $\Delta$  is technically difficult:  
careful with systematic errors
- Up to  $\sim 0.8$  fm: strong evidence for  $\Delta$   
ie.  $V_{qqq} \approx \frac{1}{2} \sum_3 V_{q\bar{q}}$
- Larger distances?
  - some 3-body potential?
  - circumstantial evidence favors  $\Delta$  over  $\Upsilon$ 
    - loop measurements  $SU(3)$  &  $SU(4)$
    - variational basis
    - wave function
- Great testing ground for vacuum description:
  - dual superconductor & Abelian monopoles  $\rightarrow \Upsilon$
  - center vortices  $\rightarrow \Delta$



High-Baryon

Density

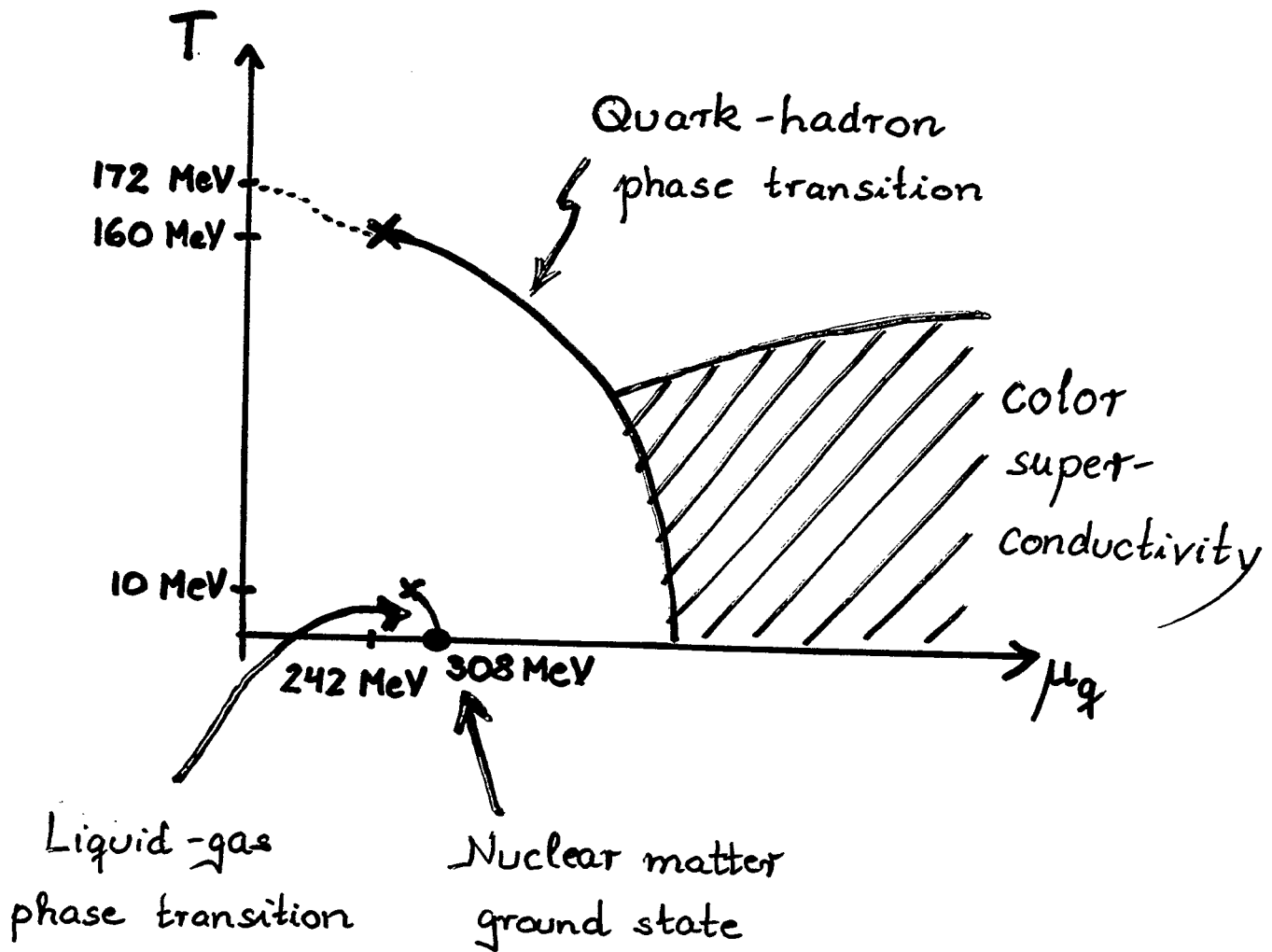
QCD matter

Dirk H. Rischke

Institut f. Theoretische Physik

Universität Frankfurt/Main

# Phase diagram of QCD matter:



## BCS theory:

$$T_c(\mu) \approx 0.57 \phi(T=0, \mu)$$

transition  
temperature  
to normal-conducting  
phase

superconducting gap  
at zero temperature

The same relation holds in QCD!  
(to leading order in weak-coupling limit)

R.D. Pisarski, D.H.R., PRD 61, 051501, 074017 (2000)

⇒ - Compute  $\phi(T=0, \mu)$ .

- Start at  $\mu \lesssim \infty$ , where  $g(\mu) \ll 1$  (due to asymptotic freedom).
- Weak-coupling limit allows for controlled approximations.

# ⇒ QCD gap equation (schematically):

On quasiparticle mass shell,  $\Phi_k^+ \equiv \Phi^+(\epsilon_k, \vec{k})$ :

almost static  
magnetic gluons  
(collinear enhance-  
ment from long-  
range interactions)

static electric  
and non-static  
magnetic gluons  
(short-range int.'s)

BCS - log  $\int \frac{dq}{\epsilon_q} \sim \ln \frac{\mu}{\phi_0}$

other stuff  
(no BCS-log)

quark self-energy

$$\Phi_k^+ = g^2 \int \frac{dq}{\epsilon_q} \Phi_q^+ \left\{ \gamma \ln \frac{\mu^2}{|\epsilon_k^2 - \epsilon_q^2|} + \beta + \beta' \epsilon_q \ln \frac{\mu}{\epsilon_q} + \alpha \epsilon_q \right\}$$

Weak-coupling solution:

$$\phi_0 = b \mu \exp\left\{-\frac{c}{g}\right\} [1 + O(g^2)]$$

$$\Rightarrow \ln \frac{\mu}{\phi_0} \sim \frac{1}{g} !$$

$$c = \frac{3\pi^2}{12}, \quad b = \frac{b_0}{g^5}, \quad b_0 \sim 1$$

D.T. Son, PRD 59, 094019 (1999)

$$b_0 = 512 \pi^4 (2/N_f)^{5/2} b'_0$$

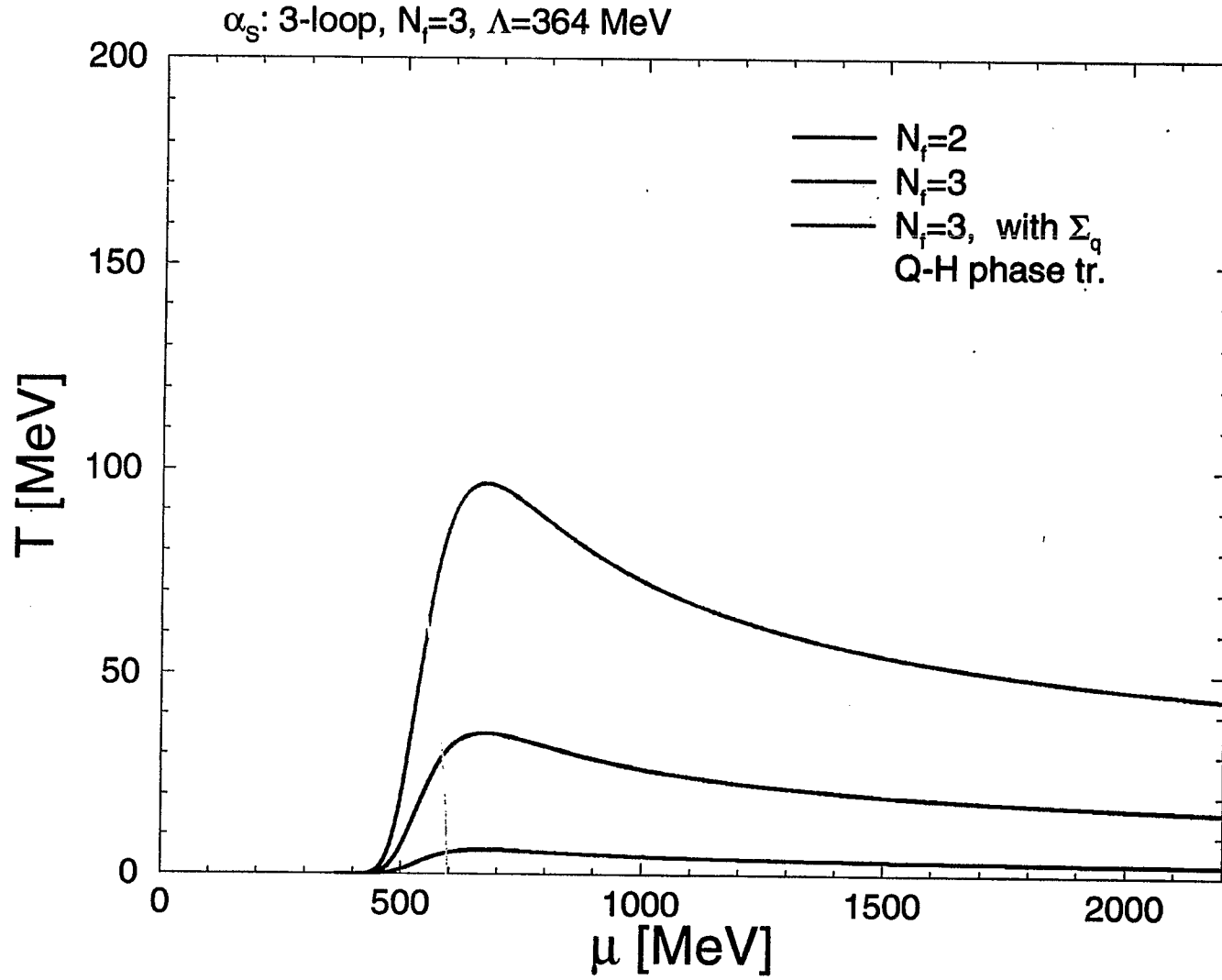
T. Schäfer, F. Wilczek, PRD 60, 114033 (1999)

R.D. Pisarski, D.H.R., PRD 61, 051501, 074017 (2000)

$$b'_0 = \exp\left(-\frac{\pi^2 + 4}{8}\right) \simeq 0.177$$

W.E. Brown, J.T. Liu, H.-C. Ren, PRD 61, 114012, P62, 054013, 054016 (2000)

Q. Wang, D.H.R. nucl-th/01100



$$T_C \simeq 0.57 \phi_{T=0}$$

as in BCS theory

R.D. Pisarski, D.H.R.,

PRD61 (2000)

051501, 074017

# Conclusions:

- At asymptotically large  $\mu$ , color-superconducting gap parameter  $\phi(T=0, \mu)$  can be reliably computed to leading and sub-leading order in  $g$ :

$$\phi = b \mu \exp\left(-\frac{c}{g}\right) [1 + O(g)]$$

- Extrapolation to  $\mu \sim 500 \text{ MeV}$  yields  $\phi \sim 20 \text{ MeV} [1 + O(g)]$

- $\Rightarrow T_c \sim 10 \text{ MeV} [1 + O(g)]$

- $\Rightarrow$  Unlikely to see diquark condensation in hot environment of RHIC.

# **Effects of Strong Color Fields on Baryon Dynamics**

**Sven Soff**

**Lawrence Berkeley**

**Laboratory**

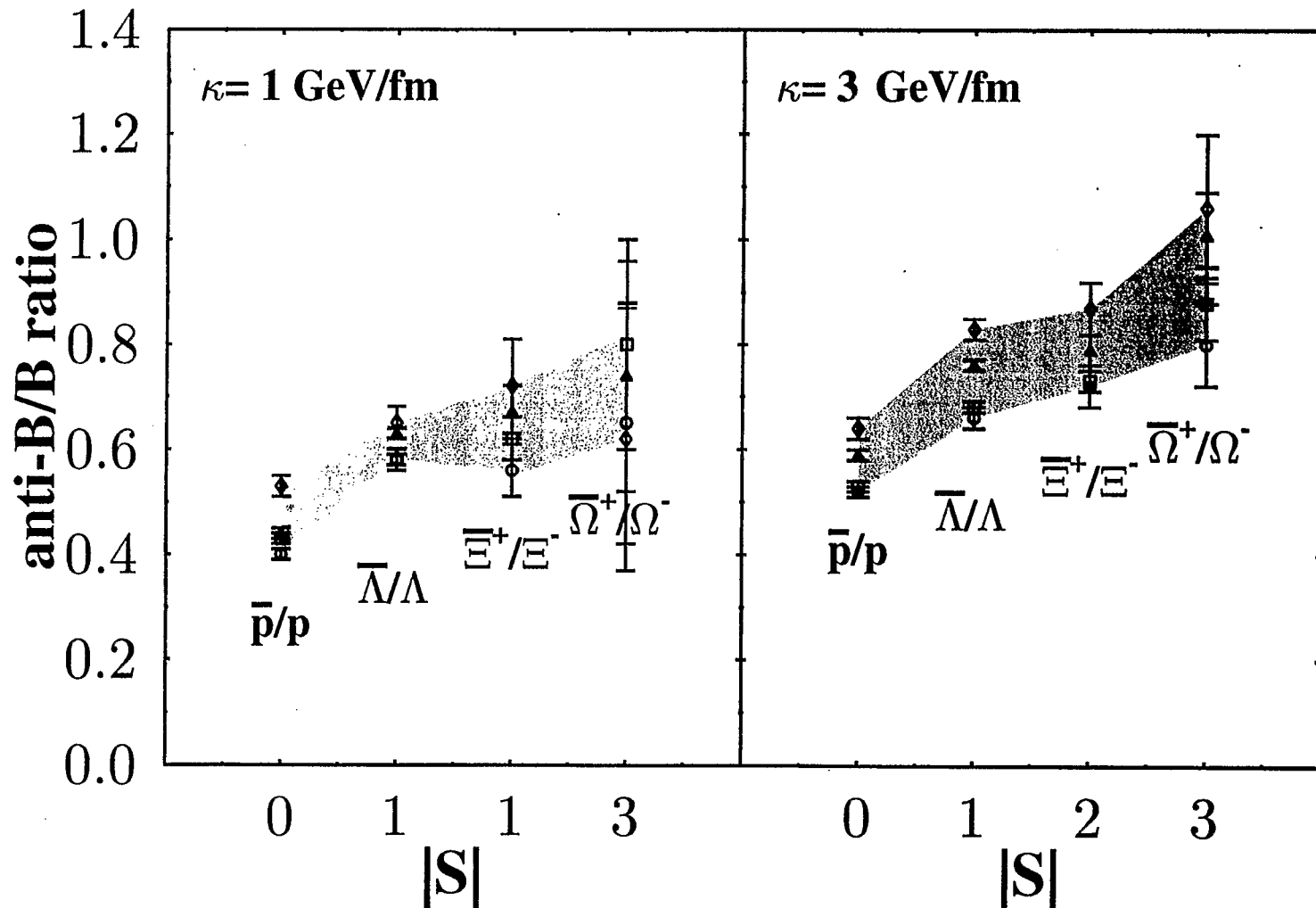
**RBRC Workshop**

**Baryon Dynamics at RHIC**

**Brookhaven, March 2002**

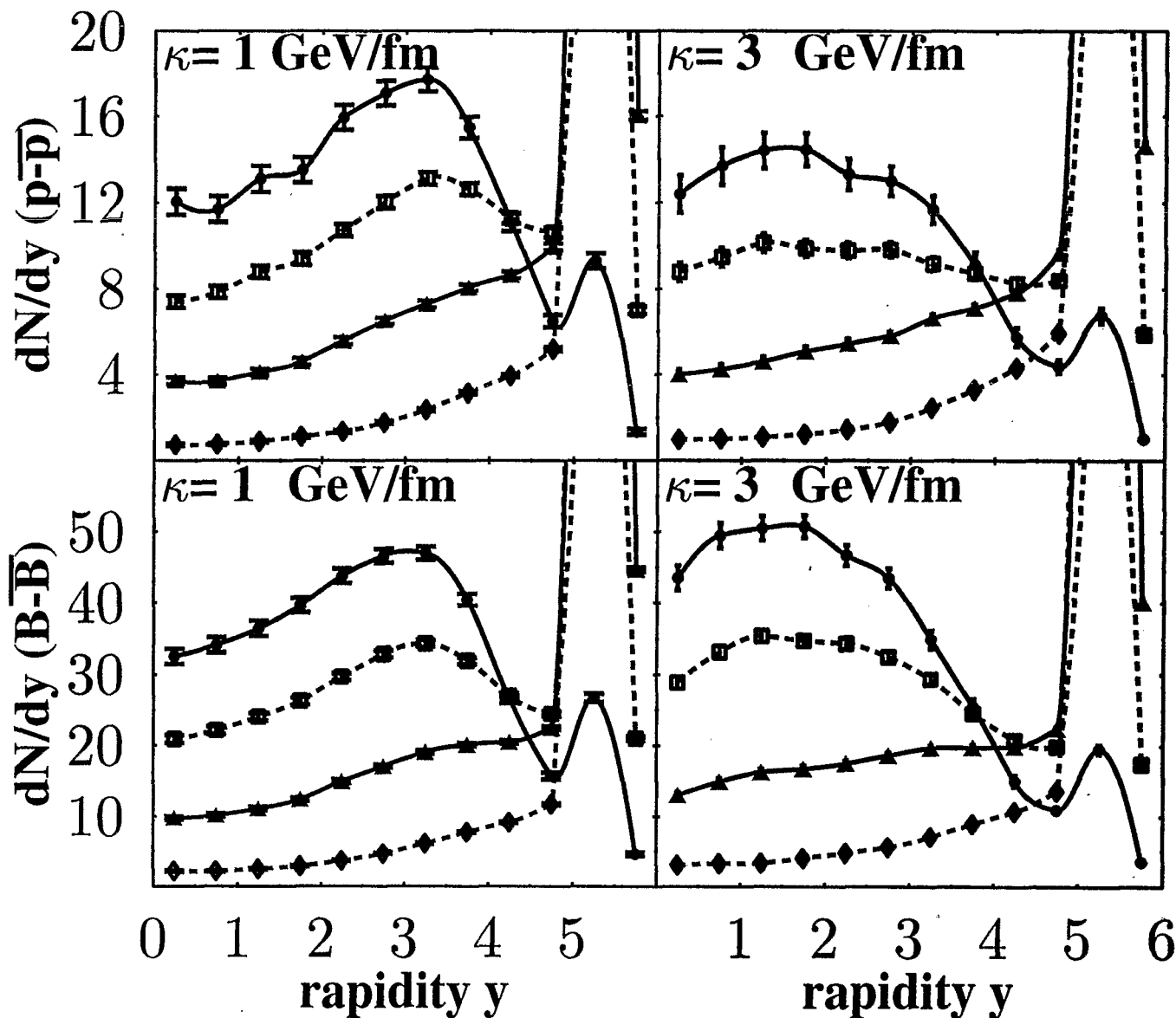
**work with H. Stöcker and Nu Xu**

# $\bar{B}/B$ Ratios @ RHIC





# Net-protons and Net-baryons



# Conclusions

---

- ⇒ Strong color fields (SCF), motivated from studies of strangeness and  $\bar{p}$  production, have large effects on the baryon dynamics
- ⇒ SCF increase the  $\bar{B}/B$  ratios
- ⇒ SCF increase strange quark and diquark pair production, reduce formation times
- ⇒ SCF modify netproton and netbaryon distributions
- ⇒ maximum shifted towards midrapidity; netbaryon number increased at midrapidity → *stopping* accompanied by conversion of netprotons into hyperon sector
- ⇒ SCF is alternative or supplementary mechanism to *junction* picture

AntiBaryon/Baryon vs. Rapidity:

Results from BRAHMS

I. G. Bearden, Niels Bohr Institute

March 28, 2002

for

Baryon Dynamics at RHIC Workshop

RIKEN BNL Research Center

## AntiBaryon/Baryon vs Rapidity: Results from BRAHMS

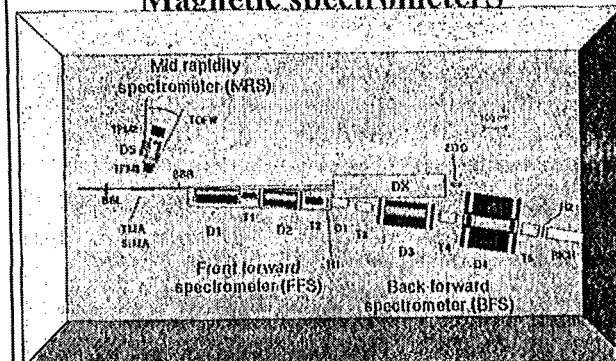
I.G. Bearden,  
Niels Bohr Institute  
for the BRAHMS collaboration

I.G. Bearden, Niels Bohr Institute

Workshop on Baryon Dynamics at RHIC  
28. Marts 2002

1

## BRAHMS: Broad Range Hadronic Magnetic spectrometers



I.G. Bearden, Niels Bohr Institute

Workshop on Baryon Dynamics at RHIC  
28. Marts 2002

3

## The BRAHMS Collaboration

I.G. Bearden<sup>1</sup>, D. Beavis<sup>1</sup>, C. Besliu<sup>10</sup>, Y. Blyakhman<sup>6</sup>, J. Brzyczczyk<sup>4</sup>, B. Budick<sup>6</sup>, H. Baggild<sup>7</sup>, C. Chasman<sup>1</sup>, C. H. Christensen<sup>7</sup>, P. Christensen<sup>7</sup>, J. Cibor<sup>1</sup>, R. Debbé<sup>1</sup>, J. J. Gaardhøje<sup>2</sup>, M. Germinario<sup>7</sup>, K. Grotowski<sup>1</sup>, K. Hagel<sup>1</sup>, O. Hansen<sup>7</sup>, A.K. Holme<sup>12</sup>, H. Ito<sup>11</sup>, E. Jacobsen<sup>2</sup>, A. Jipa<sup>10</sup>, J. I. Jordre<sup>10</sup>, F. Jundt<sup>10</sup>, C. E. Jørgensen<sup>7</sup>, T. Keutgen<sup>9</sup>, E. J. Kim<sup>6</sup>, T. Kozik<sup>3</sup>, T.M. Larsen<sup>12</sup>, J. H. Lee<sup>1</sup>, Y. K. Lee<sup>6</sup>, G. Lovhøjden<sup>2</sup>, Z. Majka<sup>3</sup>, A. Mukeev<sup>3</sup>, B. McBreen<sup>1</sup>, M. Murray<sup>3</sup>, J. Natowitz<sup>3</sup>, B.S. Nielsen<sup>7</sup>, K. Olchanski<sup>1</sup>, D. Oterdane<sup>2</sup>, R. Planetá<sup>4</sup>, F. Rami<sup>2</sup>, D. Roehrich<sup>2</sup>, B. H. Samsel<sup>12</sup>, S. J. Sanders<sup>11</sup>, I. S. Sgura<sup>10</sup>, R.A. Sheetz<sup>1</sup>, Z. Sosin<sup>1</sup>, P. Staszek<sup>7</sup>, T.S. Tveter<sup>12</sup>, F. Videbæk<sup>1</sup>, R. Wada<sup>9</sup> and A. Wieloch<sup>1</sup>

<sup>1</sup>Brookhaven National Laboratory, USA; <sup>2</sup>IRIS and Université Louis Pasteur, Strasbourg, France; <sup>3</sup>Jagiellonian University, Cracow, Poland; <sup>4</sup>Institute of Nuclear Physics, Cracow, Poland;

<sup>5</sup>Johns Hopkins University, USA <sup>6</sup>New York University, USA;

<sup>7</sup>Niels Bohr Institute, Københavns Universitet, Danmark; <sup>8</sup>Texas A&M University, College Station, USA; <sup>9</sup>Universitet i Bergen, Norge;

<sup>10</sup>University of Bucharest, Romania; <sup>11</sup>University of Kansas, USA

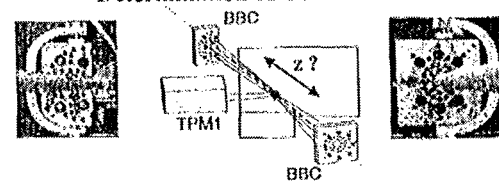
<sup>12</sup>Universitet i Oslo Norway

I.G. Bearden, Niels Bohr Institute

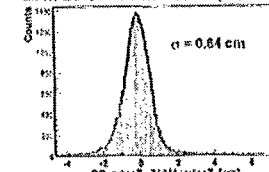
Workshop on Baryon Dynamics at RHIC  
28. Marts 2002

2

## Determination of Collision Vertex



• At in BBC measurements ( $\sigma \leq 0.7$  cm)



• Combining hits in TPM1 ( $\sigma \leq 0.2$  cm)

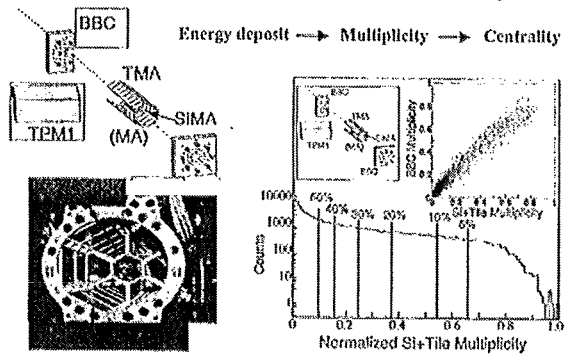
• At in ZDC measurements ( $\sigma \leq 3.5$  cm)

I.G. Bearden, Niels Bohr Institute

Workshop on Baryon Dynamics at RHIC  
28. Marts 2002

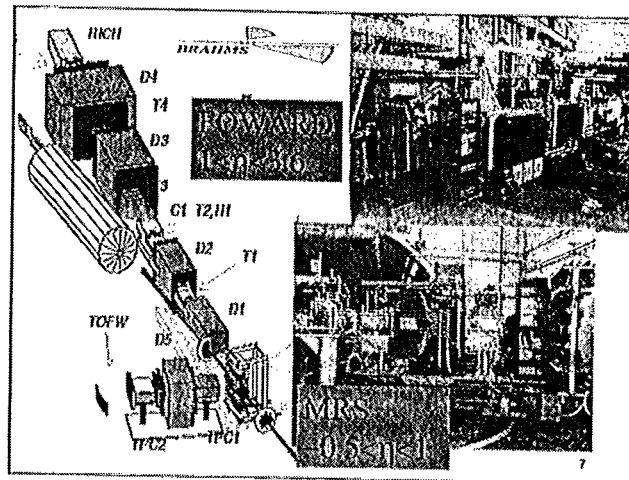
4

### Determination of Collision Centrality



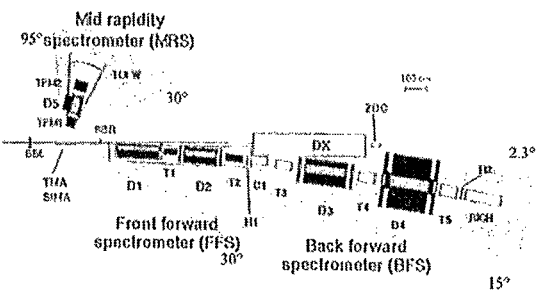
10. Bessie Nicks-Baldwin Workshop on Heavy Ion Dynamics at RHIC 25. March 2002

5



7

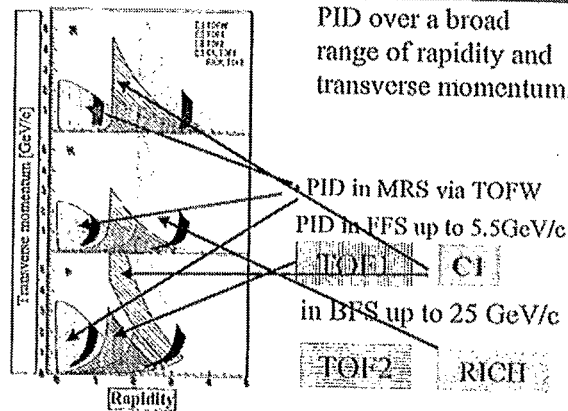
### The BRAHMS Experiment



10. Bessie Nicks-Baldwin Workshop on Heavy Ion Dynamics at RHIC 25. March 2002

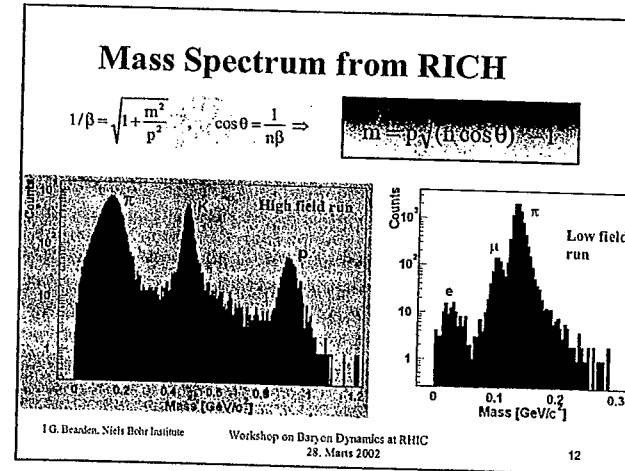
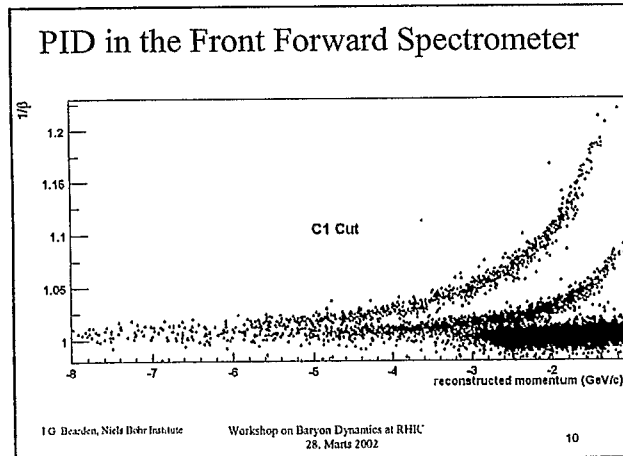
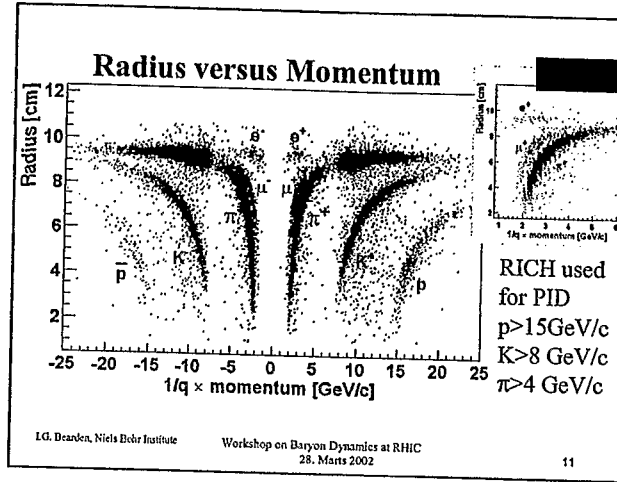
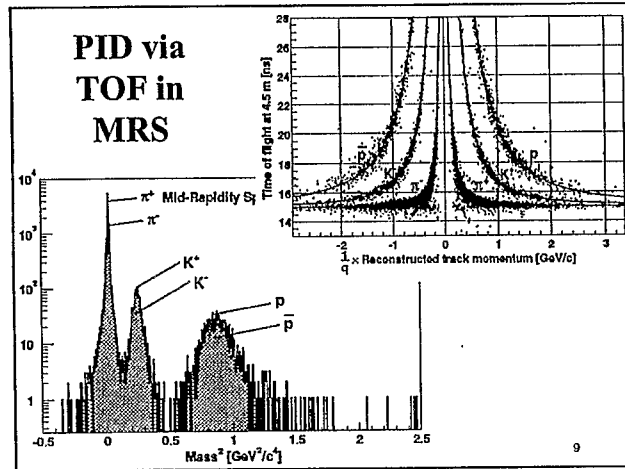
6

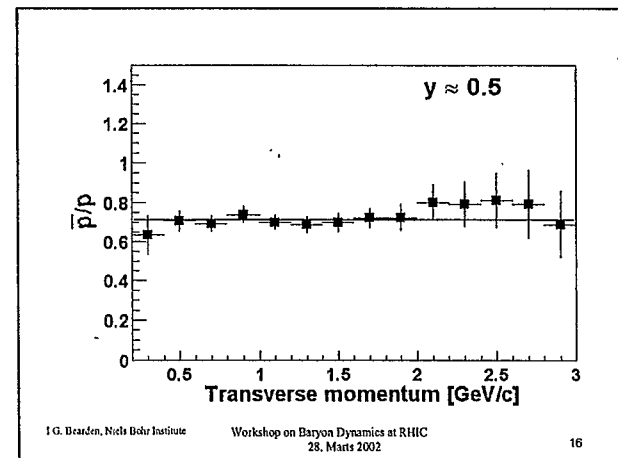
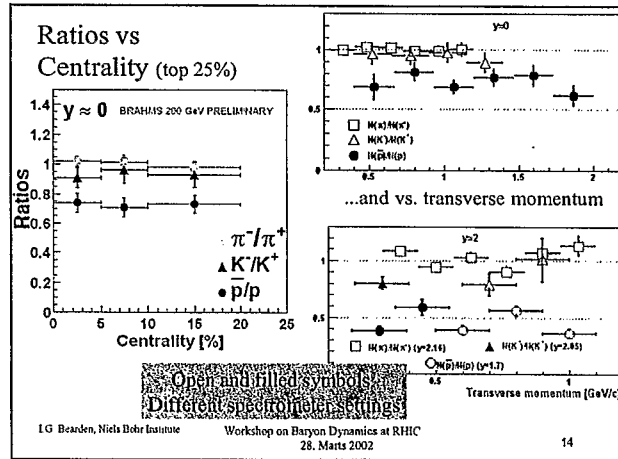
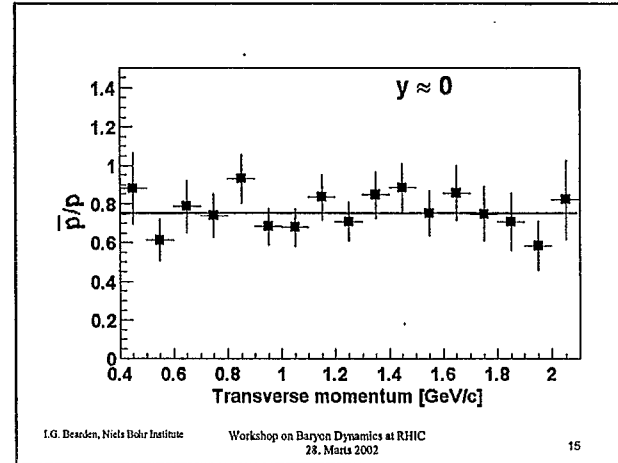
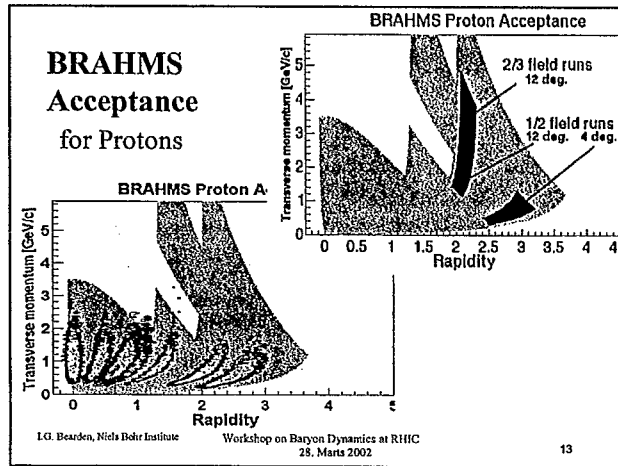
PID over a broad range of rapidity and transverse momentum.

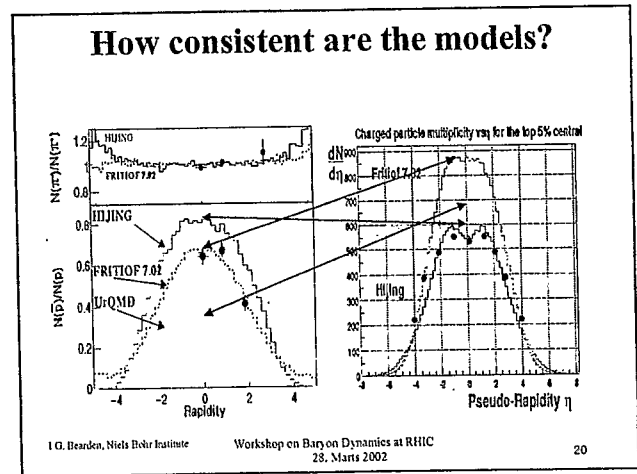
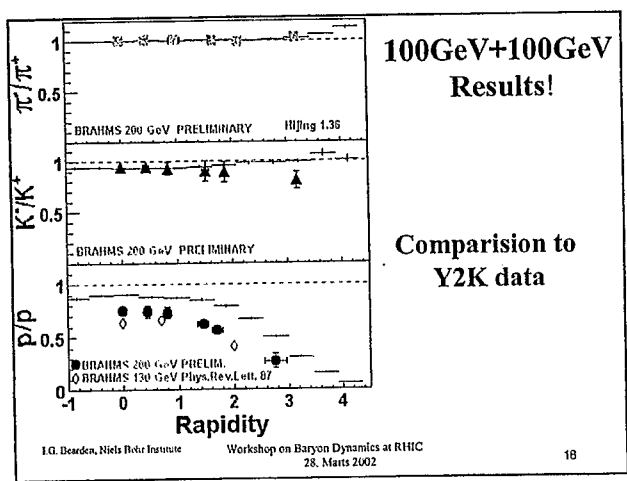
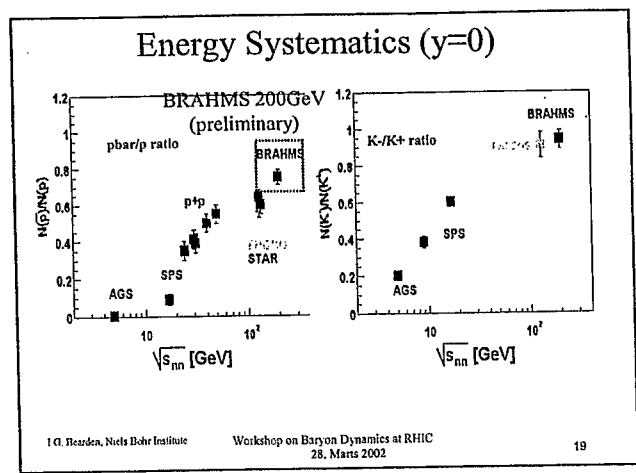
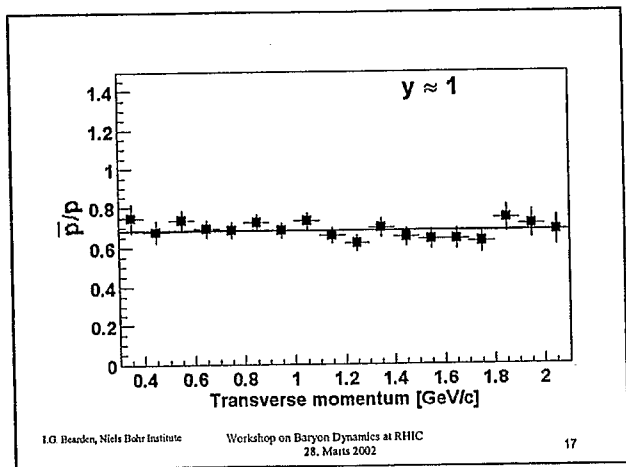


10. Bessie Nicks-Baldwin Workshop on Heavy Ion Dynamics at RHIC 25. March 2002

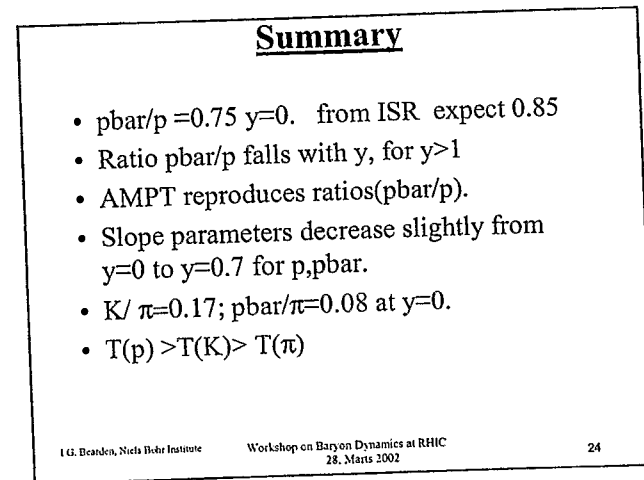
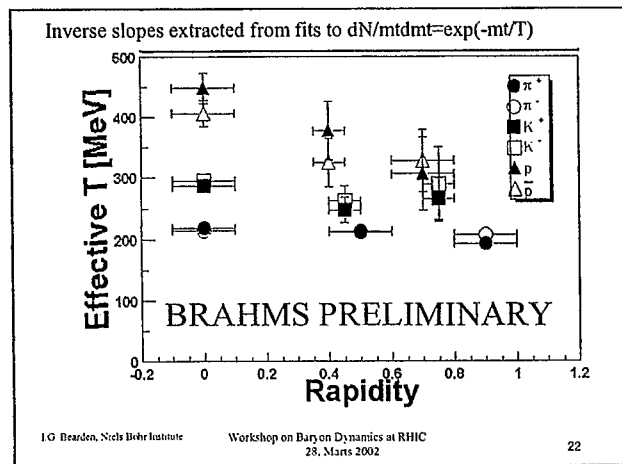
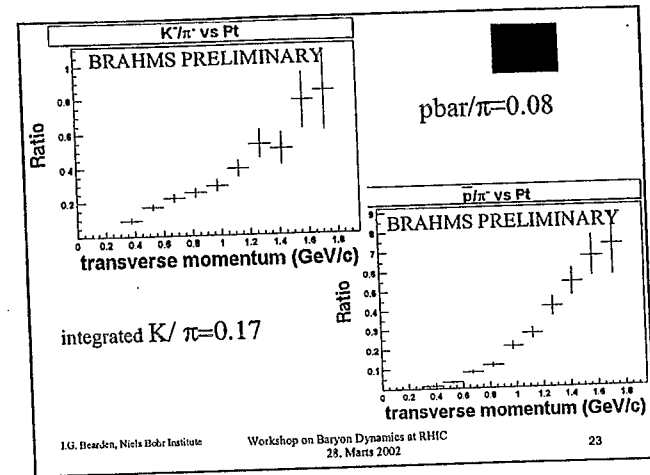
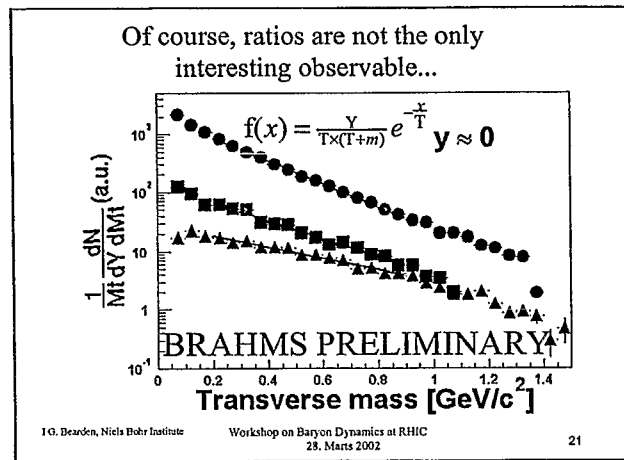
8



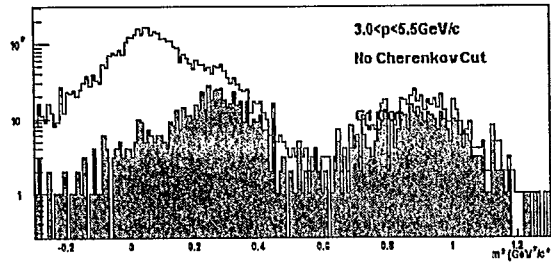




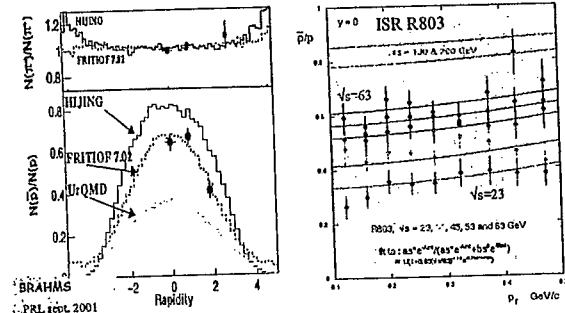




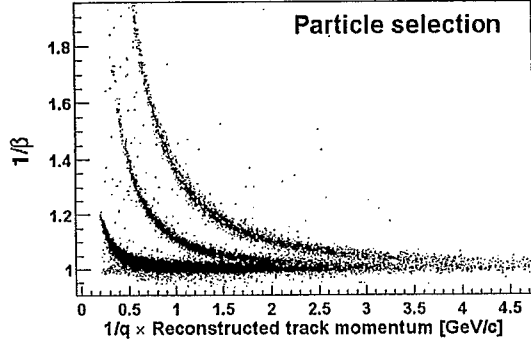
### PID in the Front Forward Spectrometer



### Bjorken limit reached for Au+Au $\sqrt{s} = 130A \text{ GeV}$ ?



### Particle selection

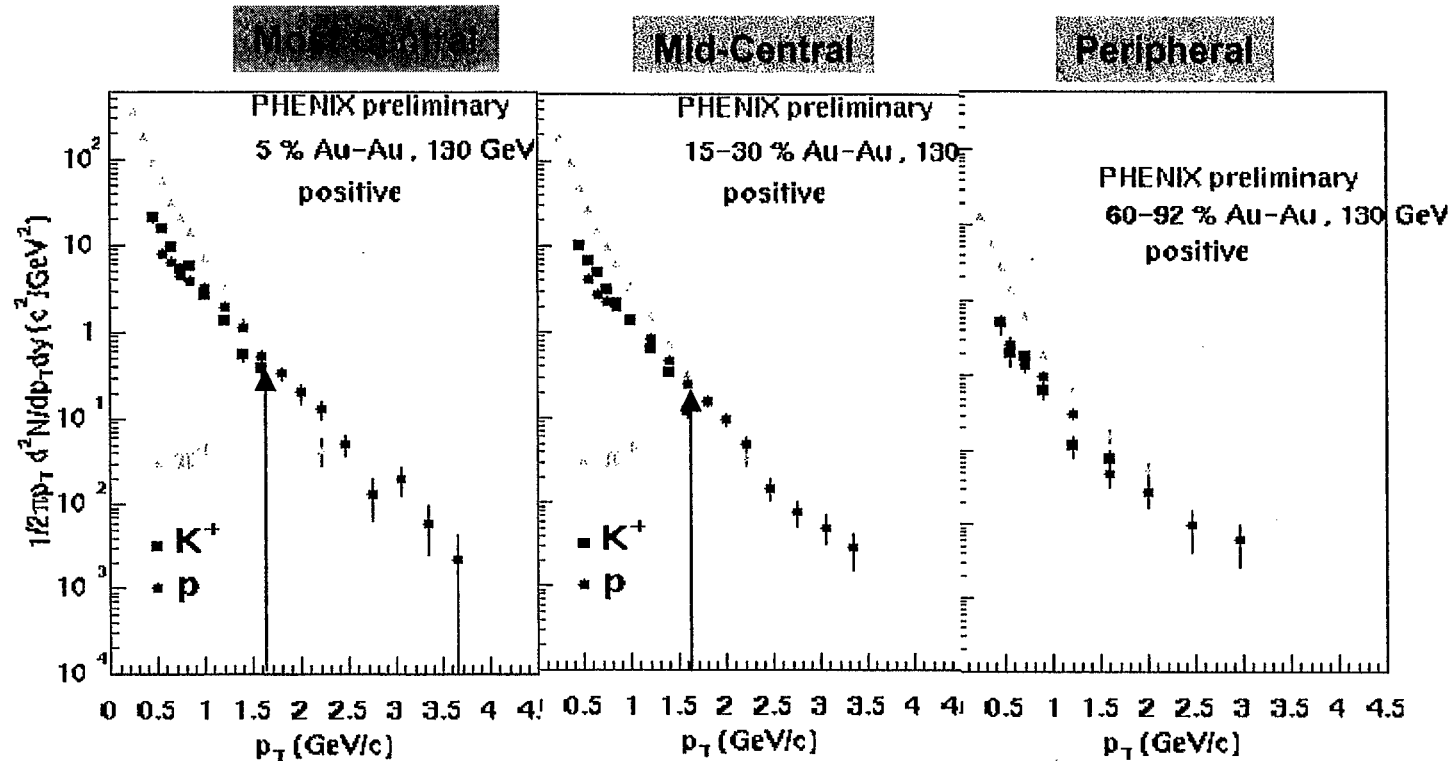


# Overview of PHENIX Results on Baryons and Identified Hadrons

Tatsuya Chujo, BNL  
March 28, 2002

for  
Baryon Dynamics at RHIC Workshop  
RIKEN BNL Research Center

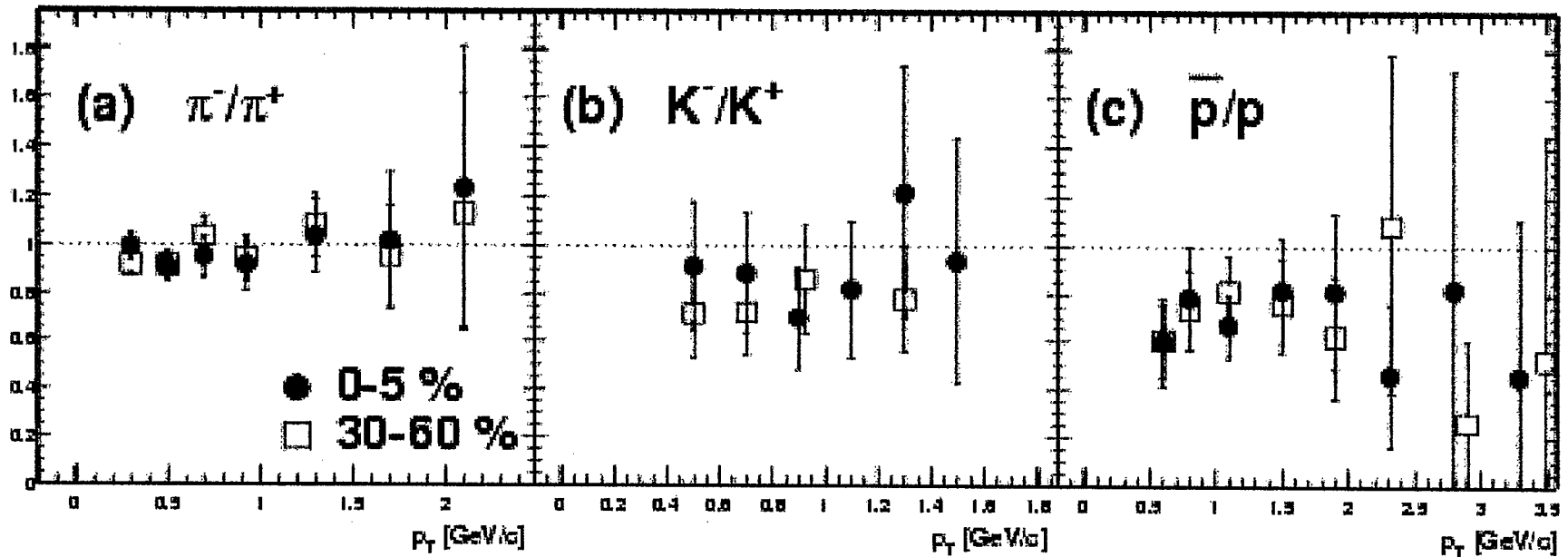
# Particle Composition @ High $p_T$



- Nucleons dominate mesons at  $\sim 1.5$ -2 GeV/c ( $\pi/p$  crossing).
- Centrality dependence of  $\pi/p$  crossing point ?
- Suppression of high  $p_T$  pions (PRL 88, 022301 (2002)) and radial flow in the protons may explain the observed crossing region in the spectra.

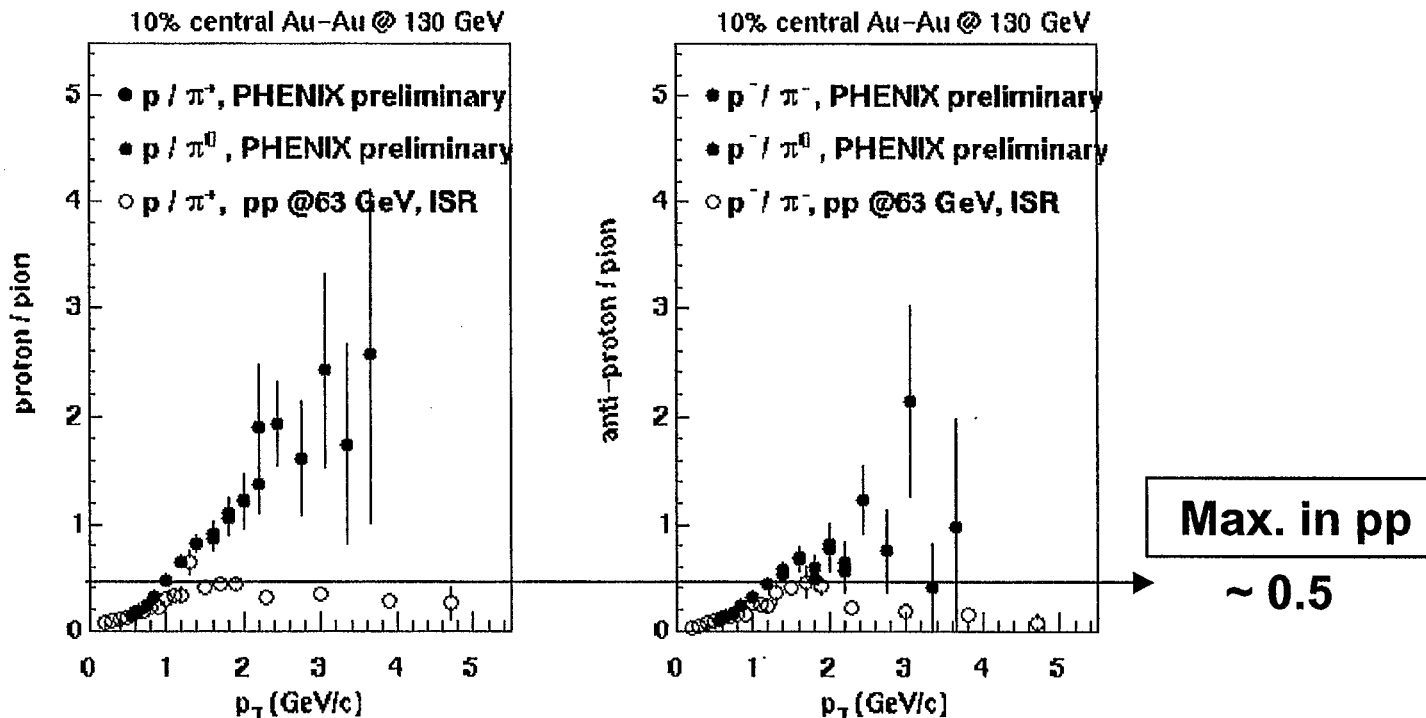
# Particle Ratio vs. $p_T$

PHENIX Preliminary



- No  $p_T$  dependence identical particle ratios in measured  $p_T$  ranges.  
 $\Rightarrow$  Consistent with the predictions of thermal model with expanding statistical system.

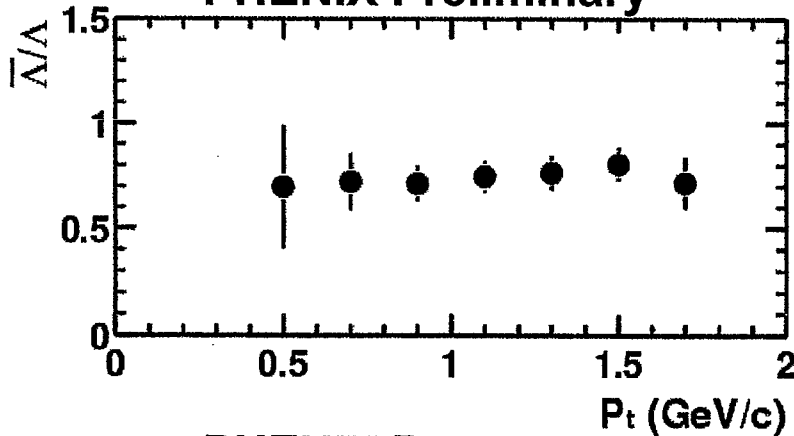
# $p/\pi$ ratio @ high $p_T$



- Used the published  $\pi^0$  results.
- Steady increase in  $p/\pi^0$  ratio with  $p_T$ , peak or saturate (?) in  $pbar/\pi^0$  ratio  $\sim 3$  GeV/c.
- $(p/\pi)_{AuAu} > (p/\pi)_{pp}$  : consistent with a strong expansion in AuAu

# $\bar{\Lambda}/\Lambda$ ratio vs. $p_T$ and $N_{part}$

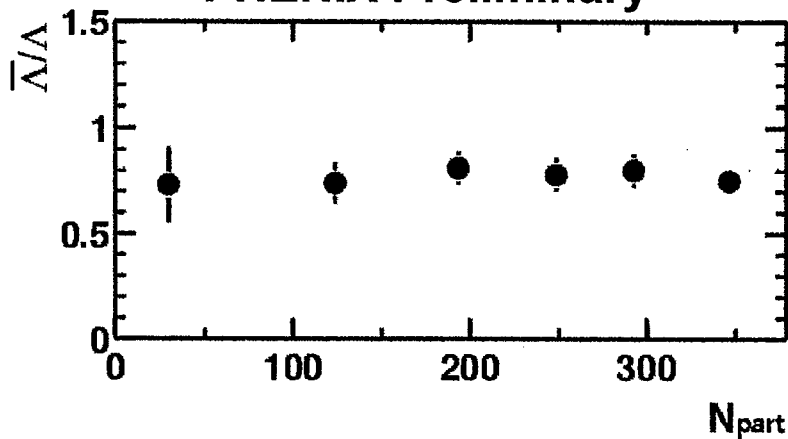
PHENIX Preliminary



- No  $p_T$  and  $N_{part}$  dependences in anti- $\Lambda/\Lambda$  ratio

- Averaged anti- $\Lambda/\Lambda$  ratio :  **$0.75 \pm 0.09$**

PHENIX Preliminary



- No  $p_T$  dependence  $\Rightarrow$  Consistent with the statistical thermal model

# Summary

- **We presented identified charged hadron spectra and ratios in Au+Au @ 130 GeV.**
  - Nucleons dominate mesons at  $\sim 1.5\text{-}2$  GeV/c ( $\pi/p$  crossing).
  - $\langle p_T \rangle$  increase with  $N_{\text{part}}$  and mass.
    - $\Rightarrow$  consistent with radial flow picture
  - (Anti) proton yields per participant rise faster than pion yields with  $N_{\text{part}}$ .
  - No centrality and  $p_T$  dependence in identical particle's ratio, including anti- $\Lambda/\Lambda$  ratio  $\Rightarrow$  consistent with thermal model.
  - $K/\pi$  and  $p/\pi$  ratio increase with  $p_T$ .
  - Measured  $\Lambda/p$  ratios and net baryon number ( $p - pbar$ ) and ( $\Lambda - \Lambdabar$ ).



# Baryons in PHOBOS

Kris Gulbrandsen (MIT, For the PHOBOS Collaboration)

Data collected during RHIC year 2000 running at  $\sqrt{s_{NN}} = 130$  GeV yielded many interesting results about baryons from all the RHIC experiments. PHOBOS had measured  $\langle \bar{p} \rangle / \langle p \rangle$  to be  $0.60 \pm 0.04(\text{stat}) \pm 0.06(\text{sys})$  (PRL 87 102301 2001) and, from this measurement, estimated  $\mu_B$  to be  $45 \pm 5$  MeV. With good agreement among all RHIC experiments on this ratio, it was evident that RHIC collision conditions were still not in the baryon free region of phase space. Data collected during RHIC year 2001 running at  $\sqrt{s_{NN}} = 200$  GeV has allowed for the extension of the current set of anti-particle to particle ratios and a first look at energy systematics in the RHIC energy regime.

The measurement is made by PHOBOS's two arm spectrometer which provides charge sign, momentum and energy loss information through the measurement of the particle's path in a 2 Tesla magnetic field and the measurement of energy lost in each plane of the spectrometer. This information is used to plot the particles'  $dE/dx$  vs momentum (and charge sign) and, by selecting equivalent regions on  $dE/dx$  vs momentum curves for positive and negative particles where particle types do not overlap, a count of identified particles can be performed.

Particle ratios are calculated using events at opposite magnet polarity for acceptance and efficiency corrections to cancel. To check this cancellation, mass distributions of identified particles and number of straight line tracks per event distributions (from tracks reconstructed in only the first 6 planes of the spectrometer where the field strength is very low) are compared at each magnet polarity to insure the field strength and trigger conditions were equivalent at the two polarities. Ratios of particles at opposite field polarity bending the same direction in our spectrometer are then taken giving two statistically independent measures of the same quantity. Corrections are then applied to the ratios for secondary production, absorption (in the beampipe and first planes of the spectrometer), and feeddown (primarily from  $\Lambda$ 's). These corrections are reduced by requiring the particles to point back to the primary vertex within 3.5 mm.  $\langle \bar{p} \rangle / \langle p \rangle$  is assigned a

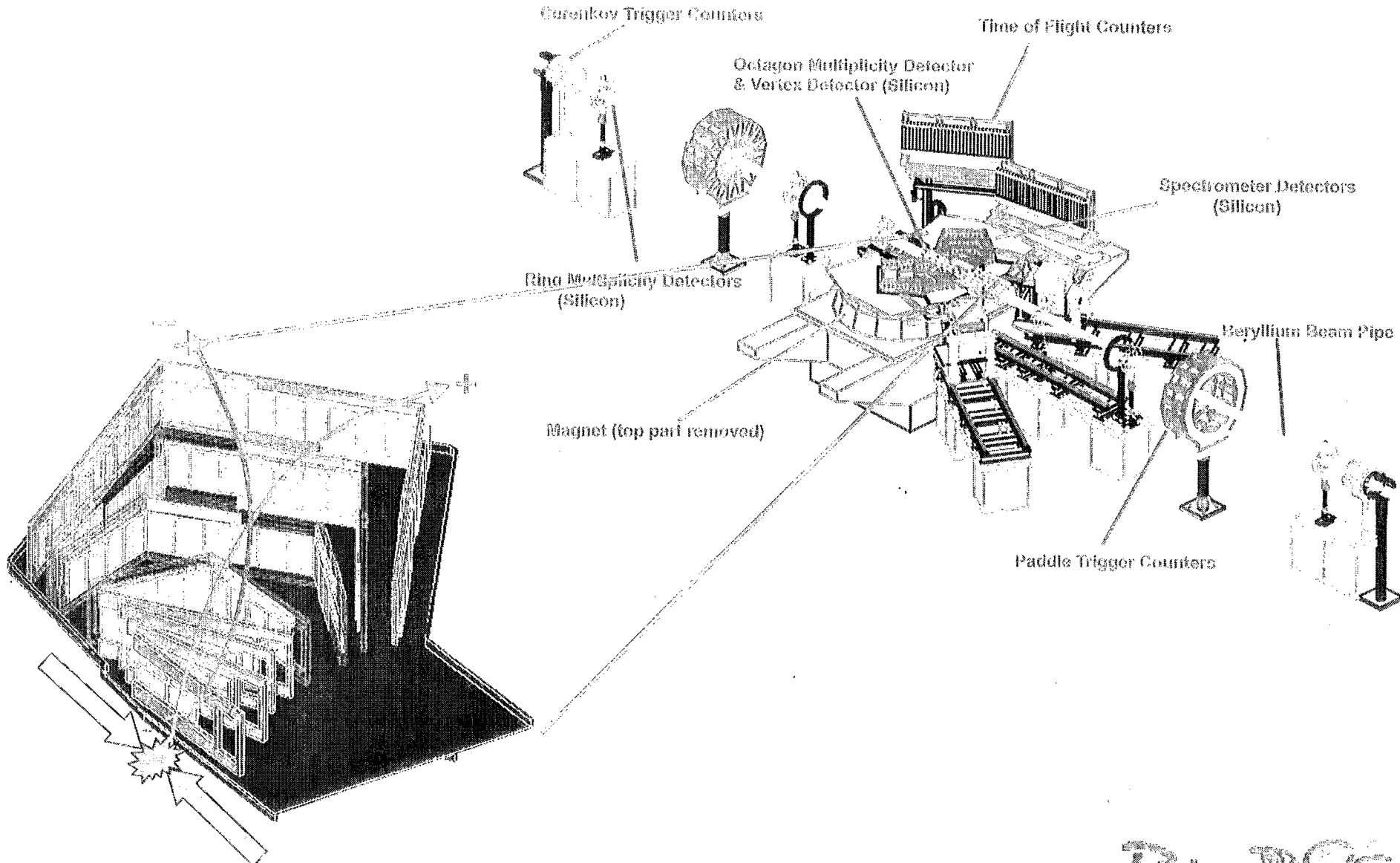
+0.7% secondary correction, +5.1% absorption correction, and -0.6% feed-down correction. Corrections for  $\langle\pi^- \rangle/\langle\pi^+ \rangle$  and  $\langle K^- \rangle/\langle K^+ \rangle$  are negligible. The resulting preliminary ratios are

$$\begin{aligned} \langle\pi^- \rangle/\langle\pi^+ \rangle &= 1.025 \pm 0.006(stat) \pm 0.020(sys) \\ \langle K^- \rangle/\langle K^+ \rangle &= 0.95 \pm 0.03(stat) \pm 0.04(sys) \\ \langle\bar{p} \rangle/\langle p \rangle &= 0.74 \pm 0.02(stat) \pm 0.03(sys) \end{aligned}$$

The systematics were arrived at by examining deviations between different methods of determining the collision vertex along with the agreement between subsets of data from each bending direction, spectrometer arm, and beam orbit condition (a noticeable shift in beam orbit was evident occurring half way through the used data set). Of those systematic checks only pions had an extra 0.015 systematic error assigned (above systematics due to vertex determination) due to deviations in the ratio when looking at data sets with different beam orbits.

A preliminary value of the baryochemical potential was estimated to be  $26 \pm 2$  MeV using a model by Redlich (QM2001 Presentation). This is nearly half the  $\sqrt{s_{NN}} = 130$  GeV value. A look at the energy dependence of  $\mu_B$  using the phenomenological model by Braun-Munzinger, Cleymans, Oeschler and Stachel (Nucl. Phys. A697: 902-912 2002) predicts the 200 GeV value within errors using data from lower energies to obtain fit parameters. This shows that, while the value of  $\langle\bar{p} \rangle/\langle p \rangle$  has increased approximately 25%, we still do not sit in a baryon free region of phase at this new energy, however phenomenological models can predict the values that are measured for these ratios well.

# Spectrometer & Tracking



51



# Calculating Ratios

- Check conditions match at both polarities
  - Field Strength  $\leftrightarrow$  Mass Distributions
  - Trigger  $\leftrightarrow$  Straight Line Tracks
- Ratio particles at opposite field polarities which bend in the same direction
- Acceptance and efficiency cancels
- Independent measurements

$$\frac{N_{\pi^-, K^-, \bar{p}}^{B+}}{N_{\pi^+, K^+, p}^{B-}} \quad \text{or} \quad \frac{N_{\pi^-, K^-, \bar{p}}^{B-}}{N_{\pi^+, K^+, p}^{B+}}$$

# 200 GeV Ratios

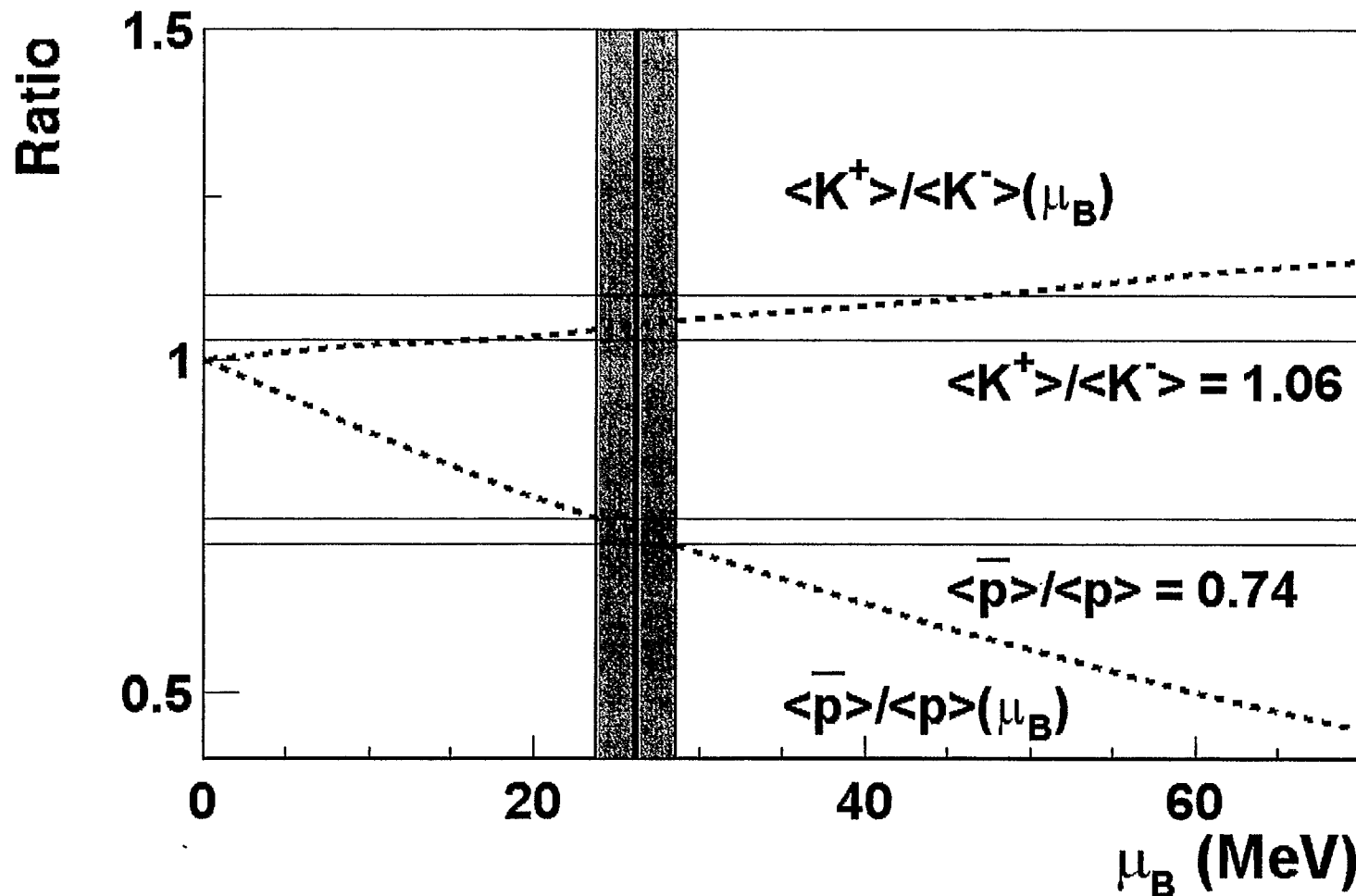
Preliminary

$$\frac{\pi^-}{\pi^+} = 1.025 \pm 0.006(\textit{stat}) \pm 0.020(\textit{sys})$$

$$\frac{K^-}{K^+} = 0.95 \pm 0.03(\textit{stat}) \pm 0.04(\textit{sys})$$

$$\frac{\bar{p}}{p} = 0.74 \pm 0.02(\textit{stat}) \pm 0.03(\textit{sys})$$

# Determination of $\mu_B$

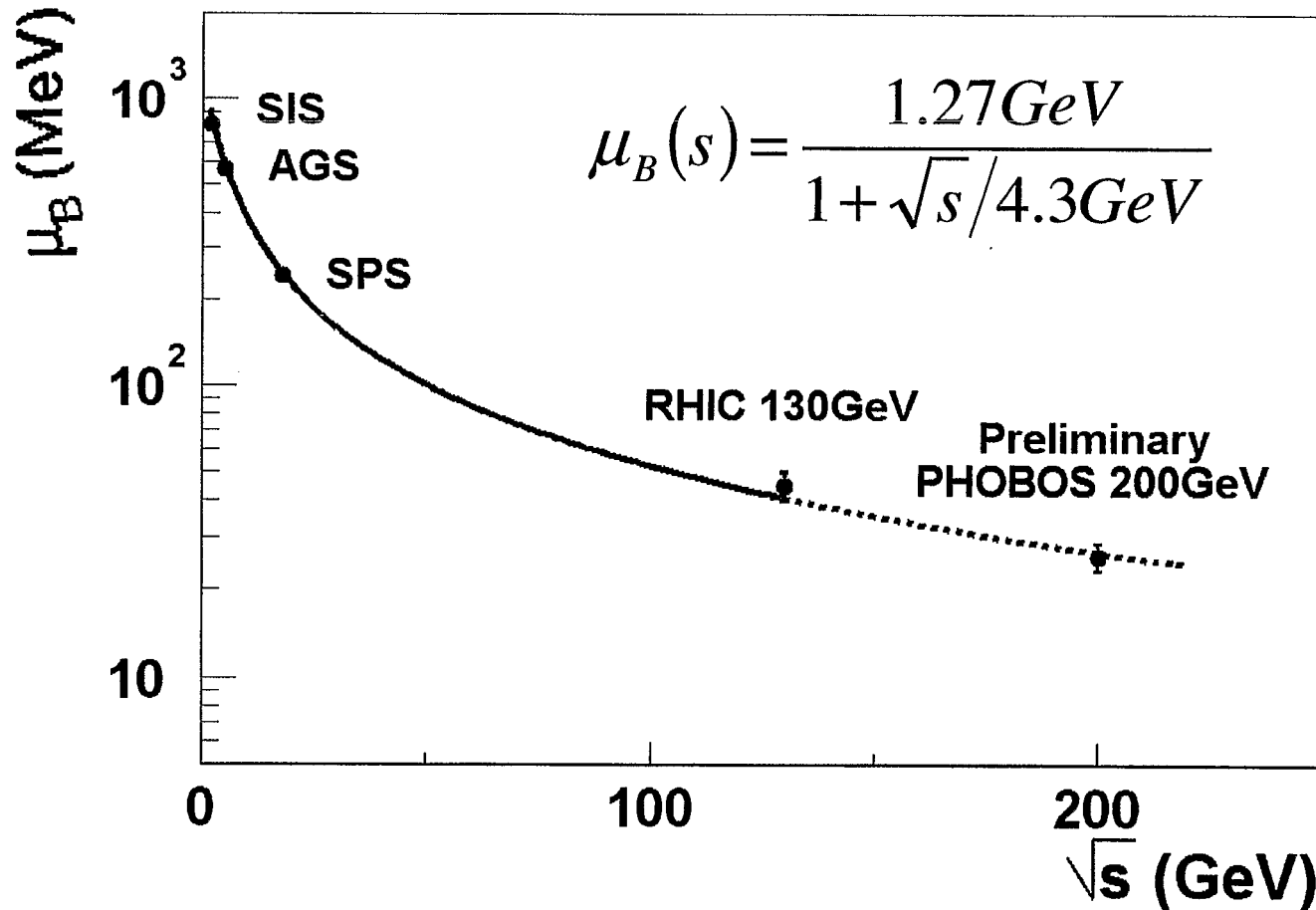


Redlich,  
QM2001 Presentation

$$\mu_B = 26 \pm 2 \text{ MeV (Preliminary)}$$

# Energy Dependence of $\mu_B$

Nucl. Phys. A697: 902-912 (2002)



Phenomenological model describes data well





# Proton and Anti-Proton Distributions from STAR

Kai Schweda, LBNL  
March 28, 2002

for  
Baryon Dynamics at RHIC Workshop  
RIKEN BNL Research Center



# Proton and Anti-proton Distributions from STAR

Kai Schweda, LBNL  
for the STAR Collaboration

1

*Baryon Dynamics at RHIC, March 28 – 30, 2002*



## Outline

- Introduction
- Analysis
- Proton and Anti-proton Distributions
- Systematics of Transverse Expansion
- Conclusions / Outlook

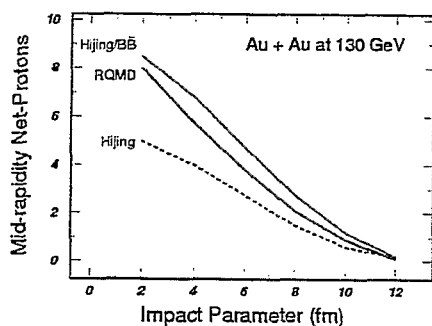
2

*Baryon Dynamics at RHIC, March 28 – 30, 2002*



## Introduction (i)

- 1) Baryon number transport is important for high energy collisions
- 2) Baryon junction mechanism needed for heavy ion collisions?
- 3) Net-proton + pair production  $\rightarrow$  proton and anti-proton yields



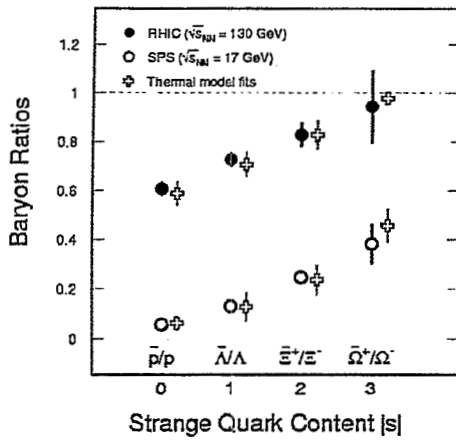
3

B2

702



# Introduction (ii)



Strange baryon ratios defined by K and p ratios!

see also J. Zimanyi et al, hep-ph/0103156

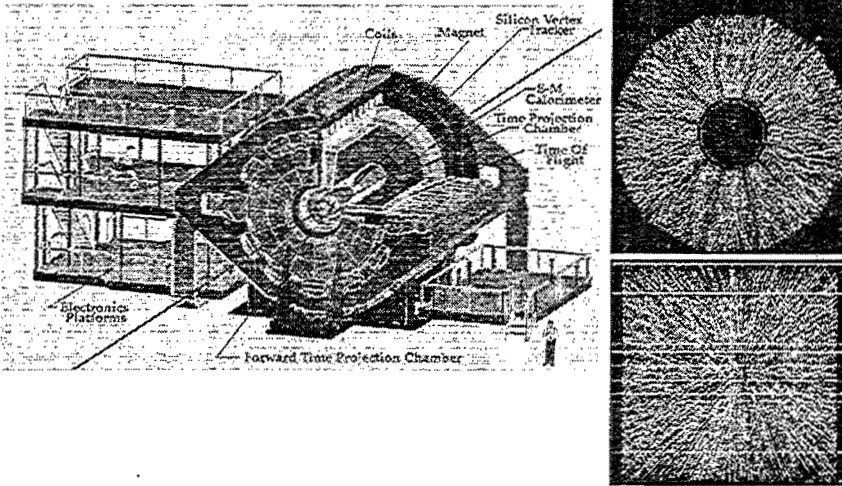
- Thermal fit by M. Kaneta

4

Baryon Dynamics at RHIC, March 28 - 30, 2002



# The STAR Experiment

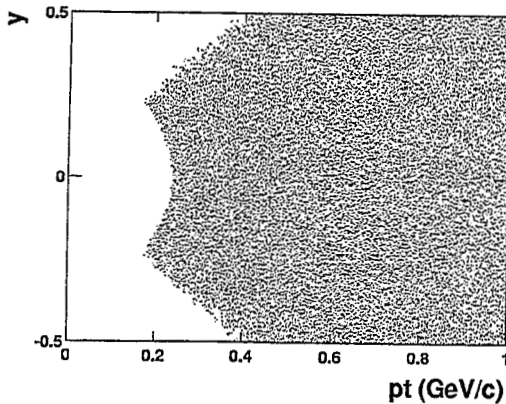


5

Baryon Dynamics at RHIC, March 28 - 30, 2002



# STAR Proton - Acceptance



- analyze at  $0.35 < p_t < 1.00$  GeV/c
- $-0.4 < y < 0.4$
- PID limit:
  - 1) low momentum - background in protons from secondary interactions,
  - 2) high momentum - contamination from  $\pi$ , K
  - 3)  $dE/dx$  resolution  $\sim 10\%$

6

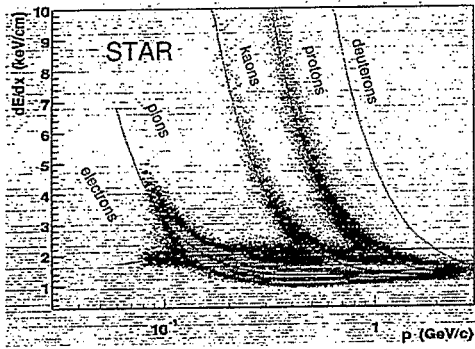
Bar

59

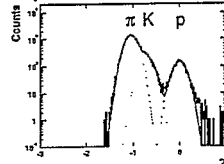
72



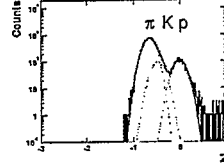
# dE/dx Particle Identification



$p_t = 600 - 650$  MeV/c



$p_t = 800 - 850$  MeV/c



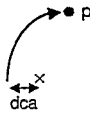
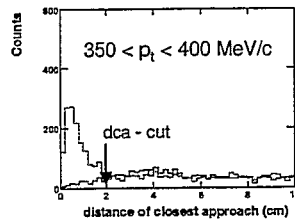
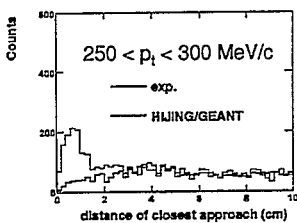
- Proton (anti-proton) ID to  $p = 1.1$  GeV/c
- $p_t < 1.0$  GeV/c,  $|y| < 0.4$

7

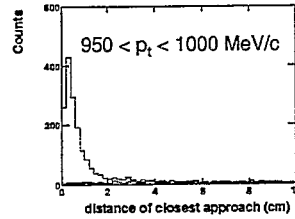
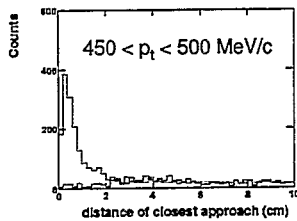
Baryon Dynamics at RHIC, March 28 - 30, 2002



## Proton Background



- Primary particles interact with detector material
- generate background protons



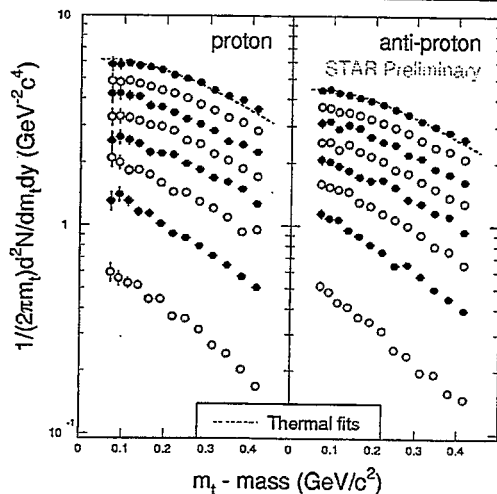
- Large background contribution at  $p_t \approx 400$  MeV/c
- Steeply decreasing at higher  $p_t$

8

Baryon Dynamics at RHIC, March 28 - 30, 2002



## $p_t$ - Distributions



Au+Au at 130 GeV

- 1) Proton and anti-proton yields as a function of centrality;
- 2) Slope increases with centrality → indicates transverse flow
- 3) Extrapolation with thermal fits;
- 4) Systematic error is large, ~ 20%.

9

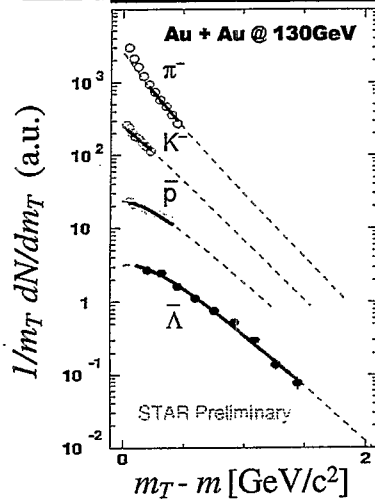
6

60

002



# Thermal Fits\*



- The bend is changing with particle mass:

$$\int_0^R r dr m_T K_1 \left( \frac{m_T \cosh \rho}{T_{th}} \right) I_0 \left( \frac{p_T \sinh \rho}{T_{th}} \right)$$

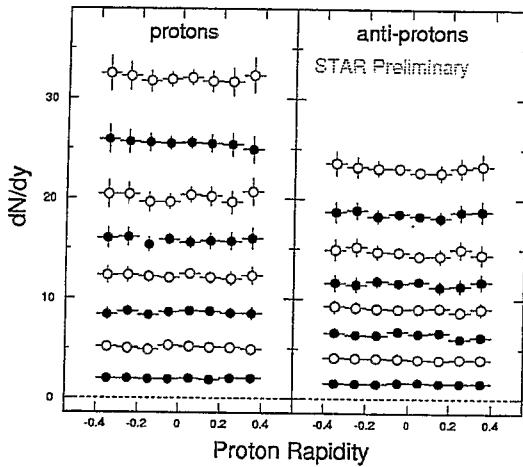
\*Masashi Kaneta, LBNL

10

Baryon Dynamics at RHIC, March 28 - 30, 2008



# Rapidity - Distributions



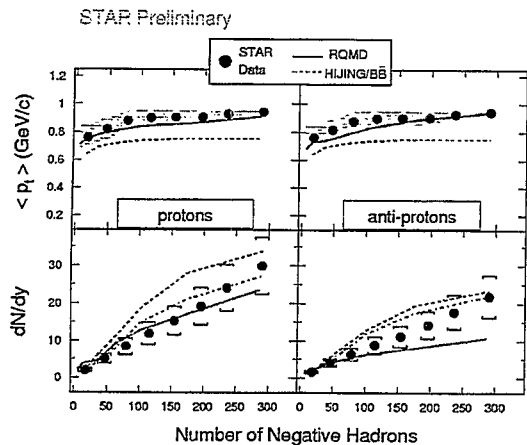
- 1) Systematic errors are larger at higher y due to larger contamination in dE/dx
- 2) dN/dy - distributions are flat for both proton and anti-protons

11

Baryon Dynamics at RHIC, March 28 - 30, 2008



# Model Comparison (i)



- increase in  $\langle p_t \rangle$  vs centrality  $\rightarrow$  radial flow
- RQMD describes transverse motion reasonably well  $\rightarrow$  hadronic re-scattering
- RQMD underestimates pbar yield due to large annihilation X-section  $\rightarrow$  re-scattering at earlier stage?

12

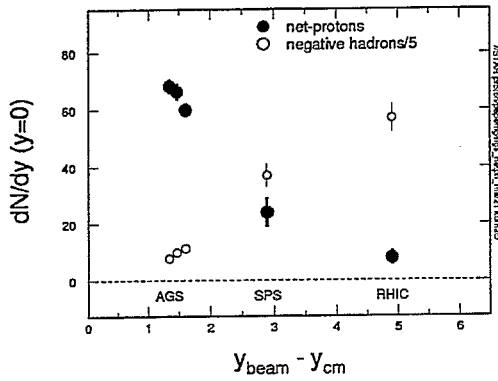
B:

61

302



# dN/dy vs Collision Energy



- While multiplicity increases with beam energy, net-proton yield is decreasing
- $p\bar{p}$  pair production dominates  $p\bar{p}$  and proton yield
- Not yet net-baryon free at RHIC
- $dN_p/dy / dN_{\bar{p}}/dy \approx \text{few } \%$

13

Baryon Dynamics at RHIC, March 29 – 30, 2002



## Summary (i)

Proton and anti-proton distributions at 130 GeV:

$p_t$  – transverse distributions

- collective expansion increases with centrality
- rescattering at hadronic or partonic stage ?  
→  $\Phi$ ,  $\Omega$ ,  $J/\psi$  are needed !

$dN/dy$  – longitudinal distribution

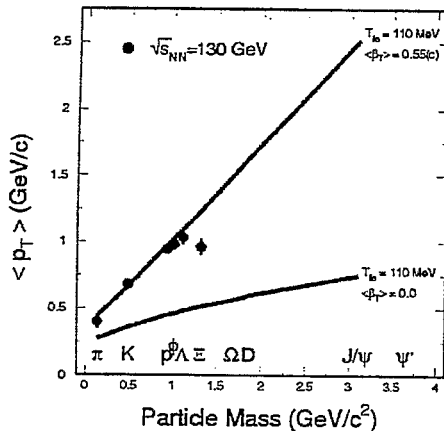
- $dN/dy$  for protons and anti-protons is flat
- no model describes results consistently  
→ larger  $p_t$  – coverage (ToF, EMC, RICH)

14

Baryon Dynamics at RHIC, March 29 – 30, 2002



## Transverse Expansion at RHIC



- 1) Thermal fit boundaries
- 2)  $K, p, \pi$ :  $\langle p_t \rangle$  shows linear mass dependence
- 3) How does  $\Omega$  behave?

M. Kaneta, H.G. Ritter, K.S., and N. Xu

15

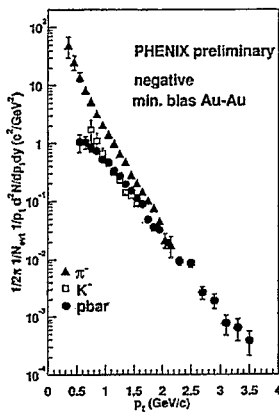
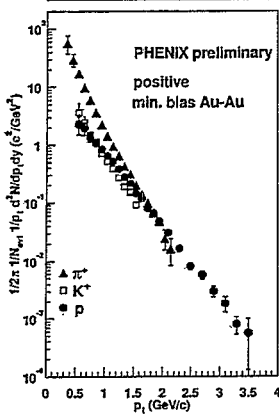
Bar

62

E



# PHENIX Min. Bias Data\*



\*nucl-ex/0112006,  
submitted to PRL

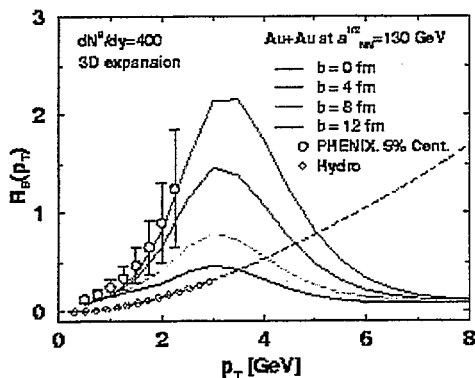
- $p(\text{pbar})/\pi \approx 1$  @  $p_T \sim 2 \text{ GeV}/c$ ,
- Indicates that  $p(\text{pbar})$  is dominant at moderately high  $p_T$ .

16

Baryon Dynamics at RHIC, March 28 – 30, 2002



## Model Comparison (ii)



I. Vitev and M. Gyulassy, (nucl-th/0104066)

non-pQCD + pQCD

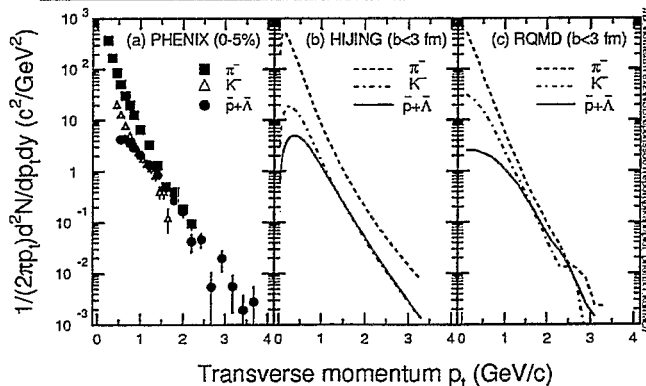
- 1) Gluon density:  $gs \rightarrow p\text{bars}$
- 2) Gluon density: Jet-quenching
- 3)  $T_0(\text{pion}) = 220 \text{ MeV}$   
 $T_0(\text{kaon}) = 275 \text{ MeV}$   
 $T_0(\text{proton}) = 400 \text{ MeV}$

17

Baryon Dynamics at RHIC, March 28 – 30, 2002



## Model Comparison (iii)



- 1) Similar to hydrodynamic calculations, RQMD provides the observed trend!
- 2) Numerous re-scattering leads to pressure gradient and collective expansion.
- 3) Re-scattering at partonic or hadronic (or both) stage ?

18

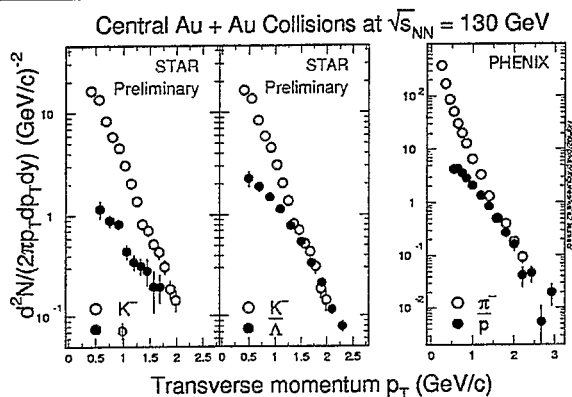
21

63

102



# STAR Data



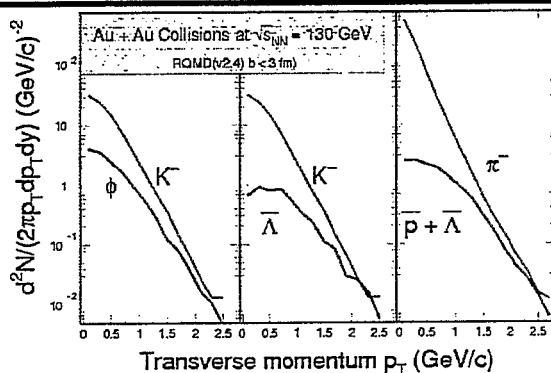
- 1)  $\rho, \bar{\Lambda}, \phi$  yields approach  $K, \pi$  with increasing  $p_T$ !
- 2) Mass effect !

19

Baryon Dynamics at RHIC, March 29 - 30, 2002



## Predictions from RQMD



- 1) RQMD provides the observed trend
- 2) Re-scattering is important at RHIC !
- 3) Re-scattering at partonic or hadronic stage ?

20

Baryon Dynamics at RHIC, March 29 - 30, 2002



## Conclusions / Outlook

- not yet net-baryon free at RHIC
  - strong collective expansion at RHIC
  - $\langle p_T \rangle$  vs. mass  $\rightarrow$  hydrodynamic feature
  - re-scattering at hadronic or partonic stage ?
- $\rightarrow (\Phi), \Omega, J/\psi$  are needed !

21

Baryon Dynamics at RHIC, March 29 - 30, 2002



# **Baryon Production and Gluonic Dynamics**

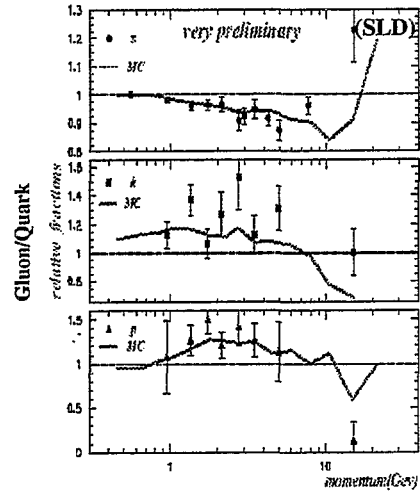
**Huan Zhong Huang**  
**Department of Physics and Astronomy**  
**University of California, Los Angeles**

**BNL/RIKEN Baryon Dynamics Workshop, March 28-30**

### Gluonic Dynamics Dominant at Mid-Rapidity at RHIC

- 1) Conceptually appealing: the gluon structure function much larger than quarks at the  $x$  relevant for mid-rapidity at RHIC; gluon-parton interaction cross sections are larger than quark-quark....
- 2) The measured ratio of anti-particle/particle close to unity: small net baryon density at mid-rapidity at RHIC; Valence quarks less important.
- 3) Multiplicity  $\leftrightarrow$  Gluon saturation model; e.g., Kharzeev and Levin, *Phys. Lett. B* 523, 79 (2001). HIJING; minijet particle production presumably induced mostly by gluons.
- 4) Elliptic flow,  $v_2$ , larger at RHIC: effective in transferring initial geometrical anisotropy to momentum anisotropy ! Strongly interacting gluonic system may be able to provide the driving force for both  $v_1$  and  $v_2$ .

### Gluon vs Light Flavor Quark Jet



-10-20% difference in baryon production between gluon and quark jets

### Baryon Yield Comparison

LEP (OPAL)

$N_{ch} = 20.92 \pm 0.24$   
 $P = 0.92 \pm 0.11$   
 $\Lambda = 0.348 \pm 0.013$   
 $\Xi^- = 0.0238 \pm 0.0024$   
 $\Omega = 0.0051 \pm 0.0013$

$p/h^+ = (8.8 \pm 1.1) \%$   
 $\Lambda/p = (38 \pm 5) \%$   
 $\Xi^-/p = (2.6 \pm 0.4) \%$   
 $\Omega/p = (0.55 \pm 0.15) \%$

STAR Preliminary

$h^+ = 290$   
 $P = 20.5 \pm 0.5$   
 $\Lambda = 12.0 \pm 0.3$   
 $\Xi^+ \sim 3.0$   
 $\Omega?$

$\bar{p}/h^+ = 7.1 \%$   
 $\Lambda/\bar{p} = (59 \pm 3) \%$   
 $\Xi^+/\bar{p} \sim 14.6\%$   
 $\Omega/\bar{p} ?$

### A+A vs e+e Collisions

- Production rate for the total number of baryons (inclusive protons and anti-protons) relative to that of mesons is similar between A+A and e+e collisions.
- The production of high mass hyperons is strongly enhanced in nucleus-nucleus collisions at RHIC.
- What determines the mass dependence for baryon production and how does the dynamical picture change from e+e to A+A collisions?

----- Multi-Gluon Dynamics -----  
 (Gluon Junctions)

### What determines the mass penalty factor?

For p,  $\Lambda$ ,  $\Xi$  and their anti-particle production

Statistical Model  $\sim m^{3/2} e^{-m/T}$

String Fragmentation  $\sim e^{-\pi m^2 / \kappa}$

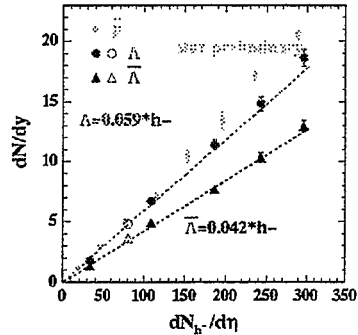
Some proposed models with different mass dependence:

Baryons through topological defect formation  
e.g., J. Ellis et al., Phys. Lett B233, 223 (1989)

OR

ALCOR – quark coalescence picture  
J. Zimanyi et al., hep-ph/0103156

### Baryon to Hadron Ratios in Au+Au Collisions

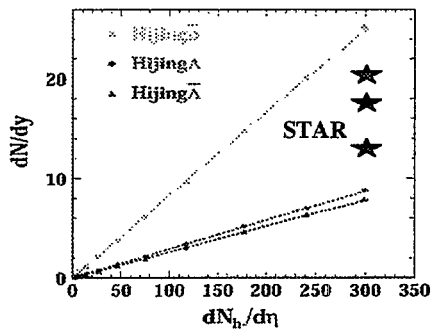


a) Approximate linear dependence of baryon on h-.

b) NA49: Mid-rapidity anti-proton/h- ~ 0.03  
STAR: anti-proton/h- ~ 0.07

STAR baryon/h is close to e+e and NA49 is below.  
Gluon dynamics and annihilation!

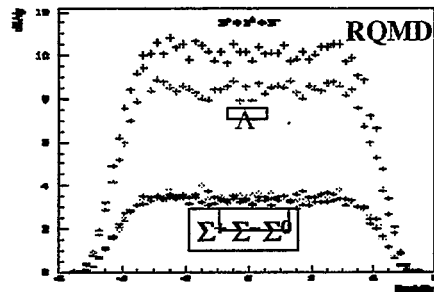
### HIJING Baryon Production does not Work



- a) anti-proton is too easy to generate! Suppressed?
- b) HIJING  $dn/d\eta$  happens to be close!  $p_T$  of baryons too small!
- c) Baryon production is not difficult. But balancing the yields of hyperons ( $\Omega, \Xi, \Sigma$  and  $\Lambda$ ) and protons requires new dynamics different from string models.

STAR Data:  $\bar{p} = 20.5 \pm 0.5$ ;  $\Lambda = 17.0 \pm 0.4$ ;  $\bar{\Lambda} = 12.0 \pm 0.3$

### Baryon Production from Diquark Fragmentation ---- Ruled Out?!



Standard string fragmentation for baryon formation through diquark tunneling out of string potential:  $e^{-\pi m^2 / \kappa}$  dependence  
 $m(\text{ud-1}) = 0.49 \text{ GeV}$   
 $m(\text{ud-0}) = 0.42 \text{ GeV}$   
predicts  $\Sigma = 0.35\Lambda$ .

If  $\Sigma = 0.35\Lambda$ , STAR data would imply  $\Xi > \Sigma$ , very unlikely!

**Where Does the Mass of Baryons Come From and How Is the Baryon Flavor Determined?**

Entities in Production Processes are:

Diquark-Masses

Constituent Quark Masses → Baryon Mass and Flavor

Strong Mass Suppression if they have to be produced from dynamical QM tunneling!

High Energy Density Gluonic Fireball:

Baryon Mass: → Mostly from gluon junction !  
(preexist in high density gluon field)

No large mass penalty is needed !



Baryon Flavor: → string break for q-qbar production !  
(the quark mass involved is not the constituent mass)

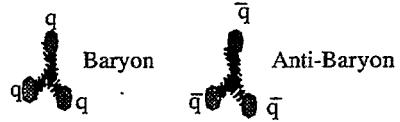
**A Novel Mechanism?!**

Basic Assumptions:

- 1) Nuclear Matter at Mid-rapidity – Gluon Dominant! (Low Net Baryon Density) and Gluons Strongly Interacting (Effective DOF unlike that of Naive QGP)
- 2) Gluon Junction Can be a Seed for Baryon Formation and Dynamically Create a Baryon Number



3) The Baryon Flavor is Determined by the Flavors of Quarks Connected to the Gluon Junction.



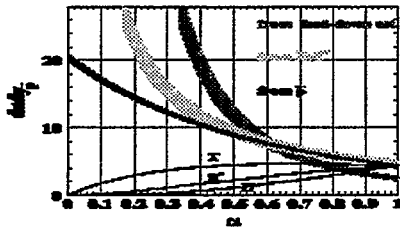
4) Baryon Production is Determined by the Probability of Gluon Junction Having Three Quarks or Anti-quarks in Hadronization and Probability of gluon junction topological configuration in a hot gluon fireball?

Vance/Gyulassy previously proposed Baryon-AntiBaryon production from dynamical gluon junction pair production from string fragmentation!

**A Consistent Picture for anti-Baryon Production**

Key Prediction of the Model:

$$\bar{\Lambda}^0 = \bar{\Sigma}^0 = \bar{\Sigma}^+ = \bar{\Sigma}^- \quad \frac{\bar{\Lambda}^0}{p} = \frac{\bar{\Xi}^-}{\Lambda^0} = \alpha \geq \frac{\bar{\Omega}}{\Xi^-}$$



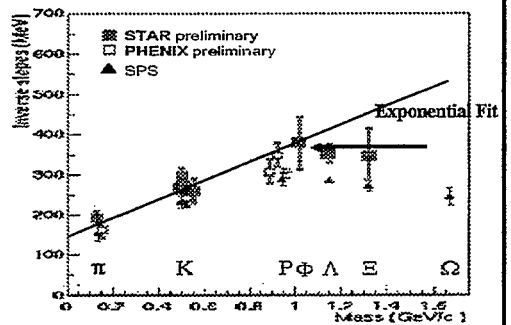
The important constraint will be from  $\Xi$  and  $\Omega$  measurement. Topological Model Predicts:

$\Xi$ -bar = 3 and  $\Omega$ -bar < 1-2

$\Sigma^0$  and  $\Lambda^0$  Measurement:

- Ratio: ~ 1.0 – Novel Mechanism
- ~ 0.35 – String Fragmentation
- ~ 0.67-0.75 – Thermal Mass Suppression

**Slope Parameters of Baryons**



Hydrodynamic:

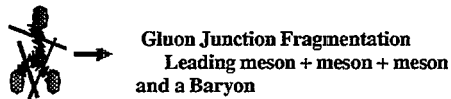
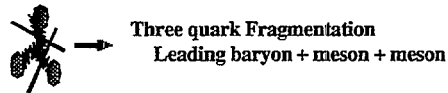
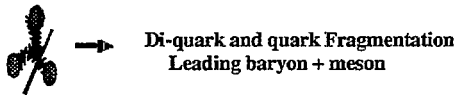
- Mass dependence – common expansion velocity
- Strange baryons freeze-out early.

Gluon Junction Picture:

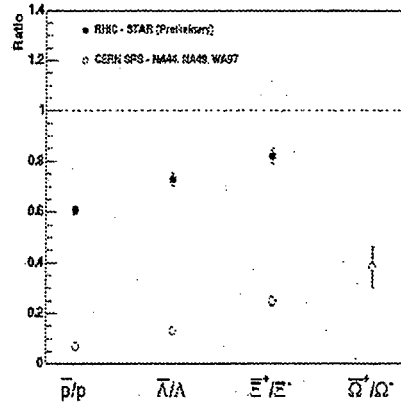
Baryon from gluon junctions approximately the same;  $m_T$  indicative of gluon energy density at the baryon formation.

- effect due to final state interactions small
- same slopes regardless of hadronic interaction cross sections.

**Schematic Representation for Baryon Number Transport Dynamics**



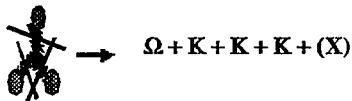
**Anti-Baryon to Baryon Ratios**



How is baryon number transferred to  $\Omega$ ? at SPS!

**Scenarios for Baryon Number Transport to Hyperons**

Direct Transport Through Gluon Junctions ...



Indirect Transport Through Pair Production Modified by Baryon Chemical Potential ...

$\Omega \bar{\Omega}$  and  $\Omega \bar{\Xi} K$   
 $\Xi \bar{\Xi}$  and  $\Xi (\bar{\Lambda}/\bar{\Sigma}) K$   
 $\Lambda \bar{\Lambda}$  and  $\Lambda (\bar{p}/\bar{n}) K$

Net Baryon Density Increases the Associated Production and Transfers net baryon number to multiply-strange baryons!

Event-by-Event STAR Hyperon Correlations  
Doable with STAR TOF and SVT Upgrade!

**Summary**

- Gluon Dynamics play an important role in particle production at mid-rapidity at RHIC.
- Multi-gluon dynamics, probably gluon junctions, may contribute to increased  $\Lambda$ ,  $\Xi$  and  $\Omega$  yields.
- The dynamics of string fragmentation model cannot reproduce the baryon and hyperon yields. The mass dependence in di-quark tunneling is problematic.
- Baryon production from gluon junction hadronization may be topological: the rate depends on topological configuration probability, not strongly on the mass of the hyperons.
- Future measurement on event-by-event hyperon correlations can shed light on mechanisms of baryon number transport to hyperons



# Hadronization, Baryon- and Meson- Dynamics at RHIC

Steffen A. Bass, Duke University and RBRC

March 29, 2002

for  
Baryon Dynamics at RHIC Workshop  
RIKEN BNL Research Center



# Hadronization, Baryon- and Meson-Dynamics at RHIC

**Steffen A. Bass**

Duke University  
& RIKEN-BNL Research Center

- Baryon- and Meson Dynamics at RHIC
- Hadronization: statistical vs. dynamical approach
- What do we learn from the Anti-Omega/Omega ratio?
- Outlook

partly in collaboration with:

M. Bleicher, K. Redlich, F. Becattini, A. Kaarenen, F. Liu, K. Werner and J. Aichelin

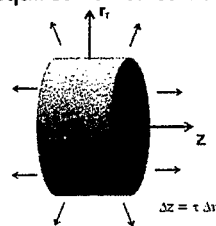
*Steffen A. Bass*

*RBRC Workshop on Baryon Dynamics at RHIC #1*



# Nuclear Fluid Dynamics

- transport of macroscopic degrees of freedom
- based on conservation laws:  $\partial_\mu T^{\mu\nu}=0$   $\partial_\mu j^\mu=0$
- for ideal fluid:  $T^{\mu\nu} = (\epsilon+p) u^\mu u^\nu - p g^{\mu\nu}$  and  $j_i^\mu = \rho_i u^\mu$
- **Equation of State** needed to close system of PDE's:  $p=p(T,\rho_i)$
- assume local thermal equilibrium
- initial conditions (i.e. thermalized QGP) required for calculation
- simple case: scaling hydrodynamics
  - assume longitudinal boost-invariance
  - cylindrically symmetric transverse expansion
  - no pressure between rapidity slices
  - conserved charge in each slice



*Steffen A. Bass*

*RBRC Workshop on Baryon Dynamics at RHIC #2*





## The UrQMD Model

- elementary degrees of freedom: hadrons, const. (di)quarks
- classical trajectories in phase-space (relativistic kinematics)
- initial high energy phase of the reaction is modeled via the excitation and fragmentation of strings
- 55 baryon- and 32 meson species, among those 25 N\*, Δ\* resonances and 29 hyperon/hyperon resonance species
- full baryon-antibaryon and isospin symmetry
- ideal for the description of excited hadronic matter
- main physics input and parameters:
  - **cross sections:** total and partial cross sections, angular distributions
  - **resonance parameters:** total and partial decay widths
  - **string fragmentation scheme:** fragmentation functions, formation time
- An interaction takes place if at the time of closes approach  $d_{min}$  of two hadrons the following condition is fulfilled:

$$d_{min} = \sqrt{\frac{\sigma_{tot}}{\pi}} \quad \text{with} \quad \sigma_{tot} = \sigma_{tot}(\sqrt{s}, |b_1|, |b_2|)$$

Steffen A. Bass

RBRC Workshop on Baryon Dynamics at RHIC #3



## A combined Macro/Micro Transport Model

### Hydrodynamics + micro. transport (UrQMD)


- |   |   |
|---|---|
| <ul style="list-style-type: none"> <li>• ideally suited for dense systems           <ul style="list-style-type: none"> <li>➤ model early QGP reaction stage</li> </ul> </li> <li>• well defined Equation of State           <ul style="list-style-type: none"> <li>➤ Incorporate 1<sup>st</sup> order p.t.</li> </ul> </li> <li>• parameters:           <ul style="list-style-type: none"> <li>– initial conditions (fit to experiment)</li> <li>– Equation of State</li> </ul> </li> </ul> | <ul style="list-style-type: none"> <li>• no equilibrium assumptions           <ul style="list-style-type: none"> <li>➤ model break-up stage</li> <li>➤ calculate freeze-out</li> </ul> </li> <li>• parameters:           <ul style="list-style-type: none"> <li>– (total/partial) cross sections</li> <li>– resonance parameters (full/partial widths)</li> </ul> </li> </ul> |
|---|---|

- matching conditions:**
- use same set of hadronic states for EoS as in UrQMD
  - perform transition at hadronization hypersurface: generate space-time distribution of hadrons for each cell according to local T and  $\mu_B$

- use as initial configuration for UrQMD

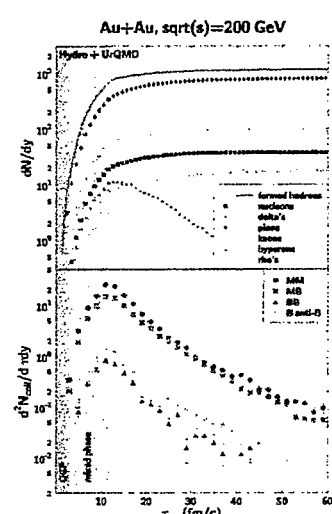
Steffen A. Bass

RBRC Workshop on Baryon Dynamics at RHIC #4




## Reaction Dynamics in a Macro/Micro Model

- initial conditions:
  - Quark Gluon Plasma
  - EoS with 1<sup>st</sup> order phase transition
  - $T_C=160$  MeV
- hadron multiplicities continue to rise after end of mixed phase
- high population of resonances, primordial and due to hadronic rescattering
- collision rates:
  - peak at end of mixed phase
  - MM and MB interactions dominate
- late kinetic freeze-out after  $\approx 35$  fm/c



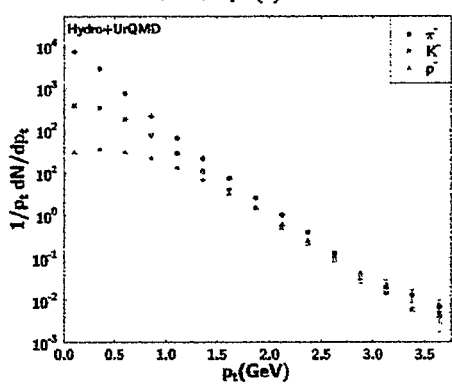
Steffen A. Bass

RBRC Workshop on Baryon Dynamics at RHIC #5

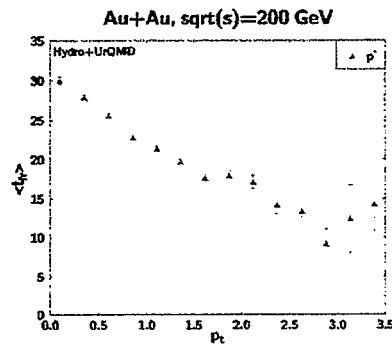


## Hadron spectra at high $p_t$

Au+Au, sqrt(s)=200 GeV



- $\langle t_{fr} \rangle$  decreases with  $p_t$
- high  $p_t$ : emission from mixed phase and phase-boundary



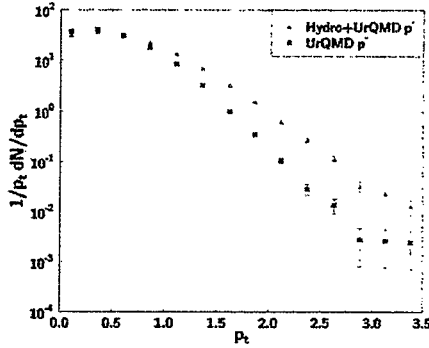
Steffen A. Bass

RBRC Workshop on Baryon Dynamics at RHIC #6



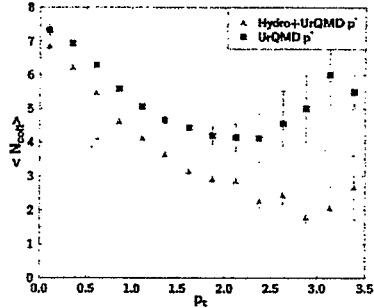
# Hydro vs. string model at high $p_t$

Au+Au, sqrt(s)=200 GeV



- string models w/o hard scattering produce insufficient high  $p_t$  hadrons

Au+Au, sqrt(s)=200 GeV



how to hadrons obtain high  $p_t$ ?

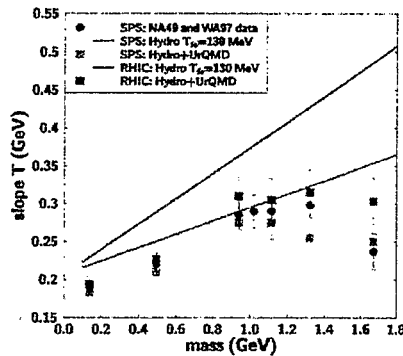
- string model: multiple rescattering
- Hydro+Micro: early freeze-out, few coll.

Steffen A. Bass

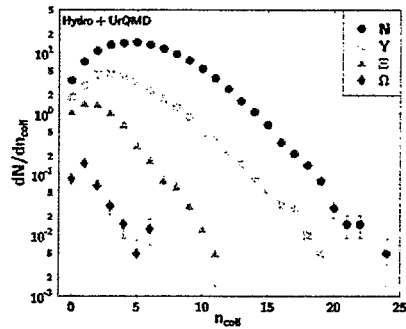
RBRC Workshop on Baryon Dynamics at RHIC #7



# Flavor Dynamics: Radial Flow



Pb+Pb SPS



- Hydro: linear mass-dependence of slope parameter, strong radial flow
- Hydro+Micro: softening of slopes for multistrange baryons
- early decoupling due to low collision rates
- nearly direct emission from the phase boundary

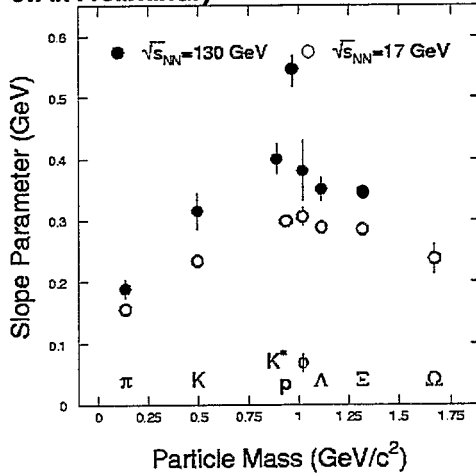
Steffen A. Bass

RBRC Workshop on Baryon Dynamics at RHIC #8



# STAR: mass dependence of $m_T$ slopes

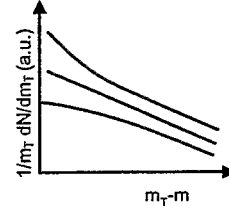
STAR Preliminary



Indication of strong radial flow at RHIC

Situation appears to be more complicated at RHIC than at the SPS

Note: inverse slope depends on the measured  $p_T$  range ( $dE/dx p < 1 \text{ GeV}/c$ )

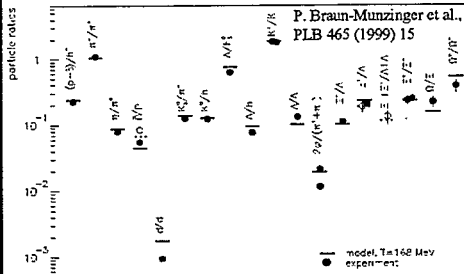


Steffen A. Bass

RBRC Workshop on Baryon Dynamics at RHIC #9



# Statistical analysis of yields/ratios



how to interpret success of fit?

- does system freeze-out at  $(T, \mu)$  or is fit a superposition of hadron species decoupling separately along a  $(T, \mu)$  trajectory?

➤ need independent verification of simultaneous/sequential decoupling!

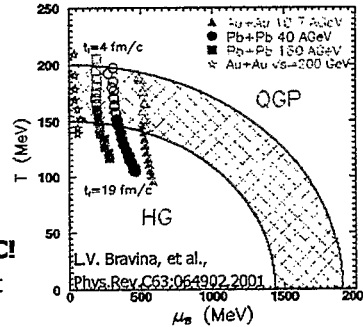
- hadron yields & ratios can be fitted in the framework of a statistical model:

$$n_i(T, \mu) = \frac{g_i}{2\pi^2} \int_0^\infty \frac{p^2 dp}{e^{(E_i - \mu_i B_i - \mu_s S_i)/T} \pm 1}$$

➤ works surprisingly well from SIS to RHIC!

- does  $T, \mu$  dependence of hadron masses affect the result of the fit? (D. Zschesche et al.)

Steffen A. Bass

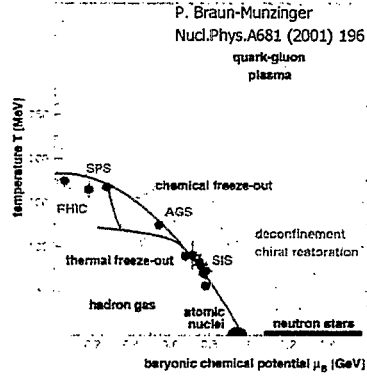


RBRC Workshop on Baryon Dynamics at RHIC #10



# Chemical Equilibration

➤ If  $(T, \mu)$  fits give point of chemical freeze-out in phase-diagram, how did the system reach this chemically equilibrated state?



- common belief: hadronic cross sections are too small to obtain chemical equilibration on the time-scale of the heavy-ion collision

➤ system evolved from QGP state

issues to be resolved:

- initial non-equilibrium processes boost particle production in hadronic scenario
- rapid equilibration through multi-particle collisions (Rapp & Shuryak, Greiner & Leupold)
- mechanism of chemical equilibration in deconfined phase is unclear (hydro+rate-eqns, PCM calculations)

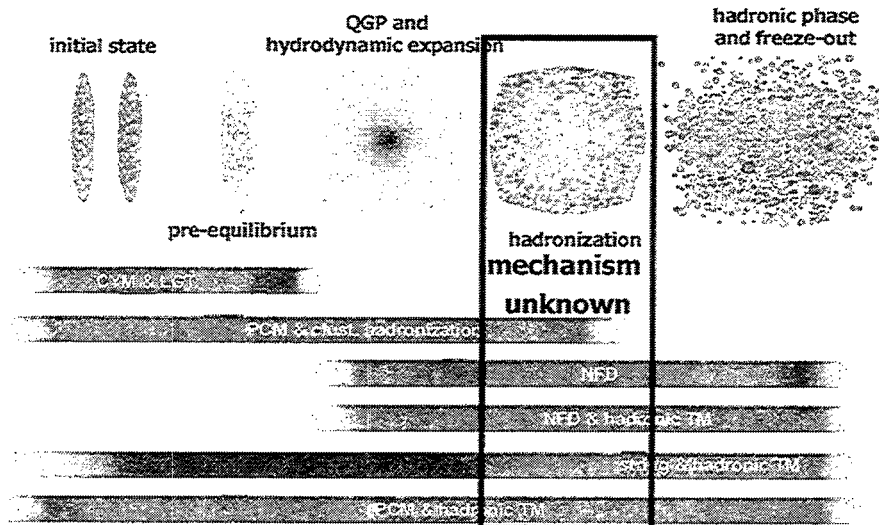
➤ Is the success of the SM a true signature of chemical equilibration or due to a generic feature of hadronization (w/o equilibration assumptions)?

Steffen A. Bass

RBRC Workshop on Baryon Dynamics at RHIC #11



# Transport Theory at RHIC



Steffen A. Bass

RBRC Workshop on Baryon Dynamics at RHIC #12

## Hadronization in a statistical model

pp  $\sqrt{s} = 27.4$  GeV

F. Becattini & U. Heinz  
Z.Phys.C76:269-286,1997

Number of St.Dev.

- the statistical model (canonical ensemble) fits hadronic yields even in elementary p+p reactions!
- chemical equilibrium in p+p reactions? (unlikely!)
- hadronization as purely statistical process

Steffen A. Bass
RBRC Workshop on Baryon Dynamics at RHIC #13

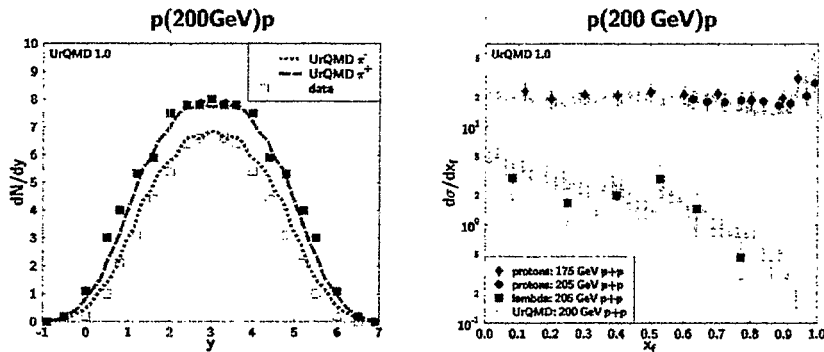
## Hadronization via String-Fragmentation

- in high energy collisions hadrons can be excited into *strings*
- a *color flux-tube* is formed by pulling one valence quark away from the remaining ones in the hadron
- if the color-field increases beyond a critical value (defined by the *string-tension*), spontaneous quark-antiquark creation from the *Dirac sea* occurs (*Schwinger mechanism*)
- newly created (anti-)quarks require a *formation time* to form hadrons
- *leading hadrons* interact with *reduced cross sections* during their formation time
- *newly created hadrons* have *zero cross section* during their formation time

Steffen A. Bass
RBRC Workshop on Baryon Dynamics at RHIC #14



## Hadronization via String-Fragmentation II



- string models require many more parameters than SMs, however, they do not only fit yields but the entire momentum space as well
- contain a model of microscopic dynamics of hadronization

Steffen A. Bass

RBRC Workshop on Baryon Dynamics at RHIC #15



## String-Fragmentation vs. Statistical Particle Production

• in a statistical model the transverse mass distribution of produced (di)quarks is exponential in  $m_{\perp}$  (Boltzmann factor):

$$\frac{dn}{dm_{\perp}} \sim e^{-m_{\perp}/T}$$

A. Bialas,  
Phys.Lett.B466 (1999) 301

• in a string model, the same distribution is given by the Schwinger term:

$$\frac{dn_{\kappa}}{dm_{\perp}} \sim e^{-\pi m_{\perp}^2 / \kappa^2} \quad (\kappa^2 : \text{string tension!})$$

➢ if Gaussian fluctuations in the string tension are introduced, one recovers an exponential form:

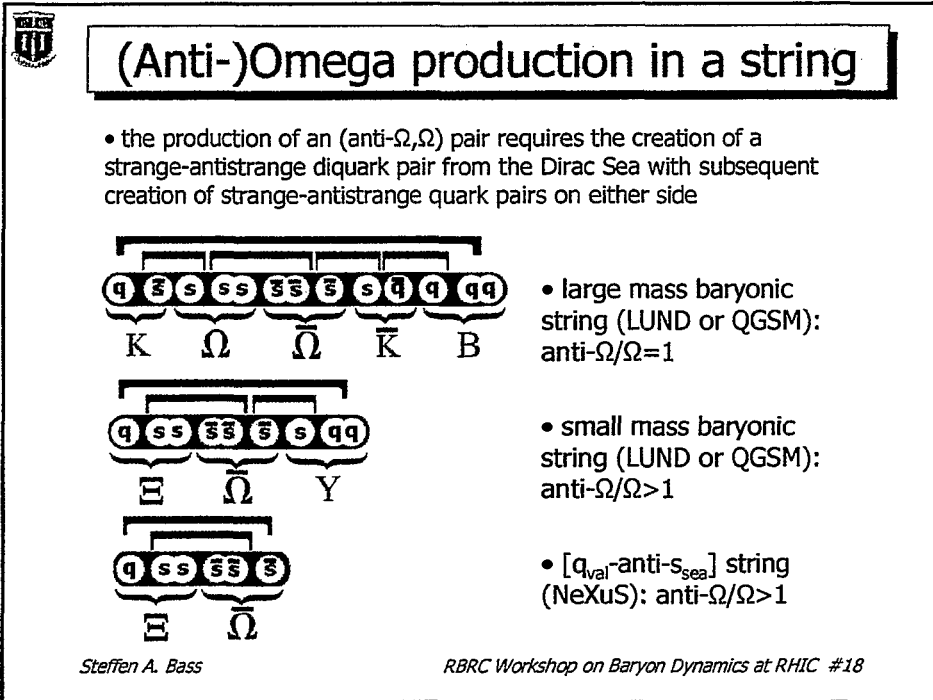
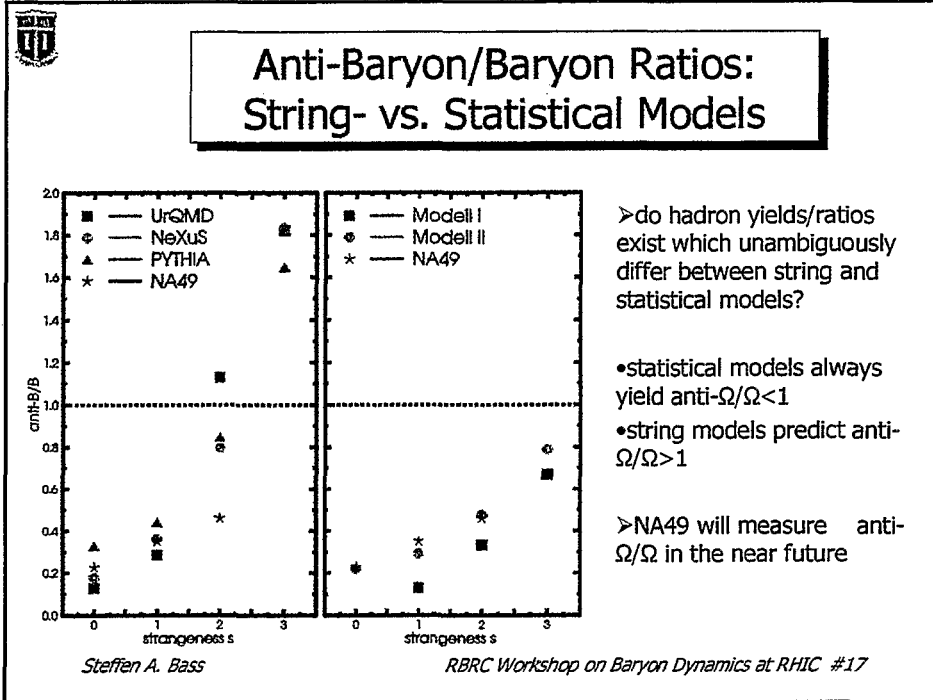
$$P(\kappa) d\kappa = \sqrt{\frac{2}{\pi \langle \kappa^2 \rangle}} \exp\left(-\frac{\kappa^2}{2 \langle \kappa^2 \rangle}\right) d\kappa$$

$$\frac{dn}{dm_{\perp}} \sim \exp\left(-m_{\perp} \sqrt{\frac{2\pi}{\langle \kappa^2 \rangle}}\right) \rightarrow \text{thermal with } T = \sqrt{\frac{\langle \kappa^2 \rangle}{2\pi}}$$

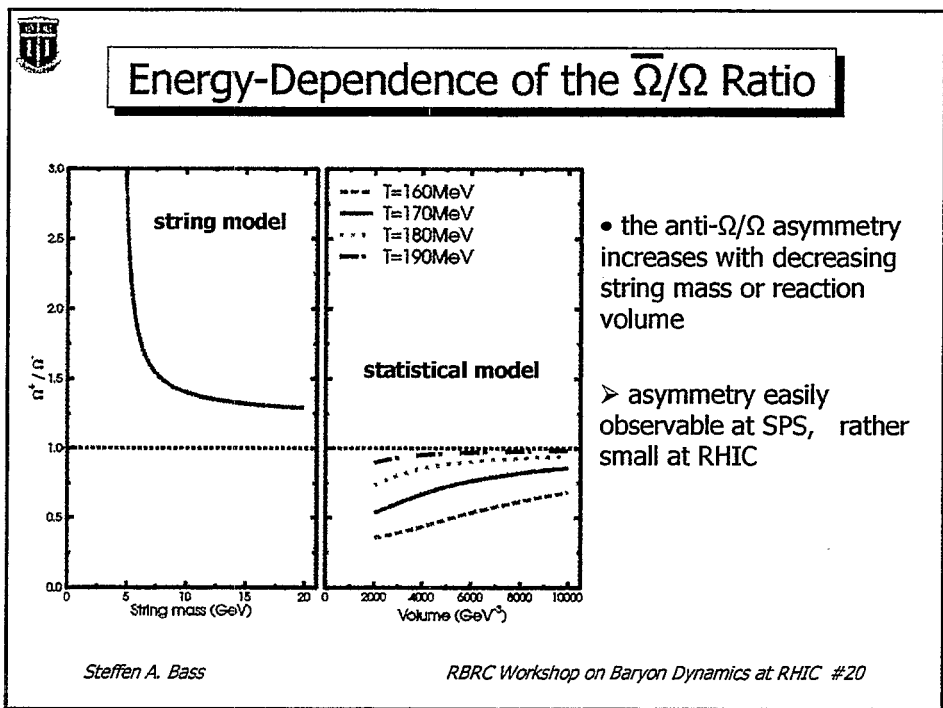
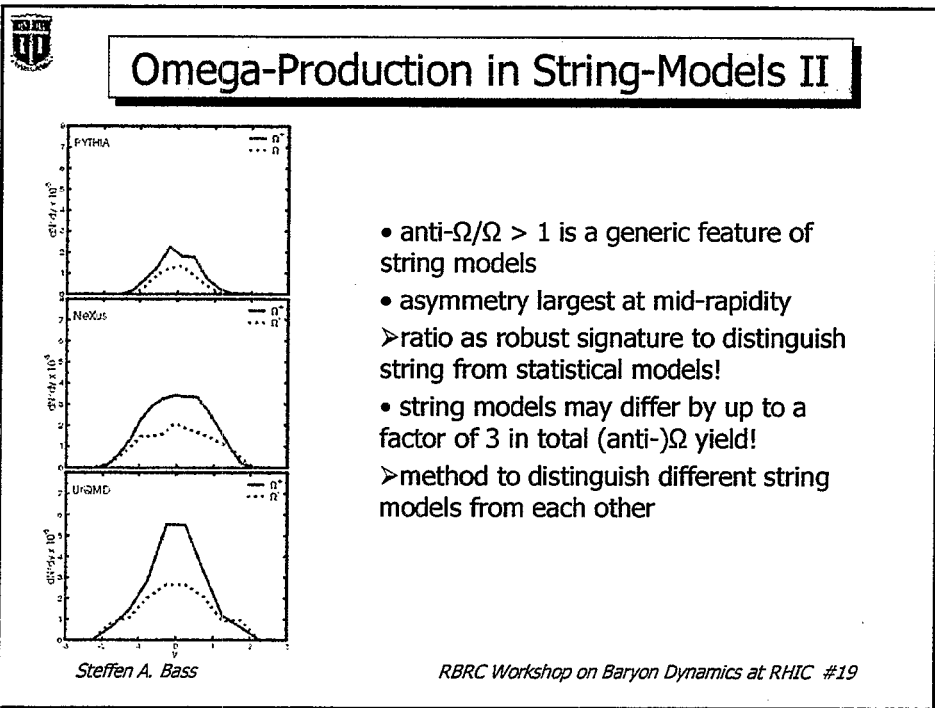
➢ can string-fragmentation be distinguished from statistical hadronization?

Steffen A. Bass

RBRC Workshop on Baryon Dynamics at RHIC #16









## Summary and Outlook

in order to make statements on the degree of chemical equilibration, either in the deconfined or confined phase, one needs to understand the dynamics of hadronization

- hadronic phase at RHIC: dominated by mesons!
- Hydro+Micro: high- $p_t$  baryons freeze out early at phase-boundary
- string fragmentation and statistical hadronization yield almost identical results, due to similarity structure: Boltzmann vs. Schwinger
- the anti- $\Omega/\Omega$  ratio provides an unambiguous observable to distinguish string fragmentation from statistical hadronization in elementary hadron-hadron reactions
  - finite size effect, clearly observable at the SPS (less dramatic at RHIC), measurement by NA49 underway

*Steffen A. Bass*

*RBRC Workshop on Baryon Dynamics at RHIC #21*

---

# Baryon Transport at RHIC

---

*RBRC Workshop, Baryon Dynamics at RHIC, March 28 – 30<sup>th</sup>, 02*

J. Barrette,  
McGill University, Montreal, Canada

C. Gale,  
McGill University, Montreal, Canada

M. Gyulassy,  
Columbia University, New York

V. Topor Pop,  
McGill University, Montreal, Canada

S. Vance,  
Brookhaven National Laboratory, Upton, NY

Xin-Nian Wang,  
Nuclear Science Division, LBNL, Berkeley

Nu Xu  
Nuclear Science Division, LBNL, Berkeley

Kirill Filimonov  
Nuclear Science Division, LBNL, Berkeley

Work in progress

# Baryon Transport at RHIC

RBRC Workshop, Baryon Dynamics at RHIC, March 28 – 30<sup>th</sup>, 02

Vasile Topor Pop



- Introduction
- Outline of Theory. Baryons Stopping. Junction physics.
- Jet Quenching. Global Observables. Nuclear Modification factors.
- Stopping Power. Baryon Distributions. Ratios.
- Transverse Momentum Spectra.  $\frac{\bar{p}}{\pi^-}$  anomaly.
- Summary and Conclusions

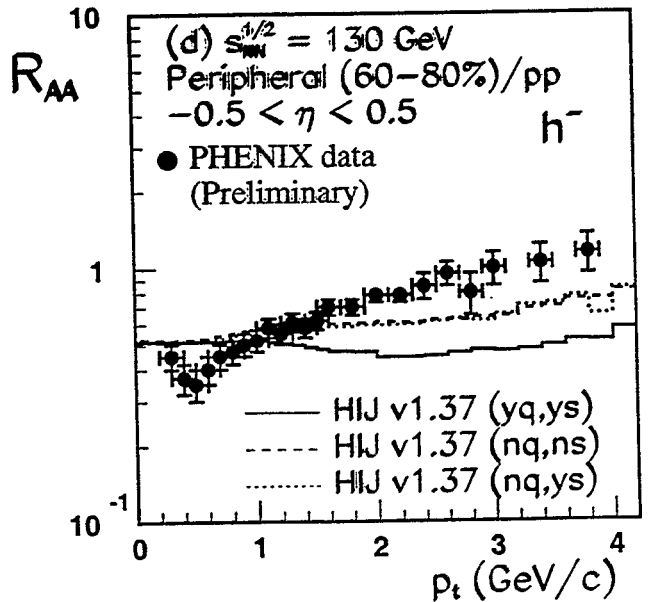
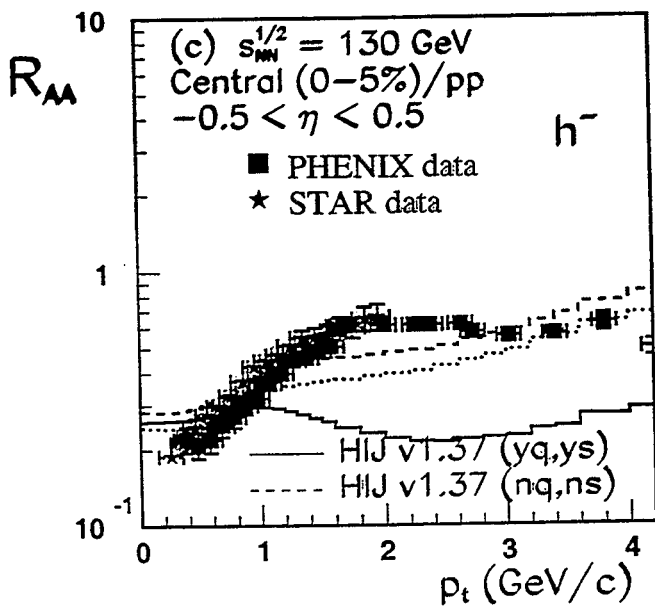
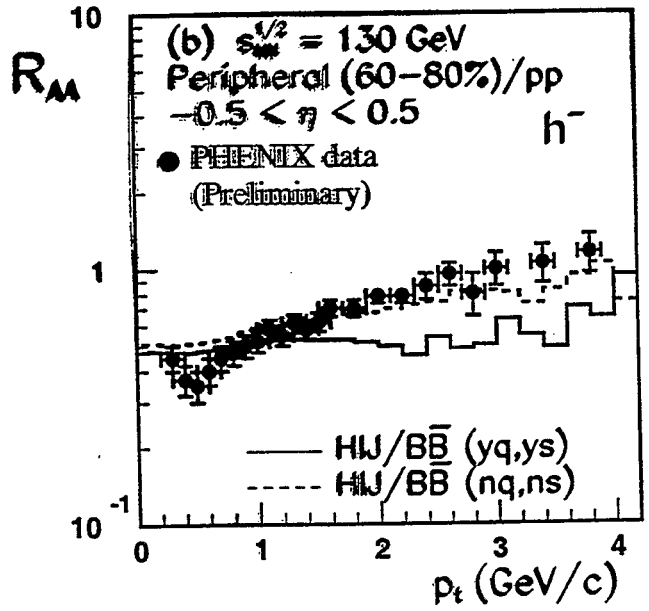
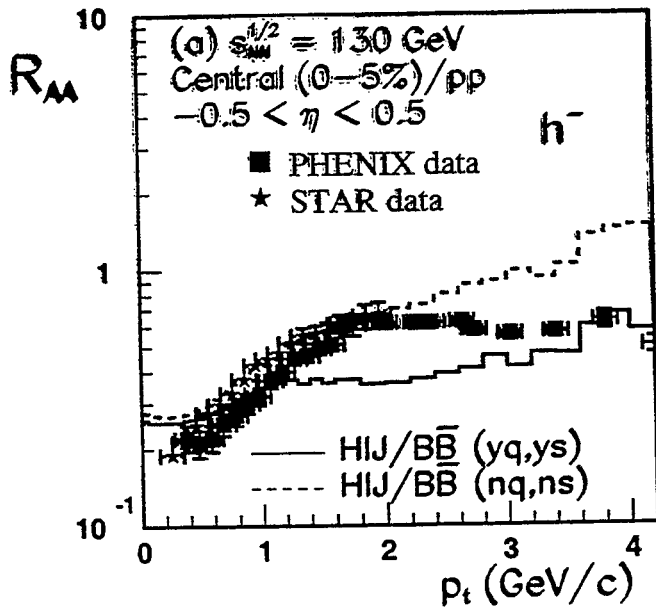
---

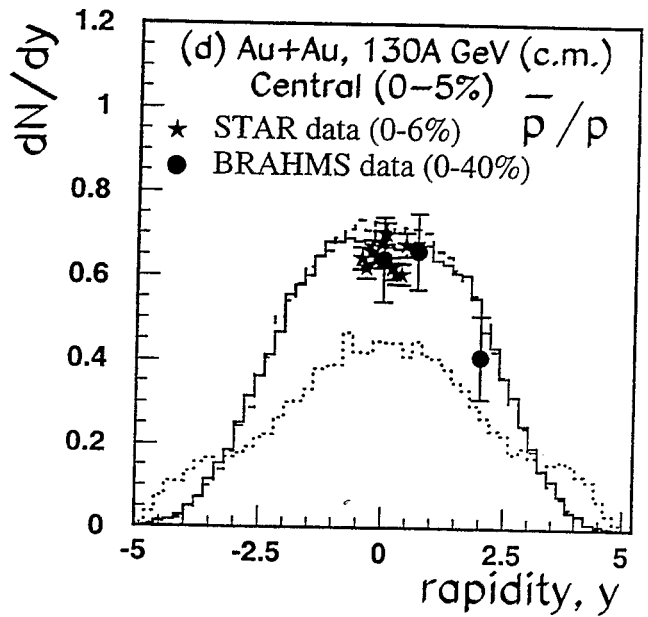
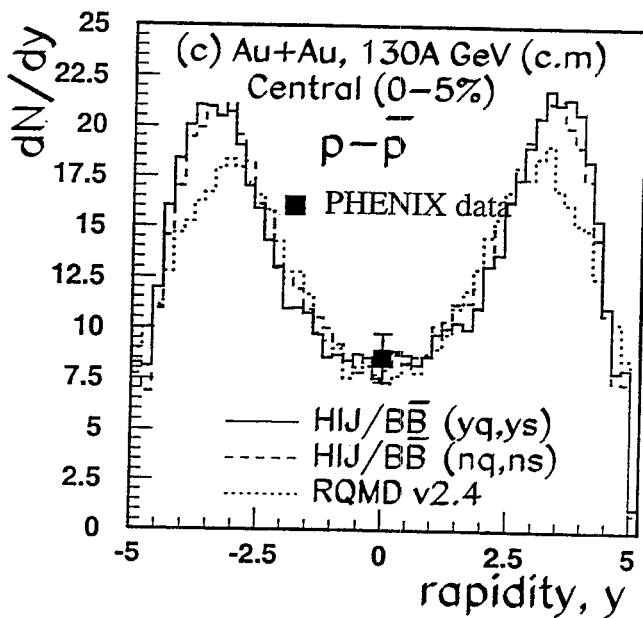
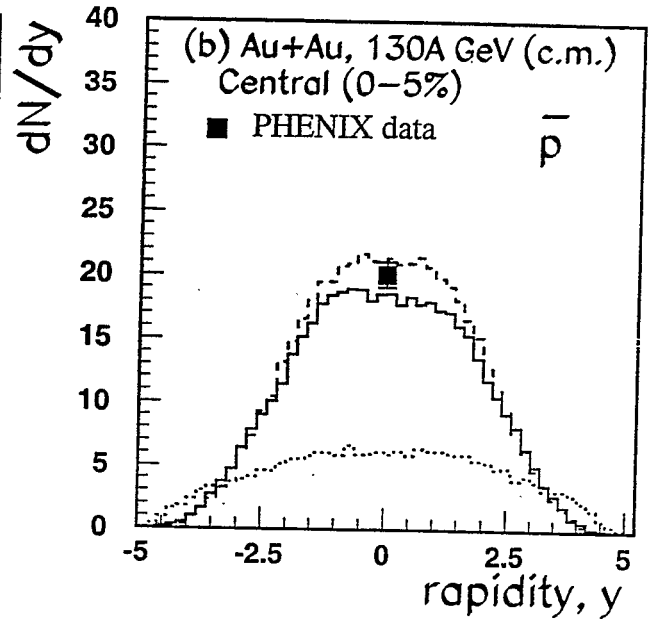
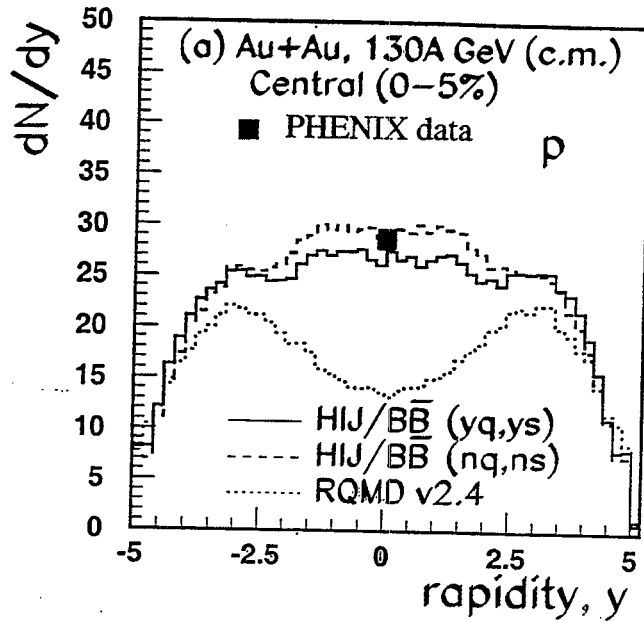
## HIJING/ $B\bar{B}$ v 1.10 Outline

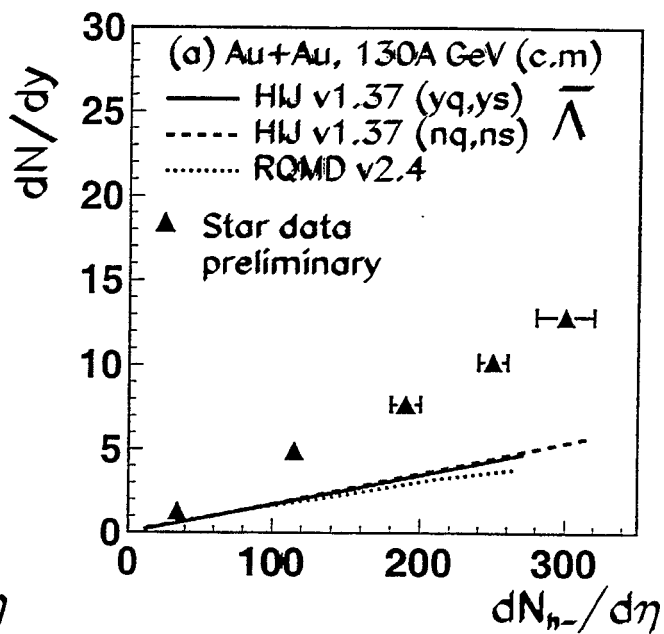
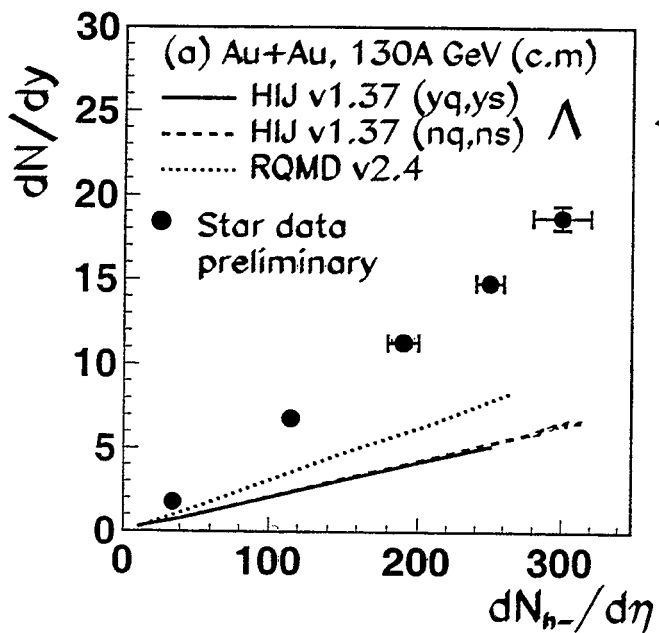
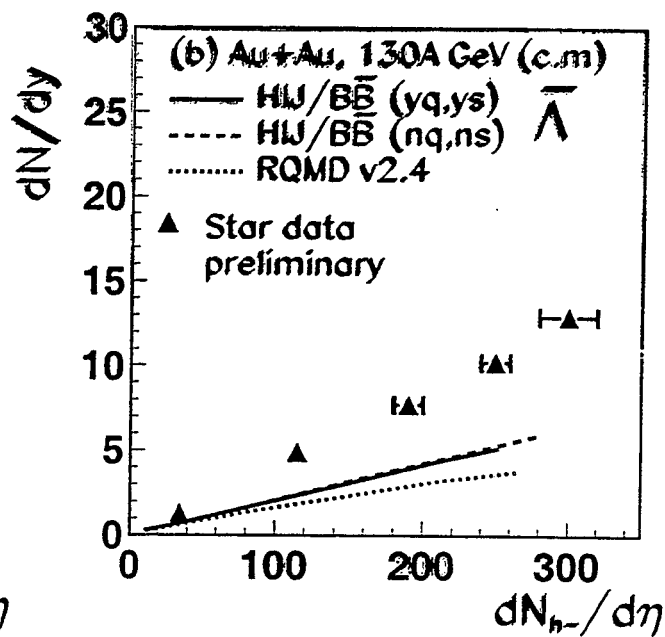
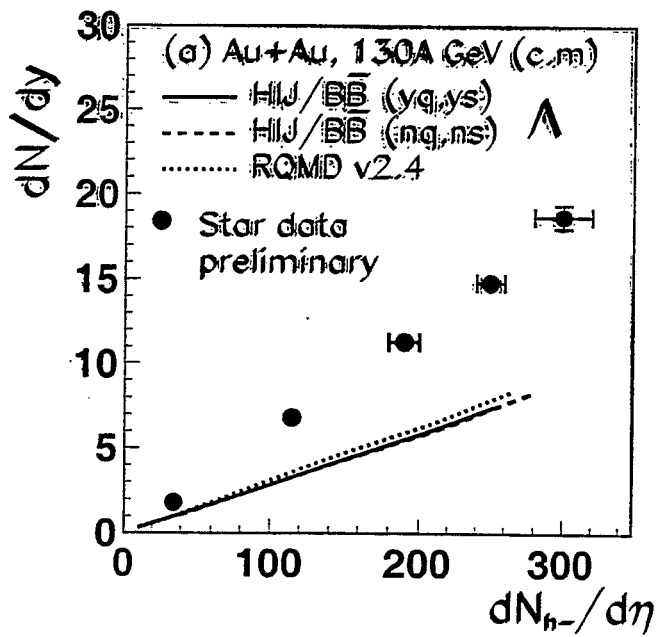
---

Experimental data at CERN-SPS on p+A and A+B interactions has revealed a large degree of stopping and strange hyperon production in the heavy nuclear systems. The stopping is significantly under-predicted by models which assume that the primary mechanism for baryon transport is diquark-quark hadronic strings (Gyulassy, Topor, Vance, 97).

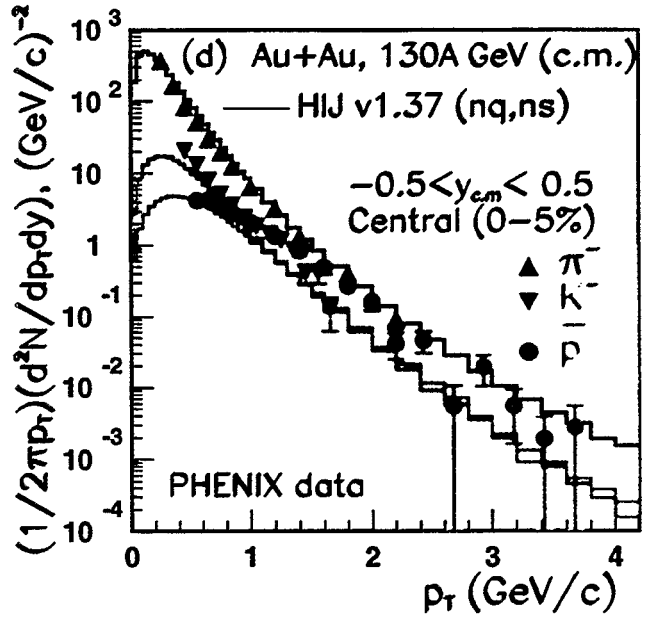
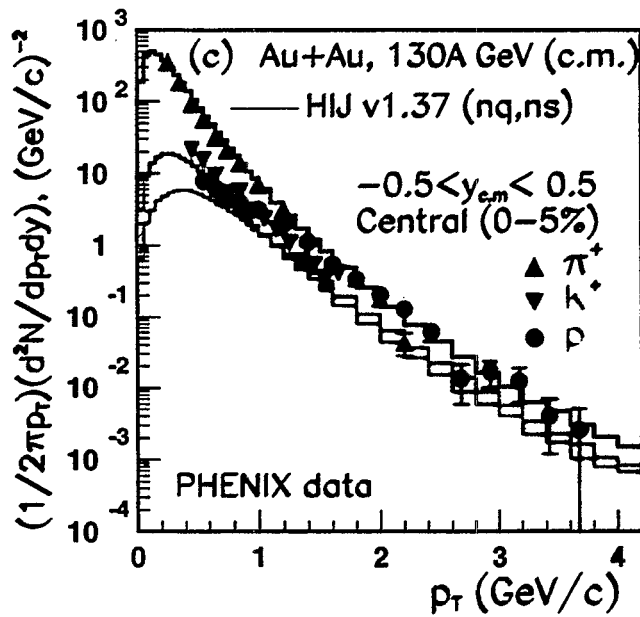
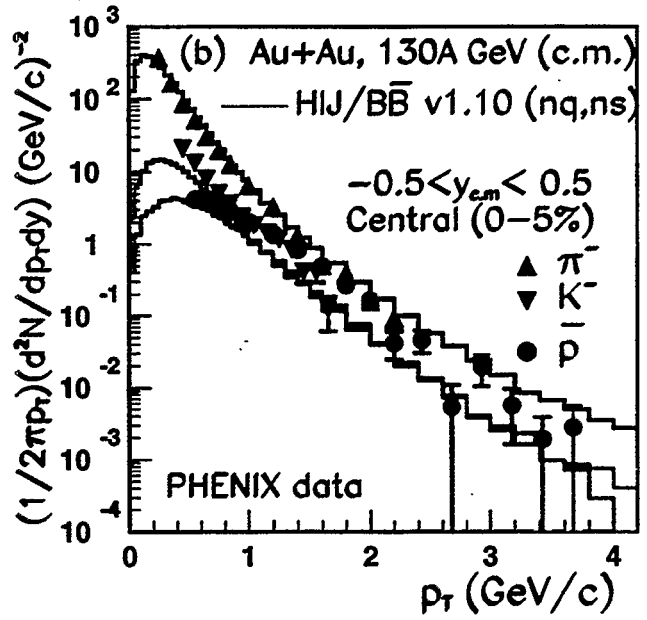
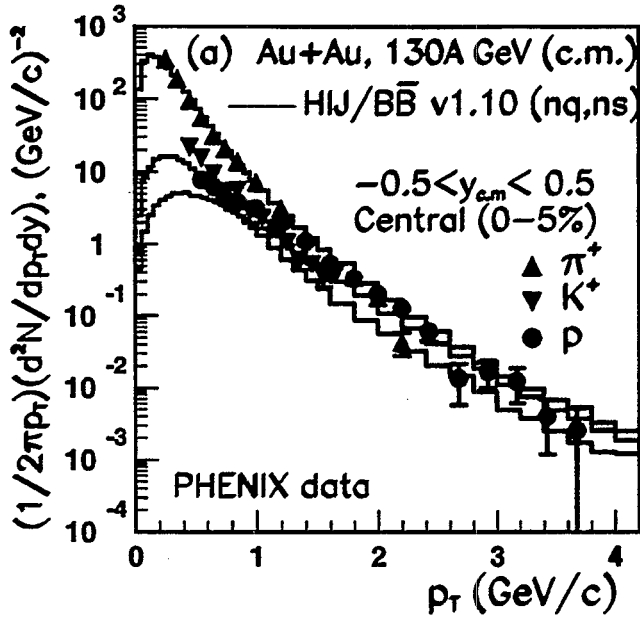
- Baryon junction mechanism, a novel non-equilibrium hadronic mechanism derived from the Y-shaped ( $SU_c(3)$ ) gluon structure of the baryon, has been introduced within HIJING/B to explain these observations. (Vance and Gyulassy, 98).
- The valence baryon junction exchange mechanism has been extended by including junction-antijunction ( $J\bar{J}$ ) loops that naturally arise in Regge phenomenology. HIJING/ $B\bar{B}$  v1.10, (Vance, Gyulassy and Wang, 99) is now available.
- Fitting  $\bar{p}$  and  $\bar{\Lambda}$  data from p+p and p+S interactions, the cross section for  $J\bar{J}$  exchange is found to be  $\sigma_{B\bar{B}} = 6$  mb. The threshold cutoff mass  $m_c = 6$  GeV, provides sufficient kinematical phase space for fragmentation of the strings and for  $B\bar{B}$  pair production. This kinematic constraint severely limits the number of allowed  $J\bar{J}$  configurations, reducing its effective cross section to  $\approx 3$  mb. **at SPS.**

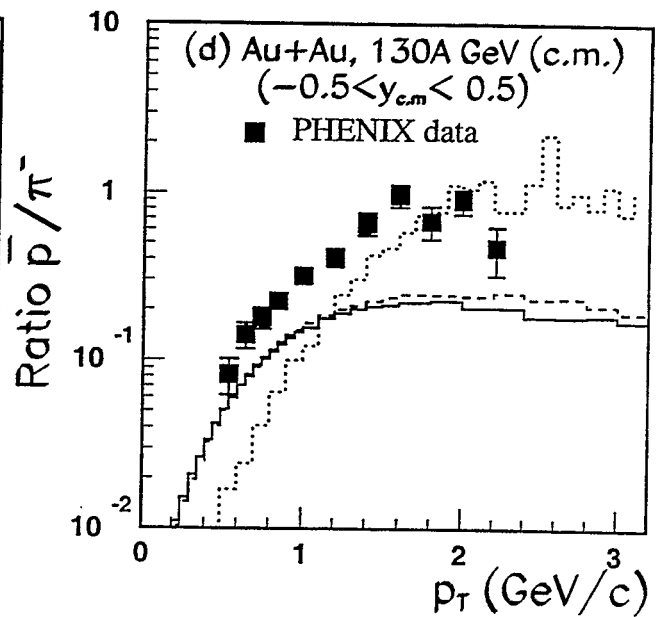
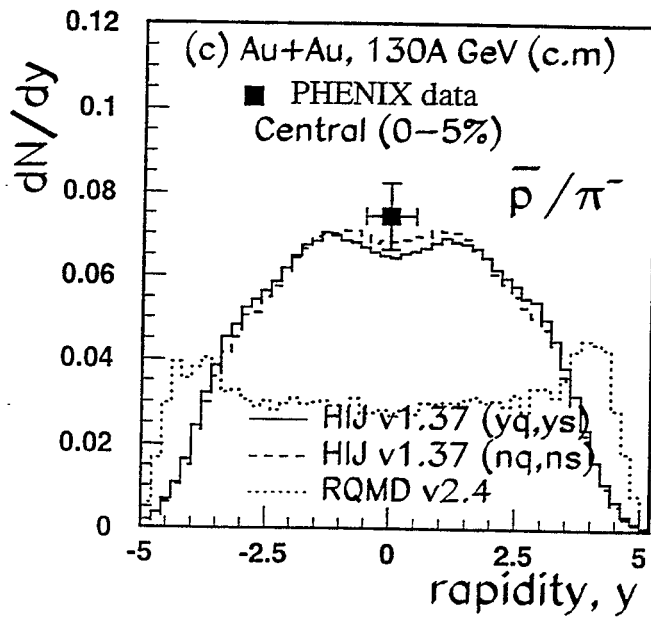
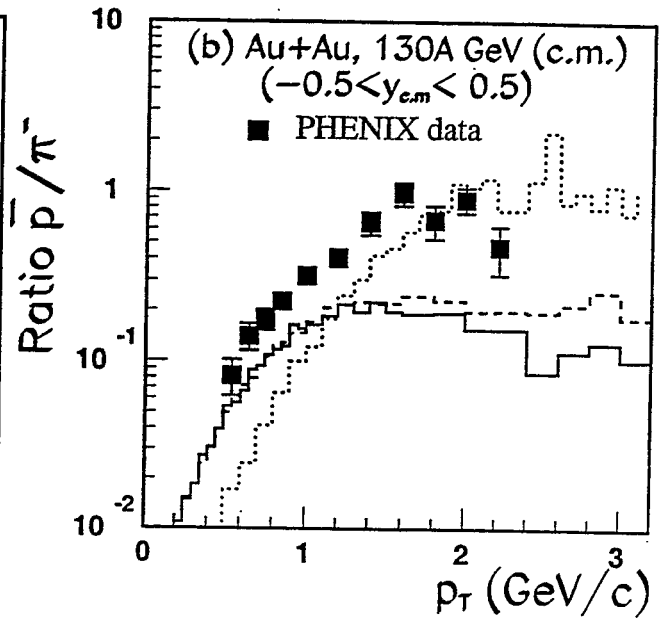
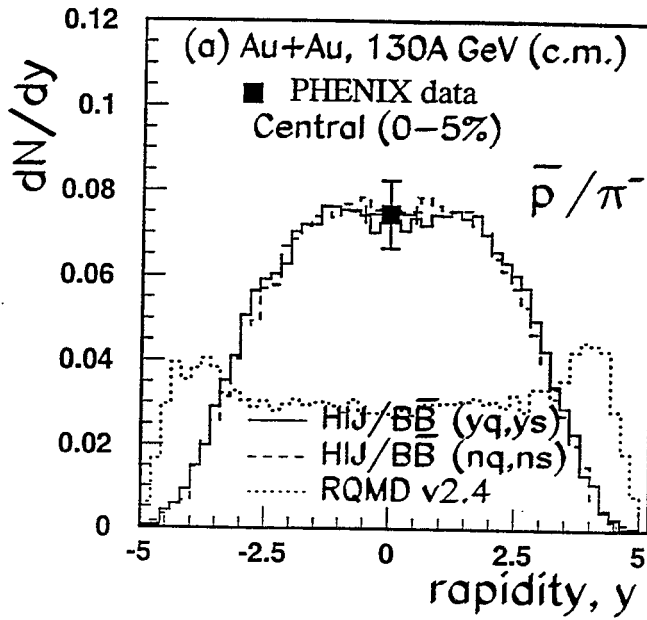


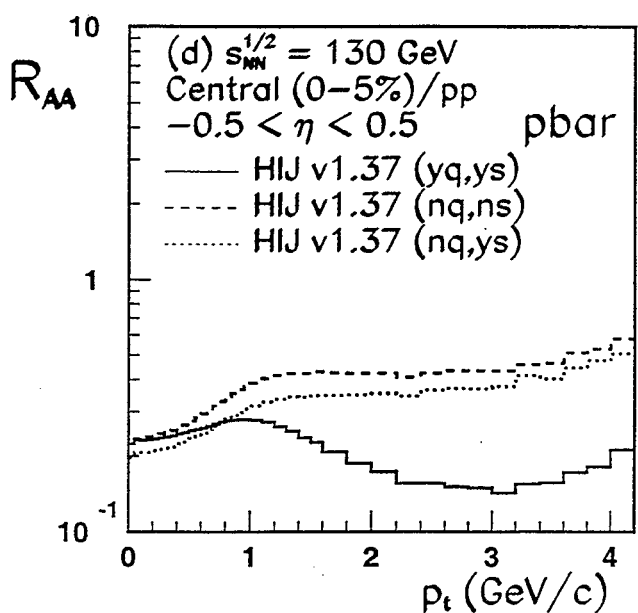
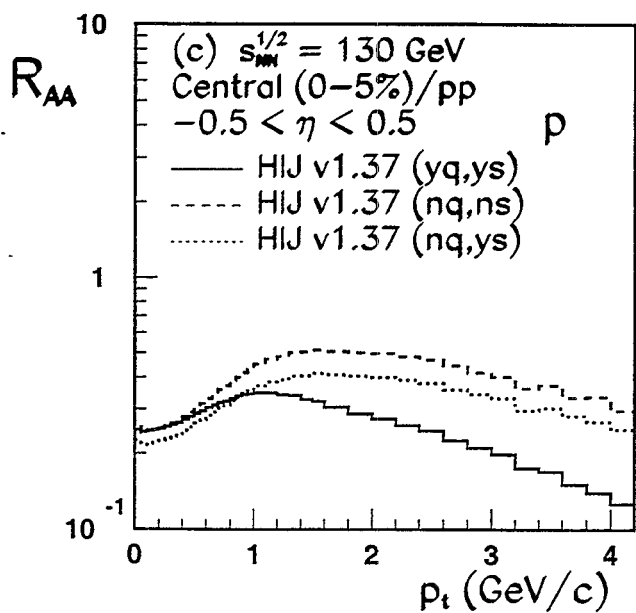
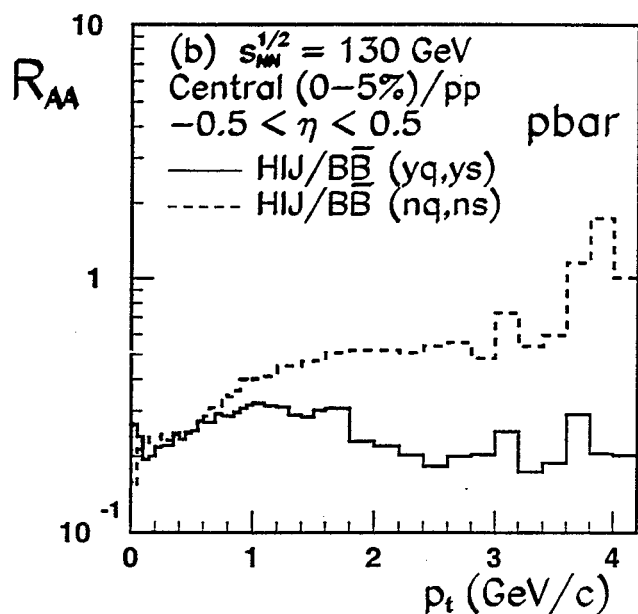
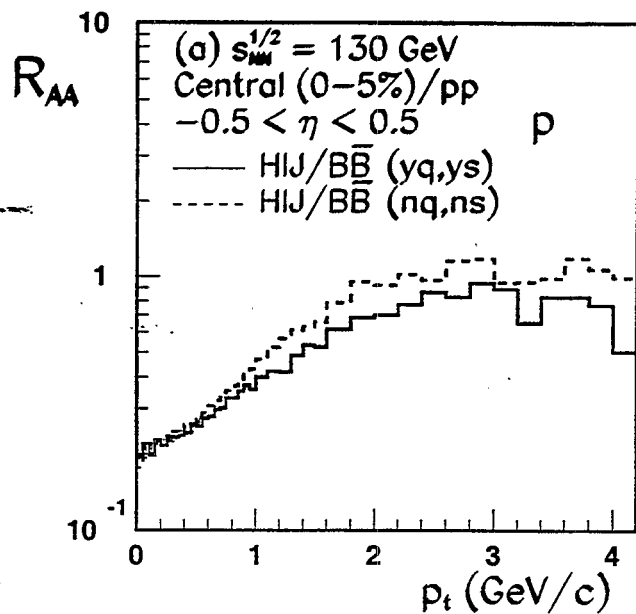












#### 4. Near future

- More data from future runs for p+p, p+A and Au+Au collisions at high  $p_{\perp}$  :, are required. Measurements of nuclear modification factors  $R_{AA}$  for  $p$ ,  $\bar{p}$ ,  $\Lambda$ ,  $\bar{\Lambda}$ .
- Data on baryon stopping in p+p and p+A collisions should be able to distinguish between the various stopping models.
- The role of the junction exchange in multiple collisions could be studied in p+A collisions.
- Finally, our detailed analysis reveal that none of the model offers at present a consistent description of the observed experimental features seen in the data.
- Further analysis and detailed comparison with data especially for identified particles spectra are necessary in the near future in order to study these interesting phenomena of interplay between soft and hard processes on different observables.

# The Relativistic Advection-Diffusion Equation

Derek Teaney

*Physics Department, Brookhaven National Laboratory, Upton, N.Y. 11973, U.S.A.*

Dissipative processes in relativistic fluids are known to create disturbance which grow exponentially [1]. This lead to a reformulation of the equations of motion by Müller and Werner Israel [2, 3]. The Müller-Israel equations are simply the Drude model applied to hydrodynamics. Here we examine the simplest of all possible of dissipative process – Diffusion. The Müller-Israel equations have the following desirable properties.

- They are derived by demanding that entropy always increase [2, 3]
- They closely model the short time response of the correlation function. The relaxation time which appears in the Drude model can be determined from from the correlation function [4].
- The form a hyperbolic system of equations [5]

The physical problem considered here is the following. I place a Gaussian drop of dye into a stream moving with a constant velocity,  $v=0.85c$ . In the non dissipative case the drop simply moves along with the stream. When diffusion is considered the drop spreads out with time. Of course for such a simple problem the solution is simple:

- 1) Go to rest frame of the stream. 2) In this frame the dye obeys the ordinary diffusion equation and the width of the drop increases with according to the following rule
- $$L^2(t) = L_o^2 + 2\lambda t; \quad (1)$$
- 3) Then boost this solution back to the frame where the fluid is moving at  $v=0.85c$ . This is the solution that

is given by the Landau-Lifshitz Relativistic Advection-Diffusion (LLRAD) equation. If the Müller-Israel Relativistic Advection Diffusion (MIRAD) equation differs from this solution, it is most certainly wrong.

The LLRAD equation is given in the first transparency. The MIRAD equation is given in the second transparency. In transparency three we analyze the eigen mode decomposition of the MIRAD equation and find two sound waves which propagate at a speed  $s_{\pm} = \frac{v \pm c_{\infty}}{1 \pm v c_{\infty}}$  where  $c_{\infty}^2 = \frac{\lambda}{\tau}$ .  $c_{\infty}$  is always less than one and is of order of the typical thermal velocity,  $c_{\infty} \sim v_{th}$ .  $c_{\infty}$  is determined by the short time response of the correlation function [4]. This is demonstrated in transparency four.

For the hydrodynamics the short time response of the correlation function should be irrelevant. Only the long the long time response should matter. Thus the final solution of the MIRAD equation should be independent of the the value of  $c_{\infty}$ . In transparency five the solution to MIRAD equation is given by the solid curves and is compared to the simple solution of the LLRAD equation. The solutions are very close to each over for a wide range of  $c_{\infty}$ . Thus the MIRAD equation provides a numerical way to finding the solution to the LLRAD equation which are numerically unstable [1]. The MIRAD equation has an additional parameter  $c_{\infty}$  but this parameter does not influence the solution. The MIRAD equation closely models the underlying short-time physics and therefore avoids unphysical solutions in the LLRAD equation which grow and ultimately swamp the real solution.

---

[1] W.A. Hiscock and L. Lindbolm, Phys. Rev. **D31**, 4 (1985).  
[2] I. Müller, Z. Phys. **198**, 329 (1967).  
[3] W. Israel, Ann. Phys. **100**, 310 (1976).  
[4] L.P. Kadanoff and P.C. Martin, Ann. Phys. **24** 419

(1963).  
[5] W.A. Hiscock and L. Lindbolm, Ann. Phys. **151**, 466 (1983).

The Advection Diffusion Equation:

Ideal Advection: Moving Along With the Stream

$$N^\mu = nu^\mu$$

Viscous Diffusion:

$$N^\mu = nu^\mu + J_D^\mu$$

For Navier Stokes:

$$J_D^\mu = \lambda(g^{\mu\nu} - u^\mu u^\nu)\partial_\nu n$$

In the rest frame of the fluid the conservation law becomes the ordinary diffusion equation:

$$\partial_\mu N^\mu = 0 \quad \rightarrow \quad \begin{cases} \partial_t n + \partial_x j = 0 \\ j = -\lambda \partial_x n \end{cases}$$

Problems:

- Two time derivatives make the initial value problem ill defined.
- Infinite propagation speeds for parabolic differential equations.
- A linear stability analysis shows that the small perturbations grow exponentially.

The Relaxation Time Approximation:

In the rest frame, it takes a time  $\tau_R$  for the current to relax. Make  $j$  a dynamic variable.

$$\begin{aligned}\partial_t n + \partial_x j &= 0 \\ \partial_t j &= -\frac{(j + \lambda \partial_x n)}{\tau_R}\end{aligned}$$

For an Arbitrary Frame:

$$\begin{aligned}\partial_\mu N^\mu &= 0 \\ DJ_D^\mu &= -\frac{(J_D^\mu + \lambda \nabla^\mu n)}{\tau_R}\end{aligned}$$

where

$$\begin{aligned}N^\mu &= nu^\mu + J_D^\mu \\ DJ_D^\mu &= u^\alpha \partial_\alpha J^\mu \\ \nabla^\mu &= (g^{\mu\nu} - u^\mu u^\nu) \partial_\nu\end{aligned}$$

Questions:

- What is the relation of the relaxation time to the microscopic correlation function.
- Is this theory causal.
- Can I solve this system.
- Long time physics should be insensitive to short timescales in the problem.

## The Reimann-Characteristic Problem

Write the equations of motion in the following form:

$$\begin{pmatrix} \mathbf{B} \end{pmatrix} \begin{pmatrix} \partial_t n \\ \partial_t j \end{pmatrix} + \begin{pmatrix} \mathbf{A} \end{pmatrix} \begin{pmatrix} \partial_x n \\ \partial_x j \end{pmatrix} = \begin{pmatrix} 0 \\ -j/\tau \end{pmatrix}$$

The eigen values/vectors of  $\mathbf{B}^{-1}\mathbf{A}$  are the signal velocities of the equation of motion.

$$s_{\pm} = \frac{v \pm c_{\infty}}{1 \pm v c_{\infty}}$$
$$c_{\infty}^2 \equiv \frac{\lambda}{\tau}$$

- Disturbances propagate with speed  $c_{\infty}$  in the local reference frame.
- $c_{\infty}$  is of order the typical thermal velocity.
- If choose  $\tau$  arbitrarily then the signals propagate faster than the speed of light.



The Werner-Israel Equation at short times

$$\partial_t^2 n + \frac{\partial_t n}{\tau} + \frac{\lambda}{\tau} \partial_x^2 n = 0$$

$$\text{Initial Conditions} = \begin{cases} n = n(0) \\ \partial_t n = 0 \end{cases}$$

At short times the correlator (after spatial fourier transforming)

$$\partial_t^2 \langle n(t)n(0) \rangle_k \Big|_{t=0} - \left[ \frac{\lambda}{\tau} \right] k^2 \langle n(0)n(0) \rangle_k = 0$$

- The short time behaviour is determined by the combination  $\frac{\lambda}{\tau}$
- $\frac{\lambda}{\tau}$  is of order a typical thermal velocity squared  $v_{th}^2$

To find  $\frac{\lambda}{\tau}$ , use the Fluctuation Dissipation Theorem:

$$2T \frac{\text{Im} \alpha(k, \omega)}{\omega} = (nn)_{k\omega}$$

where

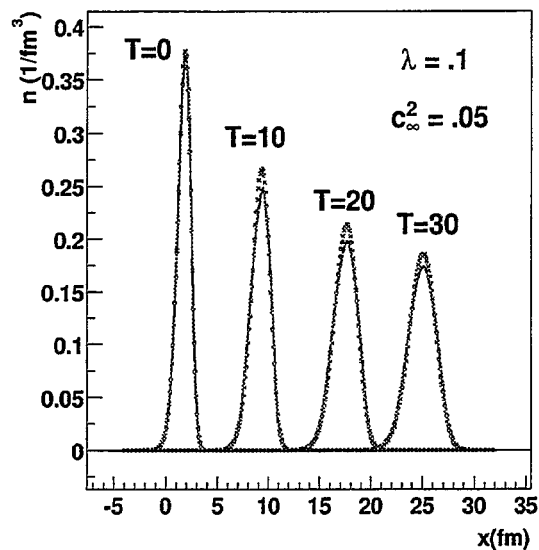
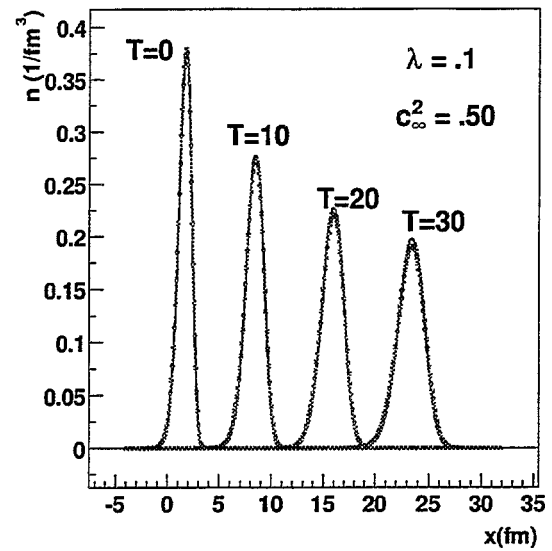
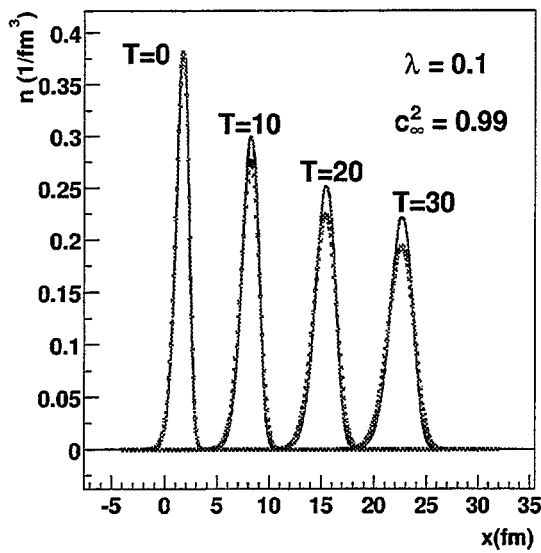
$$\alpha(k, \omega) = (i\theta(t)[n(t), n(0)])_{k\omega}.$$

We find:

$$\lim_{k \rightarrow 0} \int \frac{d\omega}{2\pi} \omega^2 2T \frac{\text{Im} \alpha(k, \omega)}{\omega} = k^2 \left[ \frac{\lambda}{\tau} \right] \langle n^2 \rangle$$

There is a sum rule relating this moment to the time derivative of the correlator at the origin.

## Small Diffusion Coefficient: $v=0.85$ !



- Red Points. Normal diffusing gaussian. The analytic solution to LLRAD of transparency #1.
- Blue Curve. The numerical solution to MIRAD equation of transparency #2.

# The $\bar{p}/\pi^-$ Anomaly at High $p_T$

Ivan Vitev

*Department of Physics, Columbia University  
538 W. 120-th Street, New York, NY 10027*

PHENIX data on  $Au + Au$  at  $\sqrt{s} = 130$  AGeV suggest that  $p$  and  $\bar{p}$  yields may exceed  $\pi^+$  and  $\pi^-$ , respectively, at high  $p_T > 2$  GeV/c. STAR data reveal a high valence proton rapidity density ( $\sim 5 - 10$ ), five units from the fragmentation regions, and a  $\bar{p}/p \simeq 0.65$  at mid-rapidity. These and other data point to novel baryon transport dynamics playing role in nucleus-nucleus reactions.

An attractive dynamical model that explains copious mid-rapidity baryon and anti-baryon production is based on the existence of topological gluon field configurations (baryon junctions and junction-antijunction loops). Junctions predict long range baryon number transport in rapidity as well as hyperon enhancement (including  $\Omega^-$ ) and considerable  $p_T$  enhancement relative to conventional diquark-quark string fragmentation. We propose that the anomalously large baryon/meson ratio as a function of  $p_T$  is due to the interplay between the jet quenched perturbative regime of hadron production and the non-perturbative QCD inspired string fragmentation mechanism. The onset of the perturbative regime depends on the mass and quark content of the hadron and can be estimated experimentally through the onset of the power law versus the  $m_T$  exponential behavior of the spectra.

In standard Regge phenomenology a Regge trajectory  $J = \alpha(0) + \alpha'(0)M_J^2$  is determined by its intercept  $\alpha(0)$  and slope  $\alpha'(0)$ . It has been argued that for junctions  $\alpha(0)_J = 0.5$  and  $\alpha'(0)_J \simeq \alpha'(0)_R/3$ . This relation through string fragmentation leads to  $\langle p_T \rangle^B \simeq \sqrt{3} \langle p_T \rangle^\pi$ . It is thus obvious that in the limit of baryon production dominated by baryon junctions and junction-antijunction loops our model predicts *approximately constant*  $\langle p_T \rangle$  for all baryon species. Corrections due to mass and phase space effects are expected to be small. The baryon junction mechanism also makes contact with  $pA$  and  $pp$  reactions where it was first proposed.

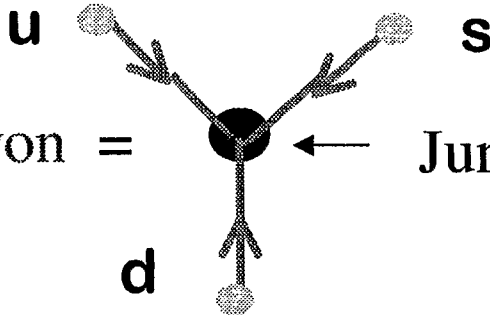
In the perturbative regime fast partons loose energy through gluon bremsstrahlung induced by multiple interactions inside the medium and for the case of jet production inside nuclear medium we have shown that  $\Delta E \sim C_R C_T \alpha^3 \int d\tau \tau \rho(\tau) \log 2E/\mu^2 L$ . Jet energy loss modifies the kinematics of the fragmentation functions into hadrons and is consistently included in the treatment of the perturbative part of hadronic spectra. At any given  $p_T$  it leads to suppression of hadrons relative to jet fragmentation in vacuum. For the  $2 \leq p_T \leq 5$  GeV/c region of interest this mechanism primarily reduces the number of perturbative pions and partly kaons.

We predict that the anomalously large  $p/\pi^+$  and  $\bar{p}/\pi^-$  ratios are limited to central and semi-central  $AA$  reactions where the quenching of pions is strong enough to expose the non-perturbative baryon junction component. In peripheral reactions the unquenched mini-jet fragmentation in mesons “obscures” the baryon junction string fragmentation contribution. We also predict that at high  $p_T > 5 - 6$  GeV/c where perturbative hadron production is dominant those ratios will converge to their PQCD computed baseline  $< 1$ . We finally note that our model suggests that it will be quite interesting to look for similar  $p_T$  and centrality behavior of the  $K/\Lambda$  ratios.

# Baryon Junctions

Veneziano, Rossi,  
NPB 123, (1977)

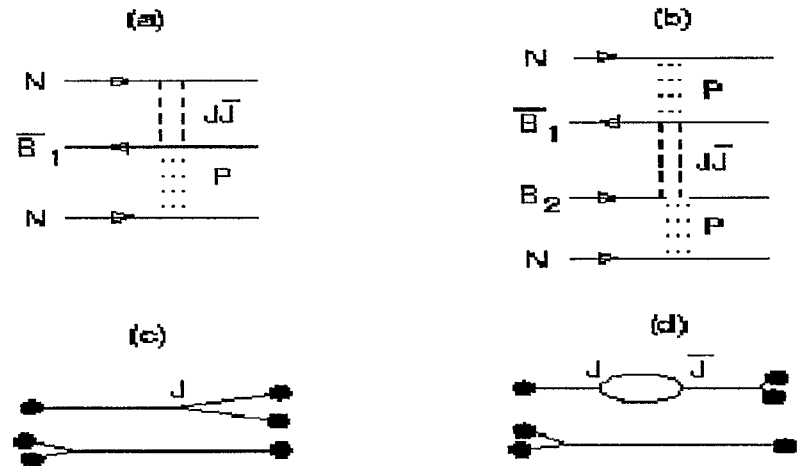
$$\text{Meson} = \bar{q}_{f'}(x_2)U(x_2, x_1)q_f(x_1) =$$



$$\text{Baryon} = \text{Junction } \Lambda = \epsilon_{i'j'k'} U^{i'i} U^{j'j} U^{k'k} u_i d_j s_k$$

- Baryon number transport via baryon junction exchange

D. Kharzeev, PLB 378,  
238 (1996)

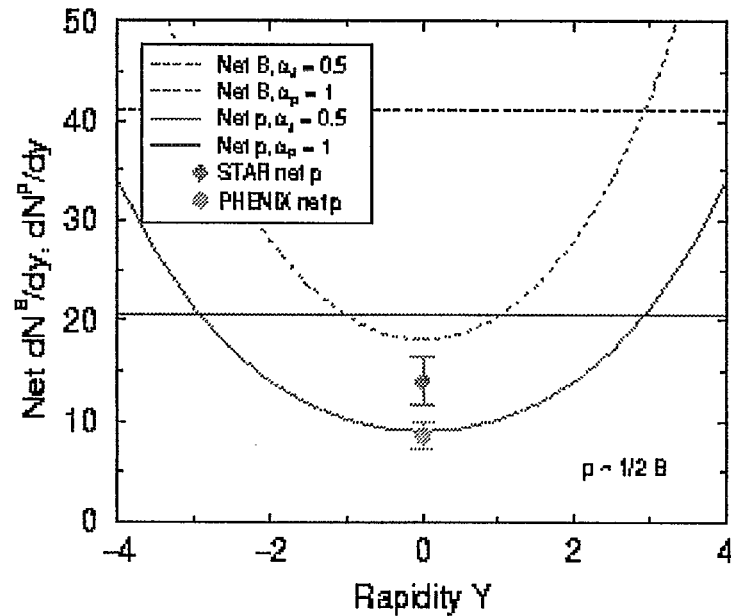


$$\frac{dN^{B-\bar{B}}}{dy} = (Z + N)(1 - \alpha_J(0)) \frac{\cosh(1 - \alpha_J(0))y}{\sinh(1 - \alpha_J(0))Y_{\max}}$$

(Integrates to 2A)

S. Vance, M. Gyulassy,  
PRL 83, 1735 (1999)

# Baryon Transport in Y and Moderate $P_T$



$\alpha_J = 0.5$  Not incompatible with data

$$\alpha_P = 1 \quad \frac{dN^B}{dy} = \frac{Z + N}{Y_{\max}} \quad (\text{off})$$

STAR PRL 87, 262302 (2001)  
PHENIX, submitted to PRL

In Regge type phenomenology:

$$J = \alpha(0) + \alpha'(0)M_J^2$$

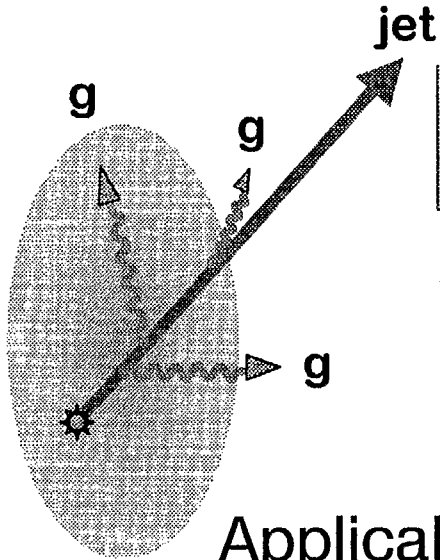
$\alpha'(0)$  Controls the “transport” in low to moderate  $p_T$ ,  $\kappa = 1/2\pi\alpha'$

D. Kharzeev,  
S. Vance :

$$\alpha'_J \simeq \frac{1}{3} \alpha'_R$$

May imply:  $T_B \simeq \sqrt{3}T_\pi$   
I.V., M. Gyulassy : Approx.  
constant  $\langle p_T \rangle$  for baryons

# Jet E-loss in QCD via the GLV Formalism



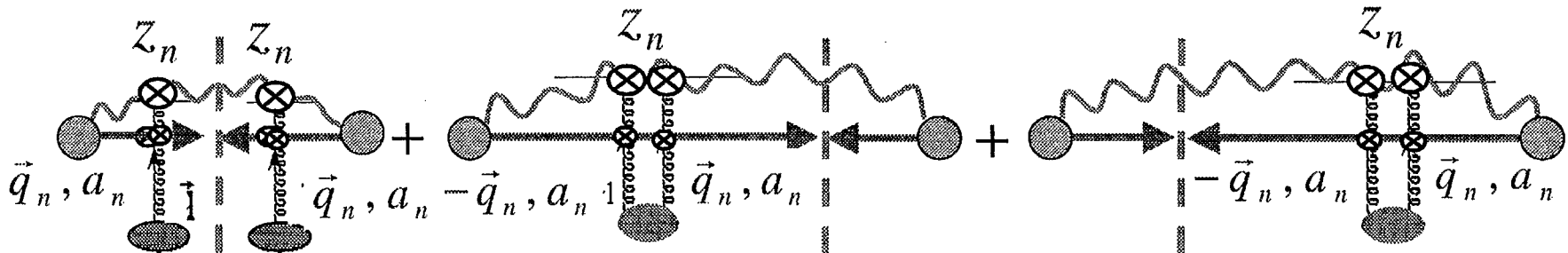
$$a) \Delta p_T^2_{GLV} \sim \alpha_s^2 \int d\tau \rho_{glue}(\tau, r(\tau)) \text{Log}\left(\frac{E_0 \mu}{\mu^2 L / \lambda}\right)$$

$$b) \Delta E^{(1)}_{GLV} \sim C_R \alpha_s^3 \int d\tau \tau \rho_{glue}(\tau, r(\tau)) \text{Log}\left(\frac{2E_0}{\mu^2 L}\right)$$

Applicable for realistic systems created in A+A collisions

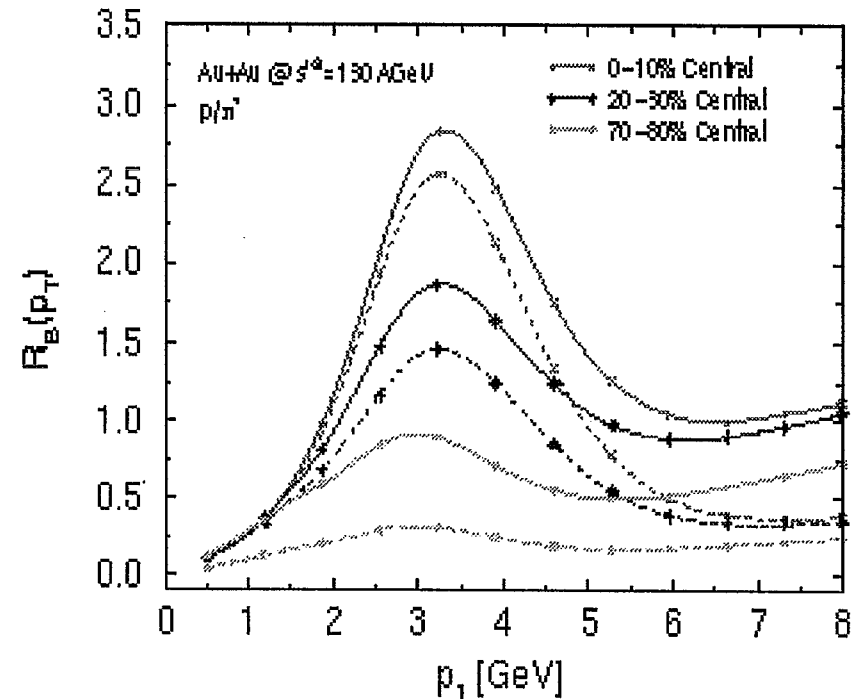
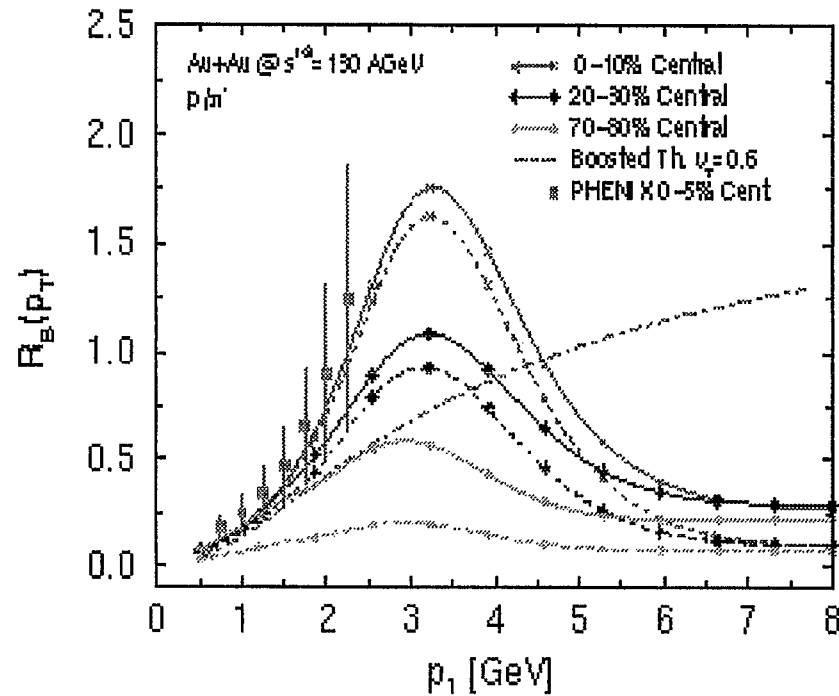
Algebraic recursive method (Reaction Operator Approach) is developed

M.Gyulassy, P.Levai, I.V.  
NPB 594, 371 (2001)  
PRL 85, 5535 (2000)



# Anomalous $p/\pi$ Ratios

I.V., M. Gyulassy, PRC in press

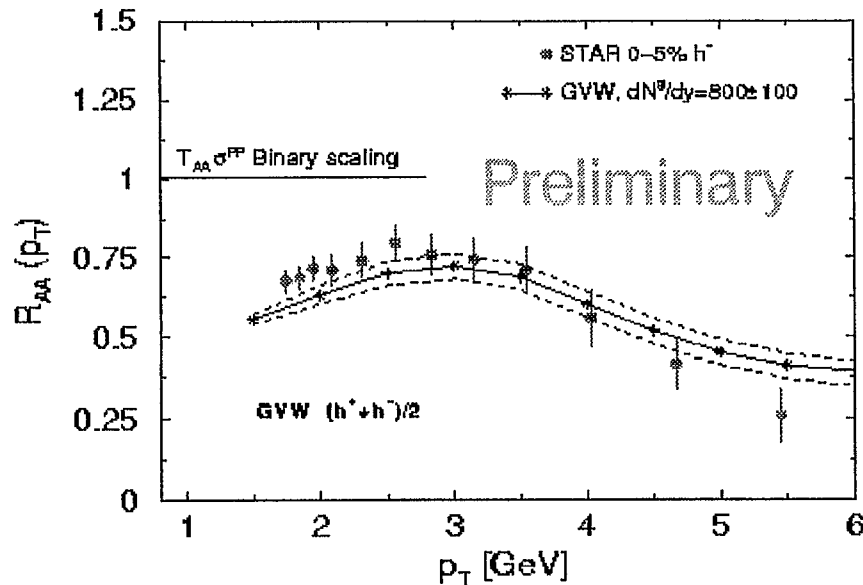


The  $p_T$  dependence of the ratios is predicted: the anomaly is limited to a finite  $p_T$  window.

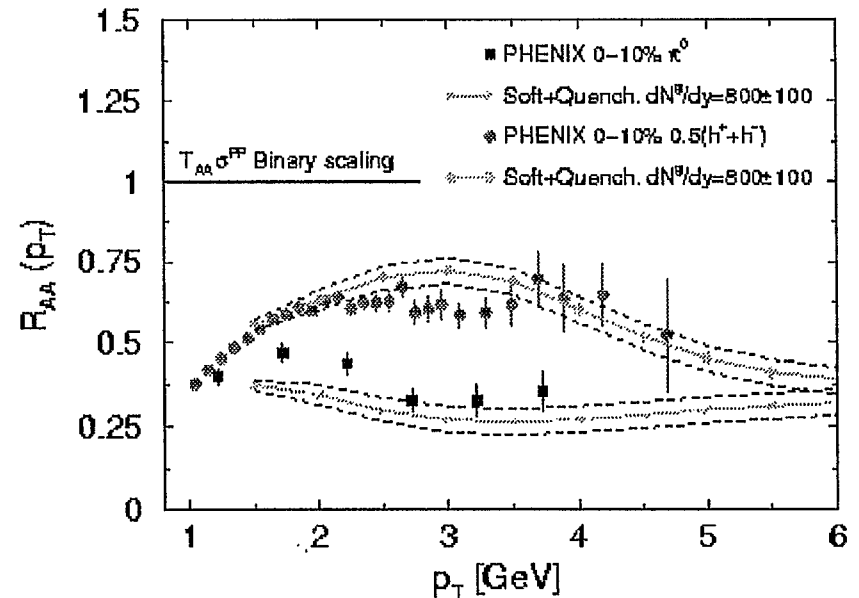
The centrality dependence of the ratios is predicted: the anomaly is limited to central and semi-central reactions.

# Suppression of Particle Spectra in a Two Component Soft+Hard Model

## STAR data

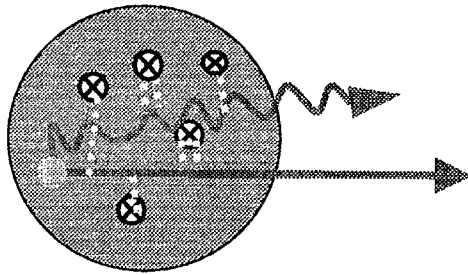


## PHENIX data

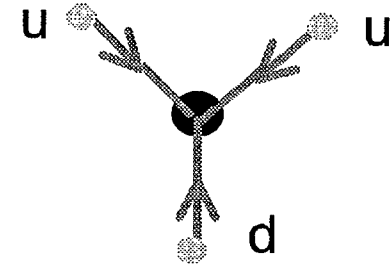


- Both STAR and PHENIX data are consistent with a factor of 2-3 suppression of the high  $p_T$  particle spectra.
- The difference in the suppression of  $\pi^0$  and inclusive charged hadrons can be understood in a dual soft+hard model with baryon transport dynamics.
- The extracted gluon rapidity density is  $dN^g/dy \sim 800$ .





## Conclusions



- In a two component model of pion and proton spectra we have incorporated the Baryon Junction phenomenology and the GLV-computed non-abelian energy loss of jets in a PQCD calculation
- We have predicted a very specific  $p_T$  and centrality dependence of the  $\bar{p} / \pi^-$  and  $p / \pi^+$  ratios (1 year ago)
- The model makes contact with existing data in p+p collisions where non-trivial  $p_T$  structure of the baryon/meson ratios is also observed
- From the suppression pattern of hadrons computed in the GLV formalism we extract  $dN^0/dy \sim 800$  at RHIC.
- The model gives a natural explanation of the different degree of suppression of  $\pi^0$  and inclusive charged hadrons



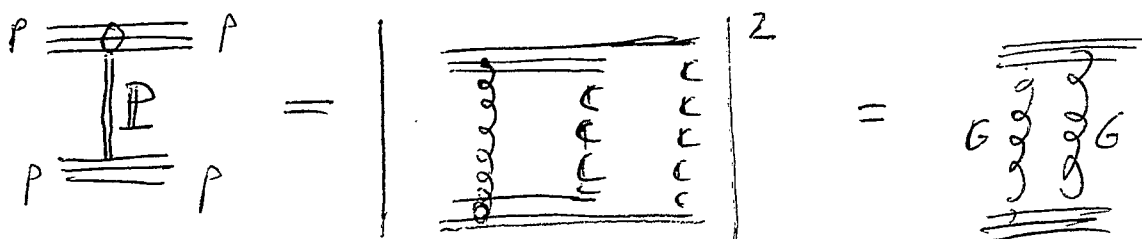
# Color Glass Condensate of Baryon Junctions

Boris Kopeliovich

BNL, March 28-30, 2002

- Perturbative QCD provides a surprisingly good quantitative description of many nonperturbative processes.

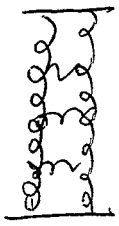
Example: the Pomeron



Two-gluon model for the Pomeron by  
F. Low and S. Nussinov.

! Predictions:  $\alpha_P(0) = 1$   $\sigma_{tot}^{PP} \sim 40 \text{ mb}$

Higher order QCD corrections push the Pomeron intercept up:

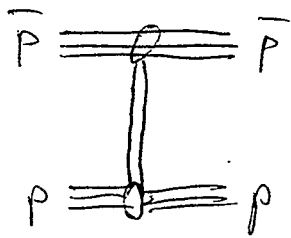


$$\alpha_P(0) = 1 + \Delta_P, \quad \Delta_P \approx 0.12 - 0.14$$

(if unitarity corrections are included)

## The Decameron

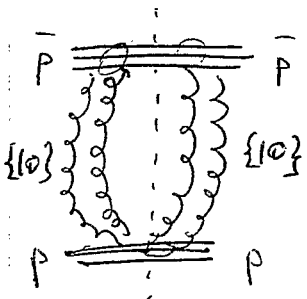
String junction - antijunction exchange



$$= \left| \begin{array}{c} \text{Junction} \\ \text{Antijunction} \end{array} \right|^2$$

G. Rossi & G. Veneziano  
1979

Perturbative interpretation: color-decuplet  $2G$  exchange



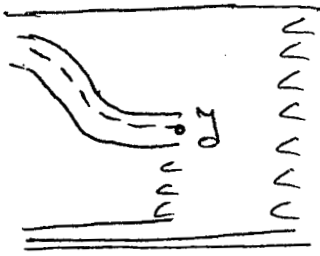
$$= \left| \begin{array}{c} \text{Decuplet} \\ \text{Exchange} \end{array} \right|^2$$

B.K.  
1987

Higher order QCD corrections in leading logs approximation:  $\alpha_D = 1 + \Delta_D$ ;  $\Delta_D > -\frac{3}{2} \Delta_P \approx -0.2$

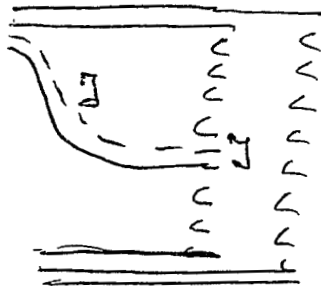
One can also estimate the absolute value of the  $\bar{p}p$  annihilation cross section in a good agreement with data!

# Baryon stopping



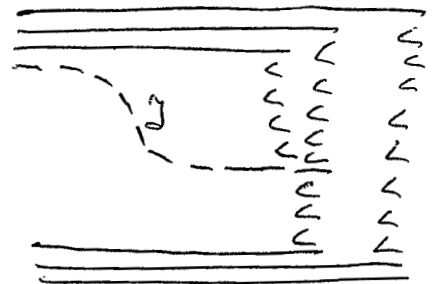
SJ transport  
by the diquark

$$e^{-\frac{3}{2} \Delta Y}$$



Valence quark  
plus junction

$$e^{-\frac{1}{2} \Delta Y}$$



Just junction  
exchange.

$$\nearrow \nearrow \sim \text{Const}$$

New mechanisms

B.K. & B. Zakharov, 1989

D. Kharzeev, 1996

$$(\alpha_{SJ} = \frac{1}{2})$$

The largest rapidity interval for stopping (7 units) is reached at HERA. Baryon asymmetry

$$A = 2 \frac{P - \bar{P}}{P + \bar{P}} = 7\% \quad \text{— predicted} \quad \text{B.K. \& B. Povh}$$

$$A = 8 \pm 1 \pm 2.5\% \quad \text{— measured by H1 Coll.}$$

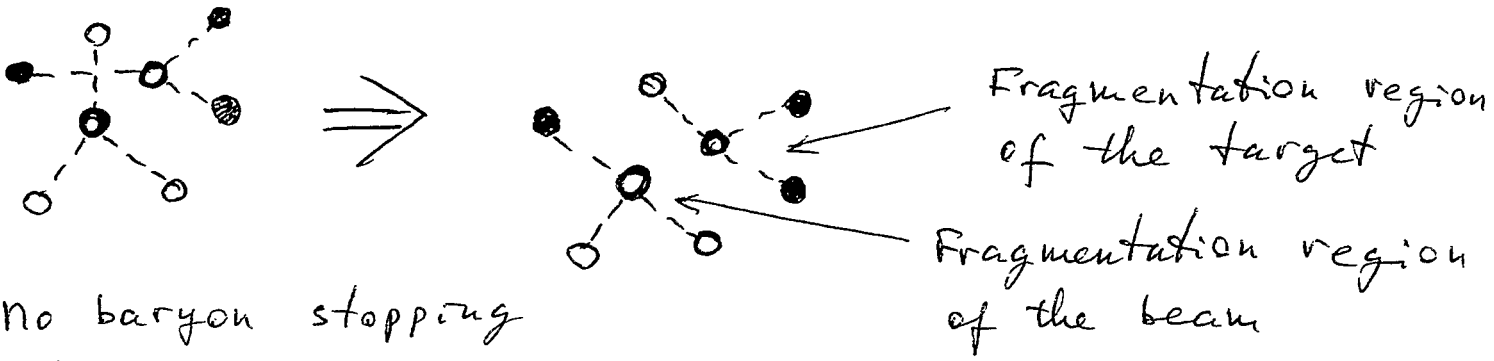
If  $\alpha_{SJ} = 1/2$ , then extrapolation of the ISR data to HERA gives  $A \lesssim 3\%$  — ruled out by the data.

# Novel mechanism of baryon stopping on nuclear targets

G. Garvey,  
B.K. & B. Povh  
2000

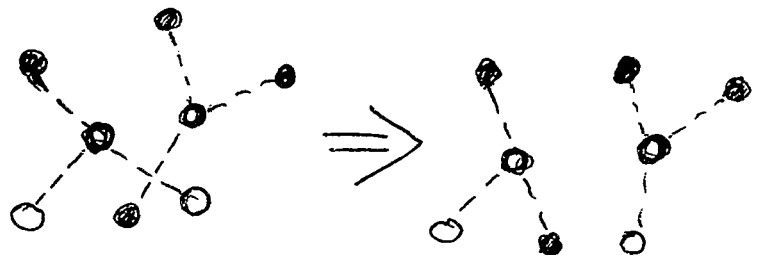
Two-step mechanism

- - beam quark
- - target quark



No baryon stopping happened

Next collision of the beam baryon junction:



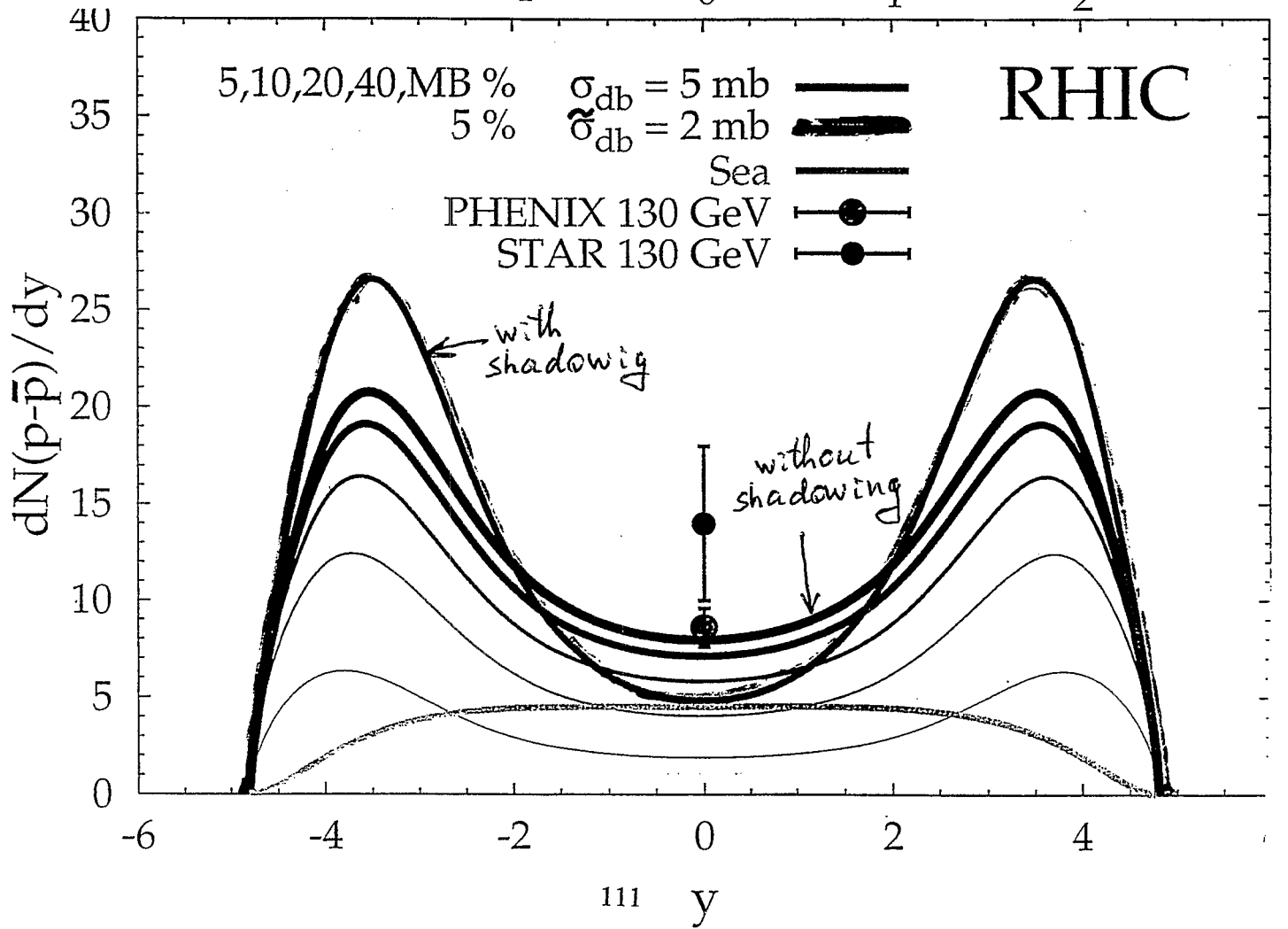
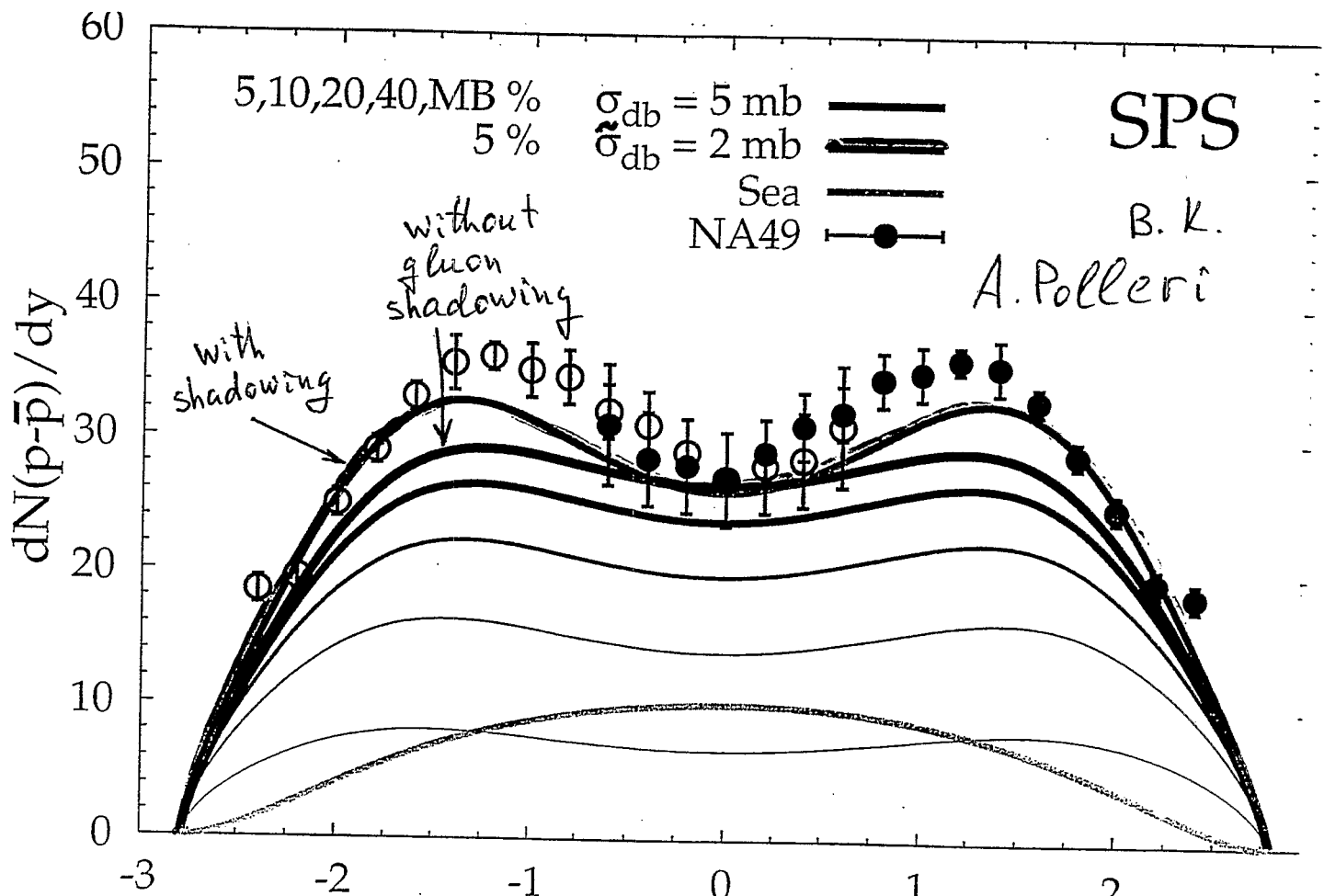
Both excited baryons have 2 target quarks, therefore, both string junctions are in the fragmentation region of the target - stopping

Since the central rapidity region is full of gluons the stopped  $\bar{3}$  stick with gluons at mid rapidities

The junction stops because of diquark breaking  $\{\bar{3}\} \Rightarrow \{6\}$ . The diquark breaking cross section

$$\sigma_{db}^N(\{qq\}_3^N \rightarrow \{qq\}_6^N) = \frac{\pi^2}{9} \alpha_s r_D^2 G_N(x, Q^2 = \frac{1}{r_D^2})$$

110 integrated gluon density



# Gluon saturation (color glass condensate)

!

Bjorken  $x$  are amazingly small

$$x = \frac{1}{F_D^2 S} \lesssim 10^{-5}$$

Shadowing is very strong

$G_A(x, Q^2)$  saturates and is  $x$ -independent

$\sigma_{db}^A$  is independent of energy and is rather small. ISR pp data for stopping need  $\sigma_{db}^A \approx 6 \text{ mb}$ .

Due to gluon shadowing  $\sigma_{db}^A \approx 2 \text{ mb}$ . Data for  $p-\bar{p}$  at SPS and RHIC are well described.

---

Junctions are stopped and produced from vacuum by the same mechanism. They are copiously produced in nuclei at small  $x$ , when gluon clouds overlap. They saturate like gluons.

## ● Predictions:

- baryons and antibaryons have the same  $P_T$  dependence (of gluons)
- saturation increases  $\langle P_T \rangle$  of  $\bar{p}$  and  $\bar{\Lambda}$  up to saturation scale: steep rise of  $\bar{p}/\pi^-$
- $\frac{\bar{p}}{p} \approx \frac{\bar{\Lambda}}{\Lambda} \approx \frac{\bar{\Xi}}{\Xi} = \frac{\bar{\Sigma}}{\Sigma}$  agree with data after isospin corrections (see talk by H.G. Fischer)



# Baryon Fluctuation

Sangyong Jeon  
McGill University  
RBRC

Collaborator: Volker Koch (LBNL)

## Fluctuation of Baryon Number

- What's the big idea?
  - \* Quarks carry  $Q_B = \pm 1/3$
  - \* Hadrons carry  $Q_B = 0, \pm 1$ .
  - \* If QGP, average  $\langle Q_B \rangle$  may be the same, but surely not the fluctuations  $\langle \delta Q_B^2 \rangle$ ?
  - \* Construct something resembling

$$R_{e^+e^-} \equiv \frac{e^+e^- \rightarrow \text{Hadrons}}{e^+e^- \rightarrow \mu^+\mu^-} = \sum_{f,c} Q_f^2$$

## How to measure $\langle \delta Q_B^2 \rangle$

- $Q_B$  is an extensive variable.

\*  $\langle \delta Q_B^2 \rangle$  contains volume (impact parameter, ...) fluctuation

$$\delta Q_B = \delta(n_B V) = \delta n_B \langle V \rangle + \langle n_B \rangle \delta V$$

\* Much better to use (no  $\delta V$ ) either

- Ratio fluctuation

$$\langle \delta R_B^2 \rangle \equiv \left\langle \delta \left( \frac{N_{\bar{B}}}{N_B} \right)^2 \right\rangle$$

or

- Voloshin's

$$\chi_B \equiv \left\langle \left( \frac{N_B}{\langle N_B \rangle} - \frac{N_{\bar{B}}}{\langle N_{\bar{B}} \rangle} \right)^2 \right\rangle = \left\langle \left( \frac{\delta N_B}{\langle N_B \rangle} - \frac{\delta N_{\bar{B}}}{\langle N_{\bar{B}} \rangle} \right)^2 \right\rangle$$

\*  $\langle N_B \rangle \gg 1$  and  $\langle Q_B \rangle \ll \langle N_B + N_{\bar{B}} \rangle$

$$\langle \delta R_B^2 \rangle \approx \chi_B \approx 4 \frac{\langle \delta Q_B^2 \rangle}{\langle N_B + N_{\bar{B}} \rangle^2} \left( 1 + O \left( \frac{\langle N_B - N_{\bar{B}} \rangle^2}{\langle N_B + N_{\bar{B}} \rangle^2} \right) \right)$$

\* At RHIC,  $N_{\bar{B}} = 0.75N_B$  or

$$\left( \frac{\langle N_B - N_{\bar{B}} \rangle}{\langle N_B + N_{\bar{B}} \rangle} \right)^2 \approx 0.02$$

Hence

$$\langle \delta Q_B^2 \rangle \approx \langle \delta R_B^2 \rangle \langle N_B + N_{\bar{B}} \rangle^2 / 4$$

up to at most 10% error. Gets better at LHC.

## QGP Result

- Assume entropy conservation
- For a non-interacting QGP

$$\begin{aligned} S_{\text{total}} &= 4 \times \left( \sum_{q=f,s,c} (\langle N_q \rangle + \langle N_{\bar{q}} \rangle) + 16 \times \langle N_g \rangle \right) \\ &\approx 7 \sum_{q=f,s,c} (\langle N_q \rangle + \langle N_{\bar{q}} \rangle) \end{aligned}$$

- $D_B = \frac{\langle \delta Q_B^2 \rangle}{\langle N_B + N_{\bar{B}} \rangle} \approx \frac{1}{9 \times 7} = \frac{1}{63}$

$\implies$  About a factor of 2 reduction from the hadronic result  
(For the charge fluctuation, a factor of 3 to 4 reductions.)

## Relationship with Balance Function (w/ S.Pratt)

$$B(\Delta y|Y) = \frac{1}{2} \left( \frac{N_{-+}(\Delta y|Y)}{N_+(Y)} + \frac{N_{+-}(\Delta y|Y)}{N_-(Y)} - \frac{N_{++}(\Delta y|Y)}{N_+(Y)} - \frac{N_{--}(\Delta y|Y)}{N_-(Y)} \right)$$

$$\frac{\langle \delta Q^2 \rangle}{\langle N_{\text{ch}} \rangle} = 1 - \int_0^Y d\Delta y B(\Delta y|Y) + O\left(\frac{\langle Q \rangle}{\langle N_{\text{ch}} \rangle}\right)$$

- $Y \rightarrow \infty \implies D \rightarrow 0$  — Charge conservation
- The sharper the  $B \implies$  The smaller the  $D$

## Conclusions

- If QGP,  $\langle \delta Q_B^2 \rangle / S_{\text{tot}}$  reduces by a factor of 2 mainly due to  $Q_B = \pm 1/3$  for quarks.
- It's better to use either the ratio fluctuation of Voloshin's  $\chi_B$  than to directly measure  $\langle \delta Q_B^2 \rangle$  — Avoid impact parameter fluctuation.
- Most serious Caveat is the diffusion in the hadronic stage  $\implies$  Need  $y_{\text{corr}} \gg |\Delta y| \gg y_{\text{total}}$

# Baryons in AMPT Model

Zi-Wei Lin, Texas A&M University

March 29, 2002

for  
Baryon Dynamics at RHIC Workshop  
RIKEN BNL Research Center

# Baryons in AMPT Model

Zi-Wei Lin

*Texas A&M University*

*work with C.M. Ko, B.A. Li, S. Pal and B. Zhang*

- A MultiPhase Transport model
- Baryon production/annihilation  
from/to multi-pion channels
- Popcorn scheme for baryon  
production
- Spectra at SPS
- Spectra at RHIC
- Summary

*Baryon Dynamics at RHIC 3/29/2002*

# Main Ingredients of AMPT Model

**HIJING** default version 1.36 (w/o jet quenching),  
using Lund fragmentation in JETSET/PYTHIA

Wang&Gyulassy, PRD44; 45;  
Gyulassy&Wang, Comp.Phys.Comm.83.

**ZPC** partonic 2-2 processes:  
 $gg \rightarrow gg, (gg \leftrightarrow qq\bar{q}, gq \rightarrow gq, \dots)$

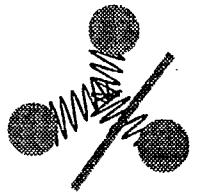
Zhang, Comp.Phys.Comm.109; Zhang,Gyulassy&Pang, PRC58.

**ART** hadronic interactions:  
Meson:  $\pi, \rho, \omega, \eta, K, K^*, \phi$ ;  
Baryon:  $n, p, \Delta, N^*(1440), N^*(1535), \Lambda, \Sigma, \Xi, \Omega$ .

Li&Ko, PRC52.

Ref to AMPT: Zhang et al, PRC61; Lin et al, PRC64, NPA698, PRC65.

# Schematic Representation for Baryon Number Transport Dynamics



→ Di-quark and quark Fragmentation  
Leading baryon + meson

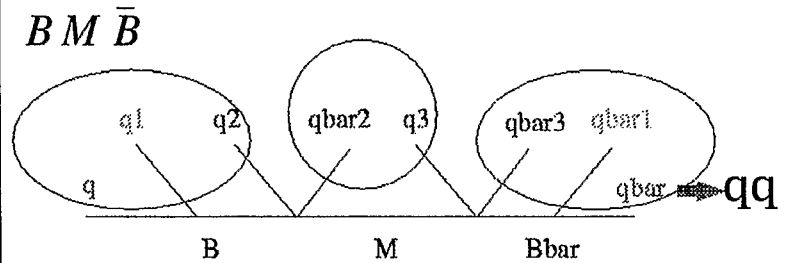
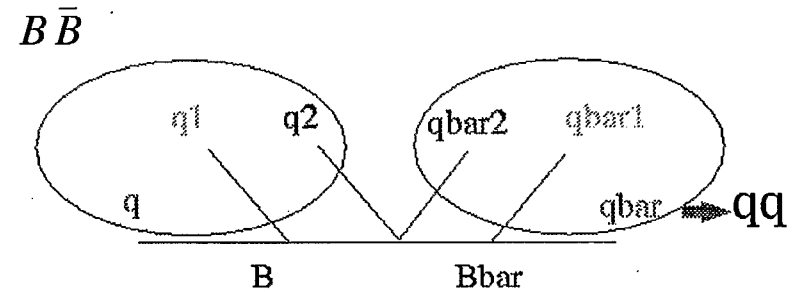
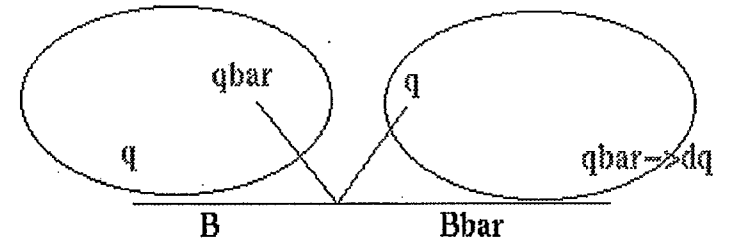


→ Three quark Fragmentation  
Leading baryon + meson + meson



→ Gluon Junction Fragmentation  
Leading meson + meson + meson  
and a Baryon

With popcorn scheme:

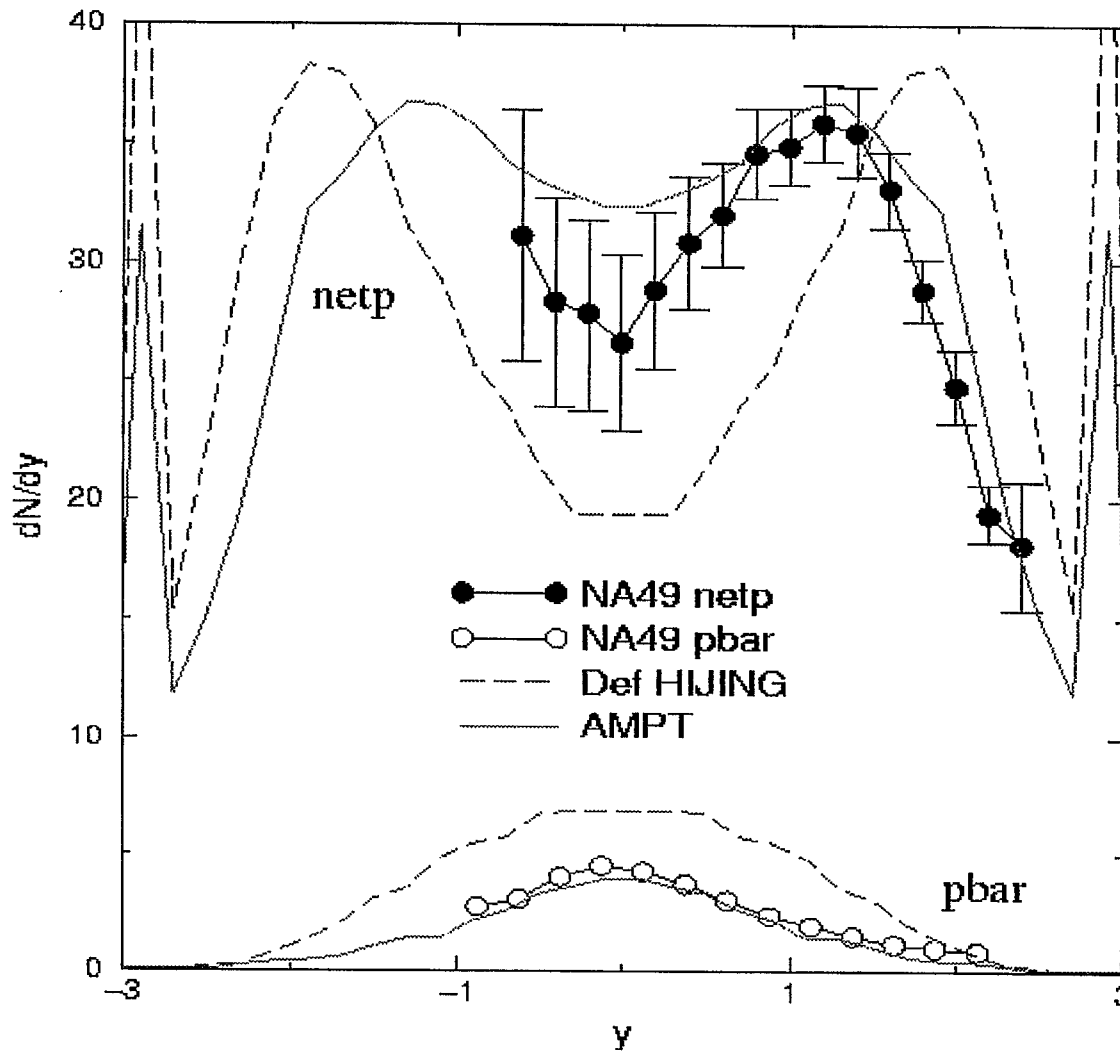


From H. Huang  
at this workshop



# Rapidity spectra at SPS

SPS  $b=0-3$  fm



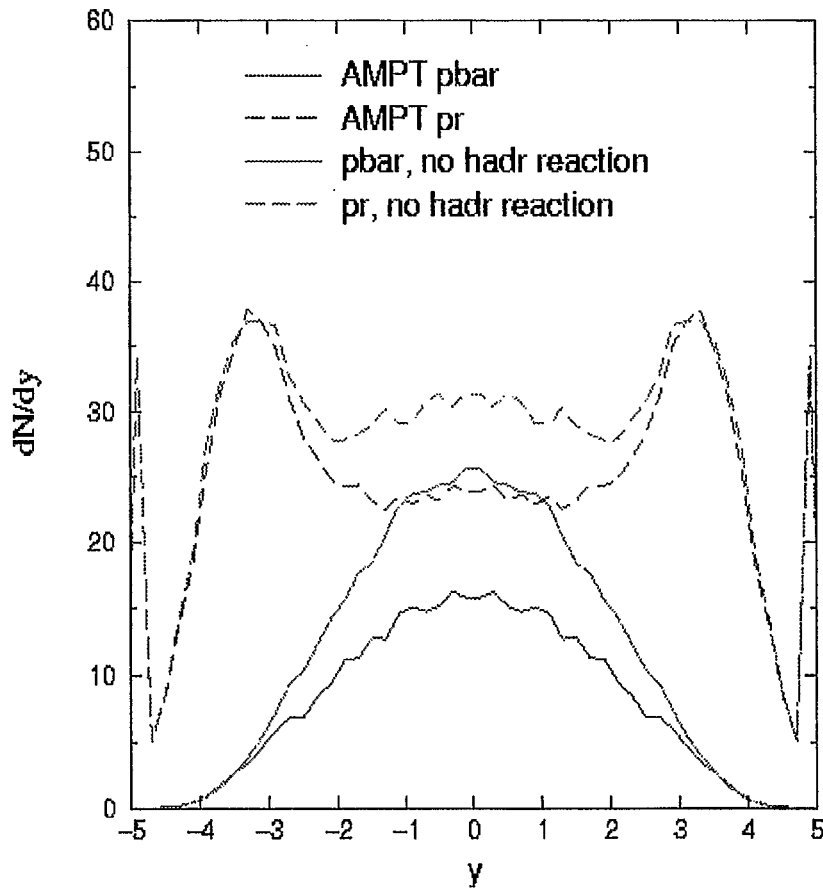
Rapidity shift due to popcorn scheme in Lund fragmentation..

pbar yield decreases from HIJING due to more annihilation than production (annihilation alone gives too low)

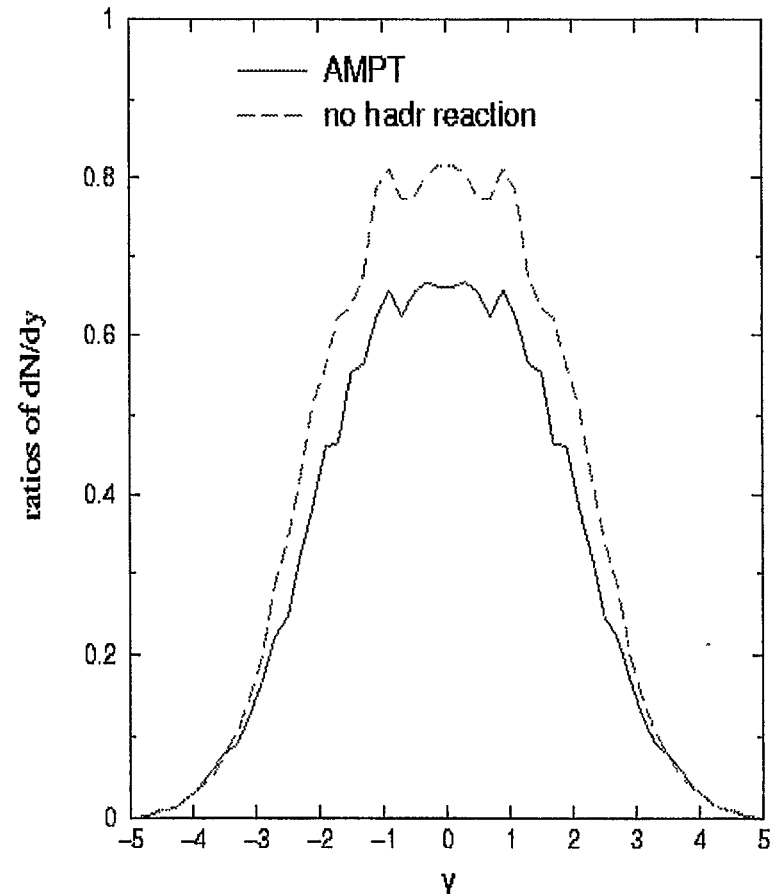
# Rapidity spectra at RHIC

# P/Pbar Ratio

130 GeV Au+Au (b=0-3 fm)



130 GeV Au+Au (b=0-3 fm)



For comparison with data from BRAHMS,  
see I. Bearden's talk at this workshop

# Summary

- AMPT model fits (net-)baryon stopping at SPS  
by popcorn scheme. (~~gluon junction fragmentation)
- Pbar yields: important contribution from  
BBbar $\leftrightarrow$ multi-pion channels
- From SPS to RHIC energy  
proton dN/dy yield has a minimum  
pbar/p ratio increases rapidly
- Final-state rescatterings  
increase  $m_T$  slope of heavy particles at SPS and RHIC  
responsible for  $p \sim \pi^+$  at  $P_T \sim 2$  GeV at RHIC 130G



# Reviving the Strong Coupling Expansion: Baryon Junctions and Other “Resonances”

Momchil Velkovsky, StonyBrook  
March 29, 2002

for  
Baryon Dynamics at RHIC Workshop  
RIKEN BNL Research Center

# REVIVING THE STRONG COUPLING EXPANSION : BARYON JUNCTIONS AND OTHER "RESONANCES"

- Strong coupling expansion in QCD
- Improved SCE; junctions and "resonances"
- Renormalization group: two representations
- SC diagrams and classical fields

Momchil Velkovsky

3/30/02

# REVIVING THE STRONG COUPLING EXPANSION: THE IDEA

- Add a hierarchy of extra terms to the lattice action (irrelevant operators), reducing the lattice artifacts at comparatively rough lattices and comparatively strong coupling.
- Hope that with the extra terms, the convergence of the SCE improves and it is applicable at smaller couplings.

Momchil Velkovsky

3/30/02

## STRONG COUPLING

On the lattice:  $S = \beta \sum_{\square} \left[ 1 - \frac{1}{N} \Re \text{Tr} (U_{ij} U_{jk} U_{kl} U_{li}) \right]$

$$\beta = \frac{2N}{g_0^2}, \quad \langle O \rangle = Z^{-1} \int (DU) O(U) e^{-S(U)}$$

Group integrals (N=3):  $\int dU U_{ij} U_{kl}^{-1} = \frac{1}{3} \delta_{jk} \delta_{il}$ ,  
 $\int dU U_{ij} U_{kl} U_{mn} = \frac{1}{3!} \epsilon_{ikm} \epsilon_{jln}$ , and any product of the  
 integrands. All other integrands give 0.

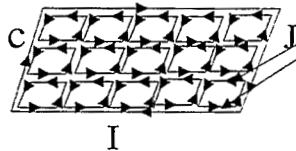
$$U_{ij} U_{kl}^{-1} = \begin{array}{|c|} \hline \uparrow \\ \hline \downarrow \\ \hline \end{array} = \left| \begin{array}{c} \uparrow \\ \downarrow \end{array} \right., \quad U_{ij} U_{kl} U_{mn} = \begin{array}{|c|} \hline \uparrow \\ \hline \uparrow \\ \hline \uparrow \\ \hline \end{array} = \left| \begin{array}{c} \uparrow \\ \uparrow \\ \uparrow \end{array} \right| =$$

If  $\beta$  small, expand the exponent. Do the integrals.

## STRONG COUPLING

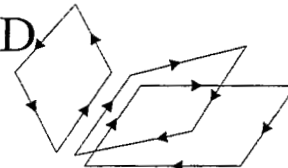
Example: Wilson loop  $W(C) = \prod_C U$ ,

$$\langle W(C) \rangle = Z^{-1} \int (DU) W(C) e^{-\beta \sum_{\square} S_{\square}(U)} = (\beta/18)^{L(C)} (1 + O(\beta))$$



**Pluses:**

- Area law (confinement) from QCD
- Baryon junctions from QCD:
- Analytic – can be continued to real time, strings

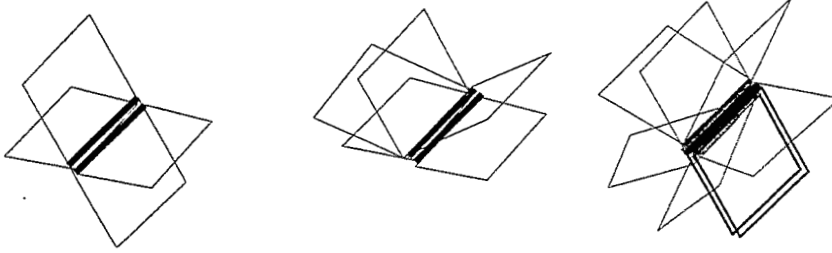


**Minuses:**

- Unphysical,  $\beta \rightarrow \infty$ , when  $a \rightarrow 0$ ; radius of convergence is outside of the scaling region.

## DIAGRAMS AND WEIGHTS

➤ All terms can be classified according to the links:



but the weights of these links are not products of  $\beta$  and  $\epsilon$ , the weight of each plaquette  $\frac{1}{k!} \left(\frac{\beta}{6}\right)^k$  can be distributed to its 4 links. The weights of the sites are always  $\sum (\delta_{ab})^m (\epsilon_{cde})^{2n}$ .

➤ To change the weight of a certain type of links, add:

$$S_{nm} = C_{nm} \Re \sum_L \prod_{\square_i, \square_j \ni L}^{I=1..n, J=1..m} [Tr U_{\square_i}] [Tr U_{\square_j}^{-1}]; \quad n - m \equiv 0 \pmod{3}$$

Momchil Velkovsky

3/30/02

## RENORMALIZATION GROUP

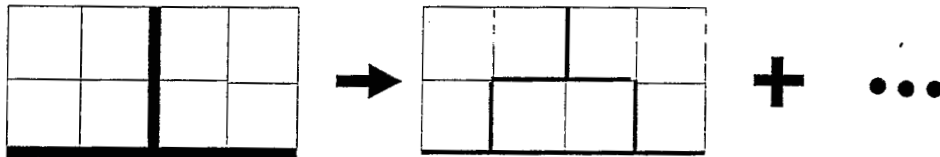
➤ RG acts in: 1. SC diagram weights space,  
2. Action coefficients space.

$$1. \quad Z = \sum_d W(d) = \sum_D W'(D), \quad W(d) = \prod f(l) g(s),$$

$$W'(D) = \sum_d W(d) A(d, D), \quad \sum_D A(d, D) = 1.$$

Can we write:  $W'(D) = \prod f'(L) g'(S)$ ?

Hints: topology (splitting links), sum  $d$  near  $D$ , lego blocks



2. Change  $f(L)$  – change  $C_{nm}$ , it depends on all simpler  $L$  ( $C$  with smaller  $n, m$ ).

\* RG acts in the space of  $C_{nm}$ !

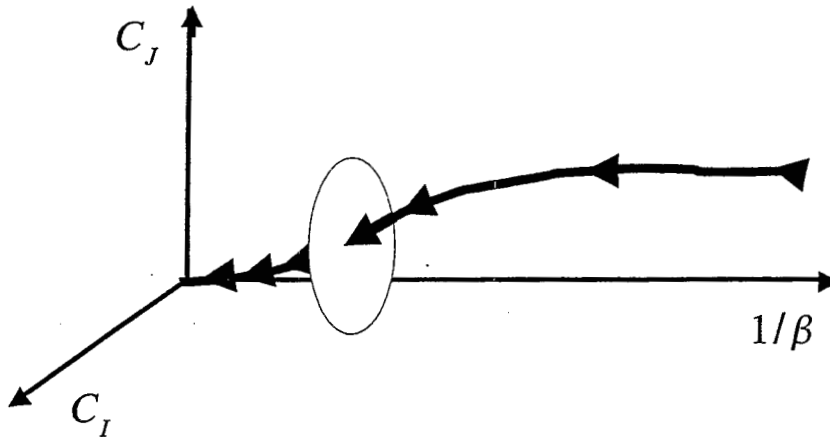
Momchil Velkovsky

3/30/02



## PERFECT ACTION

- Smaller scales → more types of diagrams → more terms in the action.
- If we are closer to the RG trajectory – less lattice artifacts. Is the convergence of the SCE better?



Momchil Velkovsky

3/30/02

## BETTER ~~PERFECT~~ ACTION

- RG trajectory going through the FP is no different than any other!

Add a few "link" terms in  $S$ , with free  $C_{nm}$  then:

1. Use lattice simulations to calculate certain correlation functions – fit the  $C_{nm}$  or
2. SCE produces analytic results! Go to Minkowski space, find appropriate observables (e.g. Baryon masses) and fit the  $C_{nm}$ . Performing a RG step should yield self consistent results!

Momchil Velkovsky

3/30/02

## WHAT CAN BE CALCULATED?

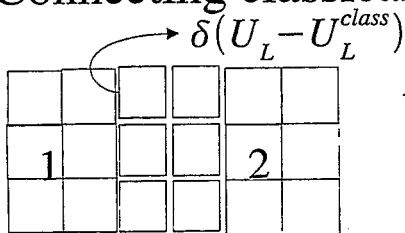
- SCE at finite temperature – reach  $T_c$  scale?
  - SCE in real time – enormous amount of data.
  - SCE in heavy ion collisions – differences and similarities with classical fields:
    1. Strong versus weak coupling.
    2. In both cases: small number of configurations in the path integral.
- SCE – quasi-classical expansion of the dual QCD action??

Momchil Velkovsky

3/30/02

## SCE AND CLASSICAL FIELDS

- Connecting classical fields with SCE diagrams :



Two classical regions:  
treated as a correlator.  
If the quasi-classical  
conditions – valid in the  
middle: maximum when 1&2 – related by EoM?

- A way to connect two quasi-classical solutions?  
E.g. The (instanton) vacuum before the collision and the  
classical expanding gluon fields after.

Analogy: In WKB, by going to imaginary time one can go  
around the region where the approximation breaks  
down. (SCE – dual quasi-classical approximation?)

Momchil Velkovsky

3/30/02

## WHERE TO START?

- Find simple test cases (observables).
- Compare with lattice.
- Fix the first extra terms in the action.
- Are there overlapping domains between SCE and other methods?



# Baryon Stopping From SIS to High energies- Expectations and reality

F.Videbæk

Physics Department

Brookhaven National Laboratory

Systematic data as function of collision system and energy was presented.

## Introduction

Stopping has been of interest in long term since it is the prerequisite for the creation of a hot and dense system. The early pp, and pA data lay the foundation and the first systematic was established by the analysis of Busza and Goldhaber [Phys.Lett.139B,235(1984)] based on FNAL data, and by the model evaluation of Date, Gyulassy and Hufner. (

## Recent low energy AA , pp, and pA data.

Very nice and complete data has emerged from experiments at AGS (E910, E941) and SPS (NA49) on pp and pA data. Rapidity and xF distributions selected and presented vs. # gray tracks i.e. target protons related to #collisions of incoming proton. Importantly data also exists for pp->nX supplementing the pp data.

The Heavy Ion data at low energies comes from SIS, E866, E917, E877, and E895 at AGS The system systematic shows a continuous development of stopping, but never reaching more than about  $\langle dy \rangle \sim 1.02$ . Still more than 40% of all protons show up in the middle 1/3 of the rapidity interval.

Data from NA49 for Pb-Pb at 158 A.GeV/c [Phys.Rev.Lett.82,2473(99)] show again considerable and much larger  $\langle dy \rangle$  than at AGS. For Pb the dy-loss is  $1.75 \pm 0.05$  and for SS  $1.63 \pm 0.16$ . Relative though to the available rapidity the  $\langle dy \rangle / y_{em}$  is constant. Thus is contrast to pp where dy is approximately constant 0.7-0.8 the dy grows from AGS to SPS approximately linearly with beam rapidity (see first two slides). The phenomenological Multichain Model that uses pA to predict AA stopping does a good job in describing the energy loss and about the observed net-proton value at mid-rapidity.

## Higher energy systematic.

The following 3 slides show systematic for pbar/p ratio and a compilation of the status of SPS and RHIC data. An iso-spin correction for p-bar over p ratios in pp collisions was suggested in nucl-ex 0106017 and applied. A smooth behavior of this quantity is observed between pp and AA up to RHIC energies.

The systematic of net baryon number demonstrates a smooth decrease with energy, a consistency between the RHIC experiments, and a net-proton yield (inclusive i.e. including feed-downs) that is higher than prediction from e.g. Hijing with the (di-quark, quark) string mechanism. The net baryon content in the lambda's is large. In the order of 25%.

## Summary

The main features of HI stopping are closely related to those in pp and pA as seen by the wealth of data from SIS to SPS energies. The data exists systematically as function of centrality, number of collisions. The development with energy and systems from pA to AA seems rather smooth. This data calls for a careful theoretical analysis. It is not unreasonable to assume that underlying mechanisms of stopping in AA can be found already in pA; with the present 130 GeV and arriving 200 GeV data the mechanism of stopping can be clarified.

It is worth to think about what other kinds of data and analysis are important to clarify stopping. I would consider the following a set of interesting candidates.

- Neutrons, anti-neutrons
- dA and pA at 100+100 GeV.
- Total energy balance.

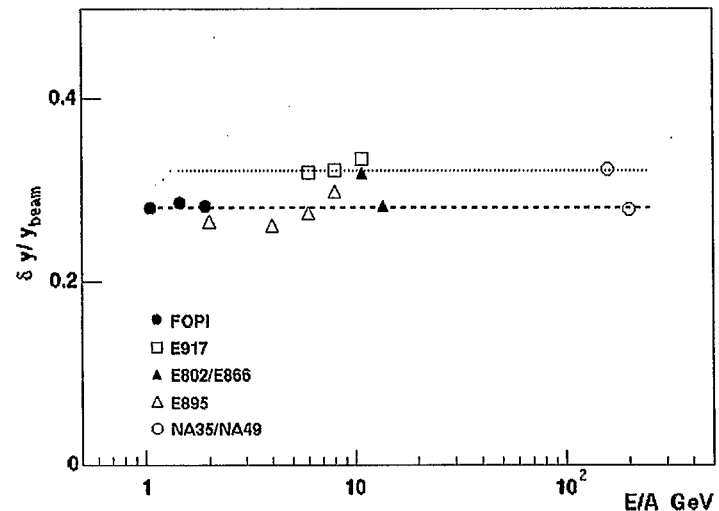
# Energy systematic

The near constant  $dy/y_{cm}$  was first demonstrated by FV and O.Hansen in PRC52,2684 (1995), but recently enhanced by adding data from FOPI by N.Hermann in Annu. Sci. Part.Rev.(99) 49,581.

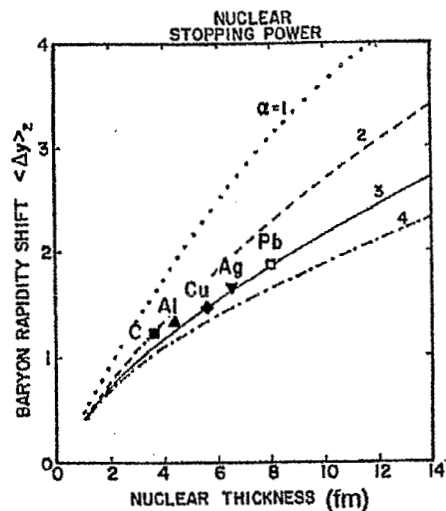
To this plot are added the recent data from AGS experiment E917, E895

At NO energy is complete stopping achieved. (thermal isotropic)

The  $dy$  increases with energy up to SPS.



# Estimates for $\delta y/y_{beam}$



$\sim 100, 120 \text{ GeV}/c$  fixed target.

Calculation of average dy loss  
(Date, Gyulassy, ..., 84)

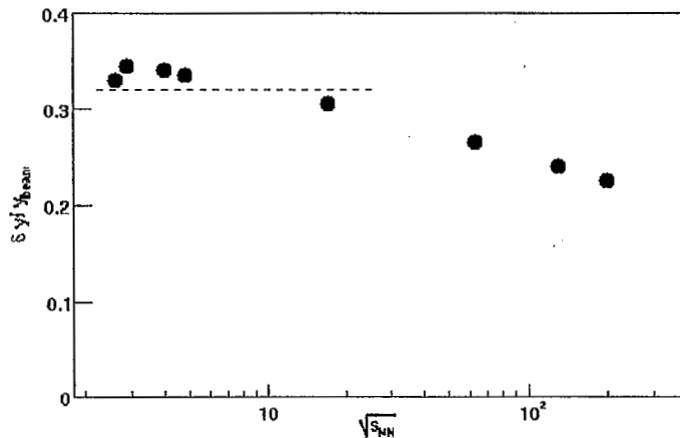
This was applied to AA (see nucl-ex 0106017 for details)

The energy losses are comparable to observed values.

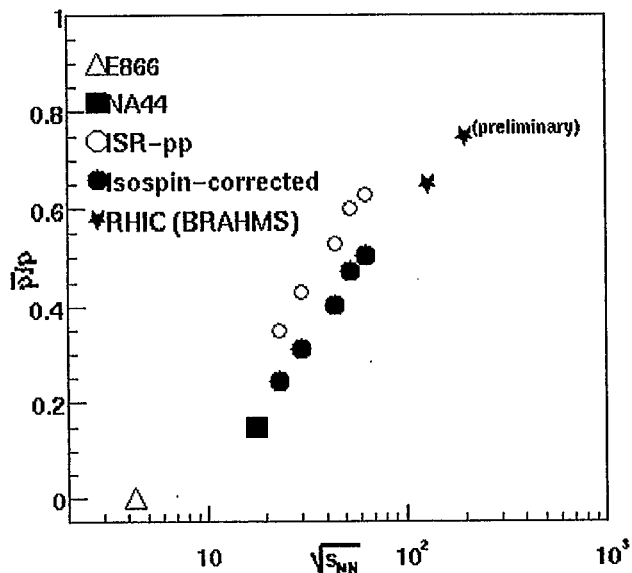
The net proton values at RHIC also close to exp ( $\sim 11$ ).

Values higher than Hijing 1.36

Calculation of average loss  $\langle \Delta y \rangle$



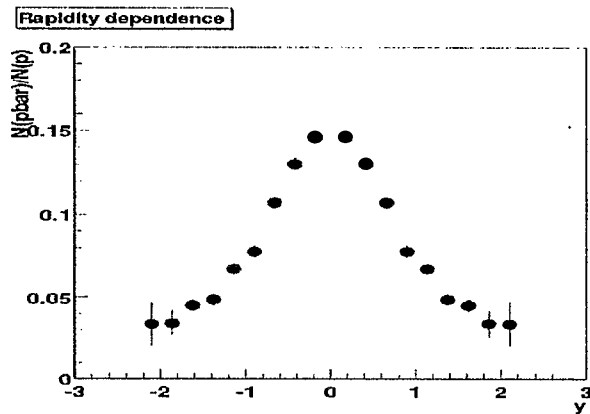
# Energy Dependence of $\bar{p}/p$



- The first data showed  $\bar{p}/p \sim 0.6-0.7$ . (STAR, BRAHMS, PHENIX, and PHOBOS) at  $y \sim 0$ . It is interesting to compare this ratio to that from lower energy data. The slide shows a survey of this ratio from lower energy AA and pp data.
- The isospin correction of the pp data is possible under the assumption that  $BB \rightarrow p\bar{p}X$  has the same cross-section as  $pp \rightarrow p\bar{p}X$  (pair production) to correct the ratios from pp collisions (see nucl-ex for details)

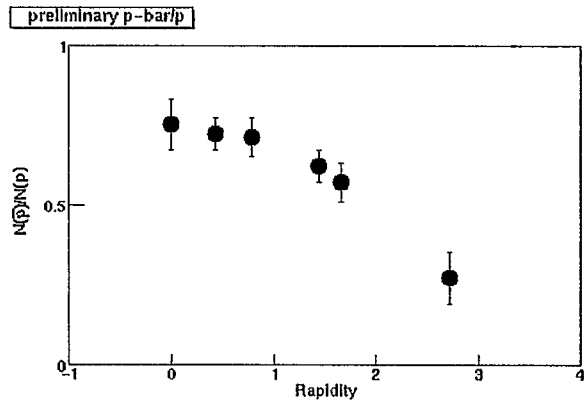


# Rapidity dependence p-bar/p



Na49.

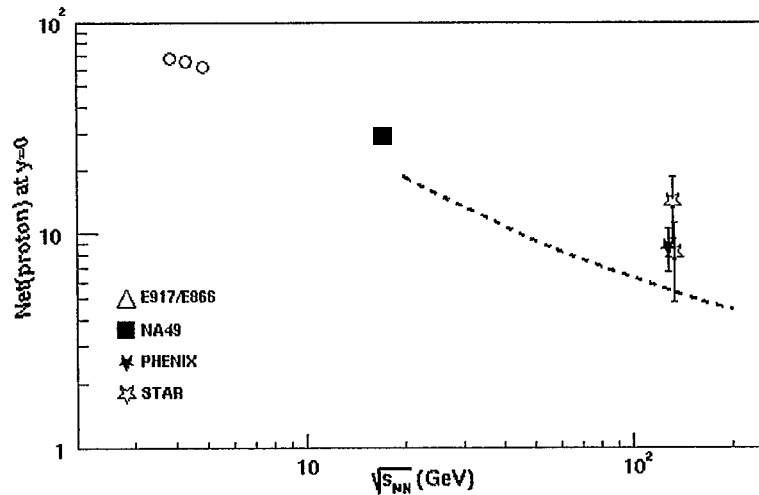
*Half Width ~2 units*



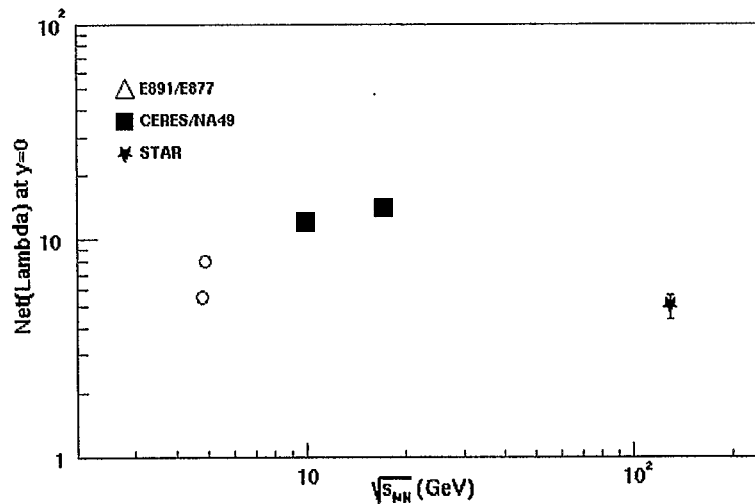
Brahms 200 GeV preliminary

*Half Width ~5 units*

# Net proton and $\Lambda$ 's



- Net protons from STAR, Phenix (130GeV)
- Is  $\sim *2$  over Hijing prediction, but close to value from Multichain model.
- Protons includes mostly hyperons decay protons.



The  $\Lambda$ 's carries a significant part of the baryon number.  
 $\sim 5 / (10 + \text{Neutrons})$   
 Can be as much as 25%.

# Strange Baryon Production in $p+A$ Collisions

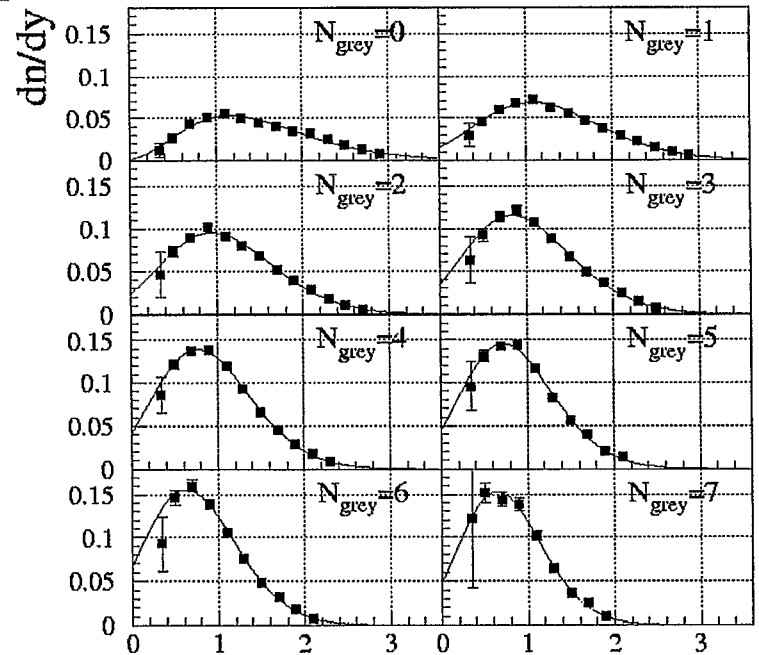
Brian Cole, Columbia  
March 29, 2002

for  
Baryon Dynamics at RHIC Workshop  
RIKEN BNL Research Center

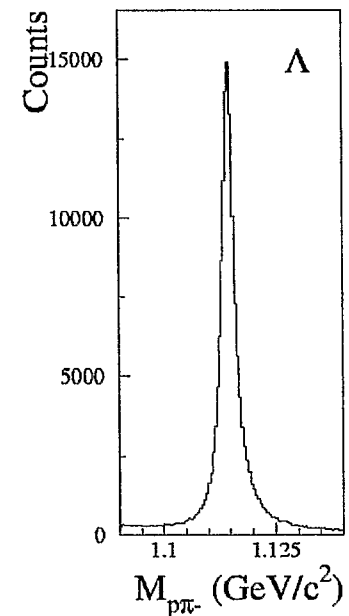
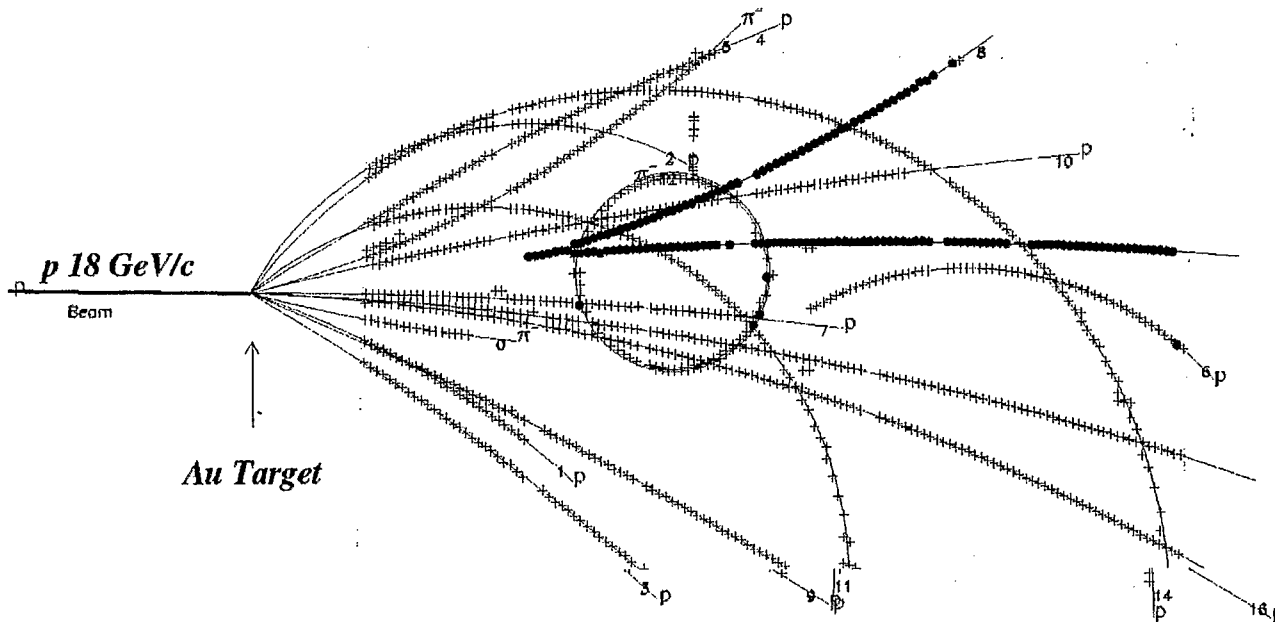
# E910 - $\Lambda$ Production

## • Analysis by X. Yang

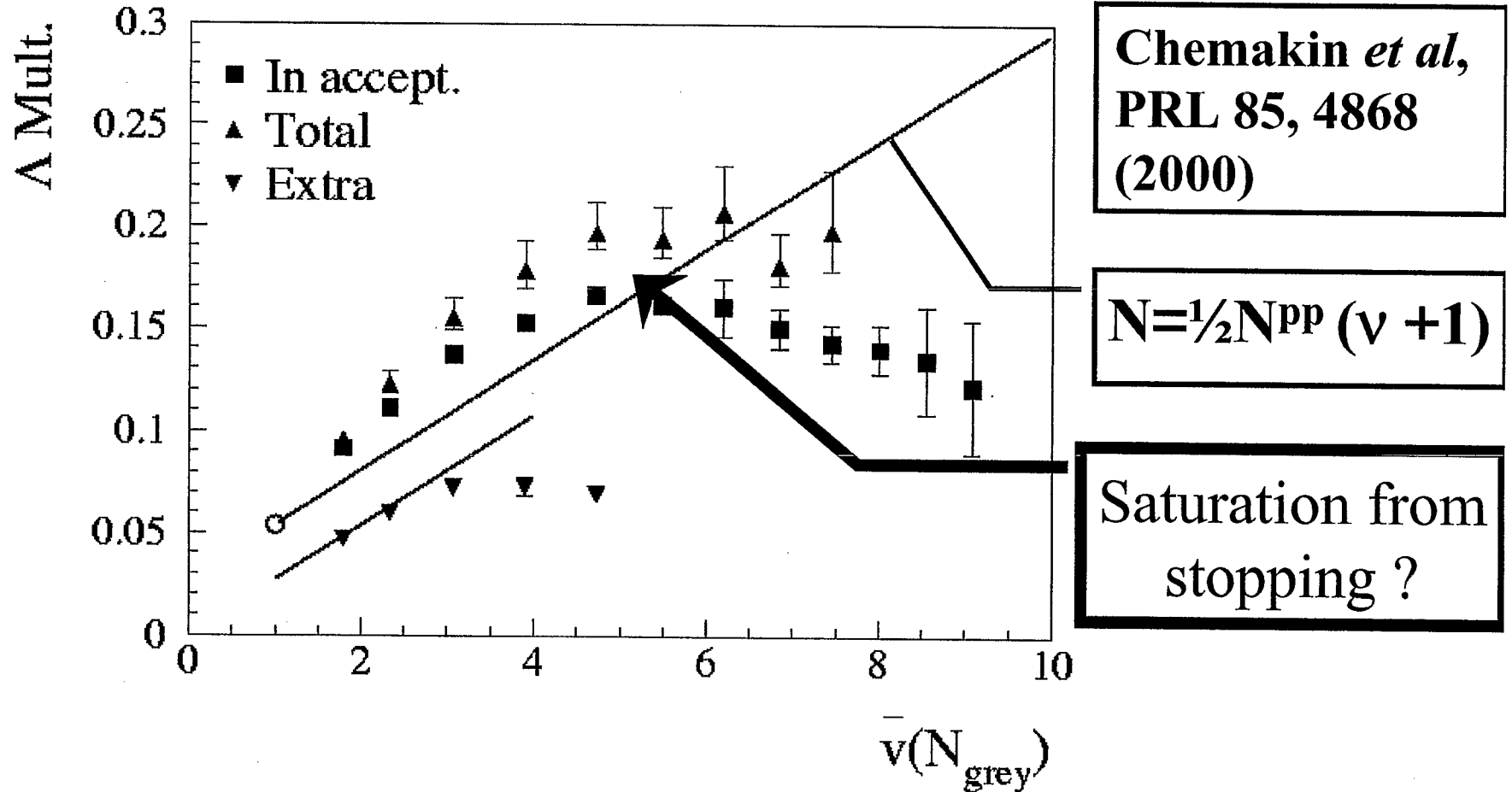
- 150k  $\Lambda$ 's in 18 GeV/c p-Au set
  - $\Rightarrow$  Good  $M_{inv}$  resolution,  $\sigma = 1.5 \text{ MeV}/c^2$
  - $\Rightarrow$  Good signal/background  $\sim 30:1$ .
- Account for missing acceptance by extrapolating w/ gamma distribution.
- "Leading" analysis - test whether  $\Lambda$  is most energetic baryon in event



y



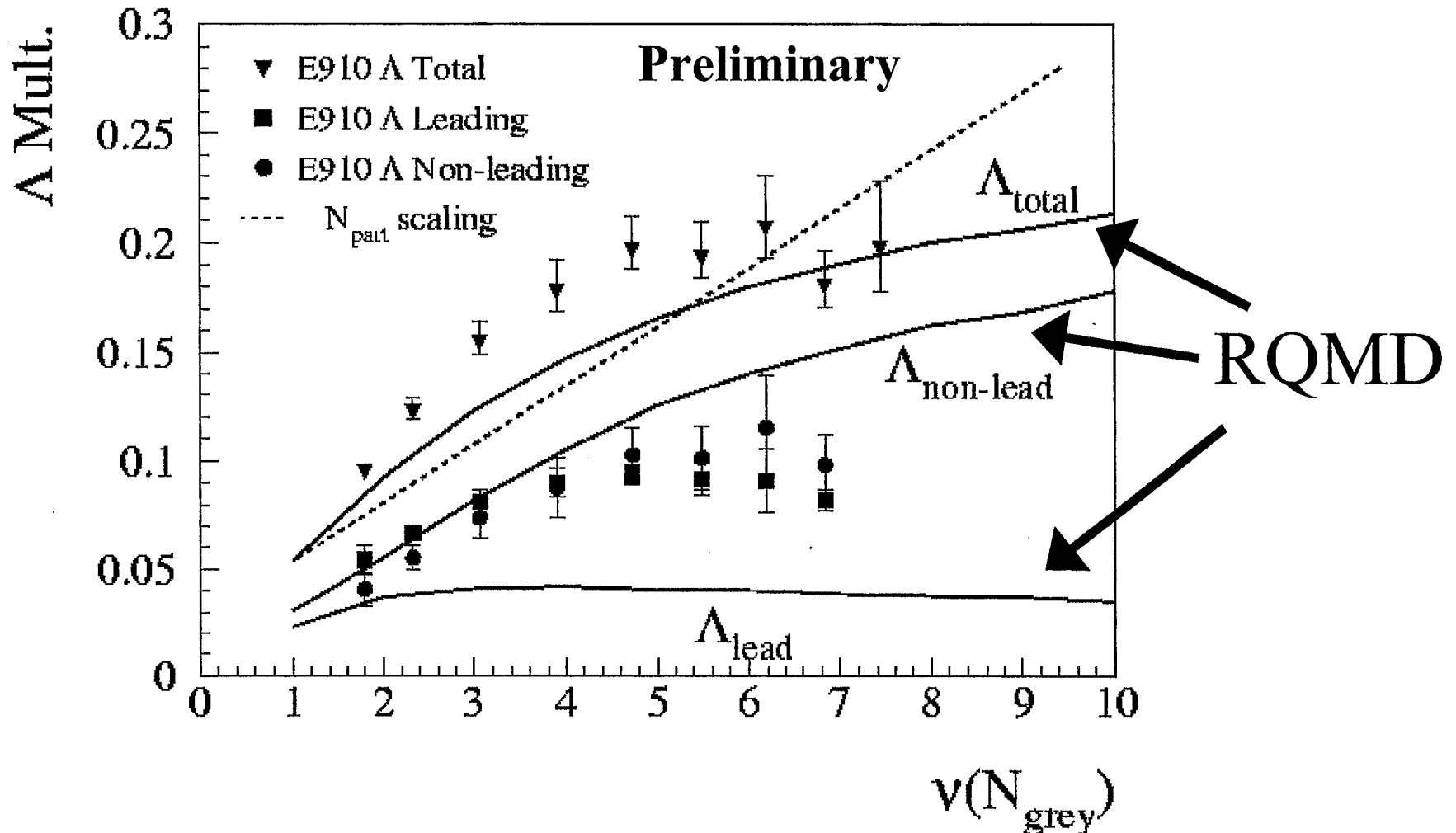
# E910: 17.5 GeV p+Au, $\Lambda$ Yield vs $v$



- Excess  $\Lambda$  production observed over # participant scaling of p-p

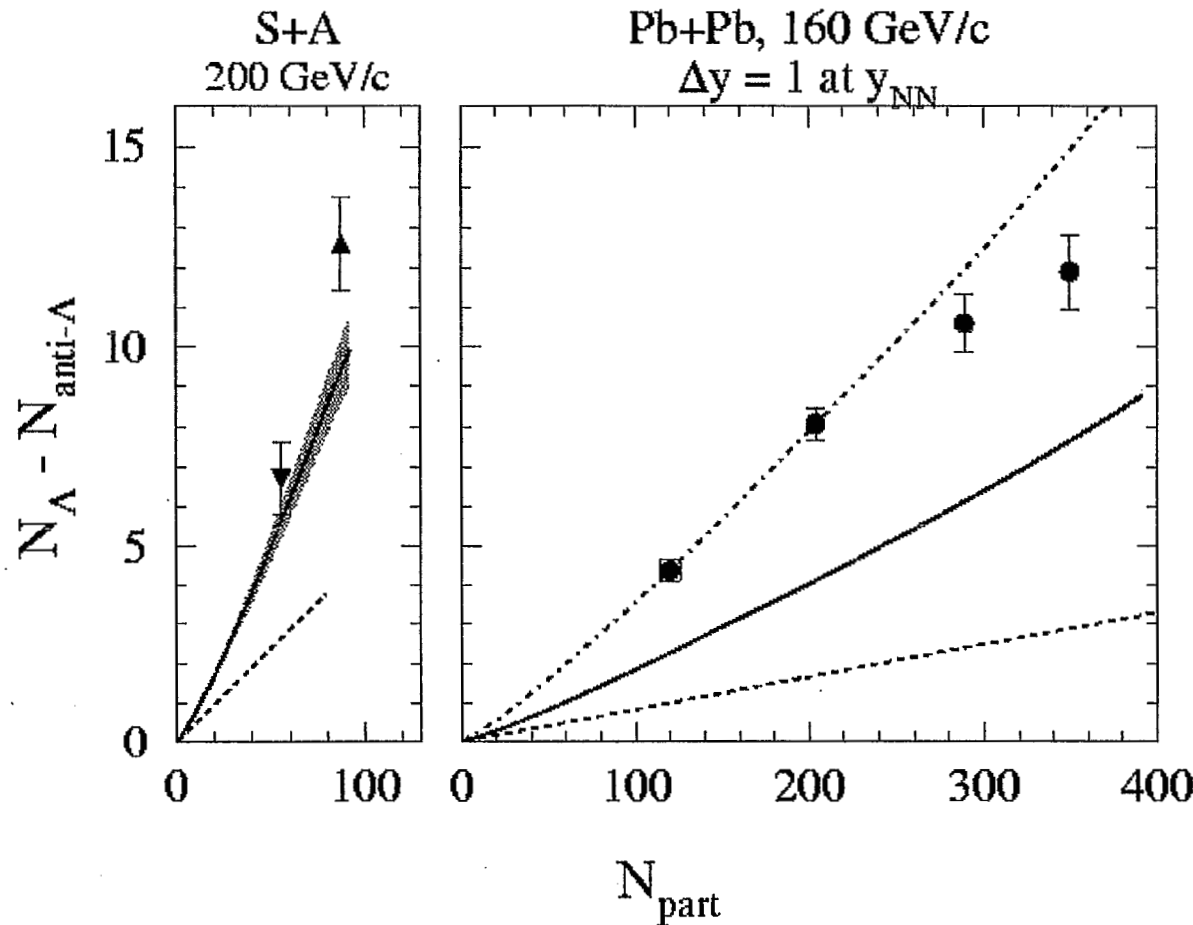
$$\Rightarrow N_{\Lambda}^{\text{proj}} = v \times \frac{1}{2} N_{\Lambda}^{\text{pp}} \text{ for } v \leq 3 \text{ ???}$$

# E910, 17.5 GeV/c p+Au, Leading $\Lambda$



- Ask “are  $\Lambda$ ’s leading baryon” event by event  
⇒ Excess due to leading  $\Lambda$ ’s (from projectile)  
⇒ **Not reproduced by RQMD.**

# E910 Extrapolation to SPS, Update

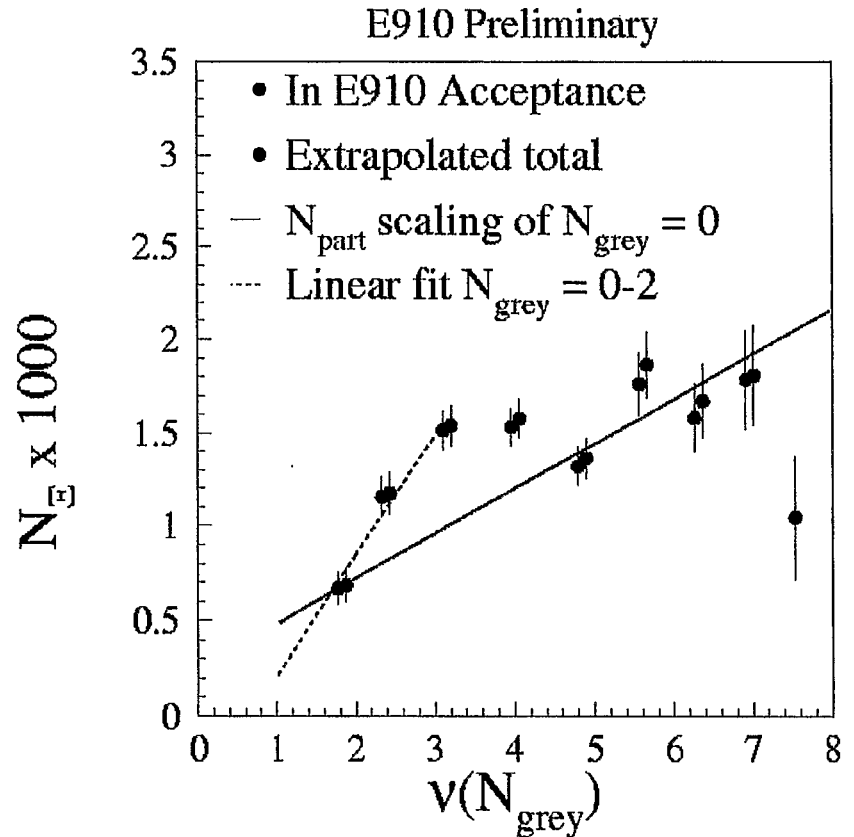
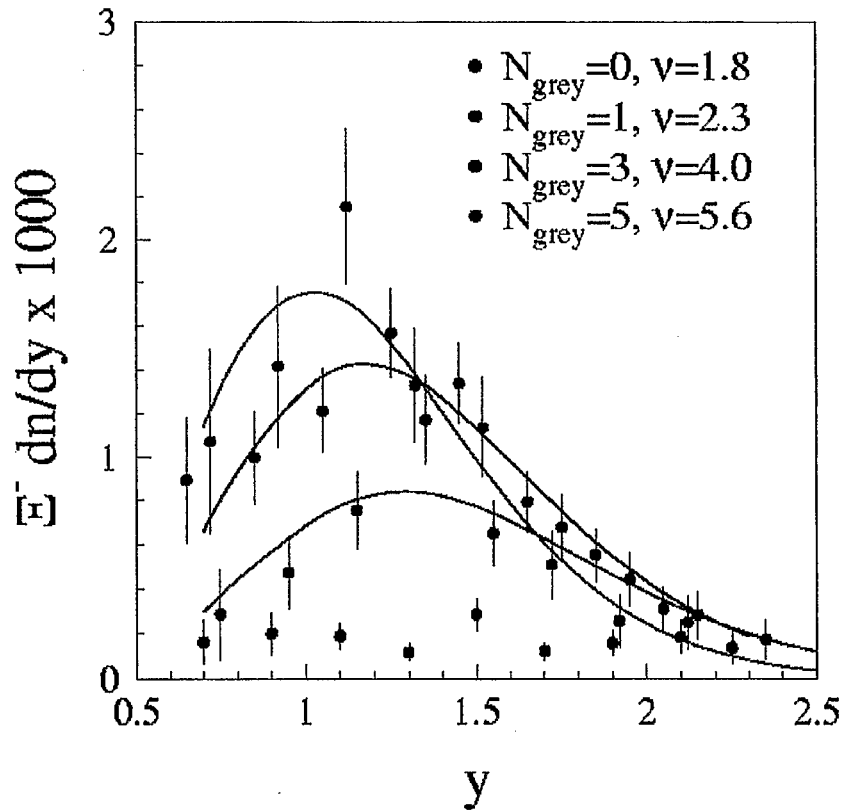


E910 Extrapolation corrected for WA97 acceptance & p-Be enhancement.

“Pure” E910 Extrapolation

- Assume  $N_{\Lambda}^{\text{part}} = \nu \times \frac{1}{2} N_{\Lambda}^{\text{pp}}$  for  $\nu \leq 3$ .
- “Extrapolate” E910 effect to Pb-Pb collisions at SPS.
- Can account for S+A  $\Lambda$  enhancement
- And Pb+Pb enhancement (after correcting for  $\Delta y$ ).

# E910 $\Xi^-$ Production



- Rapid increase in  $\Xi^-$  yield with  $v$ .

**$\Rightarrow$  Inconsistent with # participant scaling**

- $> \times 4$  increase in  $\Xi^-$  yield over  $v = 1$  with any reasonable extrapolation  $\Rightarrow > \times 8$  in A+A
- **Also due to projectile ?! (starts above  $y_{\text{NN}}$ )**



# Summary & Conclusions

---

- There is a clear enhancement of  $\Lambda$  production in p-A collisions over  $N_{\text{part}}$  scaling of p-p data.
  - Associated with multiple scattering of projectile.
- Extrapolations to A-A collisions can account for nearly all of observed  $\Lambda$  enhancement in A-A.
- A strong enhancement (x4) of  $\Xi$  production is observed in p-Au collisions.
  - Also appears to be due to projectile multiple scattering.
- Applied to Pb-Pb collisions would give  $\sim$  x8 enhancement over p-p.
  - Beware p-p and p-Be difference.
- A simple interpretation of  $\Lambda$  in terms of CQM model is consistent with p-Au  $\Xi$ , and WA97  $\Xi$ ,  $\Omega$  results.
- There also appears to be a mechanism for strongly increased anti- $\Lambda$  production after first collision.



BARYON AND BARYON PAIR PRODUCTION IN ELEMENTARY AND NUCLEAR  
HADRONIC INTERACTIONS

H.G.FISCHER

CERN

for the NA49 Collaboration

New data on baryon production from the NA49 experiment at the SPS concerning p+p, n+p and p+Pb interactions are used to establish a more precise basis of comparison with A+A collisions. In this context measurements with neutron beam (derived from deuteron beam in turn derived from Pb beam fragmentation) are particularly important.

A first comparison of proton and neutron production in p+p collisions with proton production in n+p reactions allows the establishment of isospin-weighted reference baryon distributions for heavy ion interactions, see fig.1.

The measurement of anti-proton production in p+p and n+p collisions shown in fig.2 establishes a sizeable increase of anti-proton yield from neutrons (factor 1.5-1.6) indicating a strong asymmetric baryon pair production term of the type proton/anti-neutron in p and anti-proton/neutron in n fragmentation. The definition of "net" baryon densities has to take account of this effect as anti-protons do not represent the total yield of pair-produced protons. As demonstrated in fig.3 the simple subtraction of the anti-proton yield leads to a constant invariant "net" central proton density at  $\sqrt{s}$  above 30 GeV which does not comply with baryon number conservation. The subtraction of the properly evaluated density of pair-produced protons eliminates this problem and leads to a "net" proton density approaching zero in the upper ISR energy range.

Similarly, isospin effects have also to be taken account of in strange and multiple-strange hyperon production. This leads to the prediction that the anti-Lambda yield properly measures the rate of pair-produced Lambdas

whereas anti-Xi+ production overestimates the rate of pair-produced Xi-

An overall picture of anti-baryon/baryon ratios as measured and corrected for isospin effects is shown in fig.4 for p+p collisions including a new upper limit for anti-Omega/Omega from NA49.

Finally a new evaluation of the enhancement factors of Xi and anti-Xi hyperon production in p+A and A+A collisions at the SPS as compared to p+p interactions is shown in fig.5 as a function of the number of collisions per projectile participant. It is seen that the extracted enhancement factors are of similar magnitude in p+A and A+A collisions and that the isospin correction predicted from the observed antiproton/proton pair production asymmetry reduces the apparent difference between anti-Xi and Xi enhancements.

Isospin $I = 1/2$		
Projectiles	n	p
Produced particles	n	p
$I_3$	-1/2	+1/2

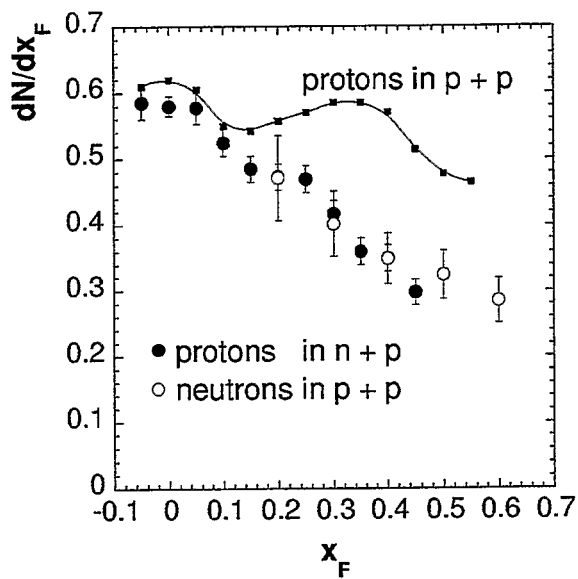


Figure 1:  $p_T$  integrated  $x_F$  distributions of protons and neutrons from  $p+p$  as well as protons from  $n+p$  interactions.

Isospin $I = 1$					
Projectiles		n		p	
Produced particles	$\bar{p}n$		$p\bar{p}$ $n\bar{n}$		$p\bar{n}$
$I_3$	-1	-1/2	0	1/2	+1

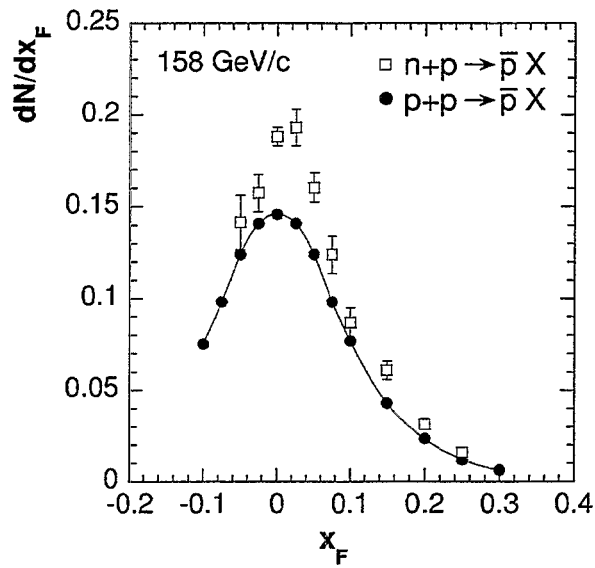


Figure 2: Anti-proton density distribution as a function of  $x_F$  for p+p and n+p interactions.

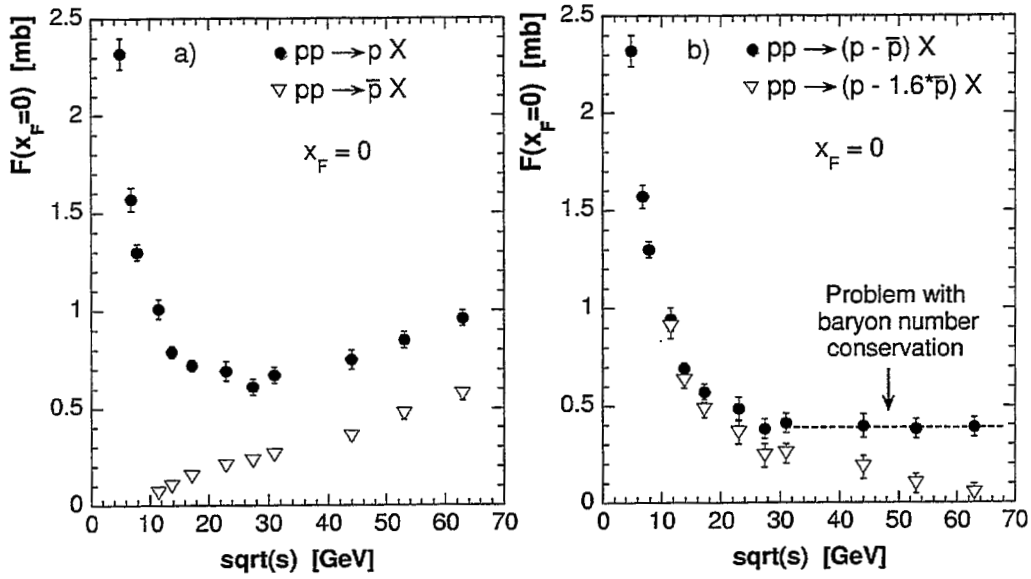


Figure 3: a)  $p_T$ -integrated invariant p and  $\bar{p}$  yields at  $x_F = 0$  as a function of  $\sqrt{s}$  b)  $p - \bar{p}$  and  $p - 1.6 \cdot \bar{p}$  as a function of  $\sqrt{s}$ .

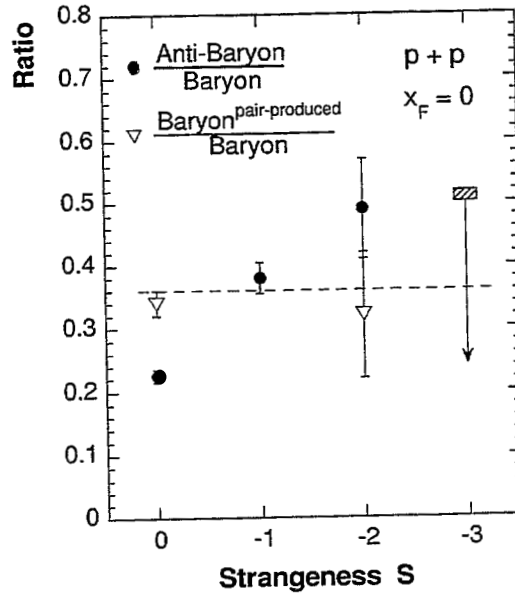


Figure 4: Anti-baryon/baryon and pair-produced-baryon/baryon ratios at  $x_F = 0$  in  $p + p$  interactions as a function of strangeness content.

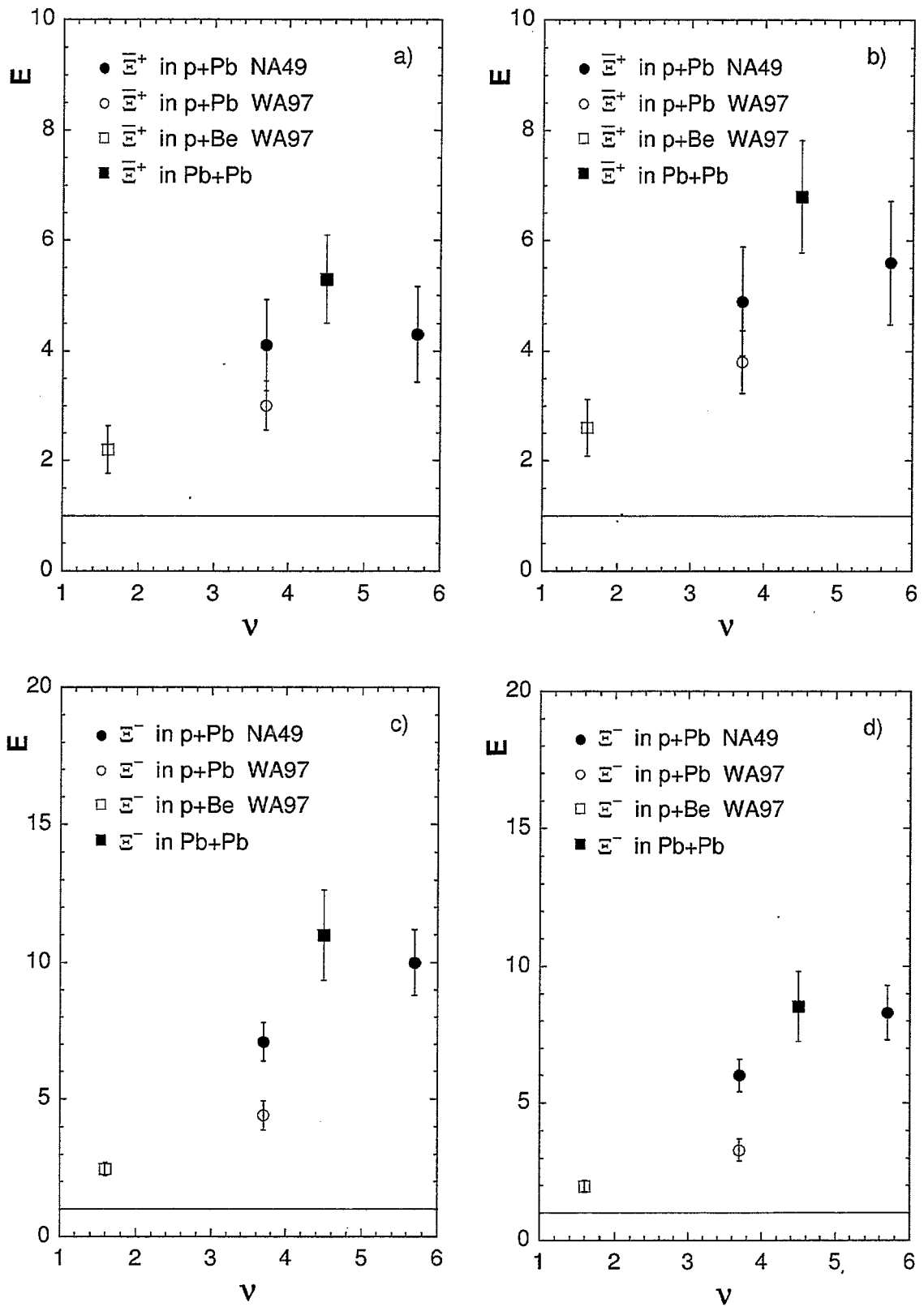


Figure 5: Enhancement factor for the production of a)  $\Xi^+$  and c)  $\Xi^-$  as measured and b), d) taking into account the isospin correction deduced from p and  $\bar{p}$  yields of p+p and n+p collisions.





# Baryon Results from E917 and the AGS

David Hofman, Univ. of Illinois Chicago  
March 29, 2002

for  
Baryon Dynamics at RHIC Workshop  
RIKEN BNL Research Center

# Baryon Results from E917 and the AGS

David Hofman  
 University of Illinois at Chicago  
 for the  
 E917 Collaboration

B.B. Back, R.R. Betts, J. Chang, W.C. Chang, C.Y. Chi, Y.Y. Chu, J.B. Cumming,  
 J.C. Dunlop, W. Eidredge, S.Y. Fung, R. Ganz, E. Garcia, A. Gillitzer, G. Heintzelman, W.F.  
 Henning, D.J. Hofman, B. Holtzman, J.H. Kang, E.J. Kim, S.Y. Kim, Y. Kwon,  
 D. McLeod, A.C. Mignerey, M. Moulson, V. Nanal, C.A. Ogilvie, R. Pak,  
 A. Ruangma, D.E. Russ, R. Seto, P.J. Stankas, G.S.F. Stephens, H. Wang,  
 F.L.H. Wolfs, A.H. Wuosmaa, H. Xiang, G.H. Xu, H.B. Yao, C.M. Zou

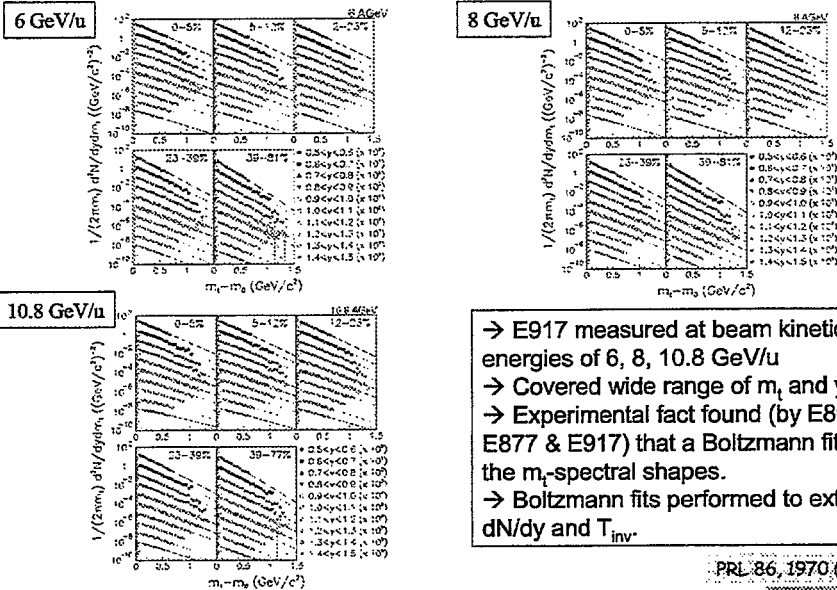
Argonne National Laboratory  
 Brookhaven National Laboratory  
 University of California at Riverside  
 Columbia University  
 University of Illinois at Chicago  
 University of Maryland  
 Massachusetts Institute of Technology  
 University of Rochester  
 Yonsei University (Korea)

E917 @ AGS

1



## Protons: Spectral yields and shapes



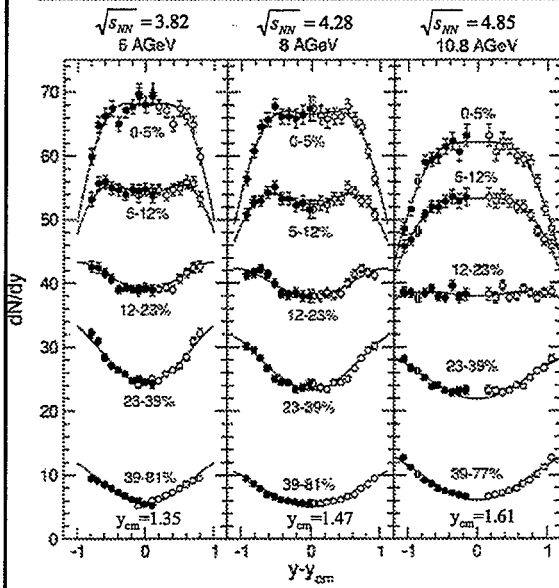
E917 @ AGS

2

PRL 86, 1970 (2001)



# Proton $dN/dy$ versus centrality



→ Can describe the data most simply with symmetric double Gaussian fits.  
 → All energies have a common smooth evolution of a bimodal shape at peripheral collisions to what appears to be still bimodal at central collisions.

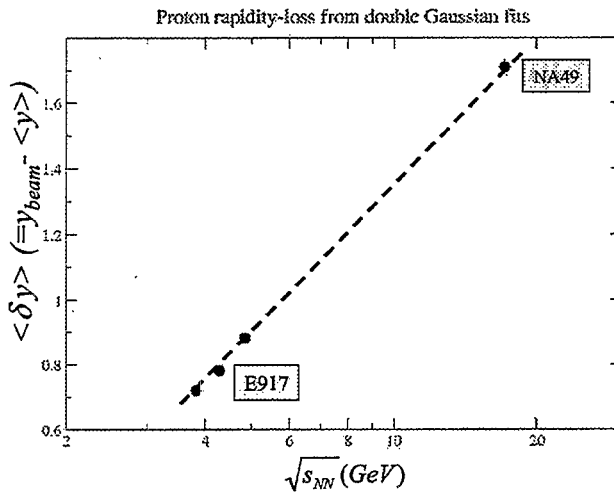
PRL 86, 1970 (2001)

E917 @ AGS

3

NUC

# Mean Rapidity Loss



→ Logarithmic energy dependence of absolute value for the rapidity loss from AGS to SPS.

→ The relative rapidity loss

$$\frac{\langle \delta y \rangle}{\delta y_{max}}$$
 varies from 0.53 to 0.59 over this same region.

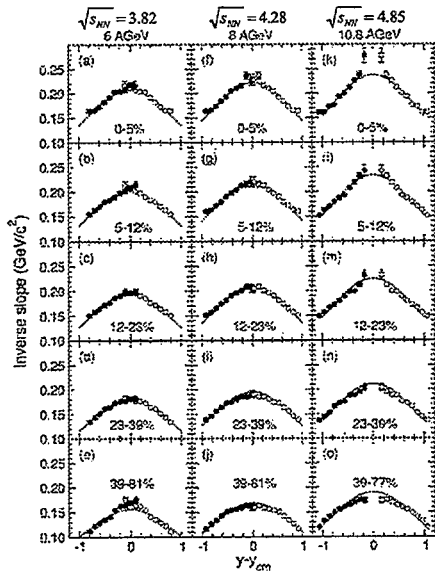
PRL 86, 1970 (2001) & PRL 82 (1999) 2471

E917 @ AGS

4

NUC

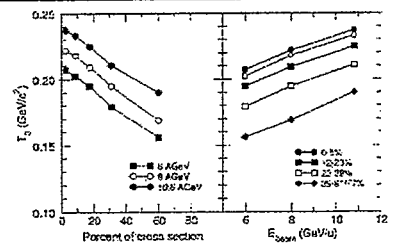
# Proton $T_{inv}$ versus centrality



→ Can describe rapidity dependence of  $T_{inv}$  with simple isotropic thermal model.

$$T(y) = \frac{T_0}{\cosh y}$$

→ Linear behavior of  $T_0$  with  $E_{beam}$  and centrality



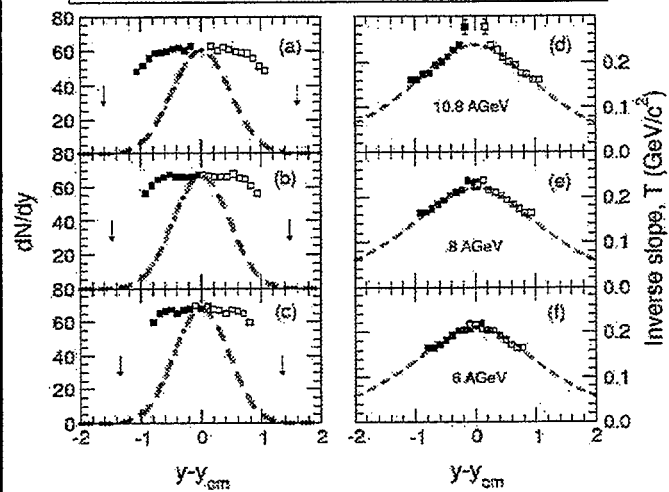
E917 @ AGS

5



# Fit $T_{inv}$ and look at $dN/dy$

Central collisions at 6, 8 and 10.8 GeV/u



→ Isotropic emission from a "stopped" thermal source fits  $T_{inv}$ , but not  $dN/dy$ .

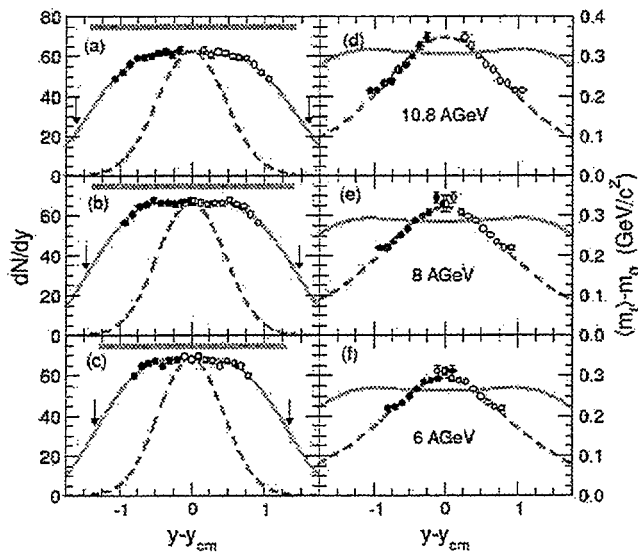
E917 @ AGS

6

PRL 86, 1970 (2001)



# Fit $dN/dy$ with boosted sources



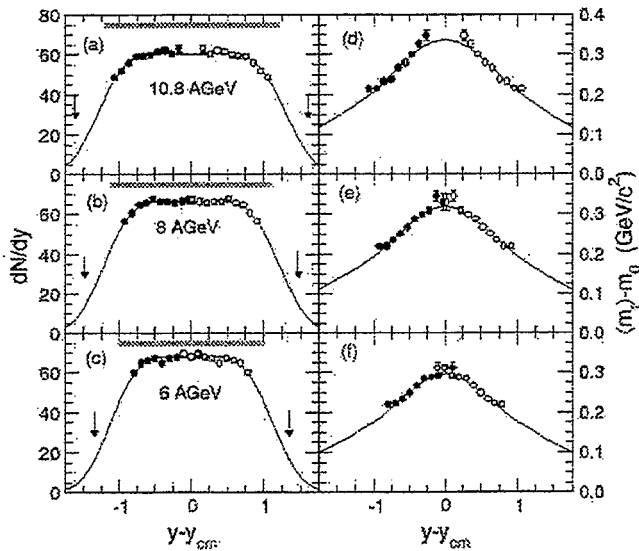
→ Emission from “boosted sources” can fit  $dN/dy$ , but not the inverse slope (or similarly the average  $\langle m_t \rangle$ )

E917 @ AGS

7

PHIC

# Simultaneous fits $dN/dy$ and $T_{inv}$



→ Emission from “boosted sources” and a Gaussian **temperature profile in rapidity space** fits both observables simultaneously.

E917 @ AGS

8

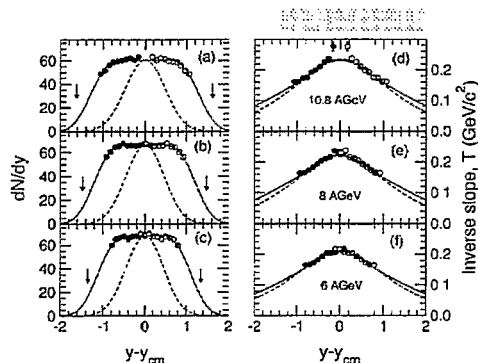
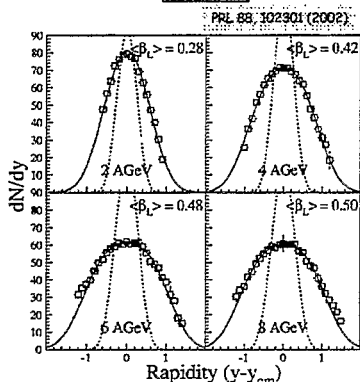
PHIC

# Comparison of AGS results

E895

Data is 5% Central

E917



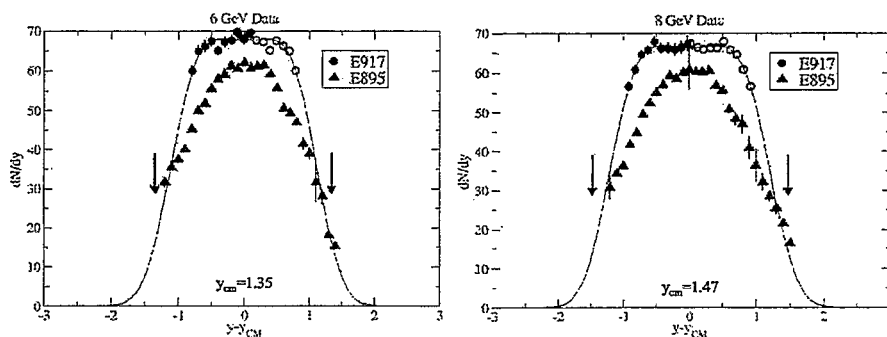
They look similar at first glance... they both show  
 (a) effect of a stationary thermal source that doesn't fit  
 (b) a longitudinally "boosted" source that does

E917 @ AGS

9

# Comparison of AGS Results

E895 & E917: Central 5% Au+Au @ 6 and 8 GeV/u



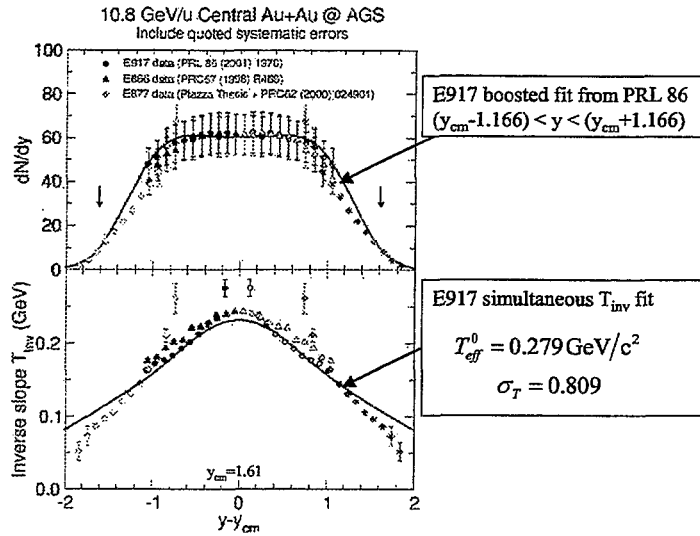
→ Shape of  $dN/dy$  and total yield appear quite different between E917 & E895.  
 E917: Integral of extrapolated "fit" gives  $N \sim 160$  (+/- 5) protons  
 E895: Integral of data + fit extrapolation gives  $N \sim 135$  (+/- 2) protons  
 → Must include systematic errors for a realistic comparison of the data!!

E917 @ AGS

10

# Comparison of AGS Results

E866, E877 & E917: Central 4 or 5% at 10.8 GeV/u



E917 @ AGS

11

PHIC

# The AGS $\bar{\Lambda} / \bar{p}$ surprise

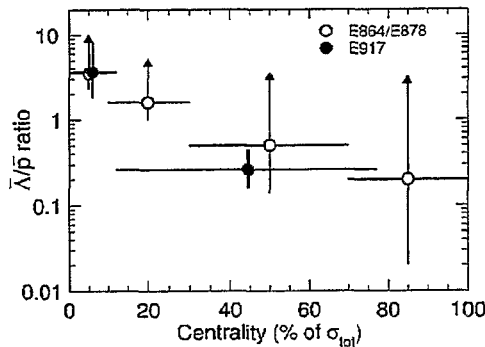
- Three AGS experiments involved in this measurement
  1. E859: Si + Au at 14.6 AGeV/c (1997)  
 (Near mid-rapidity & Central)  
 Ratio:  $2.9 \pm 0.9(\text{stat}) \pm 0.5(\text{sys})$
  2. E864 (& E878): Au + Pb at 11.5 AGeV/c (1999)  
 (Mid-rapidity, Central,  $p_t \sim 0$ )  
 Ratio:  $> 2.3$  (98% C.L.)  
 Ratio decreases for peripheral.
  3. E917: Au + Au at 11.7 AGeV/c (2001)  
 (Near mid-rapidity & Central, Peripheral)

E917 @ AGS

12

PHIC

# Antilambda/Antiproton ratio



Centrality	$\bar{\lambda}/\bar{p}_{\text{direct}}$
0-12%	$3.6^{+4.7 +2.7}_{-1.8 -1.1}$
12-77%	$.26^{+.19 +.5}_{-.15 -.4}$

Maximal values from theory:  
 UrQMD (F. Wang):  $\sim 1.3$   
 Thermal (J. Cleymans)  $\sim .9$

→ The E917 measurement at non-zero  $p_t$  is in good agreement with the elevated ratio in Si +Au collisions (E859) and the E864/E878 result at  $p_t \sim 0$ .

E917 @ AGS

13

## Summary

- E917 proton dN/dy distributions indicate a mean rapidity loss at the highest AGS energy of  $\delta y \sim 1$ . Additionally, the mean rapidity loss is found to have a logarithmic energy dependence that extrapolates nicely to SPS energies.
- Data illustrates the importance of having a good centrality measure and using all available information (e.g. dN/dy and  $T_{inv}$ ) in the data interpretation.
- E895 proton data suggest longitudinal flow can describe the proton dN/dy distribution, but E895 has qualitatively different shaped dN/dy distributions than those found by E917.
- Measured  $\bar{\lambda}/\bar{p}_{\text{direct}}$  ratio is found to be substantially larger than unity in central collisions at AGS energies.
- There are still unanswered questions at AGS.
- Emphasize the importance of including the systematic errors at all stages of data analysis, publication and modeling.

E917 @ AGS

14



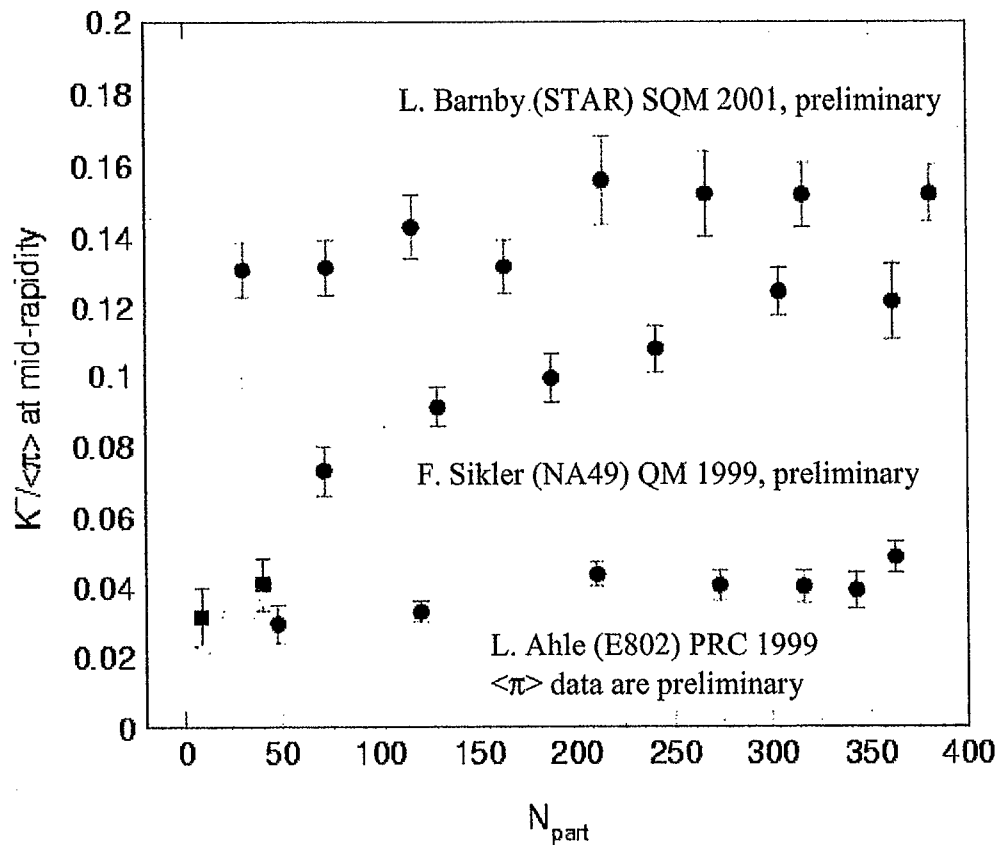


# **$K^-/\pi$ vs collision energy and centrality: What we learn from the systematics?**

**Fuqiang Wang**  
**Purdue University**



# $K^-/\pi$ vs collision energy and centrality



$K^-/\pi$  increases with energy.

Low energy:

$K^-/\pi$  increases with centrality.

High energy:

$K^-/\pi$  independent of centrality.

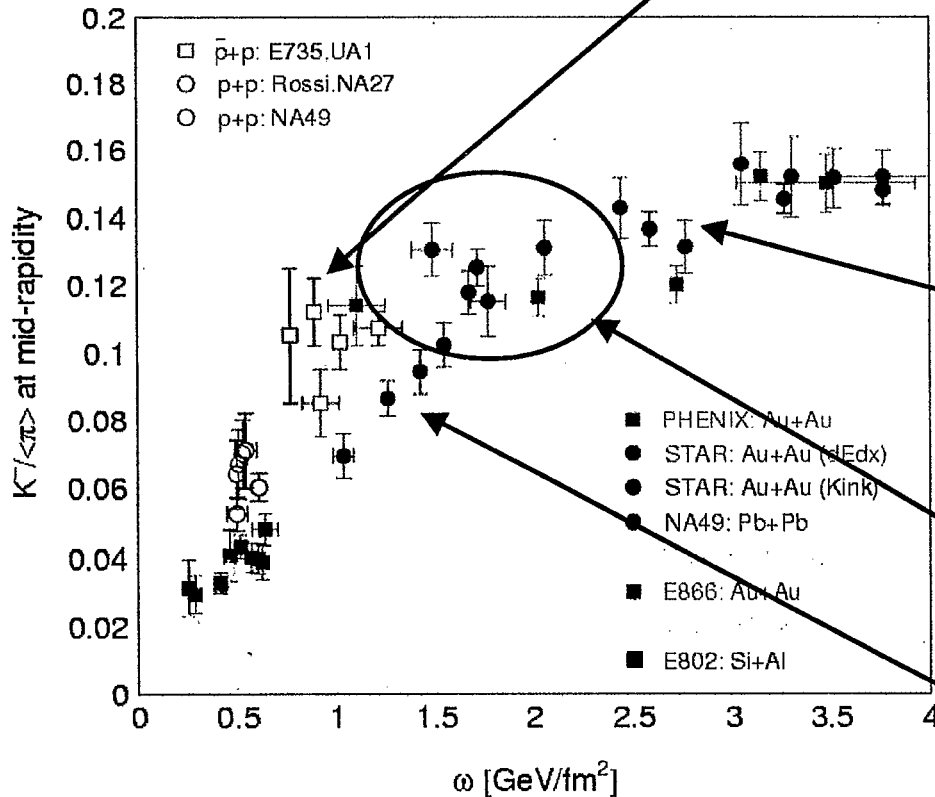
# A new variable: What does it tell us?



$$\omega = \langle m_T \rangle_c * \frac{(dN/dy)_c}{\pi R^2} * \left[ \frac{dN/dy}{(dN/dy)_c} \right]^{1/3} \approx \langle m_T \rangle * \frac{dN/dy}{\pi r^2}$$

$r_{\text{proton}} = 0.8 \text{ fm}$  (MIT Bag Model)

$K^-$  may come predominantly from gluons



$K^-/\pi$  saturates:  
Gluon saturation sets in at RHIC?  
Chem. freeze-out no longer  
sensitive to initial condition?

Turn-over purely coincidental?  
RHIC low energy data important!

$K^-/\pi$  increases at low energies

163



# Summary

- A new variable,  $\omega$ , the  $\pi$  transverse energy per rapidity per transverse area, is suggested to unify three important effects: energy, centrality,  $\langle m_T \rangle$ .
- $K^-/\pi$  seems to follow a systematic trend in  $\omega$ .
- What is the physics message?
  - $K^-/\pi$ : a sensitive probe to initial gluon density?
  - Constant  $K^-/\pi$ : evidence of gluon saturation at RHIC?
  - Phase transition between SPS and RHIC?

# Evidence for Topological Defect Production in Heavy Ion Collisions

J. I. Kapusta, S. M. H. Wong

Phys. Rev. Lett. 86, 4251 (2001)

Anomalous abundance and transverse momentum  
distribution of  $\Omega$  and  $\bar{\Omega}$  in central Pb+Pb  
collisions at 158 GeV/nucleon suggests...

that the  $\Omega$  and  $\bar{\Omega}$  are produced primarily as  
topological defects (or Skyrmions) arising from the  
formation of disoriented chiral condensates  
(DCC) with a domain size of about 2 fm.



Enhanced  $\Omega$  &  $\bar{\Omega}$  abundances may arise from the formation of topological defects (Skyrmions) associated with DCC.

Production mechanism in nuclear collisions was developed by:

De Grand (1984)

J. Ellis, Heinz, Kowalski (1989)

A.M. Srivastava (1991)

Kapusta, Srivastava (1995)

High energy heavy ion collision



high entropy



disorientation of chiral field (pions, kaons) beyond a correlation length  $\xi$



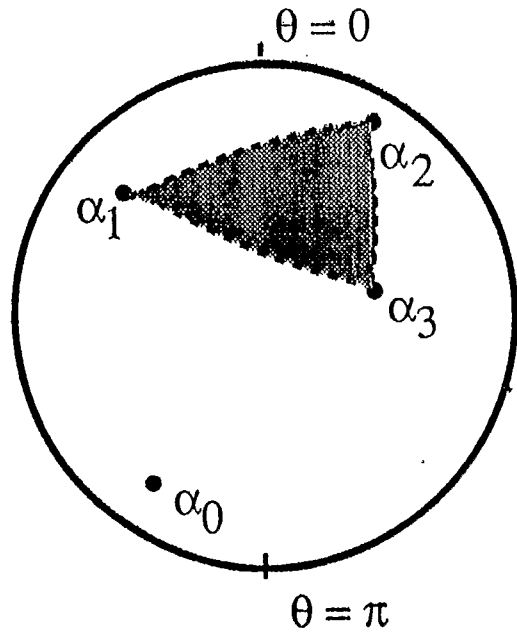
topological defects formed

probability/volume  $p = \frac{0.08}{\xi^3}$

Spergel, Turok, Press, Ryden (1991)

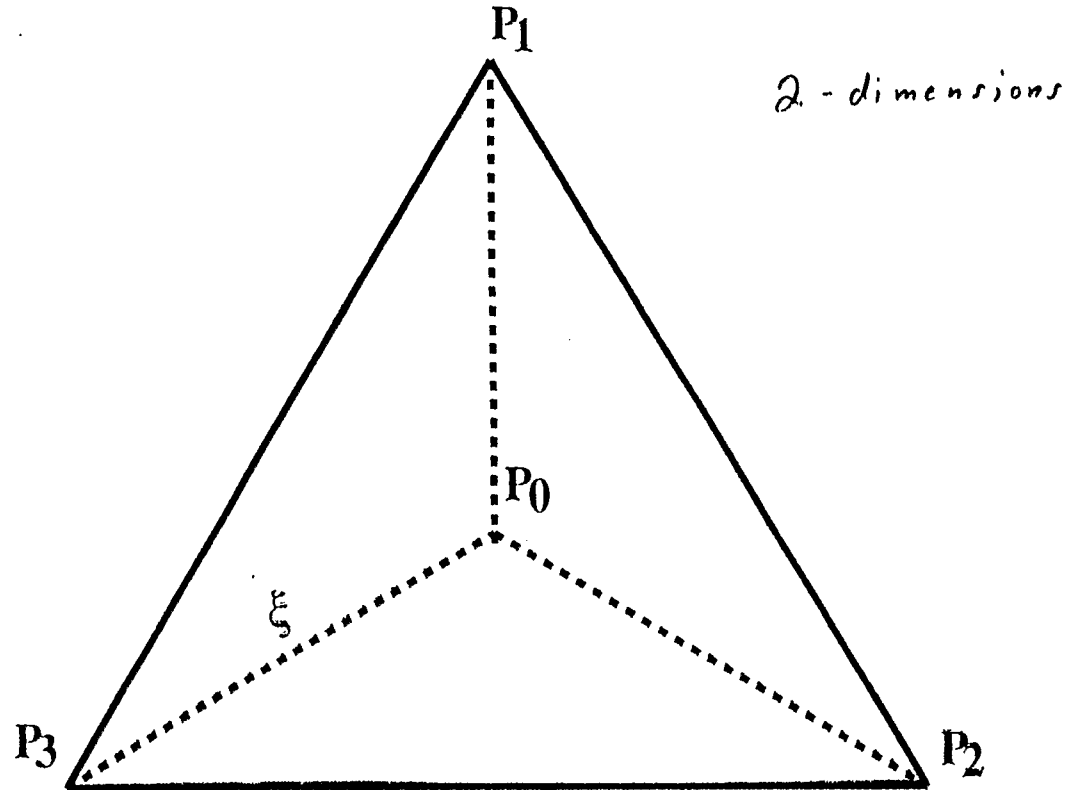
Leese, Prokopenko (1991)

flat potential:  $m_{\pi} = 0$



order parameter space

If  $\alpha_0$  lies in the image of the patch then winding number  $> \frac{1}{2}$  and will evolve into a full skyrmion.



position space

$$\text{probability / triangle} = \frac{1}{8}$$

$$\text{probability / volume} = \frac{1}{6\sqrt{3} \xi^2}$$



NA49 data on central Pb+Pb collisions  
 at 158 GeV/nucleon extrapolated to all  
 momentum space by Becattini et al.  
 together with WA97 data over central  
 rapidities:  $\bar{\Omega}/\Omega = 0.383 \pm 0.081$

$$\bar{p} = 10 \pm 1.7 > \bar{\Lambda} > \bar{\Xi}^+ > \bar{\Omega} = 0.50$$

per central collision

We assume that all  $\bar{\Omega}$  are produced as  
 topological defects, and that there is equal  
 probability to make a defect with the  
 quantum numbers of any member of the  
 baryon octet or decuplet.

$$\# \text{ Skyrmions} + \text{anti-Skyrmions} / \text{central Pb+Pb collision}$$

$$= 14 \ll 2A = 414 = \text{net baryon } \#$$

Decreased probability of DCC pointing in the  
 strange flavor direction is offset by the  
 increased probability of defect production  
 when it does.

Kapusta, Srivastava (1995)

Once produced the  $\Omega$  and  $\bar{\Omega}$  are almost indestructable!

Following rate equations of Koch, Müller, Rafelski (1986)

$$\tau(\pi + \Omega \rightarrow K + \Xi) = 160 \left(\frac{170}{T}\right)^{3/2} e^{142.5/T} \text{ fm/c} \rightarrow 370 \text{ fm/c}$$

$$\tau(K + \Omega \rightarrow \pi + \Xi) = 36 \left(\frac{170}{T}\right)^2 e^{354/T} \text{ fm/c} \rightarrow 290 \text{ fm/c}$$

$$\uparrow \\ T = 170 \text{ MeV}$$

### DCC domain size

$$\# \text{ defects} = 14 = p \cdot V$$

$$V = \frac{2000 \text{ hadrons}}{10 \cdot (0.16 \text{ nucleons/fm}^3)} \approx \frac{V_{Pb}}{\delta_{cm}}$$

$$\boxed{\xi = \text{domain size} \approx 2 \text{ fm}}$$

Predictions ranged from 1.4 to 3 fm, based on:

thermal evolution	Rajagopal, Wilczek (1993)
quenching	" " "
annealing	Gavin, Müller (1994)
bubble nucleation	Kapusta, Vischer (1997)

# Buckyballs and Gluon Junction Networks on the Femtometer Scale

T. Csörgő  
MTA KFKI RMKI, Budapest  
March 30, 2002

for  
Baryon Dynamics at RHIC Workshop  
RIKEN BNL Research Center

# Buckyballs and gluon junction networks on the femtometer scale <sup>\*</sup>

T. Csörgő<sup>a,b,c</sup> M. Gyulassy<sup>c,d</sup> D. Kharzeev<sup>e</sup>

<sup>a</sup>MTA KFKI RMKI, H-1525 Budapest 114, POB 49, Hungary

<sup>b</sup>Inst. de Fisica, USP, CP 66318, 05389-970 Sao Paulo, Brazil

<sup>c</sup>Dept. Physics, Columbia University, 538W 120th St, New York, NY 10027, USA

<sup>d</sup>Collegium Budapest, Szentháromság u. 2, H-1014 Budapest, Hungary

<sup>e</sup>Dept. Physics, Brookhaven National Laboratory, Upton, NY 11973-5000, USA

## Abstract

We explore the possibility that novel geometrical structures analogous to carbon Fullerenes may exist in Nature on the femtometer scale. The theory of strong interactions, Quantum Chromo Dynamics (QCD) predicts the existence of special topological gluon field configurations called baryon junctions and anti-junctions. Here we show that femto-scale structures, networks or closed (gluon field) cages, can be constructed in the theory of QCD as tiny cousins of familiar nano-scale structures such as carbonic Fullerenes  $C_{60}$ ,  $C_{70}$ . The most symmetric polyhedra of QCD junctions (J-balls) are characterized by the "magic numbers" 8, 24, 48, and 120, and zero net baryon number. Tubes, prisms, tori and other topological structures can also be created. In addition, special configurations can be constructed that are odd under charge and parity conjugation (CP), although the QCD Lagrangian is CP even. We provide a semi-classical estimate for the expected mass range of QCD Buckyballs and discuss the possible conditions under which such novel topological excitations of the QCD vacuum may be produced in experiments of high energy physics.

*Key words:* Fullerenes, baryon number, QCD, junction, classical and semi-classical techniques, nonstandard multi-gluon states  
*PACS:* 11.15.Kc, 11.30.Fs, 12.39.Mk

<sup>\*</sup> Dedicated to J. Zimányi on the occasion of his 70th birthday.

*Email addresses:* csorgo@sunserv.kfki.hu (T. Csörgő), gyulassy@mail-cunuke.phys.columbia.edu (M. Gyulassy), kharzeev@bnl.gov (D. Kharzeev).

## 1 Introduction

The Buckyball is the nickname for the carbon molecule Buckminsterfullerene,  $C_{60}$ , a new form of carbon discovered in chemistry in 1985 by R. F. Curl, H. W. Kroto and R. E. Smalley[1]. The molecule was named after the geodesic dome, invented by the architect Buckminster Fuller, whose geometry approximates that of a truncated icosahedral (soccer-ball) shaped structure. The discovery of Buckyballs was followed by the discovery of a wide variety of other carbon molecules with interesting geometrical properties. Carbon tubes, helices, tori, etc. opened the doorway to technology on the nanometer ( $10^{-9}$  m) scale. Carbon atoms can be arranged in novel geometric forms because the carbonic bonds can arrange into 3 way junction structures as illustrated in Fig. 1. Nano-structures have also been constructed using 3 and 4 way DNA junctions by Seaman et al. [2]. The field of nano-technology is developing rapidly using an assortment of molecular junctions as the chemical "lego" building blocks.

In nuclear/particle physics, where the distance scales are femtometers ( $10^{-15}$  m), the existence of special three-way QCD junctions (topological gluon field configurations) was predicted a long time ago[3]. Lattice QCD calculations were able to confirm the existence of such junctions only recently[4]. Data on baryon stopping and strangeness production in experiments with high energy heavy ion collisions from CERN SPS and BNL RHIC accelerators are also in agreement with model calculation assuming that QCD junctions carry the conserved baryon charge[5-8]. In this Letter, we explore what types of femtometer scale structures can be constructed from QCD using junctions and anti-junctions as a nuclear scale "lego set". Our preliminary results were presented at a Symposium on multiparticle production in high energy physics [9].

According to QCD, hadrons are composite bound state configurations built up from the fundamental quark and gluon fields. Quarks,  $\Psi_{i,f}(x)$ , carry color,  $i = 1, \dots, N_c$ , and flavor,  $f = u, d, s, c, b, t$  quantum numbers. Gluons,  $A_a^\mu(x)$ , are the vector gauge bosons intermedating the color,  $a = 1, \dots, N_c^2 - 1$ , interactions between the quarks and gluons. The form of the interaction is fixed by the principle of gauge invariance under the non-Abelian color  $SU(N_c)$  Lie group. The  $N_c = 1$  limit is Quantum Electrodynamics (QED). Gauge invariance of composite operators can only be achieved with the help of open string operators, called Wilson lines [10], that keep track of the phase along an arbitrary path,  $\Gamma$ , in space-time. In QED,  $U(\Gamma) = \exp[ie \int_\Gamma dx^\mu A_\mu(x)]$  is the well known Aharonov-Bohm phase [11] accumulated by an electron moving along a path  $\Gamma$  in an external electromagnetic field,  $A^\mu(x)$ . In QCD,  $N_c = 3$  and  $U(\Gamma)$  is a matrix defined by a path ordered exponential with dimension corresponding to that of the representation of the generators,  $T_a$ , of the Lie algebra.

Closed Wilson loops,  $\text{Tr}U(\Gamma_{xx})$ , correspond to color singlet glueball configurations in QCD, while open "strings",  $\bar{\Psi}_{i_1 f_1}(x)U^{i_1 i_2}(\Gamma_{xy})\Psi_{i_2 f_2}(y)$ , terminating with quark and anti-quark ends, correspond to mesons. Baryons are special field configurations composed of  $N_c$  quarks with their color flux strings tied together (outer product of color indices) by the Levi-Civita antisymmetric tensor,  $\epsilon_{i_1 \dots i_{N_c}}$ . In the physical ( $N_c = 3$ ) case, baryons of flavor ( $f_1, f_2, f_3$ ) are represented by the color neutral and gauge invariant operator,

$$B_{f_1 f_2 f_3} = \bar{\Psi}_{i_1 f_1}(x_1)\bar{\Psi}_{i_2 f_2}(x_2)\bar{\Psi}_{i_3 f_3}(x_3)J^{i_1 i_2 i_3}(\Gamma_1, \Gamma_2, \Gamma_3), \quad (1)$$

where the quark color indices are contracted by the baryon Junction tensor

$$J^{i_1 i_2 i_3}(\Gamma_1, \Gamma_2, \Gamma_3) = \epsilon_{j_1 j_2 j_3} U^{i_1 j_1}(\Gamma_1) U^{i_2 j_2}(\Gamma_2) U^{i_3 j_3}(\Gamma_3), \quad (2)$$

that depends on the paths,  $\Gamma_i$ , connecting the quark at  $x_i$  to an intermediate junction vertex point,  $x$ . All three paths are chromo-field flux lines oriented into the junction vertex as represented by black dots in Fig. 1. Anti-baryons can be constructed similarly with the help of an anti-Junction tensor,  $\bar{J}$ , where all the flux lines are oriented away from the vertex. Note that because of the special,  $\det U = 1$ , constraint on the symmetry group,  $SU(3)$ ,  $J^{i_1 i_2 i_3}(\Gamma, \Gamma, \Gamma) = 1$ . Thus color singlet states can be constructed from the color tensor links  $U(\Gamma)$  not only by tracing and contracting with quark fields but also by contracting with baryon junctions. The paths from a physical junction vertex must be all nondegenerate. Paths are deformable according to Stoke's theorem only if the background fields are pure gauge artifacts. In the physical, confining vacuum, or in a quark-gluon plasma, different paths correspond to configurations with different energy. In the ground state of a heavy quark baryon, the physical junction vertex ends up in the three quark plane, leading to a Y shaped chromo-field flux field configuration inside the baryon [4].

## 2 Archimedean polyhedra in QCD

The compelling theoretical arguments in favor of the existence of gauge junction and anti-junctions as inevitable components of the Standard Model led to the prediction [12] of  $M_J^0 = \text{Tr}J\bar{J} = \epsilon U(\Gamma_1)U(\Gamma_2)U(\Gamma_3)\epsilon$ , a new family of glueballs, with masses  $O(N_c)$  larger than usual glueballs corresponding to a closed string. In addition, many new exotic states formed by a multitude of quarks and anti-quarks [3,6] were predicted to exist. So far none of these structures have been observed experimentally, probably because the decay widths of these structures is too large, due to their strong coupling to light meson and baryon anti-baryon states. These previously discussed QCD structures are

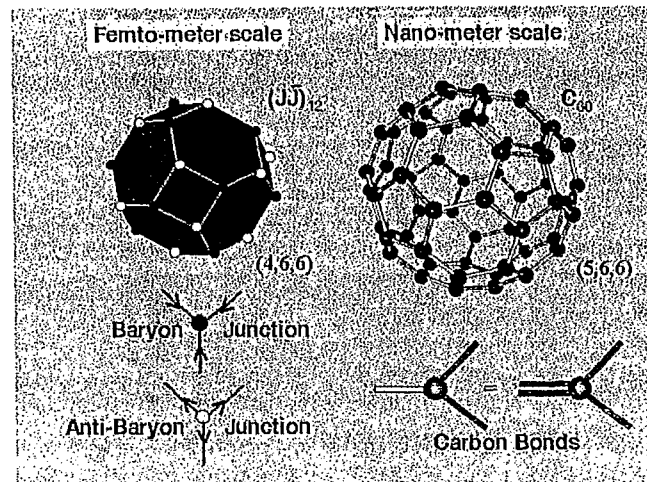


Fig. 1. Fentometer scale QCD analogs of nanometer scale (QED) carbon Fullerenes and their corresponding three way junction building blocks.

analogous to carbonic structures with low number of carbon atoms that do not possess any special geometric symmetry.

In high-energy baryon and nuclear collisions, the valence quarks carry a large fraction of the incident baryon's momentum. Those quarks thus hadronize in the fragmentation regions which are typically within one unit of rapidity,  $y = 0.5 \log[(E + p_z)/(E - p_z)]$ , from the kinematic limits. However, baryon junctions invalidate this naive picture of baryon production, since gluons carry on the average only small fraction of the baryon's momentum. Therefore, junction mechanism of baryon production (via exchange of the  $M_J^0$  Regge trajectory) predicts a much higher probability of finding the conserved valence baryon number many units of rapidity away from the incident baryons [6]. In addition, junction dynamics also naturally predicts [7] a high probability that the valence baryon emerges with multiple strangeness quantum numbers, e.g.  $\Xi^-(dss)$ ,  $\Omega^-(sss)$ , in the central rapidity region, since the final baryon is made by neutralizing the color of the gluon junction by pair production of quarks and antiquarks with arbitrary flavors. The baryon production data from SPS/CERN [7] and now RHIC/BNL [8] are consistent with these predictions and therefore lend experimental support to the important role that gluon junction dynamics plays in nuclear reactions. From a rehadronizing quark matter baryon junctions may pick up the valence quarks similarly as described by

the quark combinatorics of the ALCOR model that describes the production of multi-strange anti-baryon to baryon ratios at CERN SPS in simple terms [13]. The success of the ALCOR model implementation of quark combinatorics in predicting [14] the multistrange anti-baryon to baryon ratios at RHIC is thus consistent with a junction mechanism for the formation of baryons.

Motivated by Fullerenes, in this Letter we point out the existence of new geometric structures in QCD with high spatial symmetry. We determine the geometric structure and the characteristic "magic numbers" of these configurations, using analogies with carbon Fullerene structures. We explore some of the interesting topological structures that can be created by QCD networks and closed cages that may be produced in high energy nuclear reactions joining multiple QCD junctions and anti-junctions. Although the QCD Lagrangian is CP even, we point out that the junction and anti-junction building blocks can be used construct CP odd configurations that may also serve as domain walls between inequivalent ( $\theta$ ) QCD vacua.

In QCD, the orientation of flux lines going into (out of anti-) junctions restricts the set of allowed configurations. In particular, the number of junctions has to be equal with the number of anti-junctions on any closed path formed by the Wilson lines, which implies that QCD Fullerenes may have only even number of vertexes  $V$ , and a zero net baryon number. Recalling Euler's formula, the number of faces ( $F$ ), the number of edges ( $E$ ) and the number of vertexes ( $V$ ) of a simple (genus 0) polyhedron is related by

$$V + F = 2 + E. \quad (3)$$

Since each edge is sandwiched between a junction and anti-junction, each face must have an even number of edges. The number of faces,

$$F = N_4 + N_6 + N_8 + \dots, \quad (4)$$

is then a sum of the the number of squares ( $N_4$ ), hexagons ( $N_6$ ), etc. Each edge belongs to two faces :

$$E = (4N_4 + 6N_6 + 8N_8 + \dots)/2, \quad (5)$$

and each vertex belongs to three faces:

$$V = (4N_4 + 6N_6 + 8N_8 + \dots)/3. \quad (6)$$

The resulting Diophantic equations are solved by *any number of hexagons* and

$$N_4 - \sum_{i=4}^{\infty} (i-3)N_{2i} = 6. \quad (7)$$

This implies that there is an infinite variety of Fullerene type of structures in QCD, similarly to the case of carbon Fullerenes.

We are particularly interested in the most symmetric geometric structures in QCD, based on the expectation that configurations with the highest geometric symmetry are the most stable ones, similarly to the case of the carbon Fullerenes. If we require that all the vertex positions are equivalent with each other, we have to find the so called Archimedean polyhedra with the constraint that all faces have even number of edges. Archimedean polyhedra can be characterized by the number of vertexes or, equivalently, by their vertex structure ( $i, j, k$ ) denoting that at each vertex one  $i$ -gon, one  $j$ -gon and one  $k$ -gon is joined. The simplest such geometric structure is the  $V = 8$  cube, with vertex structure  $(4, 4, 4)$ , denoting that three squares are joined at each vertex. The cube is followed by the  $V = 24$  truncated octahedron, with vertex-face structure is  $(4, 6, 6)$ , denoting that at each vertex one square and two hexagons are joined. Allowing for octagon, and higher faces lead to only two more closed Archimedean polyhedra,  $V = 48$   $(4, 6, 8)$  and  $V = 120$   $(4, 6, 10)$ , in which one square and one hexagon are joined to an 8 or 10 sided polygon at each vertex. These are the most symmetric QCD Fullerenes as illustrated in Fig. 2.

Infinite two dimensional tiling or fences can also be created, for example  $(4, 8, 8)$ ,  $(4, 6, 12)$  and the J-graphite  $(6, 6, 6)$ . In addition, as with carbon cages, there are of course many closed structures with less symmetry such as junction  $n$ -prisms  $(4, 4, 2n)$  that can be constructed. Here we will not attempt to discuss the dynamics of elementary particle or heavy ion/nuclear collisions that may lead to the formation of QCD J-balls. In nuclear collisions, we simply assume that the observed copious production of baryons and anti-baryons (interpreted as junctions and anti-junctions) in central collisions is sufficient to allow such a configuration to form with finite probability amidst the "nuclear ashes" due to its relatively high binding energy. The carbon Fullerenes  $C_{60}$  and  $C_{70}$  were similarly found within the ashes of laser seared graphite. Another mechanism to create QCD Buckyballs may exist also, that has no analogy in Fullerene chemistry. In particular, high energy collisions of protons and anti-protons at the Fermilab Tevatron accelerator satisfy the conditions for zero net baryon number and high energy density, that are required to excite QCD Fullerenes out of the physical vacuum of strong interactions.

To estimate the relative binding energies of QCD Fullerenes, we consider the simplest model for the relative energy of J-balls consistent with QCD [6]. For a J-ball consisting of  $V/2$  junctions and  $V/2$  anti-junctions connected to

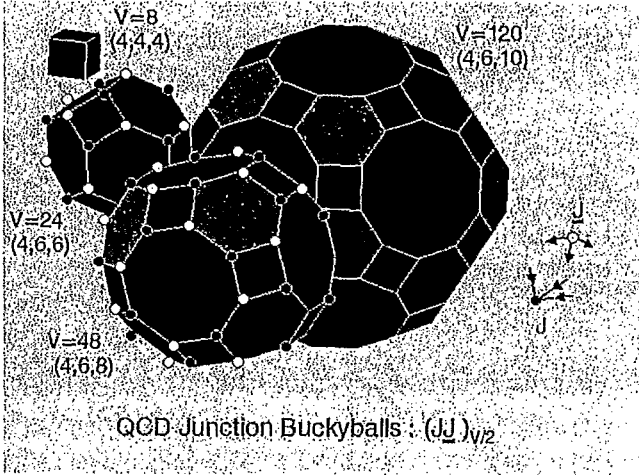


Fig. 2. The family of QCD Fullerenes,  $(J\bar{L})_{V/2}$ , with magic numbers  $V = 8, 24, 48$  and  $120$ .

form a polyhedron with  $E$  edges with lengths  $l_i$  we take the following model Hamiltonian

$$H(l_i, n_{v,i}; V, E) = \sum_{i=1}^E \left( \frac{a}{l_i} + \kappa l_i \right) + \gamma \sum_{v=1}^V \sum_{i < j=1}^3 n_{v,i} n_{v,j} \quad (8)$$

where  $n_{v,i}$ ,  $i = 1, 2, 3$  are the three unit vectors pointing away tangent to the edges at vertex  $v$ . Implicit above is that the topology is defined by these unit vectors and that the flux tubes are straight lines between vertices. The first term is a "kinetic" or "vertex localization" energy, with coefficient  $a$  that is not yet precisely known. However, one can estimate that  $a \approx \pi h$  from  $\omega = (2\pi h)/\lambda$  and assuming that  $\lambda = 2l$  that holds in the case of the lowest excitation for a string with two fixed ends. The second parameter of the effective Hamiltonian is the confining string tension,  $\kappa(T) \approx 1 \text{ GeV/fm}$ , a term that vanishes above the deconfinement temperature,  $T_c \approx 150 \text{ MeV}$ . The postulated "strain" term with strength  $\gamma$  is analogous to the Biot-Savart law in circuits and plays the role of bond angle strain in carbon nanostructures. In this model the relative binding energies are determined by the last term although its magnitude is not yet known from lattice QCD. We estimate below the possible range of  $\gamma$  and use these limiting values to give a semi-classical estimate of the mass range of the QCD Fullerenes.

For a vertex and face structure  $V$  and  $(n_1, n_2, n_3)$  the total strain energy is

$$\delta h_V = \frac{\Delta H_V}{V} = -\gamma \left[ \cos\left(\frac{2\pi}{n_1}\right) + \cos\left(\frac{2\pi}{n_2}\right) + \cos\left(\frac{2\pi}{n_3}\right) \right]. \quad (9)$$

For the  $V = 8$  J-cube with face structure  $(4, 4, 4)$  and  $\Delta h_8 = 0$ . For the  $V = 24, 48, 120$  J-balls, this strain energy per vertex is  $-1$ ,  $-(1 + \sqrt{2})/2 = -1.207$ ,  $-(3 + \sqrt{5})/4 = -1.309$  in units of  $\gamma$ . The absolute minimum is reached for the junction graphite fence which is bound with  $-3/2\gamma$  per vertex. The  $(4, 8, 8)$  and  $(4, 6, 12)$  tiles are only bound by  $-\sqrt{2}\gamma$  and  $-0.5(1 + \sqrt{3})\gamma$  per vertex. In contrast, the  $n$  prisms  $(4, 4, 2n)$  are bound by  $-\cos(\pi/n) > -1$ . Note that the  $(J\bar{L})_1 = M_j^0$  is most unfavorable due to its maximum strain energy of  $6\gamma$ . The  $V = 24$  J-ball in Figs. 1,2 with total strain energy  $-24\gamma$  may be particularly stable not only because of its relatively low strain energy but also due to its topological arrangement of junctions and anti-junctions that increases the potential barrier between adjacent  $J\bar{L}$  annihilation. The vertex structure of this  $V = 24$  QCD Buckyball,  $(4, 6, 6)$ , is the closest to that of the carbon Buckyball  $C_{60}$  whose vertex structure is  $(5, 6, 6)$ .

### 2.1 Semiclassical mass estimates for QCD Fullerenes

Let us find the semi-classical values of the Hamiltonian  $H$  to give an estimate of the expected mass range of the  $V = 8, 24, 48$  and  $120$  QCD Fullerenes. Let us first observe that the minimum of the  $H$  Hamiltonian can be determined from requiring that

$$\frac{\partial H}{\partial l_i} = 0 \quad (10)$$

for all  $i = 1, \dots, V$ , which implies that all the edges have the same length of

$$l_i = l_j = l = \sqrt{\frac{a}{\kappa}} \approx 0.79 \text{ fm}. \quad (11)$$

The mass of a QCD Fullerene can be semi-classically approximated by the value of  $H$  at this minimum,

$$M_V = \left( \frac{3}{2} \sqrt{a\kappa} + \delta h_V \right) V \quad (12)$$

Hence the mass of these QCD Fullerenes is always proportional to the number of vertexes  $V$  and the constant of proportionality is given by a sum of two terms. The first term is a kinetic term, that can be estimated as  $\frac{3}{2}\sqrt{\pi 0.197}$

GeV  $\approx 1.18$  GeV, while the second strain term is a product of a known geometrical contribution and the unknown constant of proportionality  $\gamma$ . As  $a > m_N = 0.940$  GeV, we find that without a strain term the mass of QCD Fullerenes were about 25 % higher than that of a system consisting from  $V/2$  nucleons and  $V/2$  anti-nucleons, hence if  $\gamma = 0$  these excitations are most likely unstable.

At what value of  $\gamma = \gamma_c$  were at least some of the QCD Fullerenes stable? Including the possibility of tilings, the absolute minimum of the geometrical contribution to the strain term is  $\sum_{i < j=1}^3 \mathbf{n}_i \mathbf{n}_j = -1.5$ , that can be achieved within a graphite like layer. Hence one obtains for the critical value of  $\gamma$

$$\gamma_c = \sqrt{a\kappa} - \frac{2}{3}m_N \quad (13)$$

which leads to a numerical estimate of  $\gamma_c \approx 0.16$  GeV. If in Nature  $\gamma > \gamma_c$  then (at least some high mass) QCD Fullerenes are expected to be stable against decay to baryon anti-baryon pairs, while if  $\gamma < \gamma_c$  all these objects are unstable for such decays and may exist only as short lived resonance states.

Let us now determine an absolute lower and an upper limit for the strain coefficient  $\gamma$ . If  $\gamma$  were negative, the strings were attracted to each other and the  $M_V^0$  state would be a stable bound state and it would be difficult to explain why this state has not been observed until now. Excluding this possibility, one obtains  $0 \leq \gamma$ . An upper limit on the possible values of  $\gamma$  can be obtained from requiring that even for a graphite like tiling the mass of the Fullerene should be positive, which implies  $\gamma < \sqrt{a\kappa}$ . Thus one obtains the following lower and upper limits for the mass of QCD Fullerenes:

$$\frac{3}{2}V\sqrt{a\kappa} \leq M_V < \left[ \frac{3}{2}V - \cos\left(\frac{2\pi}{n_1}\right) - \cos\left(\frac{2\pi}{n_2}\right) - \cos\left(\frac{2\pi}{n_3}\right) \right] \sqrt{a\kappa}. \quad (14)$$

Utilizing these limiting values, we obtain Table 1 that summarizes the mass range estimates for the most symmetric QCD Fullerenes utilizing the geometric strain coefficients determined by eq. (9).

Although Table 1 contains order of magnitude estimates only, we can already observe interesting patterns. In particular, the strain coefficient does not influence the mass estimate for the  $V = 8$  QCD cube, and the estimated mass is much higher than that of 8 nucleons hence this and all the low lying QCD Fullerenes are expected to be unstable as they are even more strained than the cube. The first reasonable candidate would be a  $V = B + \bar{B} = 24$  QCD truncated octahedron. The most stable candidates are expected to be the  $V = 48$

$V$	$(n_1, n_2, n_3)$	$\delta h/\gamma$	$M_{\min}$ (GeV)	$M_{\max}$ (GeV)	$M_{\text{crit}}$ (GeV)	$d$ (fm)
8	(4,4,4)	0	9.4	9.4	7.5	1.3
24	(4,6,6)	-1	9.4	28.3	22.6	2.5
48	(4,6,8)	$-\frac{1+\sqrt{2}}{2}$	11.1	56.7	45.1	3.6
120	(4,6,10)	$-\frac{3+\sqrt{5}}{4}$	18.0	141.7	112.8	6.0

Table 1

Estimated mass range for various QCD Fullerenes.  $V$  stands for the number of vertexes,  $(n_1, n_2, n_3)$  for the face structure at a vertex,  $M_{\min}$  and  $M_{\max}$  are the estimated lower and upper limits for the mass of the QCD Fullerene, together with the critical mass of stability  $M_{\text{crit}}$ . The diameter of the circumscribed sphere,  $d$  was estimated from  $l \approx 0.79$  fm and the geometrical structure.

QCD Great Rombicuboctahedron and the  $V = 120$  QCD Great Rombicosidodecahedron. These structures are compact but less strained than similarly compact lower excitations. Their compact structure and their favourable strain term may stabilize all three of them in a large domain of the allowed parameter space.

### 3 CP odd J-ball states in QCD

The junction  $n$ -prisms can be regarded as a closed ribbon of  $n J\bar{L}$  pairs. Under simultaneous charge conjugation and parity transformation, these prisms are invariant and hence CP even as are all the junction Fullerenes shown in Fig. 2. However, other nontrivial topological configurations can be constructed which are not symmetric under CP. For example an odd number of  $J\bar{L}$  pairs cannot be closed into a prism due to the oriented flux at the junctions, but after a twist to right or left can be connected into a Moebius strip. The two Moebius strips transform into each other and thus there exists a linear combination of the two that is odd under CP. Hence QCD  $J$ -ribbons can be characterized by a single "winding number" ( $i$ ) that gives the number of twists before the ribbon is closed on itself. The topology of the excitations of QCD seems to be very interesting, because not only ribbons but also tubes can be formed. The ends can be closed with caps formed by squares, octagons and decagons, satisfying eq. (5), or can be open, ending on valence quarks. The QCD femto-tubes are analogous to the carbon nano-tubes, both may have interesting chiral properties. As carbon nano-tubes, the QCD femto-tubes can be characterized by two integers  $(i, j)$ , which gives the number of steps in the direction of the lattice vectors, that connect equivalent points on the surface of the tubes. Another interesting possibility is to close the  $J$ -tube on itself, creating a toroidal structure. The femto-tubes can be closed by connecting the two ends of a



long tube, and these ends can be rotated before the connection. This gives QCD femto-tori that can be characterized by 3 winding numbers, the  $(i, j, k)$  femto-tori.

#### 4 Summary

Fullerene type of pure glue topological configurations can be constructed in QCD. These "J-balls" are QCD femto-structures with the highest geometrical symmetry. All of the QCD Fullerenes have an equal number of junctions and anti-junctions, and may have specific geometrical and topological properties. The QCD Buckyballs are CP even, other QCD structures such as linear combinations J-Moebius ribbons can be constructed that are CP odd. Topological winding numbers can be introduced to characterize these states. The QCD femto-ribbons are characterized by a single integer ( $i$ ), the femto-tubes by a pair of integers  $(i, j)$ , while the QCD femto-tori by a triplet of integers,  $(i, j, k)$ . We determined that the most symmetric (likely most stable) QCD Buckyball configurations have the magic numbers of baryons + anti-baryons  $B + \bar{B} = 8, 24, 48$  and  $120$ . Although these configurations are likely unstable, they are expected to be more stable than clusters of baryons and anti-baryons with different junction numbers, and they may appear as peaks in the spectrum of  $(B\bar{B})_n$  clusters with a given total baryon+antibaryon number. To create them, high initial energy densities and small net initial baryon number densities and large volumes are needed. Such conditions may exist in the mid-rapidity domain of central  $Au + Au$  collisions at RHIC or LHC as well as in diffractive collisions of protons and anti-protons at the Fermilab Tevatron accelerators. We suggest to search for clusters of baryons and anti-baryons with multiparticle correlation patterns of the vertices of J-balls in rapidity slices. In addition, searches for CP violating domains at RHIC should look for unusual baryon anti-baryon correlations suggested by our J-Moebii structures. Baryon junction and anti-junction networks may also help to understand the structure of domain walls between different CP vacua in QCD.

#### Acknowledgments

One of us (T. Cs.) would like to thank M. Albrow and G. Gustafson for stimulating discussions. This research has been supported by Hungarian OTKA grants T026435, T034296, the Dutch-Hungarian NWO-OTKA grant N025487, the Collegium Budapest, an US - Hungarian NSF - MTA - OTKA grant, by the Brazilian FAPESP and by the US Department of Energy DE-FG02-93ER40764.

#### References

- [1] H. W. Kroto, R. E. Smalley and R. F. Curl, *Nature* **318** (85) 165.
- [2] J. Chen and N. C. Seeman, *Nature* **350** (1991) 631-633;  
<http://seemanlab4.chem.nyu.edu/nanobib.html> .
- [3] L. Montanet, G. Rossi and G. Veneziano, *Phys. Rept.* **63** (1980) 149 - 222.
- [4] T. Takahashi *et al*, *Phys. Rev. Lett.* **86** (2001) 18.
- [5] D. Kharzeev, *Phys. Lett. B* **378** (1996) 238.
- [6] S. E. Vance, M. Gyulassy and X.-N. Wang, *Phys. Lett. B* **443** (1998) 45,
- [7] S. E. Vance and M. Gyulassy, *Phys. Rev. Lett.* **83** (1999) 1735.
- [8] C. Adler *et al*, STAR Collaboration, *Phys. Rev. Lett.* **86** (2001) 4778 - 4782
- [9] T. Csörgő, M. Gyulassy and D. Kharzeev, hep-ph/0102282, Proc. XXX Int. Symp. Multiparticle Dynamics (World Scientific, Singapore, 2001, ed. T. Csörgő, S. Hegyi and W. Kittel) p. 616 - 625
- [10] K. G. Wilson, *Phys. Rev. D* **10** (74) 2445.
- [11] Y. Aharonov and D. Bohm, *Phys. Rev.* **115** (1959) 485-491.
- [12] Y. Igarashi *et al*, *Prog. Theor. Phys. Suppl.*, **63** (1978) 49.
- [13] J. Zimányi, T.S. Biró, T. Csörgő, P. Lévai, *Phys. Lett. B* **472** (2000) 243-246
- [14] J. Zimányi, in S. A. Bass *et al*, *Nucl. Phys. A* **661** (1999) 205-260



# Theory and Phenomenology of Baryon Junctions

Dmitri Kharzeev

*Physics Department, Brookhaven National Laboratory  
Upton, NY 11973, USA*

Baryon gluon junctions are necessary to ensure the local gauge invariance of the baryon wave function:

$$B(x) = \epsilon^{ijk} \left[ P \exp \left( ig \int_{P(x,x_1)} A_\mu dx^\mu \right) q(x_1) \right]_i \left[ P \exp \left( ig \int_{P(x,x_2)} A_\mu dx^\mu \right) q(x_2) \right]_j \times \\ \times \left[ P \exp \left( ig \int_{P(x,x_3)} A_\mu dx^\mu \right) q(x_3) \right]_k .$$

The junction is the point where the gluon field fluxes from the three valence quarks (represented by the path-ordered Schwinger phase factors) meet and are anti-symmetrized in color. In the strong coupling limit, the baryon wave function thus is described by the valence quarks attached to the strings which are connected at the junction.

This picture, imposed by the local gauge invariance, has very interesting consequences for the phenomenology of baryon number transport and for the production of baryon-antibaryon pairs. Indeed, let us consider a gedanken experiment in which the junction is being kept fixed, while the valence quarks are being pulled apart. Once the quarks are separated sufficiently far, the strings connecting them to the junction will break up producing quark-antiquark pairs. The original valence quarks will thus be “dressed” by antiquarks and form mesons. However, the baryon will always emerge around the gluon junction! This simple observation suggests that even though the baryon number is, of course, associated with quarks, in high energy processes it can be dynamically traced by the non-perturbative, topological configuration of the gluon field – the junction.

In this talk, we discuss many theoretical indications pointing to the importance of baryon junctions in QCD – local gauge invariance, global center symmetry, and, possibly, the  $\theta$  dependence of the vacuum energy. Using large  $N_c$  arguments, we estimate the intercept of the junction-antijunction trajectory, which governs the energy dependence of baryon stopping in high energy  $pp$  and  $AA$  collisions. We compare predictions to the available data, and devise experimental tests of the junction picture at RHIC. Some speculations on the junction dynamics in the saturation environment are also presented.

# THEORY & PHENOMENOLOGY OF BARYON JUNCTIONS

D. KHARZEEV

BNL

1. Do we need junctions?

- local gauge invariance
- center symmetry  $Z_{N_c}$
- "new glueballs"  $M \sim N_c$   
baryons at large  $N_c$
- $\theta$ -dependence of vacuum energy,  
CP-odd domains, and junctions

2. Junctions and baryon dynamics  
 $\frac{dN_{B-\bar{B}}}{dY}$ ;  $\bar{B}/B(\sqrt{s})$ ;  $\bar{B}/\pi$ ;  $E_{byE}$

What about baryons?

⑤

$$B = \epsilon_{ijk} q^i q^j q^k$$

But again,  $\epsilon_{ijk} q^i(x_1) q^j(x_2) q^k(x_3)$

is not locally gauge-invariant

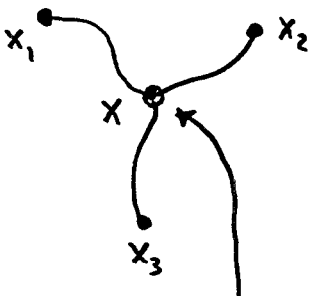
The only way to construct locally gauge-invariant state vector of the baryon:

G. Veneziano

$$B_{abc} = \epsilon^{ijk} \left[ P \exp \left( ig \int_{P(x, x_1)} A_\mu dx^\mu \right) q_a(x_1) \right]_i^x$$

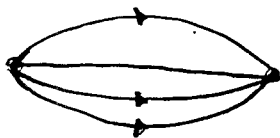
$$\left[ P \exp \left( ig \int_{P(x, x_2)} A_\mu dx^\mu \right) q_b(x_2) \right]_j^x$$

$$\left[ P \exp \left( ig \int_{P(x, x_3)} A_\mu dx^\mu \right) q_c(x_3) \right]_k^x$$



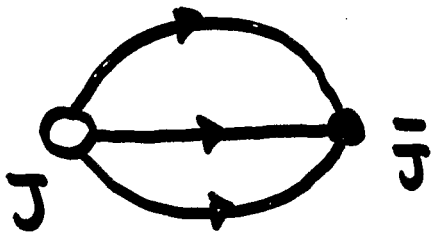
"string junction"

correlator of baryon current:




each quark is accompanied by a plane of gluons; gluons exchange color at the string junction

# "New glueballs"



$$M_J \sim O(N_c)$$

Estimate?

large  $N_c$  :  =  $\left[ \text{loop} \right]^{N_c} +$

Wilson loops factorize

$$+ O\left(\frac{1}{(N_c!)^2}\right)$$

$\Rightarrow$  "constituent meson model"

Y. Neumot.

$$M_J \approx 3 M_p \sim 2 \text{ GeV}$$

any states  
at  $\sim 2 \text{ GeV}$

strongly coupled  
to  $\bar{B}B$ ?

YES:  $f_2(1950)$   $I=0$   
 $J^{PC} = 2^{++}$

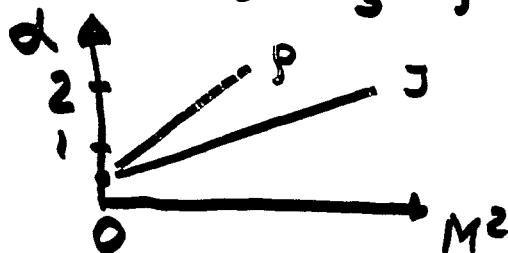
(above  $\bar{B}B$  threshold  
 $\Rightarrow$  broad)

GLUEBALL candidate

PDG: "needs confirmation"

string tension  $\sigma_J \approx 3 \sigma_p$

$$\Rightarrow \alpha'_J \approx \frac{1}{3} \alpha'_p$$



$$2 = \alpha_J(0) + \alpha'_J M_J^2 \approx$$

$$\approx \alpha_J(0) + \frac{2}{3} \Rightarrow \alpha_J(0) \approx \frac{1}{2}$$

Mueller-Kancheli diagrams

$$S_1 \approx \sqrt{s} m_+ e^{-y^*}$$

$$S_2 \approx \sqrt{s} m_+ e^{y^*}$$

$$S_1 S_2 \approx m_+^2 s$$

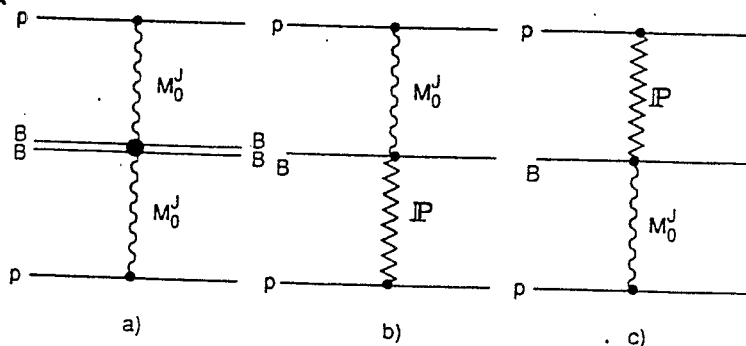


Fig. 4.

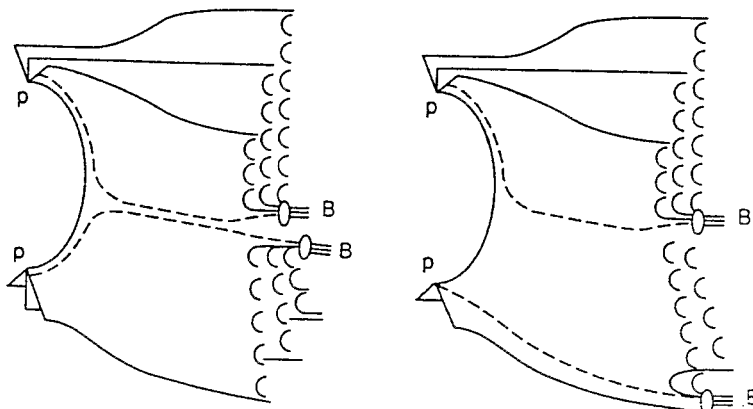


Fig. 5.

$$a): E_B \frac{d^3 \hat{\sigma}^{(2)}}{d^3 p_B} = 8\pi [G_P^M(0)]^2 f_B^{MM}(m_+^2) \left( \frac{\sqrt{s} m_+}{S_0} \right)^{2\alpha_0^J(0)-2} \sim \frac{1}{\sqrt{s}}$$

$$b)+c): E_B \frac{d^3 \hat{\sigma}^{(1)}}{d^3 p_B} = 8\pi G_P^M(0) G_P^P(0) f_B^{MP}(m_+^2) \left( \frac{\sqrt{s} m_+}{S_0} \right)^{\alpha_0^J(0) + \alpha_P(0) - 2} \times$$

$$\times \left\{ \exp[y^*(\alpha_P(0) - \alpha_0^J(0))] + \exp[-y^*(\alpha_P(0) - \alpha_0^J(0))] \right\}$$

$$\sim s^{-\frac{1}{4} + \frac{\Delta}{2}} \text{ - very slow } s\text{-dependence}$$

unusual  $y^*$  dependence

$$\alpha_0^J(0) \approx \frac{1}{2}$$

$$\alpha_P(0) = 1 + \Delta$$

$$n^a \approx \frac{3}{2} n^{inel}$$

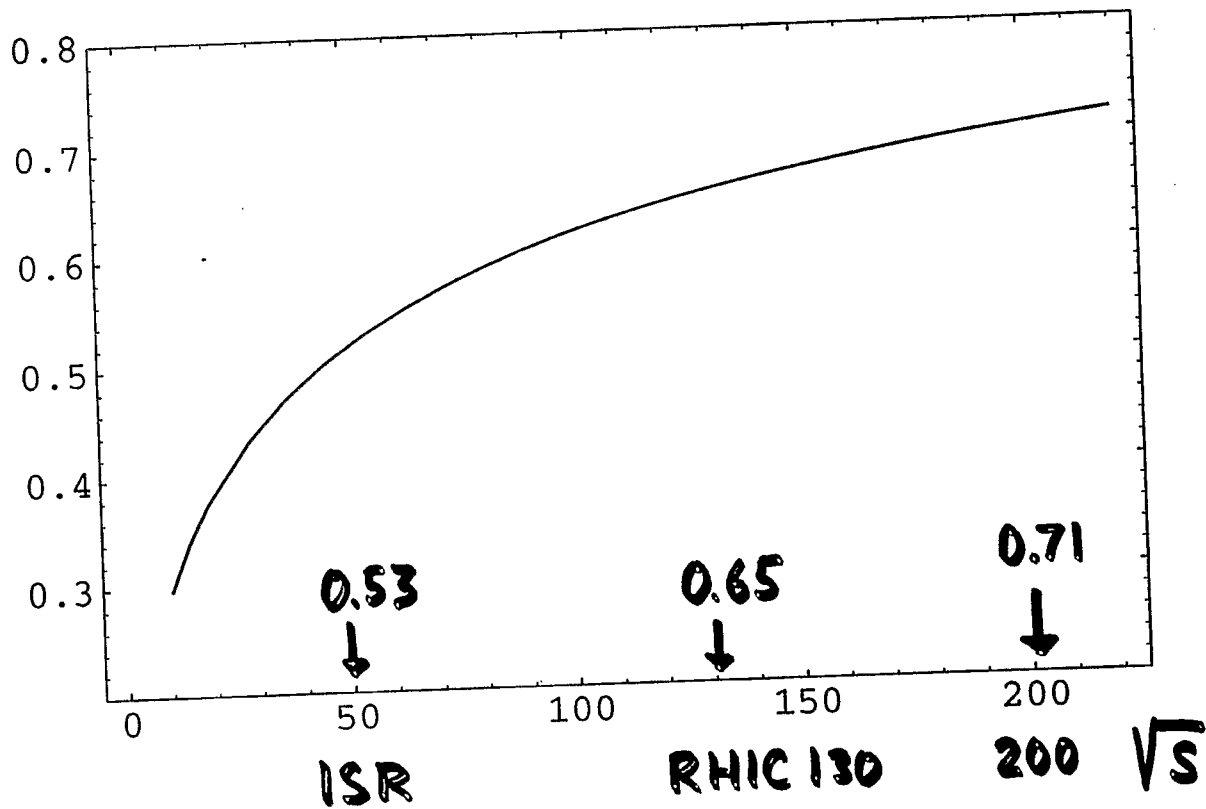
$$n^{b,c} \approx \frac{5}{4} n^{inel} \text{ - larger multiplicity}$$

$$\frac{1/p}{p} = \frac{s^\Delta}{s^\Delta + c s^{-1/4 + \Delta/2}}$$

$\Delta = 0.08$  fixed by  $\sigma_{tot}$

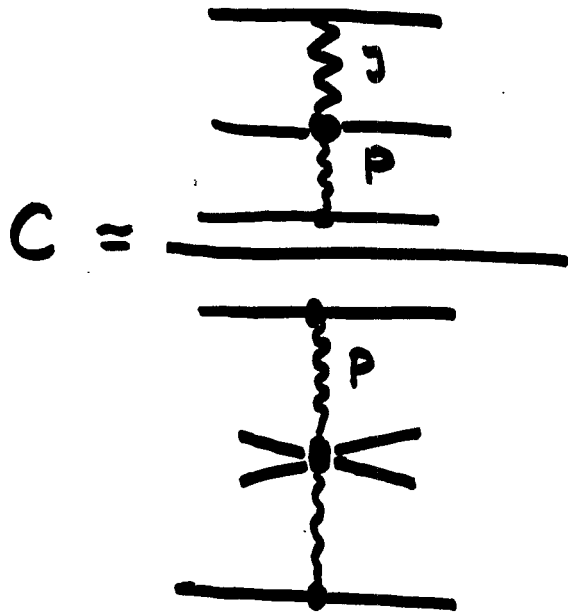
$c \approx 9$  "fitted"

$1/p/p$





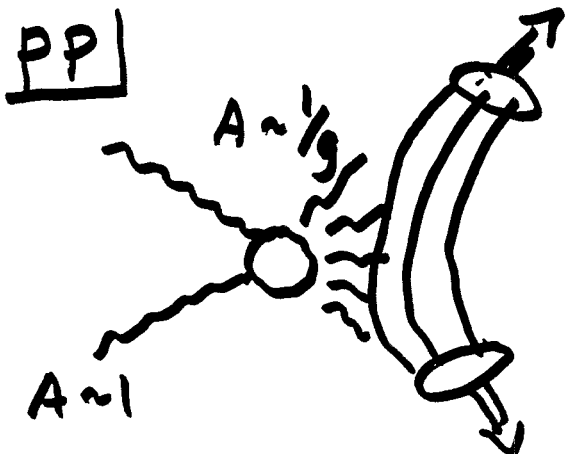
$C \approx 9$  why is it so large?



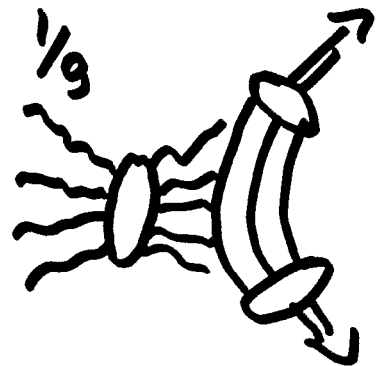
Large  $C \Rightarrow$  small probability of  $B\bar{B}$  production,  $P_{B\bar{B}}$



$P_{B\bar{B}} \sim e^{-N_c}$ , large  $N_c$   
 "JOZI" rule  
 Venezian



$e^{-\frac{1}{9^2}}$   
 AA, saturation,  
 CGC



STRONG "FLOW"  $\Leftrightarrow$  saturation  $\Leftrightarrow B\bar{B}$  production



# Recent Results on Strange Baryons From STAR

Hui Long, UCLA  
March 30, 2002

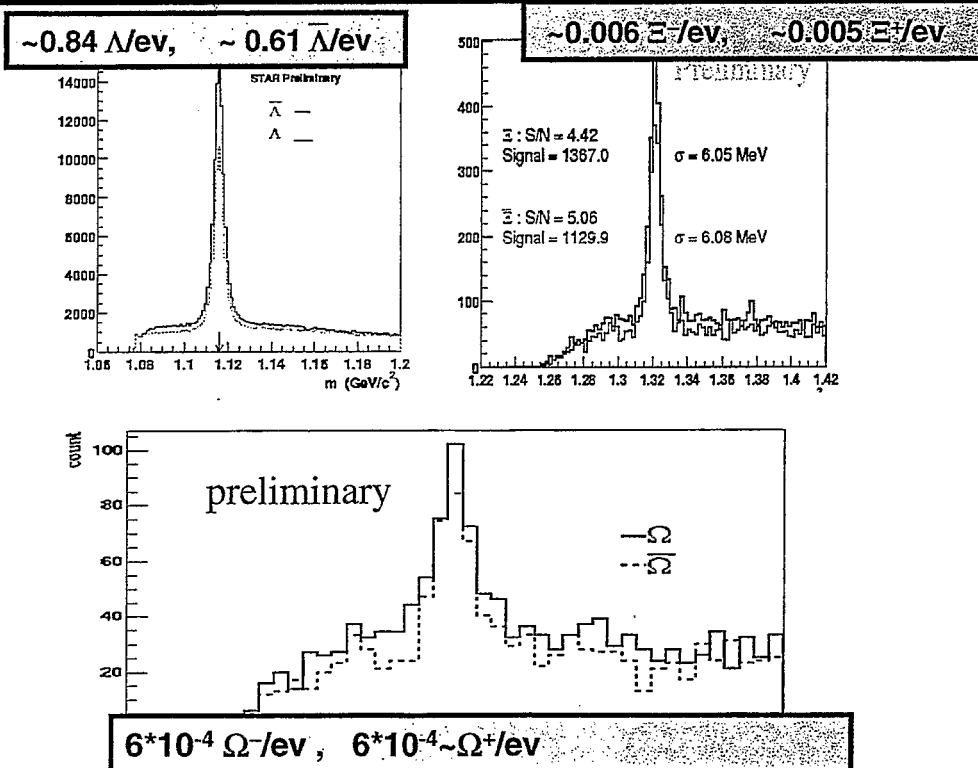
for  
Baryon Dynamics at RHIC Workshop  
RIKEN BNL Research Center



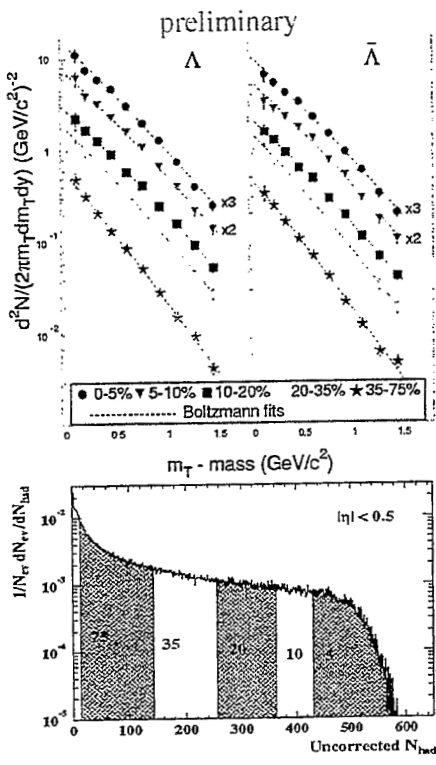
Hui Long  
 University of California, Los Angeles  
 for the star collaboration

- Outline: Experimental measurements and results of strange baryons from STAR (Au+Au at 130 GeV).
- Strange baryons at high pt.
- Strange baryon “enhancement” from pp to AA.
- Elliptic flow ( $v_2$ ) of Lambda

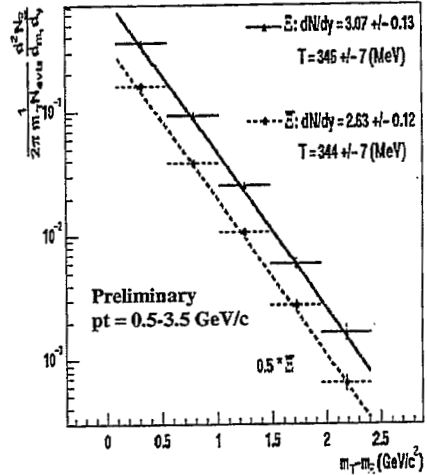
Strange Baryon Invariant Mass Spectra



# Mt spectra of (anti-) Lambda and (anti-) Cascade



Top 10% centrality



Centrality bins

## Strange baryon production as a function of centrality

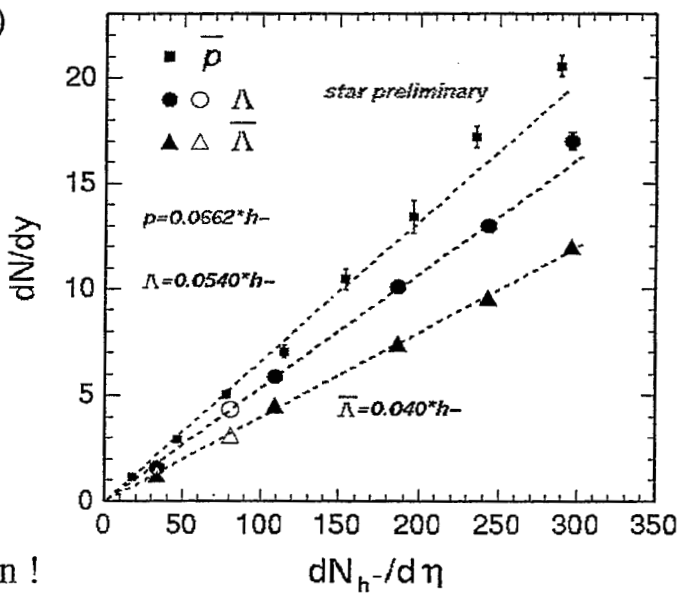
$$\bar{\Lambda}/\Lambda = (12.0 \pm 0.3) / (17.0 \pm 0.4) = 0.7 \pm 0.03$$

30% of  $\Lambda$  carry baryon numbers from the incoming nuclei

$$(\bar{\Lambda}/h^-)_{RHIC} > (\bar{\Lambda}/h^-)_{SPS}$$

$$(\Lambda/h^-)_{RHIC} < (\Lambda/h^-)_{SPS}$$

$\bar{\Lambda}$  at RHIC  $\rightarrow$  Pair Production!  
 $\Lambda$  at SPS  $\rightarrow$  Associated Production and high baryon density!



Note: spectra include feed-down contributions

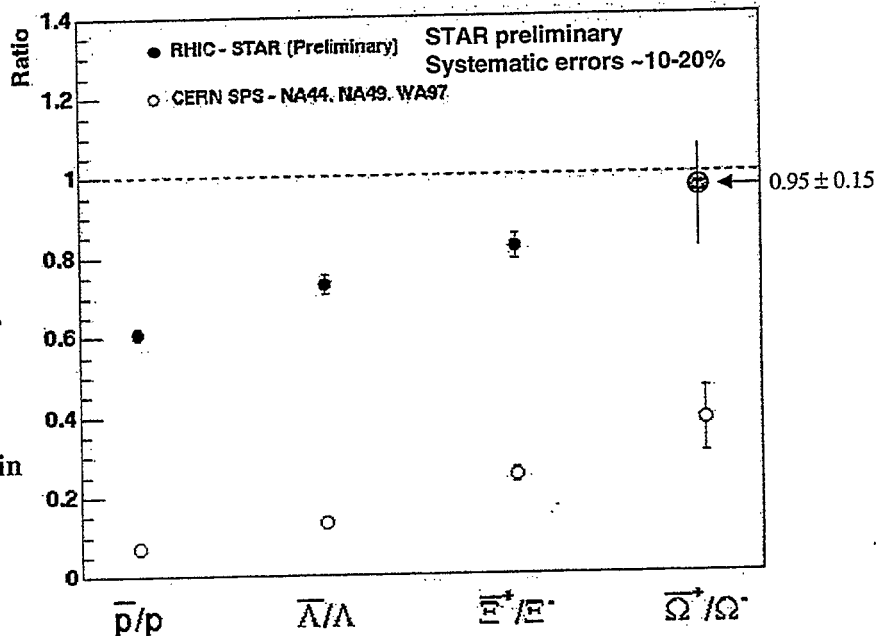
# STAR $\bar{B}/B$ Ratios

Ratio increase  
strangeness  
content increases

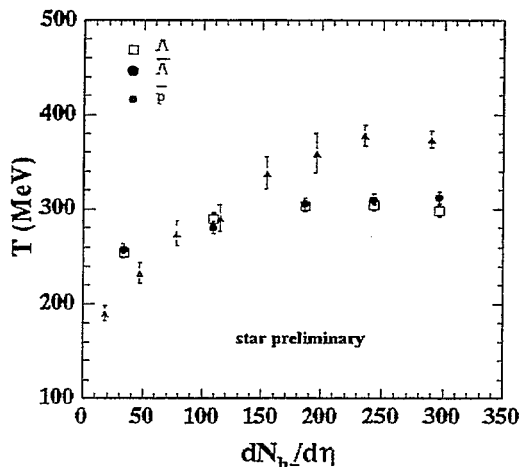
Ratios Fit Quark  
coalescence model

Strangeness  
Conservation not only  
globally, but also within  
 $|y| < 0.5$  bin!

Local Equilibrium ?!



## $m_T$ slopes vs. Centrality

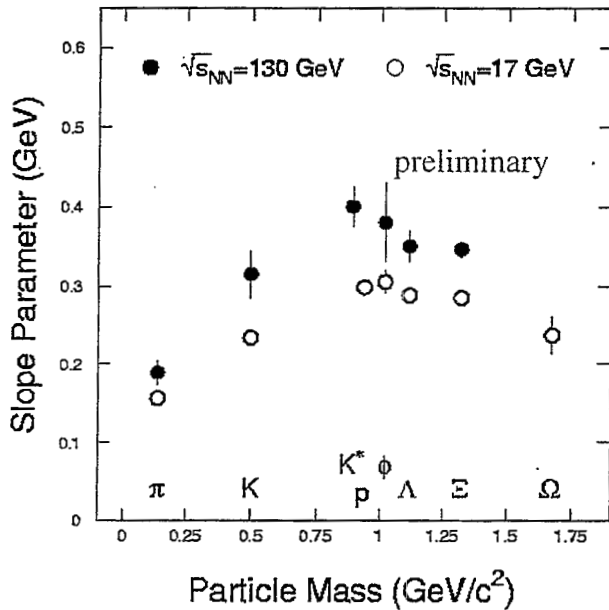


Indication of the increase of collective radial flow from the least central to the most central collisions, assuming the same freeze-out  $T$  for all collisions at the same energy.

(Proton slope is  $pt$  range dependent. But the trend in centrality dependence is also there.)

Similar  $T$  for  $\Lambda$  and  $\bar{\Lambda}$  suggests significant re-scattering during the evolution or similar production mechanism for  $\Lambda$  and  $\bar{\Lambda}$  produced from pair production and from baryon transport.

## Mass dependence of $m_T$ slopes

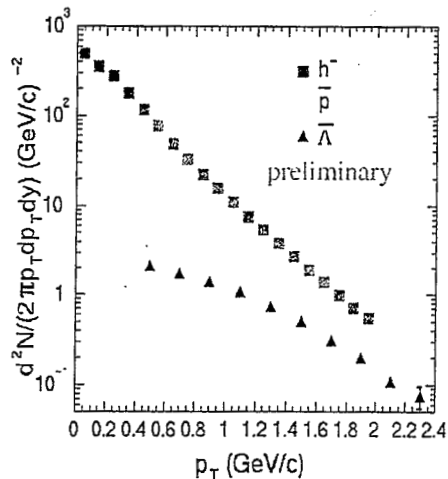


> Indication of stronger radial flow at RHIC than SPS

> Strange baryons freeze-out earlier?

STAR proton  $p_T$  coverage too small to get a reliable slope.  
PHENIX p slope  $\sim 350$  MeV in  $p_T$  region compatible to STAR  $\Lambda_s$ .

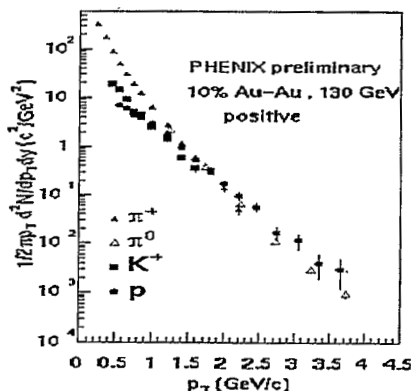
## Baryon vs. meson



Increase in baryon to meson ratio as a function of  $p_T$ .  
> 1 at high  $p_T$  ?

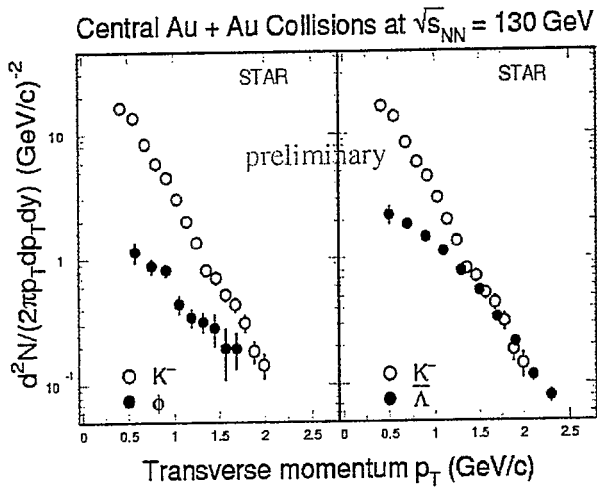
Data from  $e^+e^-$  and pQCD calculation show the ratio  $< 0.2$  even at very high  $p_T$

Consequence of radial flow or novel baryon dynamics (jet quenching effects) ?  
Vitev and Gyulassy nucl-th/0104066



$\Lambda, p$  Spectra includes feed-down contributions

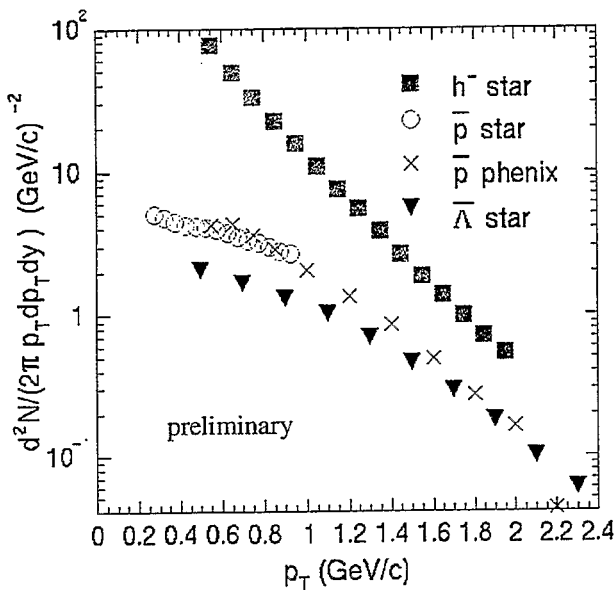
## Strange Baryon vs Strange Meson



Increasing ratio as  
function of  $p_T$ .  
Ratio > 1 at high  $p_T$

Particle mass important  
in determining the  $m_T$  shape

## Strange baryon vs. non-strange baryon



Strange hyperons constitute  
a significant fraction of total  
baryons !!

Does the hyperon to proton  
ratio depend on  $p_T$  and possibly  
the baryon “enhancement”  
mostly from hyperons?

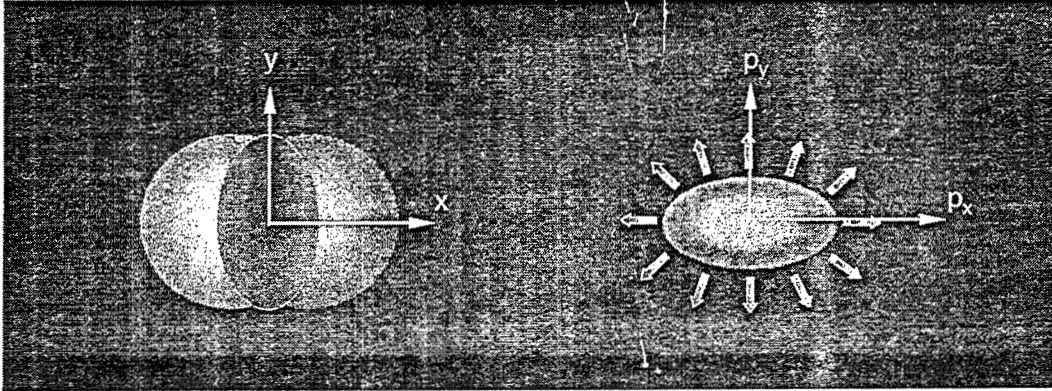
We need to understand the  
feed-down contributions in  
both the STAR and PHENIX  
data...! Very Important!!

$\Lambda, p$  Spectra includes feed-down contributions



# Event Anisotropy $v_2$

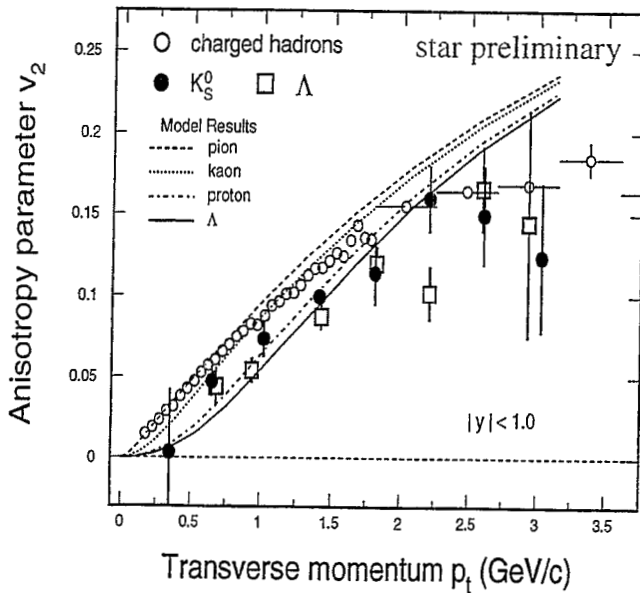
Coordinate-space-anisotropy  $\Leftrightarrow$  Momentum-space-anisotropy



$$\varepsilon = \frac{\langle y^2 - x^2 \rangle}{\langle y^2 + x^2 \rangle} \quad v_2 = \langle \cos 2\varphi \rangle, \quad \varphi = \tan^{-1}\left(\frac{p_y}{p_x}\right)$$

Sensitive to initial/final conditions and equation of state (EOS) !

$v_2(p_T, m)$  for  $\Lambda$ 's

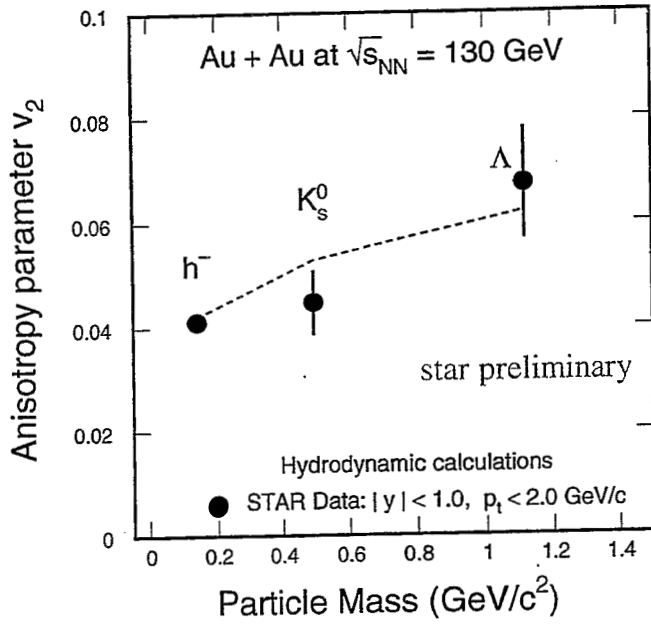


Hydro-like behavior up to 2.0 GeV/c.

$v_2$  saturates at higher  $p_T$ .

Saturation related to energy loss at high parton density in early stage.

## Integrated $V_2$ (m) of $\Lambda$

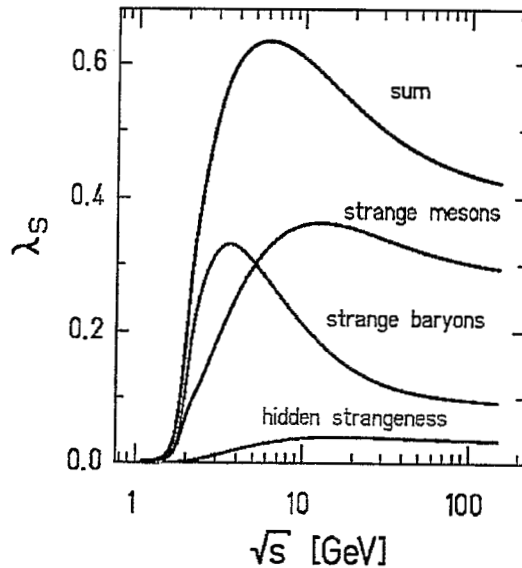


The mass dependency reflects anisotropic pressure gradient pushing massive particles outward in velocity space.

## Strange baryon production in canonical statistical calculation

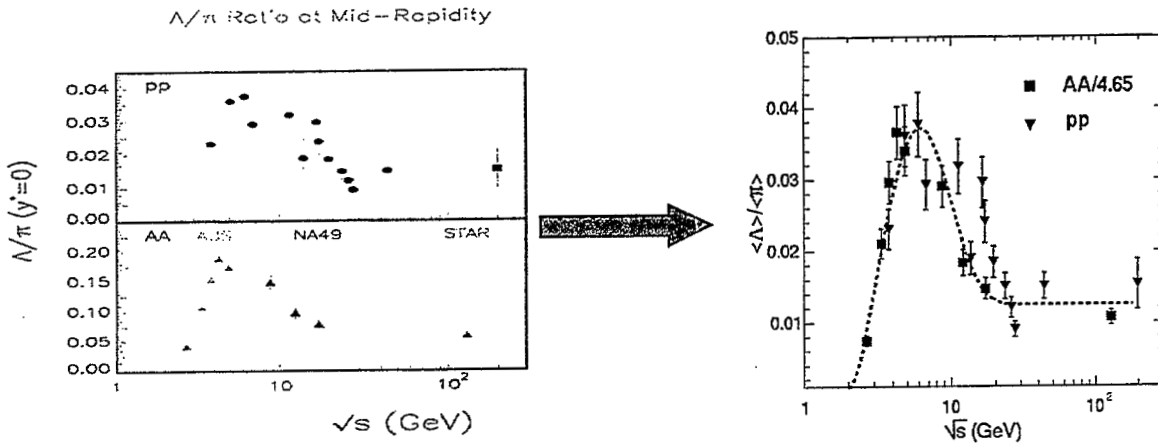
$$\lambda_s \equiv \frac{2\langle s\bar{s} \rangle}{\langle u\bar{u} \rangle + \langle d\bar{d} \rangle}$$

The decrease of baryon chemical potential coupled with only moderate increase in the associated temperature causes a decline in the relative number of strange baryons above energies of about 30 AGeV.



(PBM et al., hep-ph /0106066)

# Experimental $\Lambda/\pi$



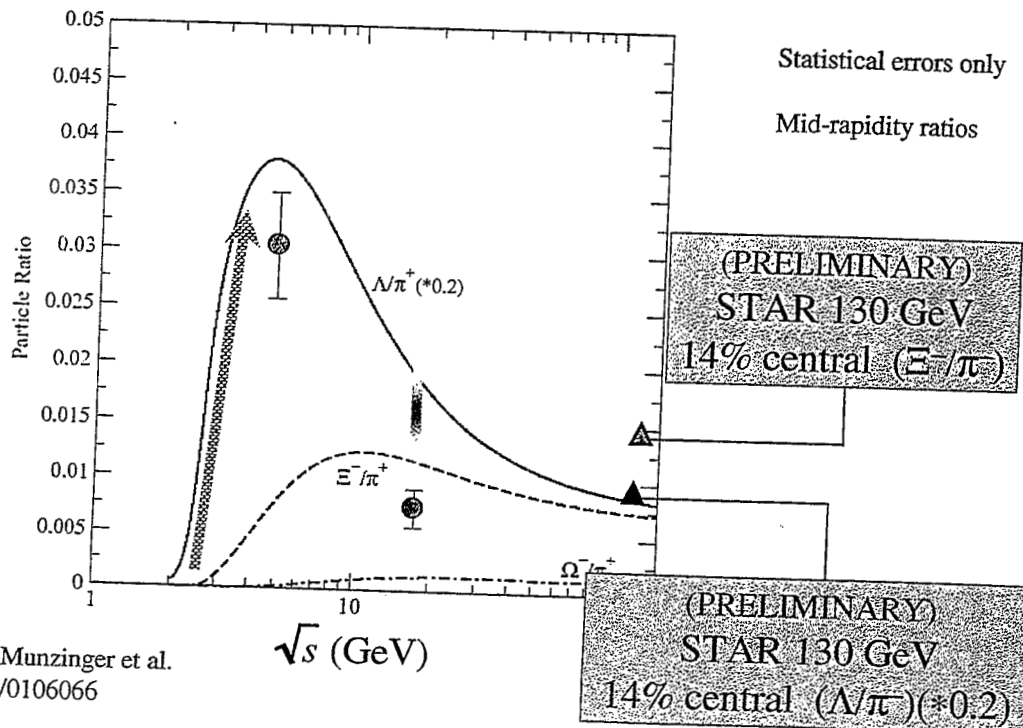
Approximately Common “enhancement” factor from pp to AA?!

→ Why beam energy independent ?

(strange baryon production mechanisms are energy dependent)

→ Why 4.65? Is this just the increase in the number of N-N collisions, the same underlying phenomenon as observed in p+A collisions by E910 (Brian Cole)?

# Experimental $\Xi/\pi$



Braun-Munzinger et al.  
hep-ph/0106066

## Conclusions

---

- 1) Successful measurements of strange baryons at STAR !!!
- 2) Interesting features in baryon ( strange baryon ) production at high pt (  $> 2$  GeV/c ) . ( “ enhancement ” in the ratio of baryon to meson or strange baryon to strange meson at high pt as compared to at low pt )

Saturated  $v_2$  of  $\Lambda$  at high pt (  $> 2$  GeV/c ).

⇒ Flow effects or novel physics at high pt ?

- 3)  $\Lambda/\pi$  ratio “ enhancement ” factor from pp to AA  $\sim$  number of average N-N collisions per participant pair in A+A.
- 4)  $\Xi/\pi$  “ enhancement ” as compared to thermal model prediction

# Anti-Baryon/Baryon ratios in PHENIX



Ilia Ravinovich

March 2002

Weizmann Institute

PHENIX collaboration



- Brazil** University of São Paulo, São Paulo
- China** Academia Sinica, Taipei, Taiwan  
China Institute of Atomic Energy, Beijing  
Peking University, Beijing
- France** LFC, University de Clermont-Ferrand, Clermont-Ferrand  
Dapnia, CEA Saclay, Gif-sur-Yvette  
IPN-Orsay, Université Paris Sud, CNRS-IN2P3, Orsay  
LLR, Ecole Polytechnique, CNRS-IN2P3, Palaiseau  
SUBATECH, Ecole des Mines at Nantes, Nantes
- Germany** University of Münster, Münster
- India** Banaras Hindu University, Banaras  
Bhabha Atomic Research Centre, Bombay
- Israel** Weizmann Institute, Rehovot
- Japan** Center for Nuclear Study, University of Tokyo, Tokyo  
Hiroshima University, Higashi-Hiroshima  
KEK, Institute for High Energy Physics, Tsukuba  
Kyoto University, Kyoto  
Nagasaki Institute of Applied Science, Nagasaki  
RIKEN, Institute for Physical and Chemical Research, Wako  
RIKEN-BNL Research Center, Upton, NY
- USA** Abilene Christian University, Abilene, TX  
Brookhaven National Laboratory, Upton, NY  
University of California - Riverside, Riverside, CA  
Columbia University, Nevis Laboratories, Irvington, NY  
Florida State University, Tallahassee, FL  
Georgia State University, Atlanta, GA  
Iowa State University and Ames Laboratory, Ames, IA  
Los Alamos National Laboratory, Los Alamos, NM  
Lawrence Livermore National Laboratory, Livermore, CA  
University of New Mexico, Albuquerque, NM  
New Mexico State University, Las Cruces, NM  
Dept. of Chemistry, Stony Brook Univ., Stony Brook, NY  
Dept. Phys. and Astronomy, Stony Brook Univ., Stony Brook, NY  
Oak Ridge National Laboratory, Oak Ridge, TN  
University of Tennessee, Knoxville, TN  
Vanderbilt University, Nashville, TN
- S. Korea** Cyclotron Application Laboratory, KAERI, Seoul  
Kangnung National University, Kangnung  
Korea University, Seoul  
Myong Ji University, Yongin City  
System Electronics Laboratory, Seoul Nat. University, Seoul  
Yonsei University, Seoul
- Russia** Institute of High Energy Physics, Protovino  
Joint Institute for Nuclear Research, Dubna  
Kurchatov Institute, Moscow  
PNPI, St. Petersburg Nuclear Physics Institute, St. Petersburg  
St. Petersburg State Technical University, St. Petersburg
- Sweden** Lund University, Lund



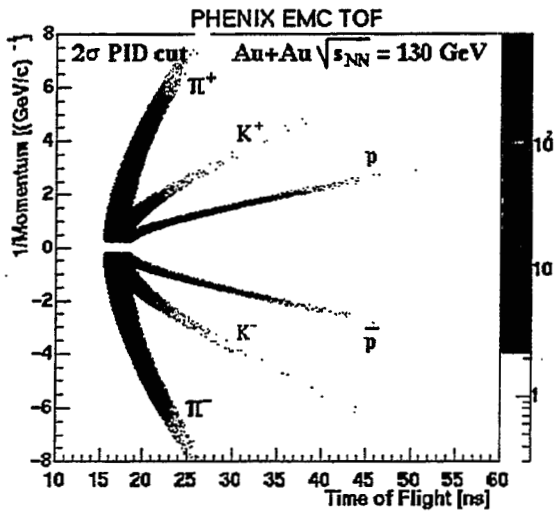
11 Countries; 52 Institutions; 430 Participants\*

\*as of January 2002

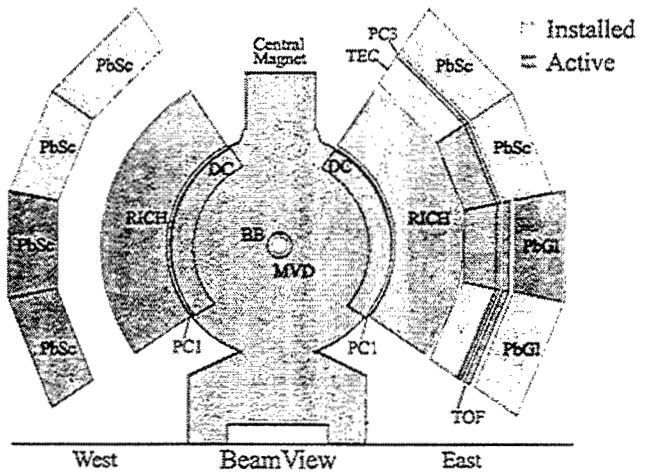
# Track definition and PID



Data: 1.3M minimum-bias events  
 Tracking: DC + PC1 + EMC, 3s matching cut  
 PID: 2s cut in mass squared distribution  
 Momentum range:  $p < 0.6$  (p),  $p < 1.4$  (p)



PHENIX Detector - First Year Physics Run

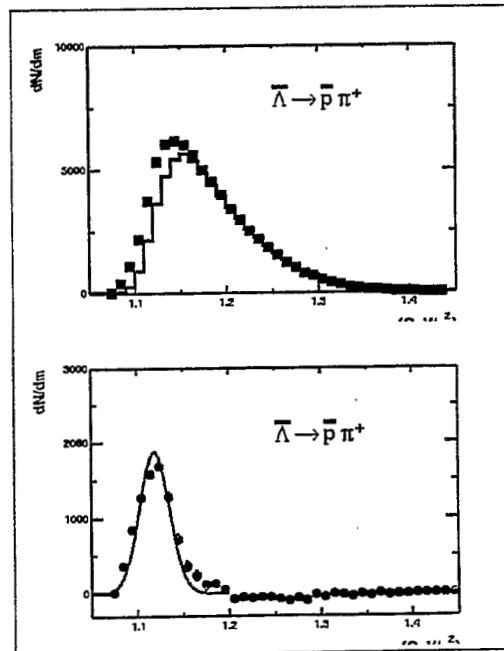
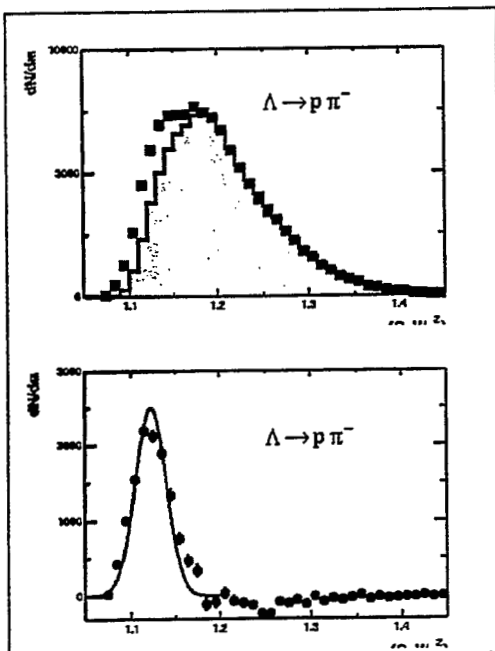


# Invariant mass spectra



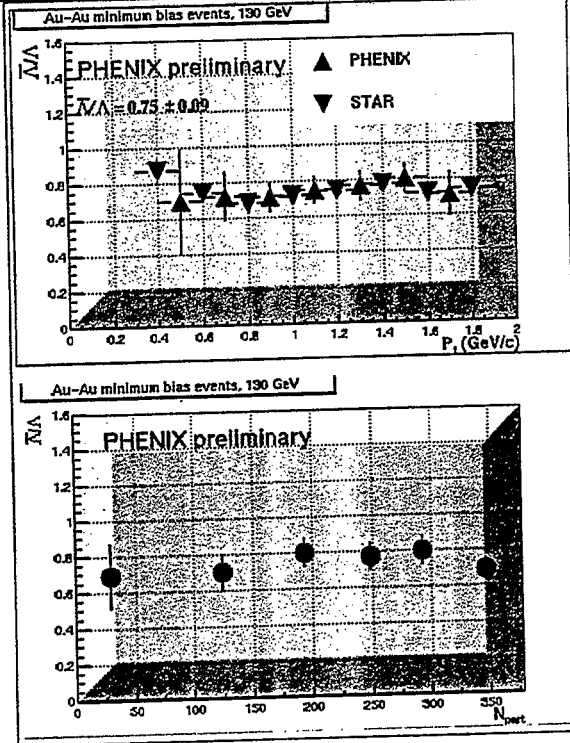
$S=11921 \pm 345$ ,  $S/B=1/2$

$S=8751 \pm 301$ ,  $S/B=1/2$



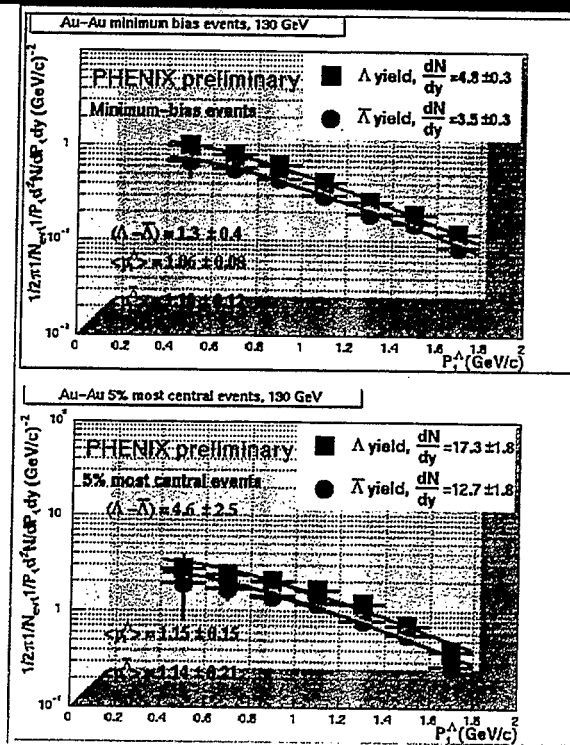
# $\bar{\Lambda}/\Lambda$ ratio vs Pt and centrality PHENIX

Ratio is  $0.75 \pm 0.09$ .  
 Ratio is consistent with STAR results (QM-2001) and statistical thermal model.  
 Ratio is constant over the whole Pt range.  
 No centrality dependence is observed.



# Transverse momentum spectra PHENIX

Extracted for minimum-bias (MB) and 5% most central events.  
 Measured Pt region:  
 $0.4 < Pt < 1.8$  GeV/c.  
 Good description by a Boltzmann distribution.  
 $T=355 \pm 11$  (366  $\pm$  13) for MB  
 $T=384 \pm 16$  (380  $\pm$  19) for 5%.  
 Yields and  $\langle Pt \rangle$  are obtained by integrating from 0 to infinity.

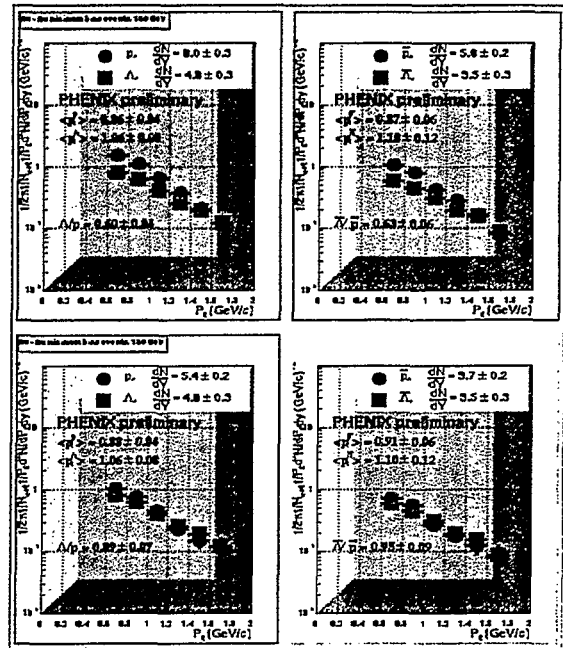


# Corrected proton spectra



$$\frac{dN^p}{dp_T dy}(i) = \frac{dN^m}{dp_T dy}(i) - \sum_{j=1}^{N_{bins}} \frac{dN^\Lambda}{dp_T dy}(j) \times BR \times w(j,i)$$

Present measurements enables us to correct the proton spectra for feed-down from  $\Lambda$  decays.  
 $\Lambda/p=0.89 \pm 0.07$  ( $0.95 \pm 0.09$ ) MB  
 $\Lambda/p=0.90 \pm 0.10$  ( $0.93 \pm 0.14$ ) 5%  
 No centrality dependence is observed.



# Net Baryon Number



Net BN	PHENIX	HIJING	HIJING/B
$\Lambda$ - $\bar{\Lambda}$ bar, min-bias	1.3 +/- 0.4	0.2	0.8
$p$ - $\bar{p}$ bar, min-bias	1.1	1.1	1.7
$\Lambda$ - $\bar{\Lambda}$ bar, 5% cent	4.6 +/- 2.5	0.8	3.2
$p$ - $\bar{p}$ bar, 5% cent	5.6 +/- 0.3	4.7	7.1

The inclusion of the gluon junction mechanism increases the net  $\Lambda$ - $\bar{\Lambda}$  and  $p$ - $\bar{p}$  baryon numbers in agreement with the data for minimum-bias events. For the 5% most central events it is true for hyperons but not for protons.



# Systematics of Nuclear Cluster Formation Rates

Zhangbu Xu, BNL  
March 30, 2002

for  
Baryon Dynamics at RHIC Workshop  
RIKEN BNL Research Center

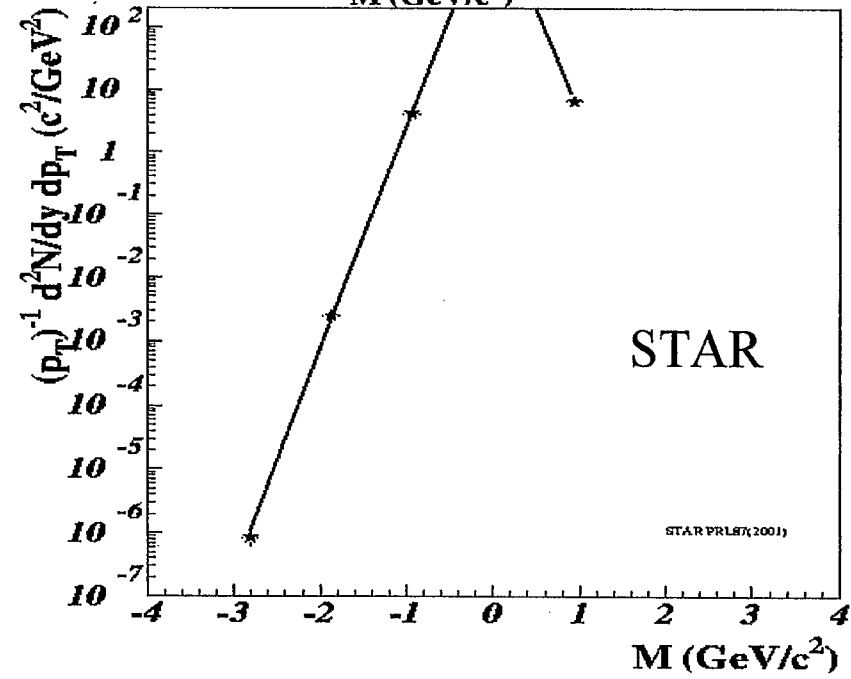
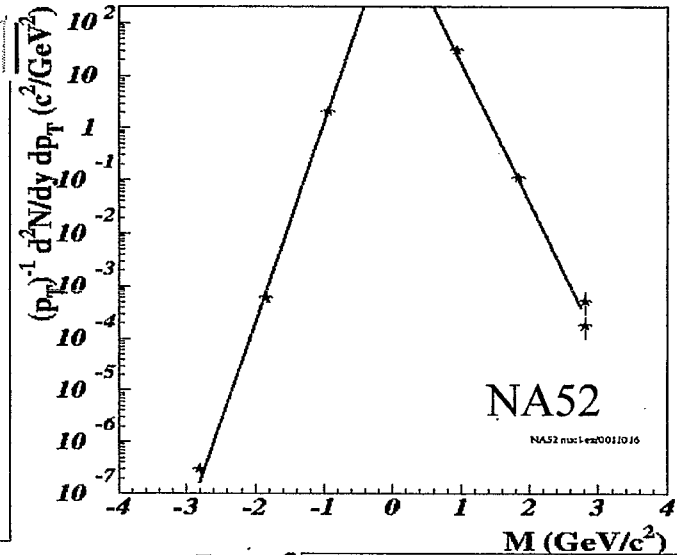
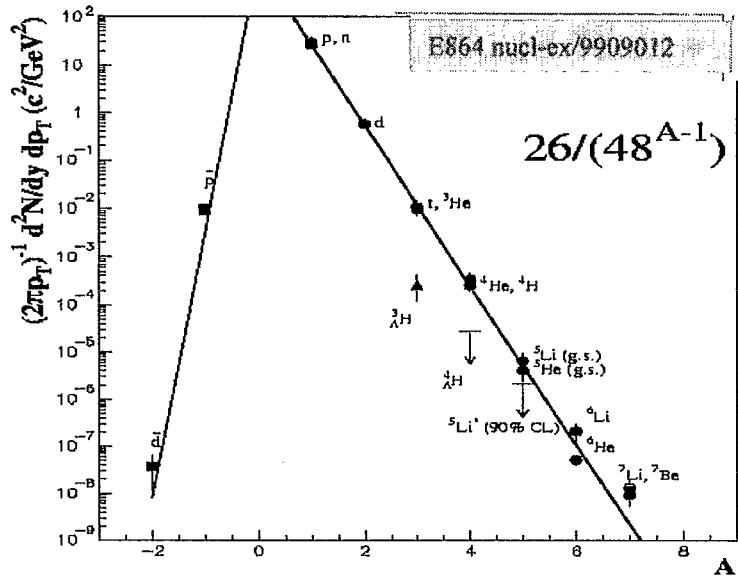
# *Systematics of Nuclear Cluster*

## *Formation Rates*

Zhangbu Xu (BNL)

- Baryon phase-space density at freeze-out depends on *earlier* condition-- (beam energies)  
But *little* dependence on beam species (pp, pA, AA)
- $\bar{d} / \bar{p}$  can measure gluon content
- RHIC is at the “saturated” antibaryon density
- “Scaling Law”  $\frac{\bar{d} / \pi}{(\bar{p} / \pi)^2}$   
related to “ $\pi$  phase-space density”

# Define Freeze-out Parameters



203

- $yield \propto \exp(-(m_n \pm \mu_b)A/T)$

R. Scheibl, U. Heinz, PRC59(1999)1585  
E864 nucl-ex/9909012

- AGS central:  $\mu_b=500\text{MeV}$ ,  $T=110\text{MeV}$
- SPS minbias:  $\mu_b=170\text{MeV}$ ,  $T=130\text{MeV}$
- RHIC central:  $\mu_b=28\text{MeV}$ ,  $T=130\text{MeV}$
- error:  $\sim \pm 10\text{MeV}$

# An Ideal Gluometer?

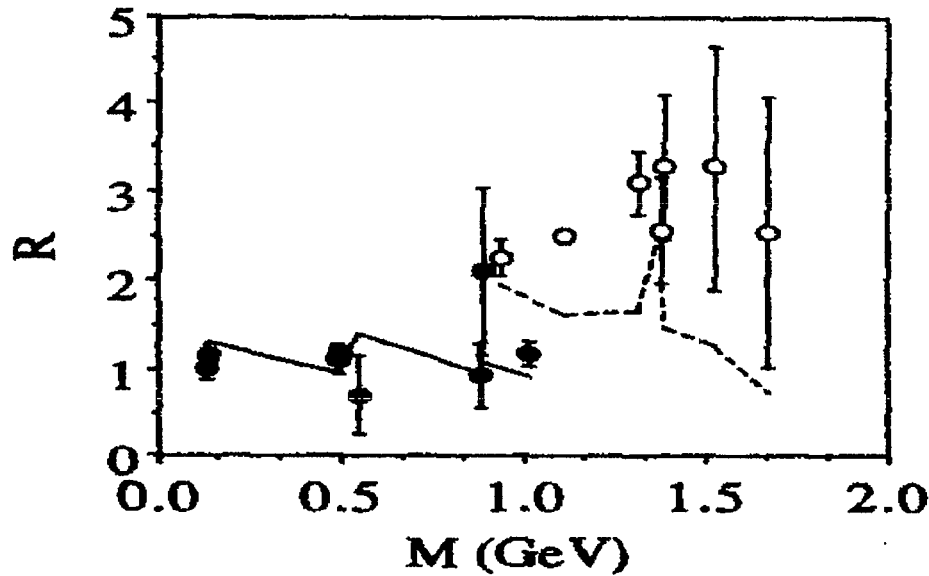
$e^+e^-$  Experiment around  $\Upsilon$  mass:

- $\Upsilon \rightarrow ggg$ : (9.46 GeV)  
high baryon production (large d/p)
- $\gamma^* \rightarrow q \bar{q}$ : (9.98 GeV)  
Lower baryon production (lower d/p)

J/ $\psi$  at BES (p/ $\pi$ )?

# Baryon Enhanced in Gluon

## Source



$$R = \frac{(\Upsilon \rightarrow ggg) \quad 1 \text{ M}}{(\gamma^* \rightarrow q \bar{q}) \quad 2-3 \text{ B}} =$$

205

$p=0.25$   
 $p+n=0.5$   
 $(0.5+1.0)/0.5=3$

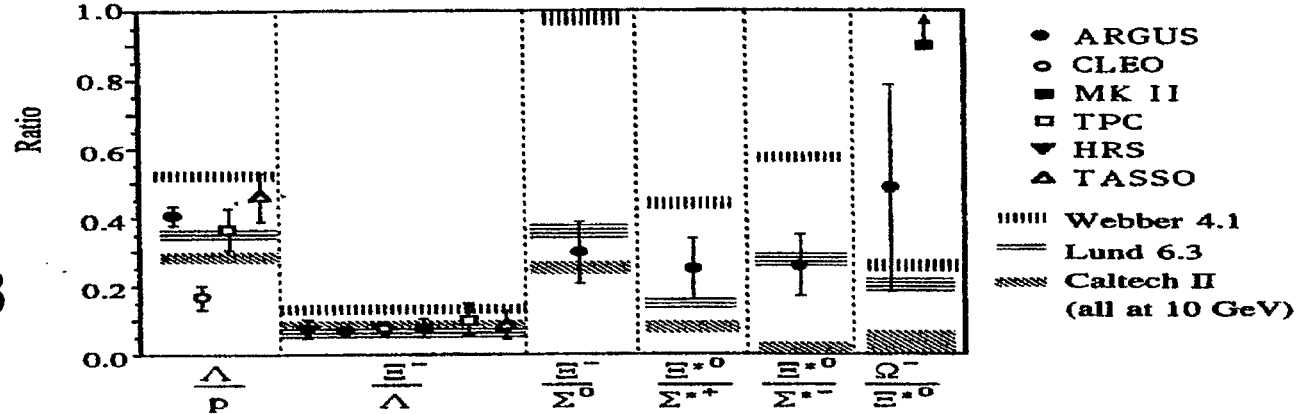
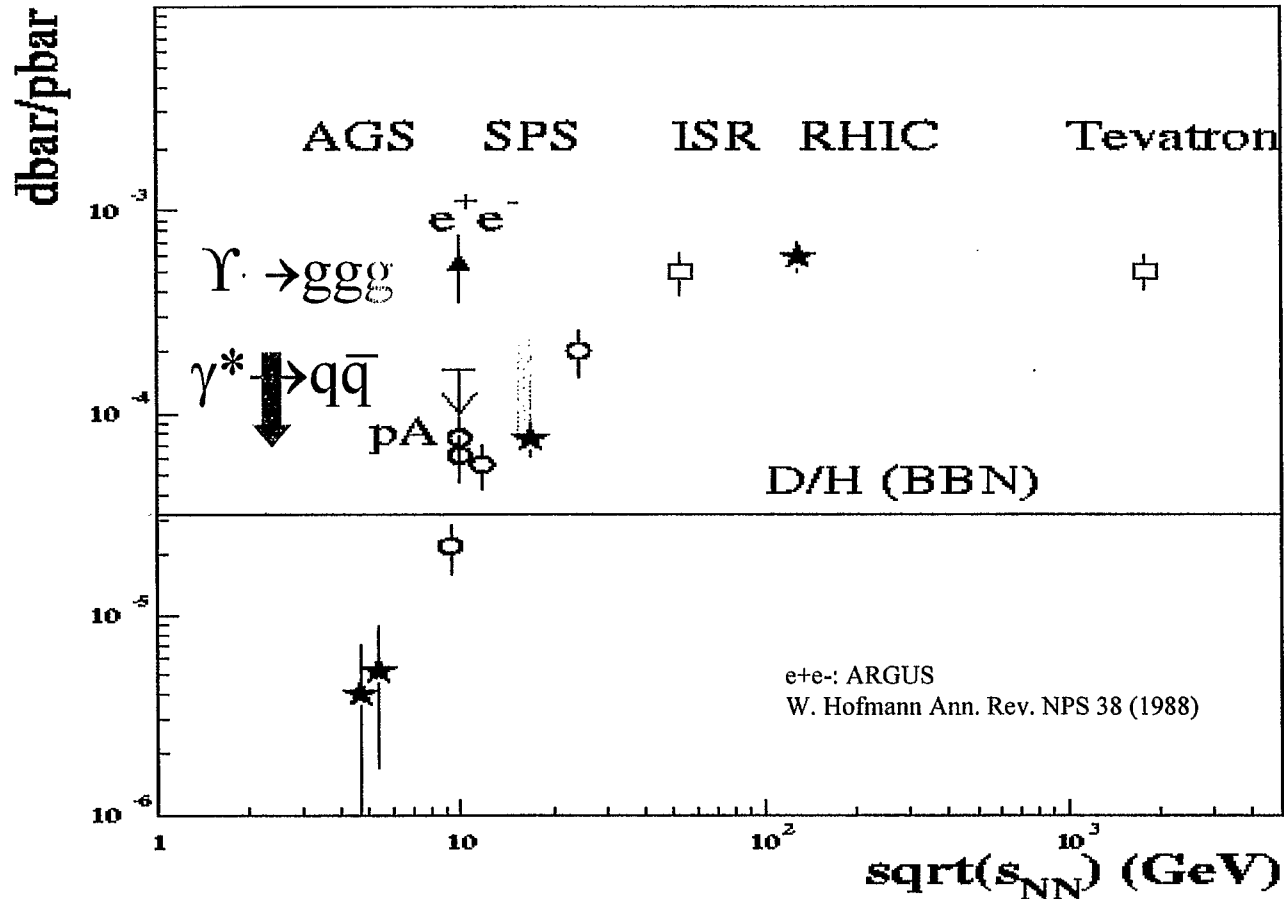


Figure 21 Strangeness suppression in baryon production. Shown are ratios of baryon cross sections for strangeness  $s+1$  and  $s$  ( $s = 0, 1, 2$ ), for baryons in the same spin multiplet. Data from  $e^+e^-$  annihilation at  $\sqrt{s} \approx 10$  GeV from ARGUS (77) and CLEO (33), and at  $\sqrt{s} \approx 30$  GeV from HRS (79, 82), MARK II (80, 83, 88), TASSO (35, 46, 84), and TPC (36, 81, 85). Shaded bands represent model predictions for  $\sqrt{s} = 10$  GeV; the results for  $\sqrt{s} \approx 30$  GeV are very similar.

# Baryons from Gluons at RHIC?

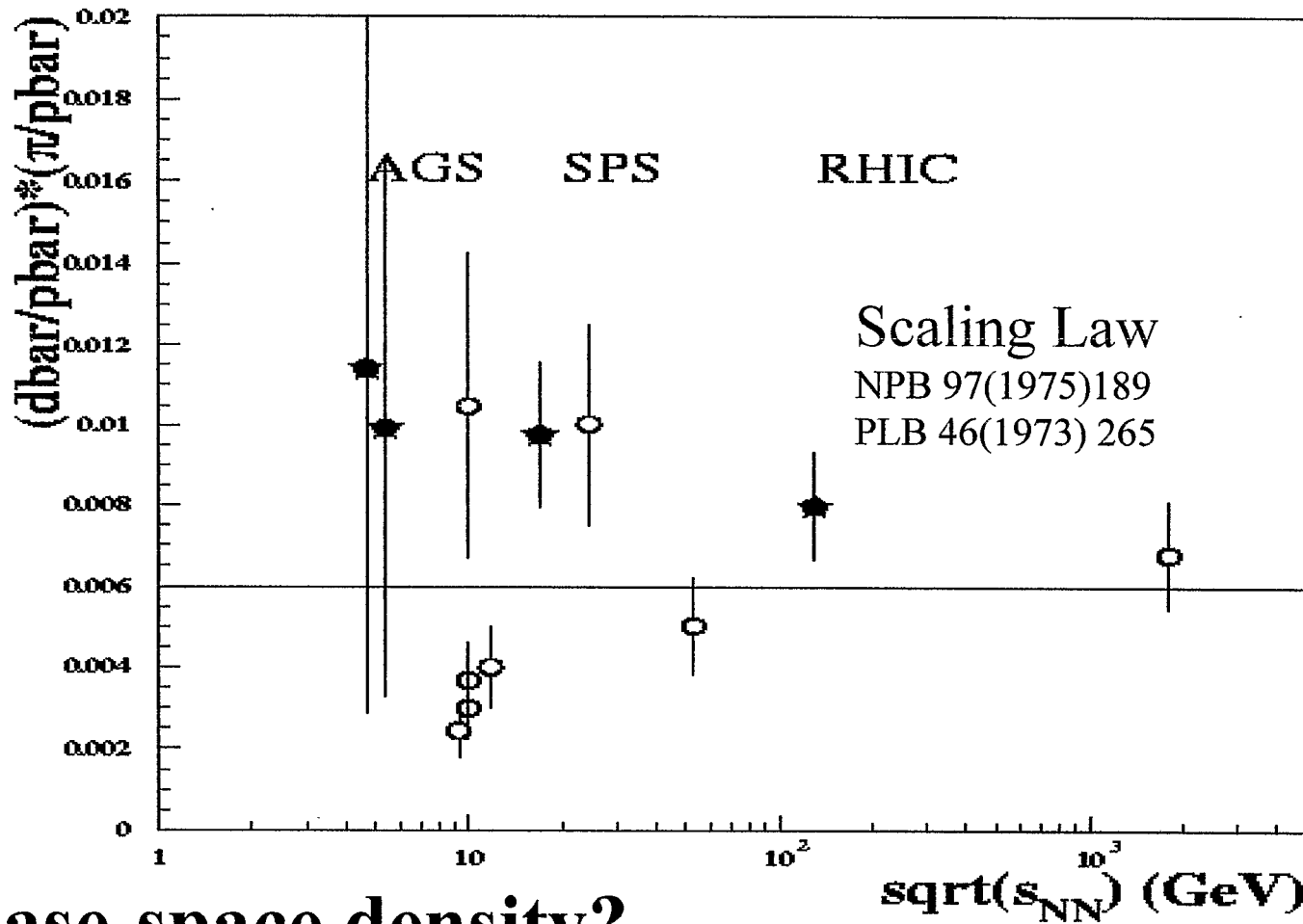


ISR energies and above:  $ggg \rightarrow B$ ?

Below:  $q\bar{q} \rightarrow B$ ?

BBN:  $p(n, \gamma)D$  at  $T \approx 1$  MeV

$$\frac{\overline{d} / \pi}{(\overline{p} / \pi)^2}$$



$\pi$  phase-space density?







# Baryon Dynamics at RHIC

March 2002

## Theory Summary


Xin-Nian Wang  
Lawrence Berkeley Laboratory

X-N Wang March 2002

Baryon Dynamics at RHIC




# Baryon Wavefunction

$$B = \varepsilon^{ijk} [Pe \int_{x_1}^x ds \cdot A(s) q(x_1)]_i [Pe \int_{x_2}^x ds \cdot A(s) q(x_2)]_j \otimes [Pe \int_{x_3}^x ds \cdot A(s) q(x_3)]_k$$


[Rossi and Veneziano'80]

## Baryonium states

$$M_0^J = \varepsilon_{lmn} \varepsilon^{ijk} [Pe \int_{x_1}^{x_2} ds \cdot A(s)]_i^l [Pe \int_{x_1}^{x_2} ds \cdot A(s)]_j^m \otimes [Pe \int_{x_1}^{x_2} ds \cdot A(s)]_k^n$$


X-N Wang March 2002

Baryon Dynamics at RHIC

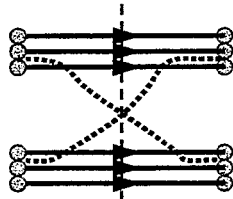


## Junctions and Baryon

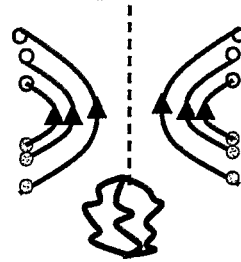
Baryonium channel could dominate baryon anti-baryon annihilation

### B-B scattering

[Kharzeev]



Double J-stopping



Single J-stopping

X-N Wang March 2002

Baryon Dynamics at RHIC



## Di-quarks and Baryons



- Possible states for  $qq$ :

$$(C, J) = (\bar{3}, 0), (\bar{3}, 1), (6, 0), (6, 1)$$

- Most attractive state:  $(\bar{3}, 0)$  also isoscalar

- Binding energy:  $\delta E = -\frac{M_{\Delta} - M_N}{2} \approx 150 \text{ MeV}$   
[Donoghue & Sateesh]

- Can di-quark scatter as a cluster?

X-N Wang March 2002

Baryon Dynamics at RHIC



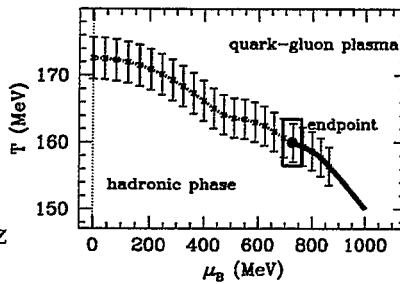
# Color Superconductivity

Dirk Rischke

- **Attractive interaction on Fermi surface:**

→ diquark condensate

$$\langle qq \rangle = q_i^a q_j^b \epsilon^{3ij} \epsilon_{ab}$$



Sandor Katz

X-N Wang March 2002

Baryon Dynamics at RHIC



# Manifest of 2-q in wavefunction

$$\psi_\mu(z) = \langle 0 | \bar{d}(z) \gamma_\mu \gamma_5 [P e^{ig \int_0^z ds A(s)}] u(0) | \pi^+(q) \rangle_{\mu^2} = \sum_n \frac{i(-i)^n}{n!} q_\mu (z \cdot q)^n A_n(\mu^2) + \text{⊗}$$

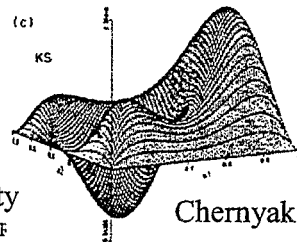
$$A_n = \int_0^1 dx \phi_\pi(x, \mu^2) x^n = i q_\mu \int_0^1 dx \phi_\pi(x, \mu^2) e^{-ixz \cdot q} + \text{⊗}$$

$\phi_\pi(x, \mu^2)$ : Quark distribution amplitude in leading Fock state

QCD sum rules  $\Rightarrow A_n$   $\langle 0 | \bar{d}(0) \gamma_\mu \gamma_5 u(0) | \pi^+(q) \rangle = i q_\mu f_\pi \Rightarrow A_0 = f_\pi$

Similarly for Baryons

$\phi_B(x_1, x_2)$  65% momentum by the u quark  
 $x_1 \rightarrow$  u quark  
 $x_2 \rightarrow$  d quark which carries helicity



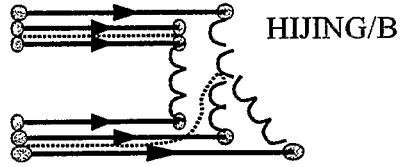
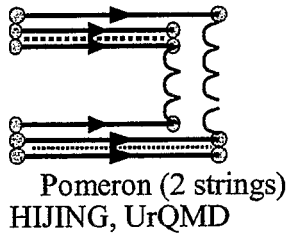
Chernyak et al

X-N Wang March 2002

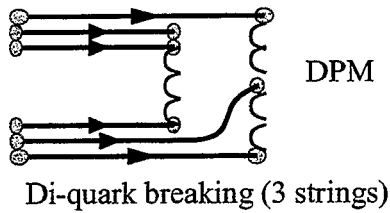
Baryon Dynamics at F



## Baryon Transport in String model



$\alpha_j = 1$ , or  $0.5$ ? [Kopeliovich]



Di-quark cross section?

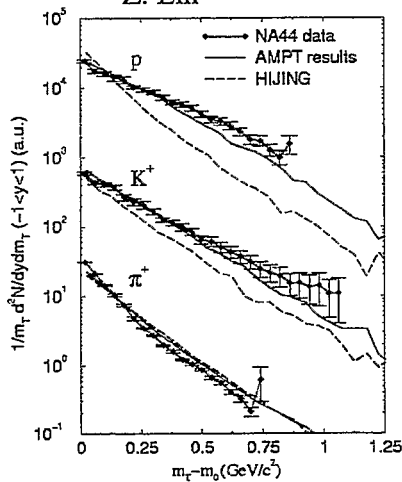
X-N Wang March 2002

Baryon Dynamics at RHIC



## Hadronic Rescattering

Z. Lin

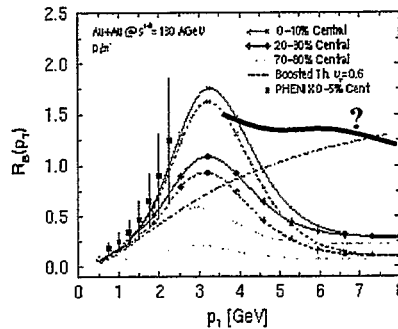


X-N Wang March 2002

Baryon Dynam

V2 points to final state  
Interaction effect:  
Partonic or hadronic?

I. Vitev





## Summary

- **Baryon is most common yet complicated objects**
- **Topologic structure leading to junction and other gluonic states**
- **Study of baryons opens up a small window into the structure of baryon and dynamics of baryon production**

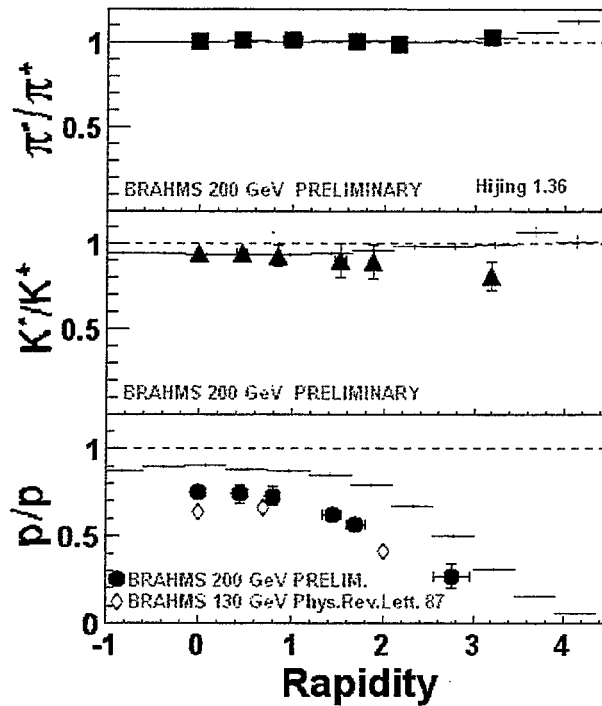


Experiment Summary  
 Craig Ogilvie  
 Iowa State University, [cogilvie@iastate.edu](mailto:cogilvie@iastate.edu)

- Highlights of new results shown at this meeting
- Experimental consistency between experiments
  - baryons, anti-baryons
- Top 10 “Baryon” results I’m excited to see at QM2002 (and beyond)

Highlights of New Results

Ratios @ 200 AGeV (I): BRAHMS



Ratios @ 200 AGeV (II): PHOBOS

$\pi^-/\pi^+$	$1.025 \pm 0.006 \pm 0.020$
$K^-/K^+$	$0.95 \pm 0.03 \pm 0.04$
$p/p$	$0.74 \pm 0.02 \pm 0.03$

### Experiment Consistency

Cent. 5% 130 GeV incl. feeddown	STAR Mar 02 (# from plot) (Syst. Schweda)	PHENIX nucl- ex/0112006	PHOBOS (y=0.5) PRL87:102301	BRAHMS PRL 87:112305
dN/dy (y=0) p	$31.9 \pm 0.7 \pm 8.0$	$28.7 \pm 0.9 \pm 4$		
dN/dy (y=0) $\bar{p}$	$22.9 \pm 0.5 \pm 5.7$	$20.1 \pm 1.0 \pm 2.8$		
(p - $\bar{p}$ )	$9.0 \pm 0.3 \pm 3.2$	$8.6 \pm 1.3 \pm \sim 1$		
$\bar{p}/p$	$0.72 \pm 0.02 \pm ?$	$0.70 \pm 0.04 \pm 0.07$	$0.60 \pm 0.04 \pm 0.06$	$0.64 \pm 0.04 \pm 0.06$

- Experimental results are consistent with each other
- Great interest in phobos and brahm's future dN/dy results for PID particles
- STAR's improved dN/dy analysis (more constraint on shape)  
–well within the systematic errors quoted by their papers

Cent. 5% 130 GeV	STAR nucl-ex/020316	PHENIX Mar '02
dN/dy (y=0) $\Lambda$	$17.0 \pm 0.4 \pm 1.7$	$17.3 \pm 1.8 \pm 2.8$
dN/dy (y=0) $\bar{\Lambda}$	$12.0 \pm 0.3 \pm 1.2$	$12.7 \pm 1.8 \pm 2.0$
Measured dN/dy (y=0) p Direct dN/dy (y=0) p		$28.7 \pm 0.9 \pm 3.2$ $19.3 \pm 0.6 \pm 2.7$
Measured dN/dy (y=0) $\bar{p}$ Direct dN/dy (y=0) $\bar{p}$		$20.1 \pm 1.0 \pm 2.2$ $13.7 \pm 0.7 \pm 1.9$

Experimental results are consistent with each other  
Phenix feed-down corrected net-proton dN/dy ~ 5-6



## Top 10 “Baryon” Results I’m Looking Forward to At QM and Beyond

### 10 Systematics

p+p, provides expt. foundation for all our physics

d+Au provides both p+Au and n+Au mixed, challenge to measure  $N_{\text{grey}}$

### 9 Degree of Strangeness Saturation

Yield of multi-strange baryons in Au+Au 200 AGeV

If strangeness fully equilibrated  $\Rightarrow \gamma_s = 1$ , what is  $\gamma_s$  at RHIC?

### 8 Nice to Get Some Understanding of why $\bar{\Lambda}/\bar{p}_{\text{direct}} \sim 1$ at RHIC, three to 5 times larger than p+p

### 7 Charmed Baryons

Baryon-junction models  $\Rightarrow$  enhanced mid-rapidity  $\Lambda$  and  $p$

could also lead to enhanced  $\Lambda_c$  ?

### 6 Accurate $\langle pt \rangle$ in Near-Peripheral Collisions,

largest difference between pp and AuAu, discriminate between onset of expansion, multiple scattering, pt kick from junction?

### 5 $\bar{p}/p$ vs pt

does  $\bar{p}/p$  in Au+Au continue to rise at high-pt (hydro) ?

or fall at high-pt (fragmentation models) ?

### 4 $\bar{p}/p$ at High-pt

current data ratio is constant as a function of pt, extend to larger pt with better statistics

In p+p, ratio decreases, because of fragmentation  $q \Rightarrow p$  dominate  $g \Rightarrow \bar{p}$

### 3 Balance Function For Baryons

### 2 Rapidity Distribution of p- $\bar{p}$ over broad range of rapidity

- p+p, d+Au and Au+Au

discriminate between models

### 1 $\Lambda$ - $\bar{\Lambda}$ and $p_{\text{direct}}$ - $\bar{p}_{\text{direct}}$ @ 200 AGeV

currently HIJING/B describes both  $\Lambda - \bar{\Lambda}$  and  $p_{\text{direct}} - \bar{p}_{\text{direct}}$

But strongly underpredicts  $\Lambda$  yield

**Baryon Dynamics at RHIC**  
**March 28-30, 2002**  
**A RIKEN BNL Research Center Workshop**

**LIST OF REGISTERED PARTICIPANTS**

NAME	AFFILIATION AND ADDRESS	E-MAIL ADDRESS
Sam Aronson	Brookhaven National Laboratory Bldg. 510A Upton, N.Y. 11973-5000	<a href="mailto:aronsons@bnl.gov">aronsons@bnl.gov</a>
Mark Baker	Brookhaven National Laboratory Chemistry Department Bldg. 555A Upton, N.Y. 11973-5000	<a href="mailto:mdbaker@bnl.gov">mdbaker@bnl.gov</a>
Anthony Baltz	RIKEN BNL Research Center Brookhaven National Laboratory Bldg. 510A – Physics Dept. Upton, N.Y. 11973-5000	<a href="mailto:baltz@bnl.gov">baltz@bnl.gov</a>
Steffen Bass	Duke University / RBRC Dept of Physics Box 90305 Durham, N.C. 27708-0305	<a href="mailto:bass@phy.duke.edu">bass@phy.duke.edu</a>
Ian Bearden	Niels Bohr Institute Blegdamsvej 17 Copenhagen, Denmark	<a href="mailto:bearden@nbi.dk">bearden@nbi.dk</a>
Hongfang Chen	USTC – University of Science & Technology of China Dept. of Modern Physics Hefei, Anhui 230027 P.R. China	<a href="mailto:hfchen@rcf.bnl.gov">hfchen@rcf.bnl.gov</a>
William Christie	Brookhaven National Laboratory Bldg. 510A Upton, N.Y. 11973-5000	<a href="mailto:Christie@bnl.gov">Christie@bnl.gov</a>
Tatsuya Chujo	Brookhaven National Laboratory Bldg. 510C Upton, N.Y. 11973-5000	<a href="mailto:chujo@bnl.gov">chujo@bnl.gov</a>
Brian Cole	Columbia University Nevis Laboratories P.O. Box 137 Irvington, N.Y. 10533	<a href="mailto:cole@nevis.columbia.edu">cole@nevis.columbia.edu</a>
Tom Cormier	Wayne State University Dept of Physics Detroit, MI 48202	<a href="mailto:cormier@physics.wayne.edu">cormier@physics.wayne.edu</a>
Tamas Csorgo	MTA KFKI RMKI Budapest 114 - PO Box 49 Hungary	<a href="mailto:csorgo@sunserv.kfki.hu">csorgo@sunserv.kfki.hu</a>
Patricia Fachini	Brookhaven National Laboratory Bldg. 510A Upton, N.Y. 11973-5000	<a href="mailto:pfachini@bnl.gov">pfachini@bnl.gov</a>
Kirill Filimonov	Lawrence Berkeley National Lab MS 70-319 1 Cyclotron Road Berkeley, CA 94720	<a href="mailto:KVFilimonov@lbl.gov">KVFilimonov@lbl.gov</a>
Hans Gerhard Fischer	CERN CH 1211 Geneva 23 Switzerland	<a href="mailto:Hans.Gerhard.fischer@cern.ch">Hans.Gerhard.fischer@cern.ch</a>

**Baryon Dynamics at RHIC**  
**March 28-30, 2002**  
**A RIKEN BNL Research Center Workshop**

**LIST OF REGISTERED PARTICIPANTS**

NAME	AFFILIATION AND ADDRESS	E-MAIL ADDRESS
Zoltan Fodor	Eotvos University Pazmany P. 1/A, Budapest, H-1117, Hungary	<a href="mailto:fodor@pms2.elte.hu">fodor@pms2.elte.hu</a>
Philippe de Forcrand	ETH Zurich CERN, Theory Division CH-1211 Geneva 23 Switzerland	<a href="mailto:forcrand@phys.ethz.ch">forcrand@phys.ethz.ch</a>
Gerald Garvey	Los Alamos National Laboratory P25 MS H846 Los Alamos, NM 87545	<a href="mailto:garvey@lanl.gov">garvey@lanl.gov</a>
Kristjan Gulbrandsen	MIT – PHOBOS Experiment Bldg 24-416 77 Massachusetts Avenue Cambridge, MA 02139	<a href="mailto:gulbrand@mit.edu">gulbrand@mit.edu</a>
Wlodek Guryn	Brookhaven National Laboratory Bldg. 510 Upton, N.Y. 11973-5000	<a href="mailto:guryn@bnl.gov">guryn@bnl.gov</a>
Miklos Gyulassy	Columbia University Pupin Lab MS5202 538 W120th St. New York, N.Y. 10027	<a href="mailto:gyulassy@nt3.phys.columbia.edu">gyulassy@nt3.phys.columbia.edu</a>
Tim Hallman	Brookhaven National Laboratory Bldg. 510A Upton, N.Y. 11973-5000	<a href="mailto:hallman@bnl.gov">hallman@bnl.gov</a>
Conor Henderson	MIT Bldg. 24-408 77 Massachusetts Avenue Cambridge, MA 02139	<a href="mailto:conor@mit.edu">conor@mit.edu</a>
David Hofman	University of Illinois at Chicago Physics Department 2236 SES, mc 273 845 W. Taylor St. Chicago, IL. 60607	<a href="mailto:hofman@uic.edu">hofman@uic.edu</a>
Matt Horsley	Yale University - WNSL 272 Whitney Ave. New Haven, CT 06520-8124	<a href="mailto:horslev@star.physics.yale.edu">horslev@star.physics.yale.edu</a>
Huan Z. Huang	UCLA Dept. of Physics & Astronomy Los Angeles, CA 90095-1547	<a href="mailto:huang@physics.ucla.edu">huang@physics.ucla.edu</a>
Shengli Huang	BNL / USTC Bldg. 118 room 205 Upton, N.Y. 11973-5000	<a href="mailto:SLHuang@rcf.bnl.gov">SLHuang@rcf.bnl.gov</a>
Kazunori Itakura	RBRC Bldg. 510A Upton, N.Y. 11973-5000	<a href="mailto:itakura@bnl.gov">itakura@bnl.gov</a>
Barbara Jacak	SUNY Stony Brook Physics & Astronomy Stony Brook, N.Y. 11794-3800	<a href="mailto:jacak@skipper.physics.sunysb.edu">jacak@skipper.physics.sunysb.edu</a>

**Baryon Dynamics at RHIC**  
**March 28-30, 2002**  
**A RIKEN BNL Research Center Workshop**

**LIST OF REGISTERED PARTICIPANTS**

NAME	AFFILIATION AND ADDRESS	E-MAIL ADDRESS
Jamal Jalilian-Marian	Brookhaven National Laboratory Physics Department, Bldg. 510A Upton, N.Y. 11973-5000	<a href="mailto:jamal@bnl.gov">jamal@bnl.gov</a>
Sangyong Jeon	McGill University Physics Department 3600 University Street Montreal, QC H3A-2T8 Canada	<a href="mailto:jeon@hep.physics.mcgill.ca">jeon@hep.physics.mcgill.ca</a>
Jay Kane	MIT 77 Massachusetts Avenue Cambridge, MA 02139	<a href="mailto:jkane@mit.edu">jkane@mit.edu</a>
Joseph Kapusta	University of Minnesota School of Physics & Astronomy 116 Church St. SE Minneapolis, MN 55455	<a href="mailto:kapusta@physics.spa.umn.edu">kapusta@physics.spa.umn.edu</a>
Sandor Katz	DESY Theory Group Notkestrasse 85 22607, Hamburg	<a href="mailto:sandor.katz@desy.de">sandor.katz@desy.de</a>
Dmitri Kharzeev	Brookhaven National Laboratory Physics Department Bldg. 510A Upton, N.Y. 11973-5000	<a href="mailto:kharzeev@bnl.gov">kharzeev@bnl.gov</a>
Che-Ming Ko	Texas A&M University Cyclotron Institute College Station, TX 77843-3366	<a href="mailto:ko@comp.tamu.edu">ko@comp.tamu.edu</a>
Boris Kopeliovich	Max-Planck-Institut fuer Kernphysik Postfach 103980, 69029 Heidelberg Germany	<a href="mailto:Boris.Kopeliovich@mpi-hd.mpg.de">Boris.Kopeliovich@mpi-hd.mpg.de</a>
Henri Kowalski	Columbia University / BNL Pupin Laboratories 538 West 120 <sup>th</sup> Street New York, N.Y. 10027	<a href="mailto:Kowalski@nevis.columbia.edu">Kowalski@nevis.columbia.edu</a>
Frank Laue	Brookhaven National Laboratory Bldg. 510A Upton, N.Y. 11973-5000	<a href="mailto:laue@bnl.gov">laue@bnl.gov</a>
Jang Woo Lee	MIT Relativistic Heavy Ion Group Bldg. 24-416, Dept of Physics 77 Massachusetts Avenue Cambridge, MA 02139	<a href="mailto:jw_lee@mit.edu">jw_lee@mit.edu</a>
Zi-wei Lin	Texas A&M University Cyclotron Institute, 3366 TAMU College Station, TX 77843-3366	<a href="mailto:lin@kopc2.tamu.edu">lin@kopc2.tamu.edu</a>
Hui Long	UCLA 136 Bronwood Avenue Los Angeles, CA 90049	<a href="mailto:long@physics.ucla.edu">long@physics.ucla.edu</a>
Tom Ludlam	Brookhaven National Laboratory Bldg. 510 Upton, N.Y. 11973-5000	<a href="mailto:ludlam@bnl.gov">ludlam@bnl.gov</a>

**Baryon Dynamics at RHIC**  
**March 28-30, 2002**  
**A RIKEN BNL Research Center Workshop**

**LIST OF REGISTERED PARTICIPANTS**

NAME	AFFILIATION AND ADDRESS	E-MAIL ADDRESS
Magdalena Markovic	Columbia University Pupin Laboratories 538 West 120 Street New York, N.Y. 10027	<a href="mailto:dmani@phys.columbia.edu">dmani@phys.columbia.edu</a>
Larry McLerran	Brookhaven National Laboratory Bldg. 510A Upton, N.Y. 11973-5000	<a href="mailto:mclerran@bnl.gov">mclerran@bnl.gov</a>
Denes Molnar	Columbia University Pupin Laboratories 538 West 120 Street New York, N.Y. 10027	<a href="mailto:molnard@phys.columbia.edu">molnard@phys.columbia.edu</a>
Yasushi Nara	RIKEN BNL Research Center Bldg. 510A Upton, N.Y. 11973-5000	<a href="mailto:nara@bnl.gov">nara@bnl.gov</a>
Craig Ogilvie	Iowa State University Department of Physics & Astronomy Ames, IA 50011	<a href="mailto:cogilvie@iastate.edu">cogilvie@iastate.edu</a>
Shigemi Ohta	RBRC/KEK Bldg. 510A Upton, N.Y. 11973-5000	<a href="mailto:ohta@bnl.gov">ohta@bnl.gov</a>
Vitaly A. Okorokov	Dep. Micro – cosmophysics Moscow Engineering Physics Institute (State University) Kashirakoe Shosse 31, Moscow 115409, Russian Federation	<a href="mailto:okorokov@rf.rhic.bnl.gov">okorokov@rf.rhic.bnl.gov</a>
Vasile Topor Pop	McGill University Dept of Physics 3600 University Street Montreal Canada H3A 2T8	<a href="mailto:toporpop@physics.mcgill.ca">toporpop@physics.mcgill.ca</a>
Iliia Ravinovich	Weizmann Institute Department of Particle Physics Rehovot 76100 Israel	<a href="mailto:Iliia.Ravinovich@weizmann.ac.il">Iliia.Ravinovich@weizmann.ac.il</a>
Corey Reed	MIT Bldg. 24-416 77 Massachusetts Avenue Cambridge, MA 02139	<a href="mailto:cjreed@mit.edu">cjreed@mit.edu</a>
Dirk Rischke	Institute for Theoretical Physics University Frankfurt J.W. Goethe-Universitaet Robert-Mayer-Str. 10 D-60054 Frankfurt am Main Germany	<a href="mailto:drischke@th.physik.uni-frankfurt.de">drischke@th.physik.uni-frankfurt.de</a>
Hans Georg Ritter	LBNL 1 Cyclotron Rd. MS 70-319 Berkeley, CA 94720	<a href="mailto:HGRitter@lbl.gov">HGRitter@lbl.gov</a>
Christof Roland	MIT ~ Relativistic Heavy Ion Group Bldg. 24-410 77 Massachusetts Avenue Cambridge, MA 02139	<a href="mailto:Christof.Roland@cern.ch">Christof.Roland@cern.ch</a>

**Baryon Dynamics at RHIC**  
**March 28-30, 2002**  
**A RIKEN BNL Research Center Workshop**

**LIST OF REGISTERED PARTICIPANTS**

NAME	AFFILIATION AND ADDRESS	E-MAIL ADDRESS
Gunther Roland	MIT Bldg. 24 77 Massachusetts Avenue Cambridge, MA 02139	<a href="mailto:Gunther.Roland@cern.ch">Gunther.Roland@cern.ch</a>
Kai Schweda	LBNL 1 Cyclotron Rd. MS 70-319 Berkeley, CA 94720	<a href="mailto:KOSchweda@lbl.gov">KOSchweda@lbl.gov</a>
Edward Shuryak	Stony Brook University Dept of Physics & Astronomy SUNY Stony Brook, N.Y. 11794	<a href="mailto:shuryak@dau.physics.sunysb.edu">shuryak@dau.physics.sunysb.edu</a>
Sven Soff	LBNL 1 Cyclotron Road, MS 70-319 Berkeley, CA 94720	<a href="mailto:ssoff@lbl.gov">ssoff@lbl.gov</a>
Hideo Suganuma	Associate Professor, Faculty of Science Tokyo Institute of Technology Main Building 1-71 Ohokayama 2-12-1, Meguro Tokyo, 152-8551 Japan	<a href="mailto:suganuma@th.phys.titech.ac.jp">suganuma@th.phys.titech.ac.jp</a>
An Tai	UCLA Dept. of Physics Los Angeles, CA 90095	<a href="mailto:atai@physics.ucla.edu">atai@physics.ucla.edu</a>
Toru Takahashi	RCNP, Osaka University Mihogaoka 10-1, Ibaraki, Osaka 567-0047, Japan	<a href="mailto:ttoru@rcnp.osaka-u.ac.jp">ttoru@rcnp.osaka-u.ac.jp</a>
Mike Tannenbaum	Brookhaven National Laboratory Bldg. 510 Upton, N.Y. 11973-5000	<a href="mailto:mjt@bnl.gov">mjt@bnl.gov</a>
Derek Teaney	Brookhaven National Laboratory Bldg. 510 Upton, N.Y. 11973-5000	<a href="mailto:dteaney@quark.phy.bnl.gov">dteaney@quark.phy.bnl.gov</a> <a href="mailto:dteaney@dau.physics.sunysb.edu">dteaney@dau.physics.sunysb.edu</a>
Gene Van Buren	Brookhaven National Laboratory Physics Bldg. 510A Upton, N.Y. 11973-5000	<a href="mailto:gene@bnl.gov">gene@bnl.gov</a>
Momchil Velkovsky	University at Stony Brook Dept. of Physics Stony Brook, N.Y. 11794	<a href="mailto:momchil@bnl.gov">momchil@bnl.gov</a>
Raju Venugopalan	Brookhaven National Laboratory Bldg. 510A Upton, N.Y. 11973-5000	<a href="mailto:raju@bnl.gov">raju@bnl.gov</a>
Flemming Videbaek	Brookhaven National Laboratory Physics Department, Bldg. 510D Upton, N.Y. 11973-5000	<a href="mailto:videbaek@bnl.gov">videbaek@bnl.gov</a>
Ivan Vitev	Columbia University 538 West 120 <sup>th</sup> Street Pupin Lab, Room 925 P.O. Box 114 New York, N.Y. 10027	<a href="mailto:ivitev@nt4.phys.columbia.edu">ivitev@nt4.phys.columbia.edu</a>

**Baryon Dynamics at RHIC**  
**March 28-30, 2002**  
**A RIKEN BNL Research Center Workshop**

**LIST OF REGISTERED PARTICIPANTS**

<u>NAME</u>	<u>AFFILIATION AND ADDRESS</u>	<u>E-MAIL ADDRESS</u>
Fuqiang Wang	Purdue University 1396 Physics Bldg. West Lafayette, IN 47907	<a href="mailto:fqwang@physics.purdue.edu">fqwang@physics.purdue.edu</a>
Xin-Nian Wang	Lawrence Berkeley National Lab Nuclear Science Division MS 70-319 1 Cyclotron Rd. Berkeley, CA 94720	<a href="mailto:xnwang@lbl.gov">xnwang@lbl.gov</a>
Nu Xu	LBNL 1 Cyclotron Road, MS 70-319 Berkeley, CA 94720	<a href="mailto:nxu@lbl.gov">nxu@lbl.gov</a>
Zhangbu Xu	Brookhaven National Laboratory Physics Bldg. 510A Upton, N.Y. 11973-5000	<a href="mailto:xzb@bnl.gov">xzb@bnl.gov</a>
Haibin Zhang	Yale University Physics Dept. 260 Whitney Ave. 454 J W Gibbs Laboratory PO Box 208121 New Haven, CT. 06520-8121	<a href="mailto:zhang@hepmail.physics.yale.edu">zhang@hepmail.physics.yale.edu</a>

RIKEN BNL Research Center Workshop  
**Baryon Dynamics at RHIC**  
March 28-30, 2002  
Physics Dept., Brookhaven National Laboratory  
\*\*\*\*\*AGENDA\*\*\*\*\*

---

Thursday, March 28

Opening Session      *Large Seminar Room, first floor, Physics Bldg. 510*

08:30 - 09:00 Registration

09:00 - 09:30 Welcome: S. Aronson, T. Hallman, & M. Gyulassy      (10, 10, 10)

Theory - Chair: Edward Shuryak

09:30 – 10:00 “Finite Chemical Potential QCD on the Lattice” - Sandor Katz, Budapest (20 + 10)

10:00 – 10:30 “The Detail Analysis of the Three-Quark Potential in SU(3) Lattice QCD” – Turo Takahashi, Osaka (20 + 10)

10:30 – 10:50 COFFEE BREAK (20)

10:50 – 11:20 “The Delta vs. Junction Configurations in Lattice QCD” – Philippe Forcrand, Zurich (20+10)

11:20 – 11:50 “High Baryon Density QCD Matter” – Dirk Rischke, Frankfurt (20+10)

11:50 – 12:15 “Effects of Strong Color Fields on Baryon Dynamics” – Sven Soff, LBNL (20+5)

12:15 – 13:55 LUNCH

Experiment Results from RHIC – Chair: Hans-Georg Ritter

13:55 - 14:30 “Results from BRAHMS” – Ian Bearden, NBI (30+5)

14:30 - 15:05 “Overview of PHENIX Results on Baryons and Identified Hadrons”  
– Tatsuya Chujo, BNL (30+5)

15:05 – 15:25 COFFEE BREAK (20)

15:25 – 15:50 “Results from PHOBOS” – Kris Gulbrandsen, MIT (20+5)

15:50 - 16:25 “Proton and Anti-Proton Distributions from STAR” – Kai Schweda, LBNL (30+5)

16:25 - 16:40 “Baryon Production and Gluonic Dynamics at RHIC” – Huan Huang, UCLA (20+5)

18:30            RECEPTION, Physics Lobby

---



---

Friday, March 29 *Large Seminar Room, first floor, Physics Bldg. 510*

Theory - Chair: *Che-Ming Ko*

- 08:30 - 09:00 "Baryons and Mesons at AA at RHIC" - Steffen Bass, Duke (25+5)
- 09:00 - 09:30 "Baryon Transport at RHIC" - Vasile Topor Pop, McGill (25+5)
- 09:30 - 10:00 "Hydrodynamic Baryon Flow" - Derek Teaney, BNL (25+5)
- 10:00 - 10:30 "The Pbar/pi- Anomaly at High pt" - Ivan Vitev, Columbia (25+5)
- 10:30 - 10:50 COFFEE BREAK (20)
- 10:50 - 11:20 "Color Glass Condensate of String Junctions" - Boris Kopeliovich (25+5)
- 11:20 - 11:50 "Baryon Fluctuations" - Sangyong Jeon, McGill (25+5)
- 11:50 - 12:20 "Baryon Distributions from AMPT" - Zi-wei Lin, Texas A&M (20+5)
- 12:20 - 12:45 "Reviving the Strong Coupling Expansion: Baryon Junctions and Other Resonances" - Momchil Velkovsky, StonyBrook (20+5)
- 12:45 - 14:00 LUNCH

Experiment Results Overview - Chair: *Mark Baker*

- 14:00 - 14:30 "Baryon Stopping From SIS to High Energies - Expectations and Reality at RHIC" - Flemming Videbaek, BNL (20+10)
- 14:30 - 14:55 "Strange Baryon Production in p+A Collisions" - Brian Cole, Columbia (20+5)
- 14:55 - 15:30 "Baryon and Baryon Pair Production in Elementary and Nuclear Hadronic Interactions" - Hans Gerhard Fischer, CERN (30+5)
- 15:30 - 15:50 COFFEE BREAK (20)
- 15:50 - 16:20 "Baryon Results from E917 and the AGS" - David J. Hofman, UIC (25+5)
- 16:20 - 16:45 "Collision Energy and Centrality: What Do We Learn From Systemic Trend?" - Fuqiang Wang, Purdue (20+5)
-

---

Saturday, March 30      *Large Seminar Room, first floor, Physics Bldg. 510*

Theory + Experiment - Chair: *Barbara Jacak*

09:00 - 09:30 “Skyrmions” – Joe Kapusta, Minnesota (25+5)

09:30 – 10:00 “J-balls” – Tamas Csorgo, Budapest (25+5)

10:00 – 10:30 “Junctions and CP-violating Domains” – Dima Kharzeev, BNL (25+5)

10:30 – 10:50 COFFEE BREAK (20)

10:50 – 11:20 “Strange Baryon Production and Azimuthal Anisotropy at RHIC”  
– Hui Long, UCLA (25+5)

11:20 – 11:50 “Baryon/Anti-Baryon Ratios” (PHENIX), Iliia Ravinovich, Weizmann (20+10)

11:50 – 12:20 “Systematic of Nuclear Cluster Formation” – Zhangbu Xu, BNL (20+10)

12:20 – LUNCH – Physics Lobby

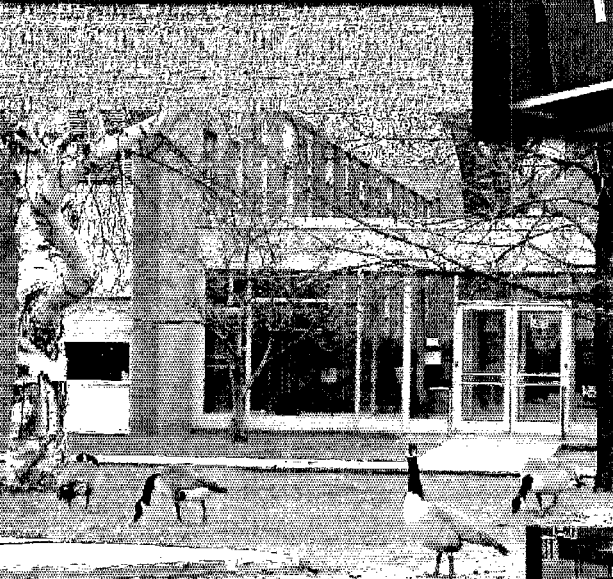
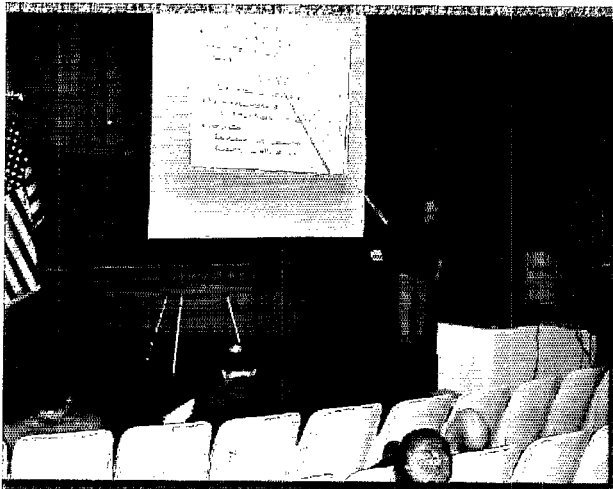
Afternoon – SUMMARY

Theory Summary, Xin-Nian Wang, LBNL (25)

Experimental Summary, Craig Ogilvie, ISU (25)

15:00 Workshop Adjourns

---



## **Additional RIKEN BNL Research Center Proceedings:**

- Volume 42 – Baryon Dynamics at RHIC – BNL-
- Volume 41 – Hadron Structure from Lattice QCD – BNL-
- Volume 40 – Theory Studies for RHIC-Spin – BNL-52662
- Volume 39 – RHIC Spin Collaboration Meeting VII – BNL-52659
- Volume 38 – RBRC Scientific Review Committee Meeting – BNL-52649
- Volume 37 – RHIC Spin Collaboration Meeting VI (Part 2) – BNL-52660
- Volume 36 – RHIC Spin Collaboration Meeting VI – BNL-52642
- Volume 35 – RIKEN Winter School – Quarks, Hadrons and Nuclei – QCD Hard Processes and the Nucleon Spin – BNL-52643
- Volume 34 – High Energy QCD: Beyond the Pomeron – BNL-52641
- Volume 33 – Spin Physics at RHIC in Year-1 and Beyond – BNL-52635
- Volume 32 – RHIC Spin Physics V – BNL-52628
- Volume 31 – RHIC Spin Physics III & IV Polarized Partons at High  $Q^2$  Region – BNL-52617
- Volume 30 – RBRC Scientific Review Committee Meeting – BNL-52603
- Volume 29 – Future Transversity Measurements – BNL-52612
- Volume 28 – Equilibrium & Non-Equilibrium Aspects of Hot, Dense QCD – BNL-52613
- Volume 27 – Predictions and Uncertainties for RHIC Spin Physics & Event Generator for RHIC Spin Physics III – Towards Precision Spin Physics at RHIC – BNL-52596
- Volume 26 – Circum-Pan-Pacific RIKEN Symposium on High Energy Spin Physics – BNL-52588
- Volume 25 – RHIC Spin – BNL-52581
- Volume 24 – Physics Society of Japan Biannual Meeting Symposium on QCD Physics at RIKEN BNL Research Center – BNL-52578
- Volume 23 – Coulomb and Pion-Asymmetry Polarimetry and Hadronic Spin Dependence at RHIC Energies – BNL-52589
- Volume 22 – OSCAR II: Predictions for RHIC – BNL-52591
- Volume 21 – RBRC Scientific Review Committee Meeting – BNL-52568
- Volume 20 – Gauge-Invariant Variables in Gauge Theories – BNL-52590
- Volume 19 – Numerical Algorithms at Non-Zero Chemical Potential – BNL-52573
- Volume 18 – Event Generator for RHIC Spin Physics – BNL-52571
- Volume 17 – Hard Parton Physics in High-Energy Nuclear Collisions – BNL-52574
- Volume 16 – RIKEN Winter School - Structure of Hadrons - Introduction to QCD Hard Processes – BNL-52569
- Volume 15 – QCD Phase Transitions – BNL-52561
- Volume 14 – Quantum Fields In and Out of Equilibrium – BNL-52560
- Volume 13 – Physics of the 1 Teraflop RIKEN-BNL-Columbia QCD Project First Anniversary Celebration – BNL-66299

## **Additional RIKEN BNL Research Center Proceedings:**

- Volume 12 – Quarkonium Production in Relativistic Nuclear Collisions – BNL-52559
- Volume 11 – Event Generator for RHIC Spin Physics – BNL-66116
- Volume 10 – Physics of Polarimetry at RHIC – BNL-65926
- Volume 9 – High Density Matter in AGS, SPS and RHIC Collisions – BNL-65762
- Volume 8 – Fermion Frontiers in Vector Lattice Gauge Theories – BNL-65634
- Volume 7 – RHIC Spin Physics – BNL-65615
- Volume 6 – Quarks and Gluons in the Nucleon – BNL-65234
- Volume 5 – Color Superconductivity, Instantons and Parity (Non?)-Conservation at High Baryon Density – BNL-65105
- Volume 4 – Inauguration Ceremony, September 22 and Non -Equilibrium Many Body Dynamics – BNL-64912
- Volume 3 – Hadron Spin-Flip at RHIC Energies – BNL-64724
- Volume 2 – Perturbative QCD as a Probe of Hadron Structure – BNL-64723
- Volume 1 – Open Standards for Cascade Models for RHIC – BNL-64722



**For information please contact:**

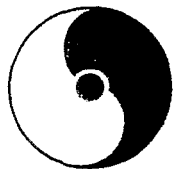
Ms. Pamela Esposito  
RIKEN BNL Research Center  
Building 510A  
Brookhaven National Laboratory  
Upton, NY 11973-5000 USA

Phone: (631) 344-3097  
Fax: (631) 344-4067  
E-Mail: [pesposit@bnl.gov](mailto:pesposit@bnl.gov)

Ms. Tammy Heinz  
RIKEN BNL Research Center  
Building 510A  
Brookhaven National Laboratory  
Upton, NY 11973-5000 USA

(631) 344-5864  
(631) 344-2562  
[theinz@bnl.gov](mailto:theinz@bnl.gov)

Homepage: <http://quark.phy.bnl.gov/www/riken.html>  
<http://penguin.phy.bnl.gov/www/riken.html>



RIKEN BNL RESEARCH CENTER

# Baryon Dynamics at RHIC

March 28-30, 2002



Li Keran

*Nuclei as heavy as bulls  
Through collision  
Generate new states of matter.  
T.D. Lee*

Copyright©CCASTA

Speakers:

S. Bass	I. Bearden	T. Chujo	B. Cole	T. Csorgo
H. G. Fischer	P. Forcrand	K. Gulbrandsen	D. Hofman	H. Huang
S. Jeon	J. Kapusta	S. Katz	D. Kharzeev	B. Kopeliovich
Z. Lin	H. Long	C. Ogilvie	V. T. Pop	I. Ravinovich
D. Rischke	K. Schweda	S. Soff	T. Takahashi	D. Teaney
M. Velkovsky	F. Videbaek	I. Vitev	F. Wang	X. Wang
Z. Xu				

Organizers: M. Gyulassy, D. Kharzeev, and N. Xu